Regulation and functions of macrophages in the adult mouse testis

A thesis submitted for the degree of Doctor of Philosophy at Monash University

August 2022

Department of Molecular and Translational Science,

Faculty of Medicine, Nursing and Health Sciences

&

Centre for Reproductive Health,

Hudson Institute of Medical Research

By

Sneha Biniwale

(Master of Biotechnology)

Under supervision of:

Professor Mark P Hedger and Professor Kate L. Loveland (Monash University, Melbourne, Australia)

Professor Dr. Andreas Meinhardt and Dr. Sudhanshu Bhushan (Justus-Liebig-University, Giessen, Germany)

JUSTUS-LIEBIG-UNIVERSITÄT GIESSEN

Regulation and functions of macrophages in the adult mouse testis

Inaugural Dissertation

Submitted to the

Faculty of Medicine

in partial fulfillment of the requirements

for the PhD-degree

of the Faculties of Veterinary Medicine and Medicine

of the Justus Liebig University Giessen

as part of the binational joint award PhD program of the Justus Liebig University Giessen and the Monash University Melbourne

by

Sneha Biniwale

of

Bharuch, India

Giessen 2022

From the Institute of Anatomy and Cell Biology
Director/Chairman: Prof. Dr. Andreas Meinhardt
of the Faculty of Medicine of the Justus Liebig University Giessen

Chair: Prof. Dr. Christine Wrenzycki
First Supervisor and first reviewer: Prof. Dr. Andreas Meinhardt
Second reviewer: Prof. Holger Reichardt
Second supervisor and Vice-chair: Prof. Gerard Schuler,

Date of Doctoral Defense: 18th Jan 2023

Table of Contents

Copyright notice

Abstract (English)

Macrophages, which regulate inflammation and dictate the course of infection, are the most important immune cell type in the testis. It has been established that the majority of macrophages in the rodent testis are 'alternatively activated' (M2, or anti-inflammatory), consistent with the immune privilege of the organ. However, there is still much to be discovered about the regulation of this testicular environment. Significantly, activins produced by Sertoli cells, pachytene spermatocytes and round spermatids, and spermatogonia in the seminiferous tubules, myoid cells in the peritubular region and Leydig cells and macrophages in the interstitium are implicated in regulating inflammatory responses by macrophages (Hedger *et al.,* 2011). Activin A is an important regulator of macrophage and dendritic cell development, and its endogenous binding protein, follistatin, has been found to be therapeutic in a number of inflammatory and immunological disease models (Hedger and de Kretser DM, 2013).

The aim of this research was to investigate the effect of activin A on the number, distribution and functions of macrophages in different compartments of the adult mouse testis, specifically the parenchyma and compartments like the rete testis, subcapsular region and tunica albuginea, using mice with reduced levels of either activin A or follistatin, by immunohistochemical studies. Additionally, macrophage subsets were studied in order to understand their functions in normal, infected and activin A-deficient mouse testes by immunofluorescence studies. Lastly, the functional regulation of the testicular macrophages was investigated by studying their gene expression profile compared to bone-marrow-derived macrophages *in vitro*.

There was a significant decrease in the total number of F4/80^{+} interstitial macrophages (31% compared with litter-mate controls) and peritubular macrophages (49%) per testis in activin-deficient *Inhba*$^{+/-}$ mice. The volume densities of the peritubular macrophages and subcapsular macrophages were also significantly reduced (53% and 36%, respectively). When F4/80^{+} macrophage subsets were studied further using expression of CX_3CR_1 (a chemokine receptor involved in leukocyte migration), MHC class II molecules (involved in antigen presentation and a marker for activated macrophages), and CD206 (a mannose-specific scavenger receptor and anti-inflammatory marker), it was observed that the volume density of interstitial macrophages was 8-9-fold higher in the interstitial and peri-epithelial regions of the

rete testis as compared to their corresponding populations in the parenchyma. The proportions of F4/80^{+}CD206^{+} interstitial and peri-epithelial macrophages in the rete testis were 71% lower than interstitial macrophages in the parenchyma and 47% lower than peritubular macrophages in the parenchyma, respectively. Additionally, there was a 70% increase in rete testis interstitial macrophages expressing MHCII as compared to the parenchyma and a 10% increase in MHCII^{+} interstitial macrophages in the rete testis of activin A-deficient mice. When infected by uropathogenic bacteria, there was considerable increase of MHCII^{+} macrophages in the rete testis at day 10 post-infection, which later resolved by day 28.

When highly-purified testicular macrophages were investigated *in vitro*, using multiplex RNAseq analysis, several key pro-inflammatory pathways, including PI3K-AKT, toll-like receptor 4 signaling, and some anti-viral responses were differentially expressed compared to bone marrow-derived macrophages. Testicular macrophages were unresponsive to stimulation by bacterial lipopolysaccharide (LPS), which correlated with low expression of genes involved in the LPS-regulated toll-like receptor (TLR4) signaling pathway (*Tlr4, Cd14, Ly96*, *Tirap, Tram1*), and higher expression of genes encoding proteins that inhibit TLR signaling via NF-κB (*Chuk, Ptpn6, Sigirr, Ikbkb*). Some transcripts encoding proteins involved in regulating anti-viral responses, including *Irf5 and* several interferon-stimulated gene transcripts (*Ifitm2*, *Ifitm3*, *Ifi35*, *Oas1a*, *Oas1g*, *Oas3*), also displayed lower expression in TMs, but other crucial anti-viral genes (*Tlr3, Tlr7, Irf1, Irf3, Mx, Ddx58*) were higher. Additionally, key regulators of mTOR/PI3K/AKT pathway that promote the anti-inflammatory/M2 phenotype (*Akt1, Pten*, *Inpp5d*, *Tsc1, Pik3r2*) were elevated in expression. Moreover, testicular macrophages expressed significantly higher transcripts of genes encoding proteins involved in antigen-presentation (MHC class II antigens, *Cd80*, *Cd86*, *Ciita*), anti-inflammatory genes (*Il10*, *Socs1*, *Nfkbiz*) and markers of alternatively activated, or M2, macrophages (*Mrc1*/CD206, *Stat3*, *Stat6*, *Gata3, Egfr*), relative to the BMMs. Overall, this analysis thereby showed several novel aspects of the anti-inflammatory nature of the testicular macrophages and their immunoregulatory roles.

In conclusion, these studies have demonstrated that activin A regulates macrophage number and function in the adult mouse testis, and have identified distinct macrophage subsets in the rete testis that appear to be both immunoregulatory and tolerogenic. Additionally, testicular macrophages have a predominantly anti-inflammatory

phenotype, and may lack the capacity to respond to some bacterial and viral infections. These studies considerably expand our understanding of the different macrophage subsets in the mouse testis, and their potential roles in regulating tolerance to sperm antigens and responses to infection.

Abstract (Deutsch)

Makrophagen steuern eine Entzündung, bestimmen den Verlauf einer Infektion und gehören damit zu den wichtigsten Immunzellen des Hodens. Man geht davon aus, dass die meisten Makrophagen im Hoden eines Nagers „alternativ aktiviert“ sind (M2 oder anti-inflammatorisch), passend zum Immunprivileg dieses Organs. Dennoch wissen wir nach wie vor zu wenig über die testikuläre Umgebung. Klar ist jedoch das Aktivine, die von Spermatogonien, Sertolizellen, pachytänen Spermatozyten, sowie runden Spermatiden in den Tubuli seminiferi, aber auch von myoiden Zellen in der peritubulären Region wie den Leydigzellen und Makrophagen im Interstitium produziert werden, eine wichtige Rolle bei der Regulation entzündlicher Antworten durch Makrophagen spielen (Hedger *et al.,* 2011). Aktivin A ist dazu ein wichtiger Regulator bei der Entwicklung von Makrophagen und dendritischen Zellen, und dessen endogener Bindungspartner Follistatin zeigt bei einigen Entzündungs- und immunologischen Krankheitsmodellen eine therapeutische Wirkung (Hedger and de Kretser, 2013).

Ziel dieser Arbeit war es die Wirkung von Aktivin A auf die Anzahl, Verteilung und Funktionen von Makrophagen in verschiedenen Kompartimenten des adulten Hodens der Maus zu untersuchen. Dazu wurden immunhistochemische Studien mit transgenen Mäusen, die nur wenig Aktivin A oder Follistatin exprimieren konnten, an Makrophagen im Parenchym sowie als weiteren Kompartimenten dem Rete testis, dem subkapsulären Bereich sowie der Tunica albuginea durchgeführt. Zusätzlich wurden verschiedene Makrophagenpopulationen mittels Immunfluoreszenz untersucht, um deren Funktionen im Hoden von Wildtyp-Mäusen, infizierten Mäusen und Aktivin A-defizienten Mäusen zu verstehen. Weiterhin wurden funktionelle Unterschiede im Profil der testikulären Makrophagen untersucht, in dem ihre Genexpressionsprofile mit denen von aus dem Knochenmark isolierten *und in vitro* kultivierten Makrophagen verglichen wurde.

Bei Aktivin-defizienten heterozygoten *Inhba*$^{+/-}$ Mäusen war die Anzahl der interstitiellen F4/80^{+} Makrophagen bezogen auf den Hoden und im Vergleich zu Wildtyp-Mäusen aus dem gleichen Wurf um 31% und die der peritubulären Makrophagen sogar um 49 % erniedrigt. Ebenfalls reduziert war die Volumendichte von peritubulären (53%) und subkapsulären (36%) Makrophagen. Bei F4/80^{+} Makrophagen, die durch die Expression von CX_3CR_1 (einen Chemokinrezeptor, der

für die Migration von Leukozyten benötigt wird), MHC II (ein Molekül, dass bei der Antigen Präsentation eine wichtige Rolle spielt und einen Marker für aktivierte Makrophagen darstellt) sowie CD206 (einen Mannose-spezifischen *Scavanger* Rezeptor und anti-inflammatorischen Marker) charakterisiert sind, war die Volumendichte interstitieller Makrophagen in den interstitiellen und peri-epithelialen Regionen des Rete Testis um einen Faktor von acht bis neun höher als im Vergleich zu den entsprechenden Populationen im Parenchyms. Der Anteil der F4/80^{+}CD206^{+} interstitiellen und peri-epithelialen Makrophagen im Rete testis war dagegen um 71% niedriger als der Anteil der interstitiellen Makrophagen im Parenchym und um 47% niedriger als der Anteil der peritubulären Makrophagen im Parenchym. Darüber hinaus war der Anteil der interstitiellen MHCII + Makrophagen im Rete testis im Vergleich zum Parenchym um 70% erhöht. Bei Aktivin-defizienten Mäusen waren die interstitiellen MHCII^{+} Makrophagen im Rete testis dagegen nur um 10% erhöht. Die Infektion mit uropathogenen E. coli Bakterien führte nach 10 Tagen zu einem beträchtlichen Anstieg der MHCII+ Makrophagen im Rete testis, der jedoch nach 28 Tagen nicht mehr nachweisbar war.

Bei der Multiplex RNAseq Analyse von hochgereinigten testikulären Makrophagen im Vergleich zu den aus dem Knochenmark isolierten Makrophagen wurden eine Reihe von wichtigen pro-inflammatorischen Signalwegen wie dem PI3K-AKT, Toll-like Rezeptor 4 (TLR4) sowie anti-virale Signalwegen differenziell exprimiert. Testikuläre Makrophagen waren hierbei unempfindlich gegenüber der Stimulation mit bakteriellem Lipopolysaccharid (LPS), was mit einer niedrigen Expression von Genen des LPS-regulierten TLR4 Signalweg einhergeht (*Tlr4, Cd14, Ly96*, *Tirap, Tram1*) sowie mit einer höheren Expression von Genen, die den TLR4 Signalweg über NF-κB inhibieren (*Chuk, Ptpn6, Sigirr, Ikbkb*). Einige Transkripte wie *Irf5* und eine Reihe von durch Interferon stimulierten Transkripte (*Ifitm2*, *Ifitm3*, *Ifi35*, *Oas1a*, *Oas1g*, *Oas3*), die alle bei der Regulation von antiviralen Antworten bedeutsam sind, zeigten eine niedrigere Expression in testikulären Makrophagen, wogegen andere wichtige antivirale Gene (*Tlr3, Tlr7, Irf1, Irf3, Mx, Ddx58*) stärker exprimiert waren. Höher exprimiert waren auch Schlüsselregulatoren des mTOR/PI3K/AKT Signalweges, die den anti-inflammatorischen M2 Phänotyp prägen (*Akt1, Pten*, *Inpp5d*, *Tsc1, Pik3r2*). Darüber hinaus exprimierten testikuläre Makrophagen auch signifikant mehr Transkripte von Genen, die für Proteine kodieren, die bei der Antigenpräsentation eine Rolle spielen

(Mhc II Antigene, *Cd80*, *Cd86*, *Ciita*), oder für anti-inflammatorische Mediatoren (*Il10*, *Socs1*, *Nfkbiz*) sowie Marker für alternativ aktivierte (M2) Makrophagen (*Mrc1*/CD206, *Stat3*, *Stat6*, *Gata3, Egfr*). Insgesamt ergaben die Analysen neue Informationen zur anti-inflammatorischen Natur testikulärer Makrophagen und ihrer Rolle bei der Immunregulation des Hodenmilieus.

Insgesamt konnte gezeigt werden, dass Aktivin A die Zahl und Funktion von Makrophagen im Maushoden regulieren kann. Darüber hinaus wurden Makrophagenopulationen im Rete testis identifiziert, die immunregulatorische und tolerogene Eigenschaften aufweisen könnten. Testikuläre Makrophagen zeigen einen klaren anti-inflammatorischen Phänotyp, der mit einem Mangel an effizienter Bekämpfung von bakteriellen und viralen Infektionen einher zu gehen scheint. Die vorliegenden Untersuchungen tragen zu einem erweiterten Verständnis der verschiedenen Makrophagenpopulationen im Hoden der Maus sowie deren Funktion bei der Entwicklung einer Toleranz gegenüber Spermienantigenen und bei der Regulation von testikulären Infektionsantworten bei.

Publications during candidature

Journal articles

1. **Biniwale, S.**, Wijayarathna, R., Pleuger, C., Bhushan, S., Loveland, K. L., Meinhardt, A., & Hedger, M. P. (2022). Regulation of macrophage number and gene transcript levels by activin A and its binding protein, follistatin, in the testes of adult mice. *Journal of Reproductive Immunology*, *151*, 103618.
2. Wijayarathna, R., Pasalic, A., Nicolas, N., **Biniwale, S.**, Ravinthiran, R., Genovese, R., Muir, J. A., Loveland, K. L., Meinhardt, A., Fijak, M., & Hedger, M. P. (2020). Region-specific immune responses to autoimmune epididymitis in the murine reproductive tract. *Cell and tissue research*, *381*(2), 351-360.

Conference proceedings

1. **Biniwale, S.**, Wijayarathna, R., Bhushan, S., Loveland, K. L., Meinhardt, A., & Hedger, M. P. (2022). *Characterization of a major macrophage subset with an immunoregulatory phenotype in the murine rete testis*. 55th Annual meeting of the Society for the Study of Reproduction, Spokane, WA, USA (2-min short oral presentation.
2. **Biniwale, S.**, Wijayarathna, R., Bhushan, S., Loveland, K. L., Meinhardt, A., & Hedger, M. P. (2022). *New insights into the immunological roles of macrophages adjacent to the rete testis and tunica albuginea.* 12th Lorne infection and immunity conference, Lorne, Australia (Poster presentation)
3. **Biniwale, S.**, Wijayarathna, R., Bhushan, S., Loveland, K. L., Meinhardt, A., & Hedger, M. P. (2021). *New insights into the immunological roles of macrophages adjacent to the rete testis and tunica albuginea.* Annual scientific meeting of the Society for Reproductive Biology, Melbourne, Australia (Poster presentation)
4. **Biniwale, S.**, Wijayarathna, R., Bhushan, S., Loveland, K. L., Meinhardt, A., & Hedger, M. P. (2021). *Analysis of macrophages in the murine rete testis: Regulation by activin.* 13th Network for Young Researchers in Andrology (virtual) (Poster presentation)
5. **Biniwale, S.**, Wijayarathna, R., Bhushan, S., Loveland, K. L., Meinhardt, A., & Hedger, M. P. (2021). *Analysis of macrophages in the murine rete testis: Regulation by activin.* 21st European Testis Workshop (virtual) (Short oral presentation)

6. **Biniwale, S.**, Wijayarathna, R., Pleuger C., Bhushan, S., Loveland, K. L., Meinhardt, A., & Hedger, M. P. (2021). *Macrophage distribution and gene expression in the testes of adult mice with altered activin and follistatin activity.* American Society of Andrology (virtual) (Poster presentation)
7. **Biniwale, S.**, Wijayarathna, R., Pleuger C., Bhushan, S., Loveland, K. L., Meinhardt, A., & Hedger, M. P. (2020). *The effects of endogenous activin activity on the number and functional properties of testicular macrophages in adult mice.* Victorian Infection and Immunity Network, Australia (Poster presentation)
8. **Biniwale, S.**, Wijayarathna, R., Indumathy S., Hosseini S., Bhushan, S., Loveland, K. L., Meinhardt, A., & Hedger, M. P. (2019). *Enumerating macrophages in the mouse testis using classical histological and immunohistochemical techniques.* Annual scientific meeting of the Society for Reproductive Biology, Sydney, Australia (Poster presentation)

Awards during candidature

1. Selected as a mentee at Industry Mentoring Network in STEM (2021-22), Australia and representing Hudson Institute of Medical Research at national level events
2. Recipient of Harold-Mitchell Travel Scholarship to virtually present at European Testis Workshop and Network for Young Researchers in Andrology (NYRA) 2021

Thesis including published works general declaration

I hereby declare that this thesis contains no material which has been accepted for the award of any other degree or diploma at any university or equivalent institution and that, to the best of my knowledge and belief, this thesis contains no material previously published or written by another person, except where due reference is made in the text of the thesis.

This thesis includes **one** original paper published in a peer reviewed journal and **two unpublished** publications. The core theme of the thesis is **regulation and functions of testicular macrophages and role of activins in adult mouse testis**. The ideas, development and writing up of all the papers in the thesis were the principal responsibility of myself, the candidate, working within the Department of Molecular and Translational Science, Monash University and Justus-Liebig University, Giessen, Germany under supervision of Professor Mark P Hedger, Professor Kate L. Loveland, Professor Dr. Andreas Meinhardt and Dr. Sudhanshu Bhushan (The inclusion of co-authors reflects the fact that the work came from active collaboration between researchers and acknowledges input into team-based research)

In the case of chapter 2*,* my contribution to the work involved the following:

Chapter	Chapter/ Publication title	Publication status	Extent (%) & nature of student's contribution
2	Regulation of macrophage number and gene transcript levels by activin A and its binding protein, follistatin, in the testes of adult mice	Published original article	70% Contributed to experimental design, data collection and analysis, writing of the manuscript

I have renumbered sections of published or prepared papers in order to generate a consistent presentation within the thesis.

Student signature: **Date:** 30-08-2022

The undersigned hereby certify that the above declaration correctly reflects the nature and extent of the student's and co-authors' contributions to this work.

Main Supervisor signature: **Date:** 30-08-2022

Acknowledgements

My doctoral journey has been a wonderful ride and I am extremely grateful for the opportunity to contribute to the world of science and to everyone who made it possible.

First of all, I would like to extend my heartfelt gratitude to Prof Mark Hedger for selecting me as a PhD candidate in his lab and supporting me throughout this exciting journey of 4 years. He always encouraged me when I was dejected and supported me with my decisions throughout my project especially during the COVID-19 pandemic. I am extremely grateful to my co-supervisors Prof. Kate Loveland (Monash University) and Prof. Andreas Meinhardt and Dr. Sudhanshu Bhushan (Justus Liebig University, Germany) for encouraging me and providing me with their invaluable scientific inputs during every conference presentation, publication and in our monthly meetings and their enthusiasm to discuss the scientific data across the seas.

I would like to thank the International Research Training Group (IRTG) on Molecular Pathogenesis of Male Reproductive Disorders between Monash University, Australia and Justus Liebig University, Germany. The financial support from Monash University in the form of Monash Graduate Scholarship and Faculty of Medicine, Nursing and Health Sciences International Tuition Scholarship is greatly acknowledged. I am indebted to IRTG coordinators Sarah Meachem and Liza O' Donnell for effectively helping me with scientific discussions and journal clubs during my candidature. My special thanks to Rose Kiarie for helping me since the day I landed in Melbourne for the first time and before during my selection phase. I would also like to thank Pia Juergens for helping me understand the processes at JLU when I needed. I extend my gratitude to Prof Michael Hickey, Dr. Nicole De Weerd and Dr Brendan Houston, my PhD panel members, for their valuable advice.

I would like to extend my heartfelt gratitude to my colleagues Rosemary Genovese, Julie Muir and Susan Hayward for providing technical support with my experiments, Julia Bender for being a wonderful colleague and project partner at JLU and Sivanjah Indumathy for teaching me the flow cytometry technique and being with me during long hour experiments. Similarly, I would like to thank JLU exchange students Rashidul Islam and Shashika Kothalawala for their support and memories during the last phase of my PhD. My special thanks to Rukmali Wijayarathna for being with me in my professional life by advising me in my experiments, timelines, sharing her

scientific and technical expertise and being a friend, I needed in my personal life. My heartfelt gratitude to my dear friend Samira Hossieni for being with me throughout my scientific and personal journey of 4 years.

I am thankful to my friend Nikita Shah for providing me emotional support during my initial days in Melbourne and being a dear friend since my college days. Similarly, I would like to thank my school friend Dipy Vasa for cheering me from the USA and my ex-colleague Sai Krishnaveni Chevooru Manda for encouraging me to apply to Monash University for doctoral studies. I am indebted to my parents, Hemangini Biniwale and Sanjay Biniwale for always believing in me in all my decisions, dreams and supporting me throughout this journey. I am extremely grateful to my brother Sanket Biniwale and sister-in-law Priti Biniwale for always looking forward to my next milestone and being proud of my achievements. I especially thank my dearest niece Saanvi Biniwale, born on the day I started my PhD journey, for being a silent cheerleader and teaching me to take on every challenge with a smile. My heartfelt gratitude to my in-laws especially mother-in-law Kalpana Khande, father-in-law Narendra Khande and grandfather-in-law Eknath Khande for supporting my decision to study further to pursue my dreams and my other niece Ira Khande for cheering me throughout. I would like to sincerely thank my maternal grandparents, Rameshchandra Chitre and Pushpa Chitre as well as paternal grandparents, Jayvantrao Biniwale and Pramila Biniwale for incorporating their values in me and encouraging me to believe in myself through their actions. I wish they were here today to witness my achievements as both paternal and maternal grandfather always wanted to see me become a doctor. Lastly, I would like to thank my husband Hemant Khande, for standing beside me like a rock throughout this journey and supporting me emotionally, with his independent scientific suggestions and at every step I needed him. I would like to dedicate my doctoral thesis to my family – my parents, grandparents, in-laws and my husband who all will be amongst the happiest to see me complete my PhD.

Abbreviations/Acronyms

Acod1	Acomitate decarboxylase
ACTR	Nuclear receptor coactivator 3 (encoded by *Ncoa3*)
ACVR1B	Activin receptor type-1B (encoded by *Acvr1b*)
ACVR1C	Activin receptor type-1C (encoded by *Acvr1c*)
Adgre1	Adhesion G protein-coupled receptor E1 (F4/80)
Adora2b	Adenosine A2B receptor
Akap4	A Kinase (Prka) anchor protein 4
AKT	RAC (Rho family)-alpha serine/threonine protein
ALDH1A2	Aldehyde dehydrogenase family 1, subfamily A2
ALK	Anaplastic lymphoma kinase
AMPK	AMP-activated protein kinase
APC	Antigen presenting cell
AROM	Aromatase
BAMBI	Bone morphogenetic protein and activin membrane-bound inhibitor
BMM	Bone marrow-derived macrophages
BSA	Bovine serum albumin
cAMP	Cyclic adenosine monophosphate
Ccl17	Chemokine (C-C Motif) ligand 17
CCL2/ MCP1	Chemokine (C-C Motif) ligand 2/ monocyte chemoattractant protein-1
CCR2	Chemokine (C-C Motif) receptor 2
CD	Cluster of differentiation
Cdc42	Cell division cycle 42
CDH1	Cadherin 1
CFA	Complete Freund's adjuvant
Ch25h	Cholesterol 25-hydroxylase
Chil3	Chitinase-like 3
Chuk	Conserved helix-loop-helix ubiquitous kinase
Ciita	Class II transactivator
Clec4a	C-type lectin domain family4, member a2
Clgn	Calmegin
Clu	Clusterin
CREB	Camp responsive element binding protein 1
CSF1	Colony stimulating factor 1
CSF1R	Colony stimulating factor 1 receptor
CTLA-4	Cytotoxic T-lymphocyte-associated protein 4
Ctsl	Cathepsin L
Ctss	Cathepsin S
CX_3CL_1	Chemokine (C-X3-C Motif) ligand 1 (Fractalkine)
CX_3CR_1	Chemokine (C-X3-C Motif) receptor 1

CXCL2	Chemokine (C-X3-C Motif) ligand 2
Cyp11a1	The cholesterol side-chain cleavage enzyme
Cyp17a1	17alpha-hydroxylase/C17,20 lyase
DAB	Diaminobenzidine
DAPI	4',6-diamidino-2-phenylindole
DC	Dendritic cells
Ddx	DEAD/DEAH box helicase
Dlst	Dihydrolipoamide s-succinyltransferase
DMEM	Dulbecco's modified eagle's medium
DMRT1	Doublesex and mab-3 related transcription factor 1
DPX	Dibutylphthalate polystyrene xylene
E	Embryonic day
EAO	Experimental auto-immune orchitis
Ear2	Eosinophil-associated, ribonuclease a family, member 2
ECM	Extracellular matrix
ED	Efferent ducts
EDS	Ethane dimethane sulphonate
Egfr	Epidermal growth factor receptor
ETC	Electron transport chain
F11r	F11 receptor
FACS	Fluorescence-activated cell sorting
FBS	Fetal bovine serum
Fcgr1	Fc receptor, Igg, high affinity i (CD64)
Fn1	Fibronectin 1
FSH	Follicle stimulating hormone
FST	Follistatin
Fstl1	Follistatin ligand 1
Gapdhs	Gadph glyceraldehyde-3-phosphate dehydrogenase
Gata3	GATA binding protein 3
GFP	Green fluorescent protein
Glul	Glutamine synthetase
GM-CSF	Granulocyte-macrophage colony-stimulating factor (CSF2)
GO	Gene ontology
HEPES	4-(2-Hydroxyethyl)-1-piperazineethanesulfonic acid
HIV	Human immunodeficiency virus
Hspa1l	Heat shock protein 1-like
IDO	Indolamine 2,3- dioxygenase
Ifitm	interferon induced transmembrane protein
IFN	Interferon
IGF-1	Insulin-like growth factor 1
Ikbkb	Inhibitor of kappa b kinase beta
IL	Interleukin

Inha	Inhibin alpha subunit
Inhba	Inhibin beta A subunit
Inpp5d	Inositol polyphosphate-5-phosphatase D (SHIP-1)
Irf	Interferon regulatory factor
IT	Interstitium
Itgam	Integrin alpha M (CD11b)
Itgax	Integrin alpha X
Itgb1	Integrin beta 1
IκBα	Nuclear factor of kappa light polypeptide gene enhancer in b-cells inhibitor, alpha
KRT8	Keratin 8
LPS	Lipopolysaccharide
M.O.M	Mouse on mouse
MACS	Magnetic-activated cell sorting
MAL	Myelin and lymphocyte protein
MAP Kinases	Mitogen-activated protein kinases
Marchf1	March1 enzyme e3 ubiquitin ligase (MARCH1)
MARCO	Macrophage receptor with collagenous structure
M-CSF	Macrophage colony stimulating factor (CSF1)
MD2	Myeloid differentiation factor 2 (encoded by *Ly96*)
MDS	Multidimensional scaling
Me1	Malic enzyme 1
MERTK	Mer proto-oncogene tyrosine kinase
MHCII	Major histocompatibility complex Ii
Mmp9	Matrix metalloproteinase 9
Mrc1	Mannose receptor, C type 1
MT-FS	Metallothionein -I follistatin
Mtor	Mechanistic target of rapamycin kinase
Mx	MX dynamin-like GTPase
MyD88	Myeloid differentiation primary response gene 88
Myo18a	Myosin xviiia
Nfe2l2	Nuclear factor, erythroid-derived 2, like 2
NFκB	Nuclear factor kappa B
NK	Natural killer
NO	Nitric oxide
NOS2	Inducible nitric oxide synthase
Oas	Oligoadenylate synthetase
OCT	Optimal cutting temperature compound
OXPHOS	Oxidative phosphorylation
PAS	Periodic acid Schiff
PAX8	Paired box 8
PBS	Phosphate buffered saline

PCR	Polymerase chain reaction
Pdha2	Pyruvate dehydrogenase E1 alpha 2
Pdk1	Pyruvate dehydrogenase kinase 1
PE	Peri-epithelial
PFA	Paraformaldehyde
Pfkm	Phosphofructokinase
PG	Prostaglandin
Pgam2	Phosphoglycerate Mutase 2
Pgd	Phosphogluconate dehydrogenase
PGE2	Prostaglandin e2
PGF2α	Prostaglandin F 2α
PGI2	Prostaglandin i2
Pgk2	Phosphoglycerate kinase 2
PI3K	Phosphoinositide 3-kinases
Pkm	Pyruvate kinase M
Plod2	Procollagen lysine, 2-oxoglutarate 5-dioxygenase 2
PPARγ	Peroxisome proliferator activated receptor gamma
PPP	Pentose phosphate pathway
PT	Peritubular region
Pten	Phosphatase and tensin homolog
Ptpn6	Protein tyrosine phosphatase, non-receptor type 6
Ptprc	Protein tyrosine phosphatase, receptor type, C (CD45)
RA	Retinoic acid
RDH10	Retinol dehydrogenase 10 (all-trans)
Retnla	Resistin like alpha
RIG-I	Retinoic-acid inducible gene I
RP105	Radioprotective 105
RT	Rete testis
RT-PCR	Reverse transcriptase polymerase chain reaction
SARM	Sterile alpha and tir motif containing 1
SC	Subcapsule
SDS	Sodium dodecyl sulphate
SEM	Standard error of the mean
Shpk	Sedoheptulokinase
Sigirr	Single immunoglobulin and toll-interleukin 1 receptor (tir) domain
Slamf8	Slam family member 8
SLC	Sertoli-like cells
Slc2a1	Solute carrier family 2 a1 (Glucose transporter 1; GLUT1)
SMAD	SMAD family member
SOCS1	Suppressor of cytokine signaling 1
Spanx4	SPANX family member N4

ST	Seminiferous tubules
Star	Steroid acute regulatory protein
Stat1	Signal transducer and activator of transcription 1
Stat3	Signal transducer and activator of transcription 3
Stat6	Signal transducer and activator of transcription 6
TA	Tunica albuginea
TAK1	TGFβ activated protein kinase 1
TBS	Tris-buffered saline
TCA	Tricarboxylic acid
TEM	Transmission electron microscopy
TGC	Testicular germ cells
TGFBR3	TGFβ receptor type 3
TGFβ	Transforming growth factor β
TH	Testicular homogenate
T_h	Helper T cell
TIF	Testicular interstitial fluid
Timd4	T cell immunoglobulin and mucin domain containing 4
Tirap	Toll-interleukin 1 receptor (TIR) domain-containing adaptor protein
TLR	Toll-like receptor
TM	Testicular macrophage
TNF	Tumor necrosis factor
Tnp1	Transition protein 1
Tnp2	Transition protein 2
Tollip	Toll Interacting protein
TR	Transition region
TRAM	Trif-related adaptor molecule
T_{reg}	Regulatory T cell
TRIF	Tir-domain-containing adapter-inducing interferon-B
TRSC	Transition region Sertoli cells
Tsc1	Tsc complex subunit 1
TTBS	Tris-buffered saline with 0.1% tween-20
Tulp2	Tubby-like protein 2
UPEC	Uropathogenic *E. Coli*
Ybx2	Y box protein 2

Chapter 1: Review of Literature

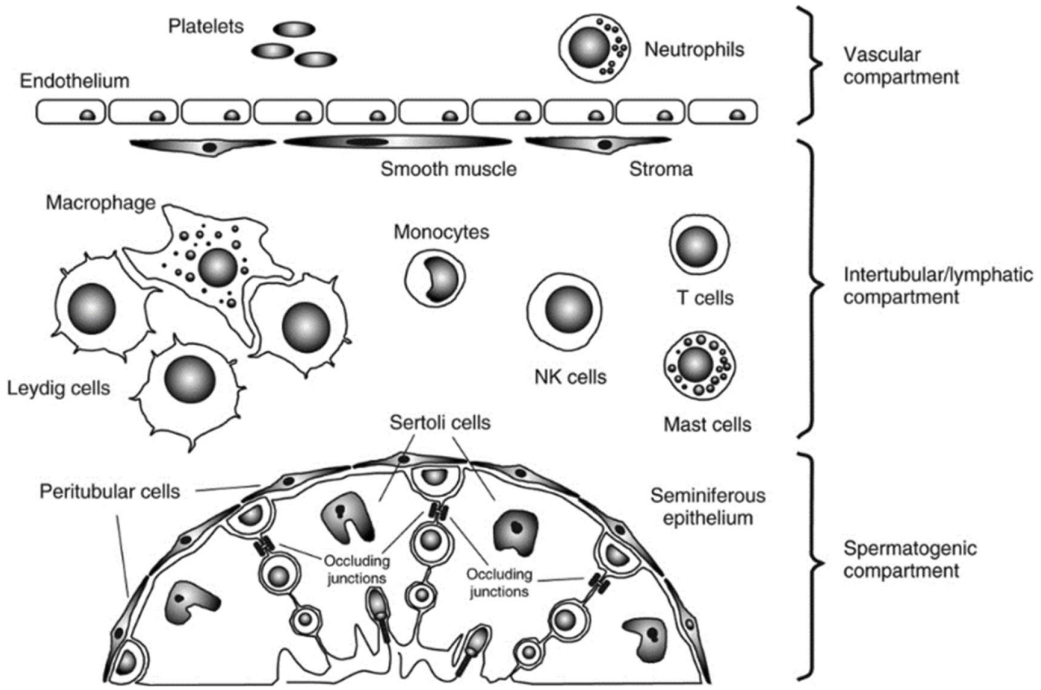

1.1 Introduction

Inflammation of the male reproductive tract has a significant impact on male health and fertility. Approximately 1/20 men suffer from infertility, much of it of unknown origin, but between 5-50% of cases (depending upon population access to health services) have an inflammatory or autoimmune involvement (Hedger, 2015, Schuppe and Meinhardt, 2005). Testicular inflammation, usually caused by urogenital infections, may lead to infertility and/ or androgen insufficiency in men, as well as long-term pain and discomfort (Aratchige *et al.,* 2008). Macrophages are the first line of defense and respond rapidly to infections and other external stimuli. They are the most abundant immune cells in the testis and are important regulators of inflammation; however, their regulation and function in this organ are still only partially understood. It has been established previously that macrophages have reduced immune responses in this environment and are known to be alternatively-activated, contributing to the status of immunological “privilege” in the testis (Winnall *et al.,* 2011b). If this were not the case, decreased survival of mature spermatozoa ultimately resulting in reduced fertility or infertility could be the result. Following testicular inflammation, resulting fibrosis can hamper spermatogenesis, leading to inefficient sperm formation, thus impairing infertility. Activin, an inflammatory mediator and a growth factor involved in the development and functional regulation of the testis, is elevated in inflammation, including in testicular inflammation. This cytokine is known to regulate inflammation and promote fibrosis, and it is hypothesized that follistatin, the activin-binding protein and its inhibitor, could improve the outcomes of testicular inflammation when used therapeutically.

This literature review focuses on summarizing the existing knowledge around the structure and functions of testis and how immune cells and somatic cells independently or in conjunction contribute to immune privilege. Additionally, the biology of activin and follistatin and their roles in the development and function of the testis, as well as in inflammation, will be discussed.

1.2 The male reproductive tract

The male reproductive tract comprises a pair of testes, efferent ducts and epididymides enclosed in the scrotum, which are connected to paired vas deferentia and the accessory sex glands (Fig. 1). These glands include the paired seminal

vesicles, the prostate gland and bulbourethral glands in the human male. Mice have two additional accessory glands; the ampullary glands and preputial glands (Knoblaugh and True, 2012).

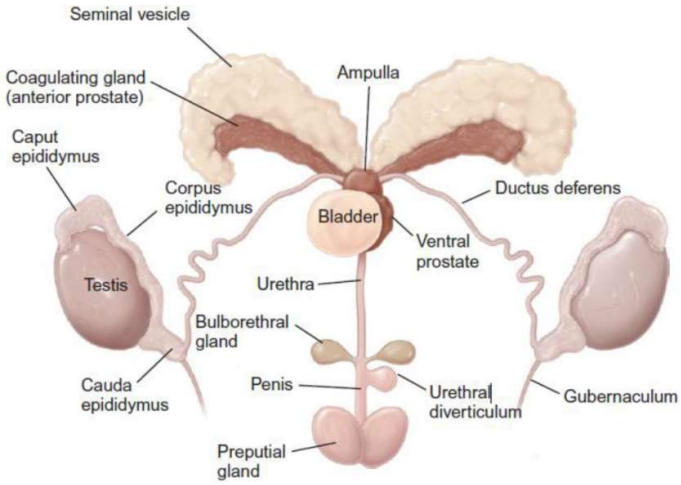

Figure 1: *Schematic diagram of the murine male reproductive tract (With permission from Knoblaugh and True, 2012)*

The reproductive glands collectively produce secretions that become part of the semen ejaculated from the urethra (De Kretser *et al.,* 1982). Sperm are produced in the testes. Spermatogonial stem cells undergo complex processes of mitosis and meiosis to form a mature sperm in the process called spermatogenesis. The mature sperm from the testis travel to the epididymis via the rete testis and efferent duct system. The epididymis is the storage site for mature sperm until ejaculation. The testis is also a major site for androgen production by somatic cells known as Leydig cells.

1.2.1 Structure and function of the testis

The male gonad has two main functions to perform: production of the male gamete - sperm - and synthesis of androgens, especially testosterone. The outermost layer of the testis is the tunica albuginea or capsule, which surrounds a complex structure of seminiferous tubules. These tubules collectively join to form the rete testis connecting them to the epididymis via the efferent ducts. Internally, the testis is compartmentalized histologically and functionally into the seminiferous tubules, where spermatogenesis takes place, and the interstitial tissue, which includes the vasculature, lymphatics, interstitial fluid and somatic cells, i.e., Leydig cells and

immune cells, such as macrophages, T cells, mast cells, and NK cells (Hedger, 2002). Macrophages are the most abundant immune cells in the interstitium of the testis. The seminiferous tubules consist of an outermost basement membrane, with closely associated Sertoli cells forming the epithelium. These cells are known as 'nurse cells' because of their ability to functionally support the growing spermatogonial stem cells and developing spermatogenic cells. Additionally, the Sertoli cells create the 'blood-testis barrier' by forming highly specialized tight junctions between adjacent cells. This barrier provides protection from immune cells in the interstitium and provides a supportive environment for the developing sperm within the seminiferous epithelium. Developing spermatogonia undergo a complex series of mitoses and meiosis to form primary spermatocytes and then the haploid round spermatids. Subsequently, they develop into elongated spermatids and eventually spermatozoa by spermiogenesis and are released into the lumen (Fig. 2). The basement membrane of the tubule is surrounded by peritubular cells, including myoid cells and macrophages with a stellate-like appearance, which differ from interstitial macrophages in various aspects to be discussed later. The peritubular myoid cells provide structural support to the tubules and help the movement of the mature sperm from the lumen into the epididymis by peristaltic contractions (Fijak *et al.,* 2017).

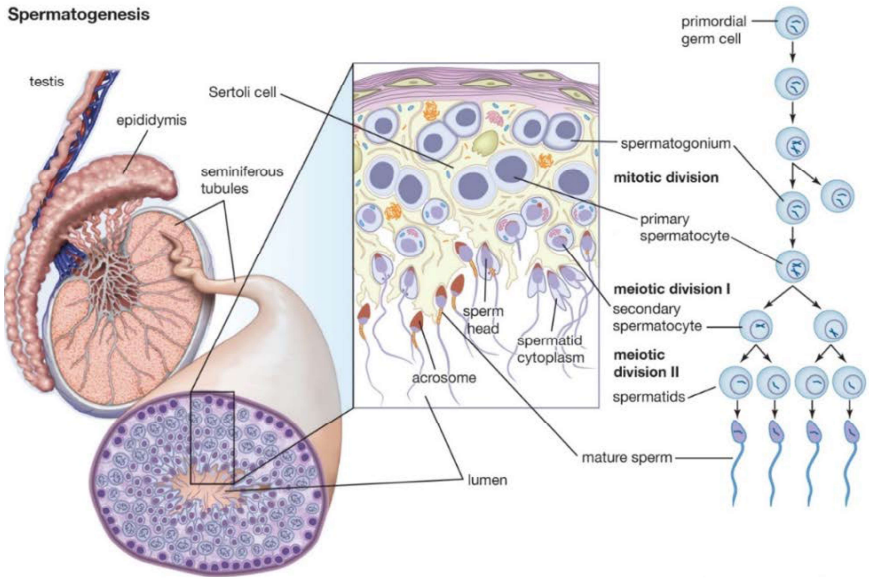

Figure 2: *Schematic diagram of the structure of the human testis and seminiferous epithelium (By courtesy of Encyclopedia Britannica, Inc., copyright 2011; used with permission)*

1.2.1.1 Structure and function of Sertoli cells and blood-testis barrier

The adult Sertoli cell is a large epithelial cell with a flattened surface towards the basement membrane of a seminiferous tubule and an extensive cytoplasm with numerous lateral and apical processes constituting the seminiferous epithelium along with the developing germ cells (Russell *et al.,* 1990, Hess and Vogl, 2015). Sertoli cells form specialized junctions comprising of adherens, gap and tight/ occluding junctions interspersed with actin-based Sertoli cell cytoskeletal structures and short tubulobulbar complexes, forming the blood- testis barrier, which protects a specialized environment for meiotic and post-meiotic germ cell development (Stanton, 2016, Mruk and Cheng, 2015). These junctions are formed at puberty and are principally maintained by occludin and claudin-11 proteins expressed by Sertoli cells themselves (McCabe *et al.,* 2016). Sertoli cells are orchestrators of spermatogenesis and perform numerous important functions in the testis, such as fetal germ cell development, regulation of androgen production, supporting the testicular vasculature, phagocytosis and maintenance of immune privilege (O'Donnell *et al.,* 2022). Sertoli cells are responsible for release of spermatids during spermiation which decides the sperm output produced during spermatogenesis (O'Donnell *et al.,* 2011, Kumar *et al.,* 2018). Disturbances in the Sertoli cells signaling pathways and hormone levels leads to spermiation failure, generally characterized by the retention and phagocytosis within Sertoli cells (O'Donnell *et al.,* 2011, Saito *et al.,* 2000). Additionally, Sertoli cells play an important role in immune privilege (explained later in section 1.3) by compartmentalizing the seminiferous epithelium and expressing a number of important immunoregulatory molecules, such as activins and inhibins belonging to the transforming growth factor β (TGF-β) superfamily, and indoleamine 2,3-dioxygenase (IDO), which are involved in inducing tolerogenic dendritic cells and regulatory T (T_{reg}) cell development (Cesaris *et al.,* 1992, Selawry *et al.,* 1991, Wyatt *et al.,* 1988, Nikolova *et al.,* 1992, Kaur *et al.,* 2014, Hedger, 2015, Bhushan *et al.,* 2020). Sertoli cells are a key regulator inducing the production of tolerogenic T_{reg} cells directly or indirectly through activation of the professional antigen presenting cells (APCs), the macrophages and dendritic cells (Kaur *et al.,* 2014, Tung *et al.,* 2017). *In vivo* studies with Sertoli cells have shown that they possess immunosuppressive properties that prevent grafts from being rejected when co-transplanted (Kaur *et al.,* 2017, Kaur *et al.,* 2014, Tung *et al.,* 2017).

1.2.1.2 The rete testis (RT) and transition region (TR)

The cellular organization of the rete testis epithelium is different from that of the seminiferous epithelium. A mature rete testis consists of flattened or squamous to cuboidal-shaped epithelial cells lining anastomosing channels within the basal lamina as opposed to mature Sertoli cells forming a blood-Sertoli cell barrier within the seminiferous epithelium in rodents (Kulibin and Malolina, 2020, Malolina and Kulibin, 2019, Major *et al.,* 2021) (Fig. 3). The rete epithelial cells are referred as 'Sertoli-like' cells (SLC) and express Sertoli cell-related genes, such as *Wt1, Sox9, Gata4 and Vim*, indicating that these rete cells share similarities with Sertoli cells. However, immature and mature rete testis cells specifically express PAX8 (a transcription factor responsible for mesonephros development), CDH1 (an adherens junction protein expressed in epithelial cells), KRT8 (an intermediate filament protein in the epithelia of many tissues) and few cells express DMRT1 (a transcription factor responsible for Sertoli cells differentiation), which are not expressed on Sertoli cells from seminiferous tubules (Malolina and Kulibin, 2019). Moreover, these SLCs continue to proliferate into adulthood, potentially providing a reservoir of Sertoli cell progenitors, and lack Sertoli cell tight junctions (Figueiredo *et al.,* 2016, Figueiredo *et al.,* 2021). The rete testis and seminiferous tubules are separated by the transition region (TR), also known as the tubuli recti, consisting of cells resembling the phenotype of Sertoli cells. These cells have been referred to as 'modified' Sertoli cells or transition region Sertoli cells (TRSCs) by different research groups (Kulibin and Malolina, 2020, Figueiredo *et al.,* 2021, Major *et al.,* 2021). These TRSCs are columnar cells with oval-shaped nuclei and peripheral heterochromatin (Aiyama *et al.,* 2015, Dym, 1974). They have tight junctions in the apical region, but the TR epithelium along the basolateral region is discontinuous and lacks Connexin 43, an important gap junction protein. Additionally, there are no mature spermatogenic cells in the TR or rete testis epithelium (Figueiredo *et al.,* 2021).

In addition to sperm transport, studies in rodents indicate that the mature rete testis also plays a role in fluid resorption, because the epithelial cells of the rete testis and the transition region possess endocytic activity and regulate the composition of the rete fluid by carrying out receptor-mediated endocytosis (Hermo and Dworkin, 1988, Turner *et al.,* 1984, Morales *et al.,* 1984).

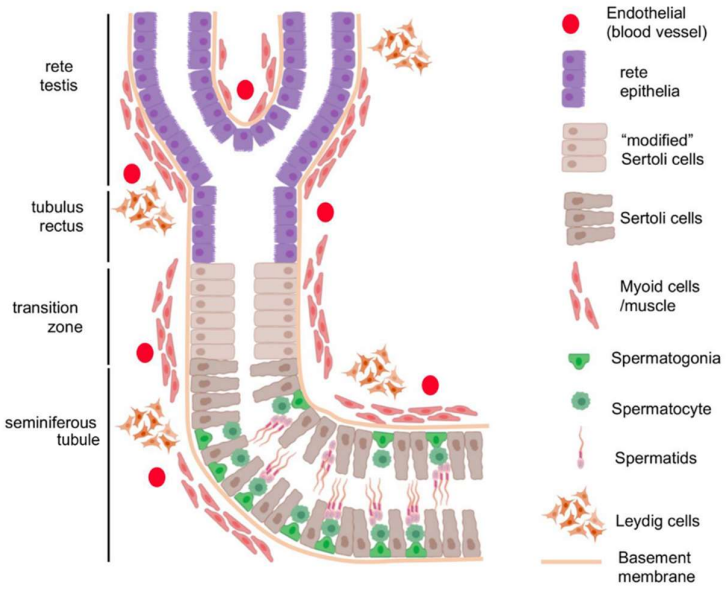

Figure 3: *Anatomy of the rete testis and transition region of the testis in rodents (modified from Major et al., 2021 and used with permission)*

1.2.2 The efferent ducts

The efferent ducts, or vasa efferentia, are small parallel tubules connecting the rete testis to the caput epididymis. The epithelium of the efferent ducts consists of cuboidal/ columnar cells that are either ciliated or nonciliated and the epithelium is surrounded by a basement membrane and a smooth muscle layer, with some species including the mouse also showing basal cells and intraepithelial lymphocytes or macrophages (Hess, 2002). Non-ciliated cells are present in greater proportion in the proximal region, whereas ciliated cells are distributed more towards the epididymal region (Ilio and Hess, 1992). The non-ciliated cells are the major cell lining the efferent duct and reabsorb the luminal fluids, thereby increasing the concentration of sperm several-fold (Clulow *et al.,* 1998). Fluid resorption involves multiple functions, including solute transport, passive water permeability, endocytosis and secretion (Clulow *et al.,* 1998).

1.3 Immunophysiology of the testis

Testicular interstitial macrophages are the most abundant immune cells in the interstitial area of the testis in all known species, followed by T cells, NK cells and dendritic cells (DC) (Hedger and Hales, 2006). A ratio of approximately one interstitial macrophage to four Leydig cells is well-established in experimental rodent testes (rat and mouse) and they are closely associated through cytoplasmic interdigitations,

which form during sexual maturation (Hutson, 1992). Several studies indicate that development and maintenance of macrophages and Leydig cells is interdependent: macrophage-deficient osteopetrotic mice with an inactivating mutation of a critical macrophage cytokine, CSF1, (*Csf1*$^{op/op}$ mice) are infertile, with reduced Leydig cells and low testosterone (Cohen *et al.,* 1996). Additionally, another study demonstrated that adult rats treated with ethane dimethane sulphonate (EDS), which specifically depletes Leydig cells, resulted in reduced macrophage numbers (Wang *et al.,* 1994). Recent studies have shown that the tissue-resident macrophages in the murine testis are derived from several waves of hematopoiesis, initially arising from primitive yolk-sac macrophages, followed by fetal monocytes (myeloid cells which later differentiate into macrophages) and later from nascent bone marrow-derived cells (Wang *et al.,* 2021). In the absence of inflammation or endocrine disruption, they are largely self-maintaining with minimal replenishment from circulating monocytes (Lokka *et al.,* 2020, Wang *et al.,* 2021, Meinhardt *et al.,* 2021). The peritubular lining of the seminiferous tubules contains peritubular macrophages and myoid cells. The peritubular macrophages differ significantly from the interstitial macrophages in expression of cell markers, response to external stimuli, shape, functions and are derived from different waves of recruitment (Lokka *et al.,* 2020, Mossadegh-Keller *et al.,* 2017). Additionally, peritubular macrophages express elevated levels of major histocompatibility complex class II (MHCII) antigens, and hence one of their roles is predicted to be to act as antigen-presenting cells to regulatory T cells (T_{reg} cells) to protect the developing sperm from antigen-specific immune responses (Welsh *et al.,* 2009, Tung *et al.,* 2017).

Other monocyte-derived cells, specifically dendritic cells, which may or may not have a common lineage (dendritic cells can also develop from specific myeloid and lymphoid DC precursors in the bone marrow and circulation), are distinct from testicular macrophages with less efficient phagocytic properties, but they are more highly effective APCs (Fig. 4) (Banchereau and Steinman, 1998). Lymphocytes are more densely distributed in the rete testis and adjacent areas than in the remainder of the interstitium of all species investigated (Ritchie *et al.,* 1984). Lymphocytes make up about 10-20% of the total leukocyte population in the rat and human testis (Hedger and Hales, 2006) and mainly comprise T cells (both $CD4^+$ and $CD8^+$) and NK cells, but not B cells in normal mouse, rat and human testis (Ritchie *et al.,* 1984). Their

numbers increase significantly during inflammation and infectious conditions and some T-cells become memory T-cells in order to respond to the same antigen more rapidly in their next encounter. Moreover, there is evidence of increased numbers of intratesticular lymphocytes in men with infertility and sperm autoimmunity (El-Demiry *et al.,* 1985). In contrast to T cells, which are part of the adaptive immune system, NK cells have functions in innate immunity and provide protection against viruses and tumour formation. Interestingly, a significant proportion of NK cells in the testis are NK T cells (Hedger and Hales, 2006), which typically play a major role in controlling graft rejection responses (Sonoda *et al.,* 2001).

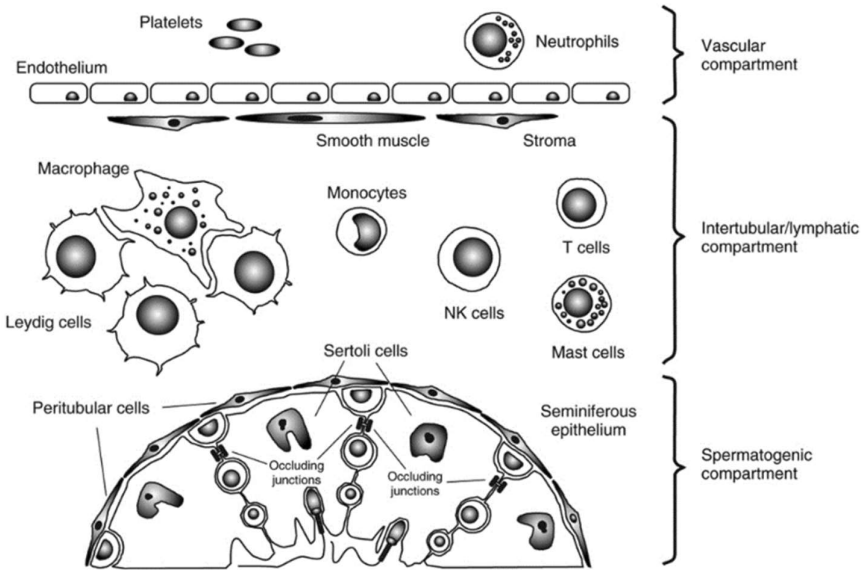

Figure 4: *Distribution of testicular cell types in the vascular, interstitial and spermatogenic compartments (Figure adapted from Hedger and Hales, 2006)*

1.3.1 Immune responses, inflammation, and fibrosis

Immune privilege is defined as the protection of the spermatogenic cells from the host immune response, extending to tolerance of foreign tissue grafts placed within the testicular environment (Meinhardt and Hedger, 2011). Immune privilege of the testis first came to light from studies on prolonged allograft and xenograft survival within the testicular interstitium (Head *et al.,* 1983). In the testis, more mature germ cells possessing autoimmune antigens are separated from the immune cells of the interstitial tissue by the blood-testis barrier, which develops approximately two weeks postnatally in mice, coinciding with the onset of meiosis (Hintz and Goldberg, 1977). Macrophages have long been implicated in maintaining immune privilege in the testis

by possessing immunosuppressive properties. However, an immune-privileged environment does not mean that effective inflammatory or immune responses cannot occur (Hedger, 2015). Innate immunity, the first line of defense against infections, involves recognition of pathogen-associated molecular patterns (found on bacteria, virus, fungus and protozoa) by pattern recognition receptors, such as the toll-like receptors (TLRs). Several studies have demonstrated that macrophages, polymorphonuclear cells and NK cells, in particular, express the majority of these pattern recognition receptors and have the capability to initiate inflammation, thereby clearing pathogens and protecting the host (Hedger, 2011, Meinhardt and Hedger, 2011, Hedger, 2015).

Inflammatory conditions in the testis have been commonly studied by using bacterial lipopolysaccharide (LPS), a toll-like receptor 4 (TLR4) ligand or uropathogenic *E. coli* (UPEC) and various experimental auto-immune orchitis (EAO) models in mice and rats. Recognition of LPS by TLR4 on these cells trigger inflammatory signaling pathways involving mitogen-activated protein (MAP) kinases and the inflammatory transcription factor, nuclear factor kappa B (NF-κB). As a result, pro-inflammatory genes including IL1α and β, IL6, inducible nitric oxide synthase (NOS2) and the immunoregulatory cytokine, activin A, are secreted (Bhushan *et al.,* 2015, Winnall *et al.,* 2011a, Hedger and Hales, 2006). These typically inflammatory molecules are also involved in regulation of mitosis, meiosis, and maintenance of Sertoli cell tight junctions and various stages of seminiferous epithelium. Ultimately, production of these molecules by immune cells, either resident or in circulation, can disturb the normal functions of the seminiferous epithelium and spermatogenesis (Hedger *et al.,* 2011).

Acute infection leads to fibrosis of the testis that involves disruption of blood–testis barrier, thickening of the lamina propria, and atrophy of seminiferous tubules. Additionally, the number of immune cells, including $CD4^+$, $CD8^+$, T cells, T_{regs}, macrophages, dendritic cells, mast cells and, depending on the etiology, neutrophils, B cells and plasma cells increases and androgen production is impaired, both in rodents and men (Fijak *et al.,* 2018). Key elements of adaptive immunity involve the effective processing and presentation of antigens to immune cells that is mediated by MHC class I (MHCI) molecules present on most cell types and MHC class II (MHCII) molecules on the surface of macrophages and dendritic cells. These MHCI and MHCII

molecules deliver short antigenic peptides to the cell surface allowing them to be recognized by $CD8^+$ (cytotoxic) and $CD4^+$ (helper and regulatory) T cells, respectively (Kotsias *et al.,* 2019, Roche and Furuta, 2015). These peptides may originate from endogenous (e.g., self-antigens) or external sources (e.g., infectious pathogens). During this process of antigen presentation, co-stimulatory molecules expressed by APCs (CD80, CD86 and other B7 family members) and T- cells (CD28 and CTLA-4) play an important role through surface ligand-receptor interactions (Kotsias *et al.,* 2019, Roche and Furuta, 2015).

1.4 Macrophage polarization and functions in general

In general, tissue-resident macrophages can originate from the yolk sac, fetal liver, and hematopoietic stem cells in bone marrow during development and have tissue-specific functions upon maturation (Schulz *et al.,* 2012). Macrophages of the brain (microglia) originate from the yolk sac; Langerhans cells of skin, alveolar macrophages of lung, Kupffer cells of liver and heart macrophages originate from both fetal liver and yolk sac, whereas those from intestine, dermis of skin and lamina propria in lung originate from the mononuclear phagocytic lineage (Schulz *et al.,* 2012). Macrophages have several functions in common, including expression of markers of the mononuclear phagocyte (i.e., macrophage and monocyte-derived dendritic cell) lineage, mobility, phagocytic and bactericidal properties, tissue-restructuring capacity, and the ability to present antigen to $CD4^+$ T cells (either T_{reg} or T helper cells), which are the master regulators of antigen-specific immune responses. However, macrophages differ widely in their patterns of cytokine secretion, proteases, and other bioactive secretions in different tissues (Rutherford *et al.,* 1993). Moreover, they also differ in their functional polarization status in different tissues. Macrophages can be broadly classified as pro-inflammatory (M1) or anti-inflammatory/tolerogenic (M2). Generally, M1 macrophages sustain inflammatory responses by secreting pro-inflammatory cytokines and recruit new macrophages to the inflamed tissue, whereas M2 macrophages are resolve inflammation, phagocytose apoptotic cells and release anti-inflammatory mediators (Pace *et al.,* 1983, Stein, 1992). These macrophage phenotypes differ in the metabolic signatures that help them to regulate lipid and amino acid metabolism and affect their responses and their tissue-specific functions (Jha *et al.,* 2015, Meiser *et al.,* 2016). Pro-inflammatory macrophages rely mainly on glycolysis and have a deficient TCA cycle resulting in accumulation of itaconate and

succinate. Conversely, anti-inflammatory macrophages have elevated oxidative phosphorylation (OXPHOS), and their TCA cycle is intact, thus continuing the electron transport chain (ETC) (Jha *et al.,* 2015, Meiser *et al.,* 2016). Pro-inflammatory macrophages are induced by microbial pattern recognition receptor ligands, such as LPS, or pro-inflammatory cytokines, such as IFNγ or TNF, and typically are characterized by their ability to kill pathogens and present to T-cells through expression of CD80, CD86, MHCII and other B7 family receptors (Mosser and Edwards, 2008, Chen *et al.,* 1995). Conversely, anti-inflammatory macrophages generally are induced by IL-4 or IL-13, express the mannose receptor CD206 (encoded by *Mrc1* gene) and produce anti-inflammatory and pro-fibrotic factors, such as TGF-β/activin and insulin-like growth factor 1 (IGF-1), thus actively suppressing inflammation and promoting repair (Mantovani *et al.,* 2013, Stein, 1992).

Maturation of macrophage function is regulated by the cytokines CSF1 (M-CSF) and CSF2 (GM-CSF), and recruitment of macrophages into tissues is stimulated by chemokines. In the rat testis, CSF1 and the chemokines, monocyte chemoattractant protein 1/CCL2 and fractalkine/CX_3CL_1, regulates macrophage recruitment and activity (Winnall and Hedger, 2013). The normal rat testis expresses high levels of CSF1 and low CCL2 (Gerdprasert *et al.,* 2002). However, LPS treatment *in vivo* increases CCL2 levels in Leydig cells, peritubular cells, and testicular macrophages (Gerdprasert *et al.,* 2002). According to Sierra-Filardi and colleagues, bone marrow-derived macrophages (BMMs) matured with CSF1 are inclined towards M2 polarization by producing high levels of CCL2, producing the anti-inflammatory cytokine IL-10 in response to LPS (Sierra-Filardi *et al.,* 2014).

1.4.1 Origin and phenotypes of testicular macrophages

Macrophages in the testis, similar to the other organs of the body, are potent immunoregulators and thereby control inflammatory responses. They are present in relatively low numbers following birth, but increase in number during sexual maturation (Head and Billingham, 1985). Testicular macrophages play an important role in tissue development, vascular remodeling, and organogenesis in postnatal organs, in addition to their basic phagocytic and bactericidal functions. In the developmental stages between E11.5-E12.5 in the mouse, macrophages play a critical phagocytic role by engulfing germ cells that do not migrate into the gonads and are retained in the mesonephros (DeFalco *et al.,* 2014). This observation is supported by the finding that

Sertoli cells are never found outside cords after E12.5 in normal mice, whereas a macrophage-depleted model had visible clusters of Sertoli cells in the interstitium at this time (DeFalco *et al.,* 2014). This suggests that macrophages regulate Sertoli cell function from an early age. Moreover, there are indications of macrophages playing an important role in testis cord morphogenesis by regulating vascularization (DeFalco *et al.,* 2014).

Testicular macrophages are heterogeneous in their distribution, phenotype, and function (Gerdprasert *et al.,* 2002a). There are two major populations of testicular macrophages, based on their location within the tissue. In addition to the typical tissue-resident macrophages within the interstitium, testicular macrophages with stellate-like appearance reside in the peritubular region along with myoid and other peritubular cells near the basement membrane of the seminiferous tubule in adults (De Falco *et al.,* 2015). In the mouse, interstitial macrophages are principally derived from embryonic progenitors, while peritubular macrophages originate from bone marrow hematopoietic stem cells after birth (Mossadegh-Keller *et al.,* 2017). They both differ in shape and size, marker expression, putative functions, transcriptional activity, and their anatomical location (Mossadegh-Keller *et al.,* 2017). The interstitial macrophages are physically associated with Leydig cells through cell-to-cell interdigitations (Miller *et al.,* 1984, Hutson, 2006). They produce 25-hydroxycholesterol, which is a precursor for testosterone biosynthesis. On the other hand, the peritubular macrophages are known to participate in the regulation of spermatogonial development and spermatogenesis: transient depletion of these macrophages resulted in disrupted spermatogonial differentiation in a mouse model (Mossadegh-Keller *et al.,* 2017, DeFalco *et al.,* 2015). Murine testicular macrophages can be identified based on expression of marker molecules, including the cell adhesion molecules, F4/80 and the integrin CD11b, and the fractalkine receptor, CX3CR1, but are mostly negative for CD11c (dendritic cell marker) and Ly6c (marker for monocytes) (Mossadegh-Keller *et al.,* 2017, Bhushan and Meinhardt, 2017). Interstitial macrophages are characterized by the marker expression pattern of $CD64^{+}CSF1R^{+}MerTK^{+}MHCII^{low}$, while peritubular macrophages are identified by $CD64^{-}CSF1R^{-}MerTK^{-}MHCII^{high}$, where MER proto-oncogene tyrosine kinase (MerTK) is an indicator of reduced phagocytic function (Mossadegh-Keller *et al.,* 2017, Bhushan and Meinhardt, 2017). These two macrophage populations can be further distinguished on the basis of expression of

genes for anti-inflammatory cytokines *Il10* and *Marco* (interstitial macrophages) and *Il1β* (peritubular macrophages) (Mossadegh-Keller *et al.,* 2017).

1.4.2 Macrophage function in testicular homeostasis

In addition to protecting the developing germ cells, testicular macrophages perform classical macrophage functions related to homeostasis, including phagocytosis of pathogens and apoptotic cells and chemotaxis for leukocyte migration and recruitment, tissue remodeling, connective tissue degradation (proteases) and synthesis [production of extracellular matrix (ECM) components] (Wang *et al.,* 2017, DeFalco *et al.,* 2014). Additionally, they play important roles in regulating steroidogenesis and spermatogonial development. Testicular macrophages have been shown to produce 25-hydroxycholesterol, a cholesterol precursor for testosterone biosynthesis, thereby stimulating Leydig cell steroidogenesis, proliferation and differentiation during development and recovery after damage (Gaytan *et al.,* 1994, Cohen *et al.,* 1996, Nes *et al.,* 2000). The number of spermatogonia was reduced upon macrophage ablation in the adult mouse testis, probably due to defects in differentiation or proliferation of spermatogonia (DeFalco *et al.,* 2015). Testicular macrophages express the enzymes ALHD1A2 and RDH10 for retinoic acid (RA) synthesis, and RA induces differentiation of spermatogonia as well as entry into meiosis (DeFalco *et al.,* 2015, Hogarth and Griswold, 2010). In the neonatal testis, macrophages have been implicated to play a role in testicular vascularization and spermatic cord formation, thus helping in normal organ development (DeFalco *et al.,* 2014).

1.4.3 Testicular macrophage functions during inflammation

In biopsies of patients with idiopathic infertility, disrupted spermatogenesis is frequently associated with leukocytic infiltrates and fibrosis (Schuppe and Meinhardt, 2005). Moreover, testicular macrophages increase in ‘Sertoli cell only’ syndrome patients and in acute orchitis (Fijak *et al.,* 2011, Schuppe and Meinhardt, 2005). Inflammation induced by LPS also causes a decline in testosterone levels and Leydig cell function (O’Bryan *et al.,* 2000). Acute orchitis caused by uropathogenic *E. coli* (UPEC) in mice resulted in increased testicular macrophage numbers and cytokine expression accompanied by low testosterone and disrupted spermatogenesis (Bhushan *et al.,* 2011). Fijak and colleagues reported massive germ cell loss,

inflammation, and testicular fibrosis in an EAO rodent model (Fijak *et al.,* 2011). Interestingly, supplementation of testosterone or the anti-inflammatory drug, ethyl pyruvate, reduced inflammation and macrophage numbers in this model. Moreover, LPS-induced inflammation in rats reduced the production of several pro-inflammatory cytokines and enzymes: TNF, IL-1β, IL-6, CCL2 and NOS2 (Gerdprasert *et al.,* 2002a, Gerdprasert *et al.,* 2002). Another example of testicular damage related to inflammation is the aromatase-overexpressing ($AROM^+$) transgenic mouse that is infertile and has a phenotype characterized by chronic inflammation with large numbers of $CD68^+$ macrophages (Li, 2009).

Bacterial (*E. coli* or *Klebsiella* sp.) or viral infections (HIV-1, Zika virus and mumps orthorubulavirus) are frequent causes of inflammation in the human testis (Le Tortorec et al., 2020, Pleuger et al., 2020). Macrophage numbers increase during inflammation, as observed following acute LPS stimulation or UPEC-induced epididymo-orchitis in rodent models (Gerdprasert *et al.,* 2002, Bhushan *et al.,* 2011, Klein *et al.,* 2020). In the mouse model, inflammation resolves at day 31 after an initial influx of $Ly6G^+$ neutrophils, $F4/80^{lo}CD11b^{hi}$ inflammatory macrophages and $Ly6C^{hi}CD11b^{hi}$, thus showing a remarkable ability of the testicular macrophages and testis to resolve inflammation (Wang *et al.,* 2021, Nicolas *et al.,* 2017).

Differential activation of inflammatory pathways in testicular macrophages provides a rationale for their subdued inflammatory capacity. Our research group has previously shown that immune response of testicular macrophages is skewed towards an alternatively activated phenotype in rats when treated with both classical (LPS and IFNγ) or alternative (IL-4) activation ligands (Winnall *et al.,* 2011a). Bhushan and colleagues showed that, compared to peritoneal macrophages in rats, isolated testicular macrophages express low levels of mRNA for TLR and NF-κB signaling pathway genes, such as CD14, MD2, Toll/IL-1R domain–containing adaptor-inducing IFN-b (TRIF), TRAM (TRIF-related adaptor molecule), MAL, TNFR-associated factor 6 and TAK1 (Bhushan *et al.,* 2015). Additionally, TLR4 protein was marginally detected, whereas the expression of SARM (negative regulator of TLR3 signaling) and RP105 (negative regulator of MD2/TLR4 signaling) were significantly higher (Bhushan *et al.,* 2015). Moreover, IκBα degradation was blocked in LPS-treated testicular macrophages. In fact, testicular macrophages showed the characteristics of regulatory macrophages by expressing lower levels of nitric oxide (NO), pro-inflammatory

cytokine IL-12 and higher levels of IL-10 (Bhushan *et al.,* 2015). Several groups have shown potential roles of prostaglandins, androgens, corticosterone, and CSF1/CSF2 in maintaining this immunoregulatory phenotype. Testicular interstitial fluid contains remarkably high concentrations of prostaglandins PGE2, PGI2, PGD2, and PGF2α, with Sertoli cells, Leydig cells, peritubular myoid cells and testicular macrophages as the main production sites in the testis (Frungieri *et al.,* 2015, Carpenter, 1974, Winnall *et al.,* 2007). Prostaglandins are implicated in polarization of macrophage phenotypes by inhibiting TNF production, and upregulating IL-10 via the cAMP-CREB signaling pathway (MacKenzie *et al.,* 2013, Harris *et al.,* 2002). Moreover, it has been established that testosterone has immunosuppressive properties and attenuates the development of EAO in mice (Meinhardt *et al.,* 2018). In addition, testosterone treatment suppressed the NF-κB signaling pathway by delaying IκBα degradation upon LPS induction in rats, with decreased production of proinflammatory cytokines (Wang *et al.,* 2017). The same study also showed that corticosterone in the testicular interstitial fluid (TIF) is an important autocrine regulator in maintaining testicular macrophage function and phenotype. Corticosterone belongs to the glucocorticoid family of steroid hormones and elicits a wide range of biological effects, including immunosuppressive and anti-inflammatory actions (Slominski *et al.,* 2020, Ahmed *et al.,* 2019). Recently, Zhang and colleagues showed that activation of AMP-activated protein kinase (AMPK), a master regulator of cellular and systemic energy homeostasis, facilitates macrophage differentiation to an anti-inflammatory phenotype (Zhang *et al.,* 2020).

1.4.3.1 Experimental auto-immune orchitis models and the role of macrophages

Experimental autoimmune orchitis in rodents is a well-established model of human chronic testicular inflammation (Tung and Teusher, 1995). EAO is characterized by production of testicular autoantibodies, elevated inflammatory mediators, including TNF and activin A, interstitial leukocytic infiltration, severe lesions of the seminiferous tubules, fibrosis, and germ cell apoptosis, resembling the histopathology of some cases of human idiopathic spermatogenic disturbance (Fijak *et al.,* 2018). In 1987, Tung and his colleagues showed that active and passively induced EAO in mice had different effects on macrophages populations and their probable functions (Tung *et al.,* 1987). In active EAO, mice were immunized with mouse testicular homogenate in Complete Freund's adjuvant (CFA) containing *Mycobacterium tuberculosis*, followed

by an i.p injection of *Bordetella pertussis*, whereas in passive EAO (i.e., adoptive transfer of EAO), single cell suspensions of regional lymph node and spleen cells were stimulated with irradiated syngeneic spleen cells and mouse testis homogenate and then transferred into untreated syngeneic recipients. Passive EAO and active EAO were found to differ in the predominant locations of involvement in the male gonad. In passive EAO, the straight tubules, rete testis, and ductuli efferentes were the predominant initial sites of inflammation in addition to intralymphatic granulomata in the subcapsule. In contrast, orchitis affecting the seminiferous tubules closest to the capsule was a more common early lesion in active EAO. In this study, rete testis and subcapsule showed increase in F4/80$^+$ macrophages, of which 30% were MHCII in normal testis, which further increased 10-20-fold in mice immunized with TH, CFA or pertussis extract on day 5. Another study by Itoh and colleagues showed that immunization of a susceptible mouse strain with syngeneic testicular germ cells alone could induce lymphocytic inflammation of autoimmune origin without the use of any adjuvant (Itoh *et al.,* 1991). In this model, the lymphocytic infiltration started around the tubuli recti, later spreading to the seminiferous tubules (Itoh *et al.,* 1995). These studies indicate that the rete testis and the efferent ducts are the special regions in the germ cell compartment of the testis where transferred T cells most readily encounter target antigens and highlight these regions and the subcapsular region as susceptible sites for initiation of orchitis.

1.5 Sertoli cells and the transforming growth factor-β (TGF-β) superfamily

The canonical TGF-β family of cytokines comprises three homodimeric proteins in mammals (β_1, β_2, β_3) (Hedger and Hales, 2006). They are widely expressed, and are implicated in development, tissue remodeling and immunoregulation in the testicular environment. In the testis, they are produced principally by Sertoli cells; however, they are also produced by peritubular cells and Leydig cells in fetal and premature testis, although their production decreases considerably during sexual maturation (Avallet *et al.,* 1994). In the postnatal testis, they also have been localized to the spermatogenic cells in a development-specific pattern of expression (Hedger and Hales, 2006). The receptors for TGF-β are found in both spermatogenic and somatic cells. TGF-β_1 and TGF-β_2 are known to regulate apoptosis in gonocytes (precursor germ cells responsible for production of spermatogonial stem cells), but not in Sertoli cells and Leydig cells (Olaso *et al.,* 1998). Moreover, they are postulated to regulate the

development of Leydig cells from immature to adult rats by inducing the expression of extracellular matrix proteins (Dickson *et al.,* 2002). In addition, TGF-β_3 appears to play a crucial role in opening and closing the blood-testis barrier by regulating Sertoli cell tight junction dynamics (Lui *et al.,* 2003).

1.5.1 Activin and follistatin biology

Activins belong to the TGF-β superfamily owing to their structural and sequence similarity (Ling *et al.,* 1986). They were first isolated for their capacity to release follicle stimulating hormone (FSH) from the anterior pituitary gland and were initially named as the 'FSH releasing protein'. Activins are disulfide-linked homodimers of the β subunits of the FSH-inhibiting hormone, inhibin, forming activin A ($\beta_A\beta_A$) and activin B ($\beta_B\beta_B$) (Vale *et al.,* 1986). Other activin subunit homodimers that lack the capacity to regulate FSH have been found: activin C (Hotten *et al.,* 1995) activin D (Oda *et al.,* 1995) and activin E (Fang *et al.,* 1996), as well as heterodimers of the activin subunits, but activin A and activin B have been most studied. They are synthesized as inactive dimeric precursors, which dissociate to their active form on release, unlike other TGFβ family members, that require enzymatic or acid hydrolysis for activation (Gray and Mason, 1990, Walton et al., 2012). Inhibins are heterodimers of a structurally-related α-subunit (encoded by the *Inha* gene) and one of the β-subunits linked with disulphide bond (encoded by the *Inhba* or *Inhbb* genes), forming inhibin A ($\alpha\beta_A$) and inhibin B ($\alpha\beta_B$), respectively (Ling *et al.,* 1986, de Kretser and Robertson, 1989). Inhibins are competitive antagonists of the activins. Another inhibitor of activin bioactivity is follistatin, the activin-binding protein, which does not share structural similarity to the activins (Robertson *et al.,* 1987). Follistatin is a monomeric protein of either 315 or 288 amino acids, produced by alternative mRNA splicing, known as FST288 and FST315, respectively (Inouye *et al.,* 1991, Shimasaki *et al.,* 1988). The former is predominantly tissue-bound because it binds to heparan sulphates on cell surfaces, whereas the heparan-binding site of FST315 is physically obstructed, and it is able to circulate freely in the blood (Sugino *et al.,* 1993). Follistatin is a high-affinity binding protein for the activins, and reportedly has a higher affinity for activin A than for activin B. Binding of activin to FST288 or FST315 facilitates its internalization by cells mediated by cell surface heparan sulphates, which leads to lysosomal degradation of the activin-FST complex (Hashimoto *et al.,* 1997).

Both activins A and B act through a serine/threonine kinase receptor pathway similar to other TGF-β superfamily members (Fig. 5). In brief, activins bind to a Type II activin receptor (ACVR2A or 2B) on the surface of the target cell, which in turn binds and phosphorylates a Type I receptor. Activin A recruits the type I receptor Alk4 (ACVR1B), while activin B can recruit either Alk4 or Alk7 (ACVR1C) (Tsuchida *et al.,* 2004). As a result, activin B may have a broader spectrum of activity (de Kretser *et al.,* 2012). Binding of activin to its receptor induces SMAD intracellular proteins that act as signal transducers for the broader TGF-β superfamily. Receptor-regulated SMADs, SMAD-2 and/or 3, are phosphorylated by the Type I receptor, and form a transcription factor complex with the common partner (co)-SMAD, SMAD-4. This complex is translocated to the nucleus where it triggers target gene transcription to initiate cell division and apoptosis (Lin *et al.,* 2006). Activins can also activate MAP kinase pathways in inflammatory or infection states (Eramaa *et al.,* 1992). Mice with activin A or follistatin knockouts die at birth, consistent with the biological importance of these molecules during development (Matzuk *et al.,* 1995b, Matzuk *et al.,* 1995c).

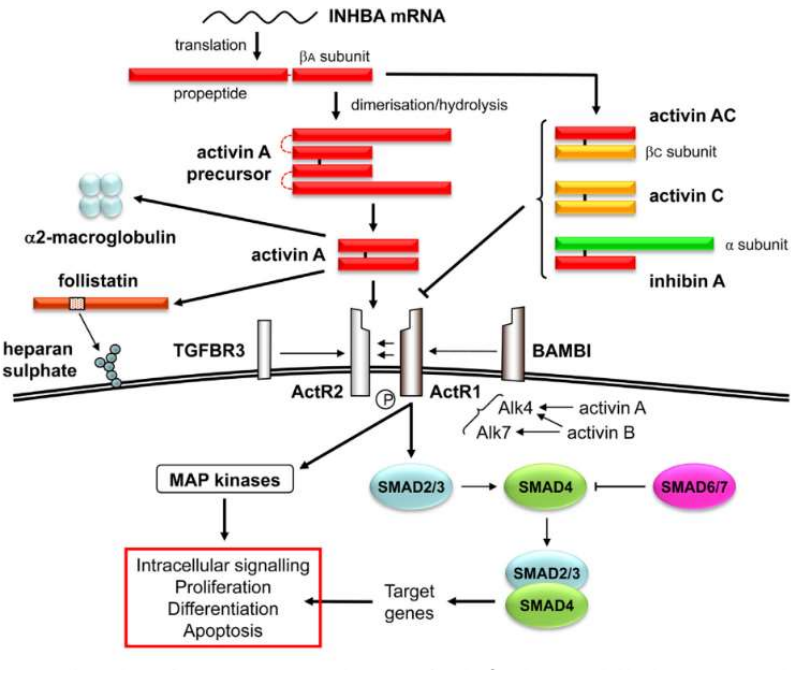

Figure 5: *The activin signaling pathway and its regulation. Activin binds to a receptor type II on a target cell surface, which binds and phosphorylates receptor type I. This leads to activation of intracellular proteins SMADs 2 and 3 forming a heteromeric transcription factor complex with SMAD4. This complex is transported to the nucleus*

to carry out functions such as cell division and apoptosis. Regulation of activin activity can occur through the action of binding proteins, such as follistatin and α2-macroglobulins, competitive inhibition by the α-subunit and βC-subunit to form inhibins and inactive activin dimers, or non-activating transmembrane receptors, such as BAMBI and TGFBR3 [figure adapted from Hedger and de Kretser, 2013].

In the testis, activins are produced by Sertoli cells, pachytene spermatocytes and round spermatids, and spermatogonia in the seminiferous tubules, myoid cells in the peritubular region and Leydig cells and macrophages in the interstitium of mice, rats, and human (Hedger *et al.,* 2011). Data suggests that Sertoli cells are the major production site of activins in the normal testis, but this has not been definitely established (Winnall *et al.,* 2011b, Winnall and Hedger, unpublished data). Outside the testis, activin A is abundant in myeloid lineage cells, such as dendritic cells and macrophages, epithelial cells, mast cells and stromal cells (Hedger and de Kretser, 2013). The βA and βB subunits are widely expressed, but α-subunits are mainly produced in the gonads and hence inhibins are abundant in gonads of mouse, rat, and human (Anderson *et al.,* 1998). Notably, rats have 10-fold higher levels of activin A in the testicular interstitial fluid than in the circulation (O'Bryan *et al.,* 2005).

Activins are involved in development and function of cells, including those of myeloid and lymphoid lineage (Hedger and de Kretser, 2013). Activin A is involved in regulation of embryogenesis, stem cell development, cell growth and survival, inflammation, fibrosis, immune cell development and regulation. While similar actions for activin B may be anticipated, the functional roles of activin B have not been well-studied to date. Activin C and activin E are found predominantly in the liver. However, they lack activin receptor signaling activity, and are believed to act as competitive antagonists to activin A and activin B, similar to the inhibins (Gold *et al.,* 2009).

1.5.2 The role of activins in testis function

Activin A is a local regulator of Sertoli cell proliferation and germ cell development. *Inhba*$^{-/-}$ mice lacking activin A have smaller testes and low Sertoli cell numbers when compared with their littermate controls at the day of birth (Mendis *et al.,* 2010). Moreover, they produce double the number of gonocytes. This disruption of the Sertoli cell: gonocyte ratio, resulting in testicular dysgenesis and ultimately failure in testicular cord formation, indicates the requirement for an appropriate balance in activin A levels

at early ages (Archambeault and Yao, 2010). Activin A and activin B also regulate the proliferation of spermatogonia (Mather *et al.,* 1990, Kaur *et al.,* 2014). Metallothionein-I follistatin (MT-FS) transgenic mice having high follistatin and low activin levels showed spermatogenic arrest and hence infertility, demonstrating the importance of maintaining the right balance of activins in the reproductive tract (Guo *et al.,* 1998).

During the normal seminiferous tubule cycle, activin A levels increase during stage VIII, coinciding with the release of mature sperm into the seminiferous tubule lumen (Okuma *et al.,* 2006). Activins are known to play a role in reorganizing the inter-Sertoli cell tight junctions, which occurs after stage VIII when spermatocytes need to cross the blood-testis barrier (Hedger and Winnall, 2012). Additionally, expression of activin receptor ACVR2B increases in type A spermatogonia and Sertoli cells at stage IX-XI of seminiferous cycle, when activin A peaks, while ACVR2A expression is low (Matzuk *et al.,* 1995a). The transgenic mouse model of *Inhba*$^{BK/BK}$, which has increased expression of activin B and reduced activin A, displays reduced testis size, delayed maturation of type A spermatogonia into spermatocytes and hence delayed onset of fertility. In contrast, *Inhbb*$^{-/-}$ mice have normal testicular weight and are fertile. Hence, it seems that activin A is more essential than activin B for proper functioning of testicular mechanisms (Vassalli *et al.,* 1994).

1.5.3 Regulation of activins in the testis

Activin production and its activity are regulated at multiple levels. As mentioned earlier, inhibins and follistatin are key regulators of activin activity. In addition, membrane bound co-receptors such as BAMBI and the TGF-β receptor type 3 (TFGBR3/ betaglycan), or serum carrier proteins, such as the α2-macroglobulins, are reported to play an important role in regulation of activin activity at the cell surface (Hedger and de Kretser, 2013). BAMBI and TGFBR3 are transmembrane proteins that are homologous to type 1 activin receptors and hence interfere in interaction of activin and its receptors (Fig. 5). However, they lack the intracellular kinase domain required for signaling and thereby block the signaling cascade (Barbara *et al.,* 1999). Regulation of activin activity can occur through concurrent production of the inhibin α-subunit or β_C subunit, which form non-activating dimers with the β_A and β_B subunits that compete for the activin receptor complex. Inhibin A and inhibin B bind to the ACVR2 activin cell surface receptors and prevent its dimerization with type 1 receptors through the activity of TGFBR3 (Mathews and Vale, 1991). Follistatin has affinity to activins similar to the

affinity of activin to its receptors. Both isoforms of follistatin attach to cell surfaces and remove activins by a lysosomal degradation pathway (Hashimoto *et al.,* 1997).

1.5.4 Activins in immunoregulation and inflammation

It is increasingly evident that the activins play an important role in maintaining this immunoregulated environment. Levels of activin A increase at sites of inflammation in many clinical diseases and models of inflammatory disease, and inhibition of activin by treatment with follistatin, or other antagonists of activin action, is able to ameliorate inflammation and its sequelae in many disease models (Hedger *et al.,* 2011). This role of activin A involves the regulation of macrophage activation and development, which leads to an increase of pro-inflammatory cytokines, including IL-1β and TNF (Yamashita *et al.,* 1993). As shown in figure 6, monocytes can differentiate into an activated macrophage or a dendritic cell under the influence of activin A (Hedger *et al.,* 2011). An activated macrophage induces inflammation in the testis by secreting pro-inflammatory cytokines or into an M2 macrophage leading to tissue repair or fibrosis. On the other hand, dendritic cell differentiation can lead to either antibody-mediated immunity/ allergy/ tolerance or cell-mediated immunity/ autoimmunity/rejection.

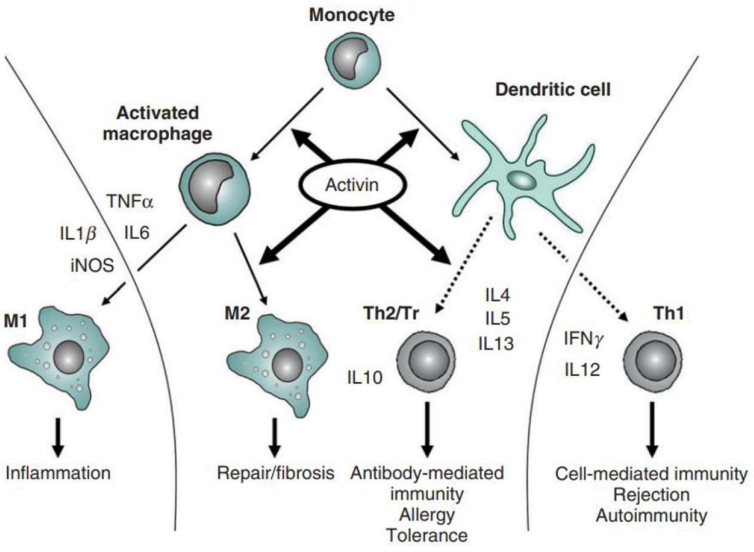

Figure 6: *Schematic of the effects of activin A on immune responses. Activin A promotes immune responses by modulating the differentiation of monocytes towards dendritic cells or activated macrophages. In activated macrophages, activin A regulates the immune response towards the M2 phenotype while inducing a Th2/Tr*

response in T cells. IFNγ: interferon gamma; IL1β, 4, 5, 6, 10, 12, 13: interleukin 1 beta, 4, 5, 6, 10, 12, 13; iNOS: inducible nitric oxide synthase; TNFα: tumor necrosis factor; Th1, 2: T helper cell 1, 2; Tr: regulatory T cell (Hedger et al., 2011); with the permission of the publisher, license number: 5184551193188).

Recently, activin A deficiency has been shown to reduce total macrophage numbers in the testicular compartments (see thesis chapter 2; Biniwale *et al.,* 2022). Activin A induces regulators of fibrosis and is a stimulator of fibroblast and mast cell development (Funaba *et al.,* 2003). On the other hand, extended exposure to activin A results in release of anti-inflammatory cytokines and an anti-inflammatory phenotype of macrophages and stimulates the development of T_{reg} cells (Huber *et al.,* 2009). Furthermore, activin A stimulates the development of dendritic cells, but restricts maturation of T cells by dendritic cells (Robson *et al.,* 2008). It also regulates polarization of macrophages towards the M1 and M2 subsets (Ogawa *et al.,* 2006). Additionally, activin A stimulates development of antigen-specific immune suppressor T_{reg} cells (Huber *et al.,* 2009), whereas it directly or indirectly inhibits peripheral T cell development by producing pro-inflammatory cytokines and inducing apoptosis of B cells (Brosh *et al.,* 1995, Kaur *et al.,* 2014). The levels of activin increase in acute and chronic inflammation. Interestingly, inhibition of activin reduces inflammation, sepsis, fibrosis and even reduces mortality rates in these conditions (Hedger and de Kretser, 2013). Various reports indicate the activation status of the immune cell and the duration of exposure is responsible for the switch between pro-inflammatory or anti-inflammatory roles of activins (Hedger and de Kretser, 2013). Thus, activin is an immunoregulatory cytokine in normal as well as inflamed conditions, and its role in regulating these processes in the testis needs to be determined.

1.6 Summary and Conclusions

Activins have complex effects on the macrophage function and early inflammatory events, but also induce the development of anti-inflammatory/tolerogenic M2 responses in macrophages. Interestingly, the effect of activin on macrophage development is complex and can lead to either M1 or M2 polarization depending upon other influences in the environment. The factors and pathways responsible for the alternate activation of macrophages in the testis involving activins has not been studied in detail to date. The altered levels of activin and follistatin in experimental mouse models can provide insights into the respective roles of activins in maintaining

the unique phenotype of the testicular macrophages and pathways responsible for their maintenance.

1.7 Research aims

Activins are known to play an important role in maintaining the immune environment of many tissues and are involved in the recruitment, maturation, and activation of macrophages (Chen and Ten Dijke, 2016). Activin A has both pro-inflammatory and anti-inflammatory/tolerogenic activities and has differential effects on macrophage function based on their activation status and the dose and length of exposure (Hedger *et al.,* 2011). The **first aim** of the project was to investigate regulation by activin of the number and distribution of macrophages in different compartments of the adult testis using the classical macrophage marker F4/80, in mice with reduced levels of either activin A or follistatin. Gene transcripts involved in macrophage regulation and function were also measured in comparison with those of other testicular somatic cells.

Interstitial and peritubular macrophages in the parenchyma of the testis are the most studied macrophage populations in the testis, whereas the macrophages in minor compartments of the testis, i.e., the rete testis, subcapsule and tunica albuginea have received less attention. The rete testis and subcapsule have been reported to be primary sites of inflammation in different experimental EAO models (Tung *et al.,* 2017). The **second aim** of the project was to study macrophage subsets in these minor compartments and understand their functions in normal, UPEC-infected and activin A deficient mice testes based on the results from aim 1. Additionally, $CD68^{+}$ macrophages in the adult human rete testis were qualitatively assessed compared with the mouse.

Our research group has previously shown that immune response of testicular macrophages is skewed towards an alternatively activated phenotype in rats when treated with both classical (LPS and IFNγ) or alternative (IL-4) activation ligands (Winnall *et al.,* 2011a). Additionally, rat testicular macrophages express low levels of adapter molecules (CD14, MD-2 and MyD88) required in the TLR4 signaling pathway as well as their inability to activate NF-κB signaling pathway upon stimulation TLR ligands LPS and poly (I:C) (Bhushan *et al.,* 2015). These studies only examined a selected subset of functional genes and proteins, and employed macrophage preparations that contained small, but significant, numbers of other testicular somatic

and germ cell types, which may have complicated the results. The **third aim** of the project was to isolate highly purified testicular macrophages from adult mouse testis and to investigate the functional profile of these macrophages in detail using multiplex RNAseq analysis, in order to identify critical pathways involved in their functional regulation.

Chapter 2: Regulation of macrophage number and gene transcript levels by activin A and its binding protein, follistatin, in the testes of adult mice

Published original manuscript: *Journal of Reproductive Immunology* 2022; 151, 103618

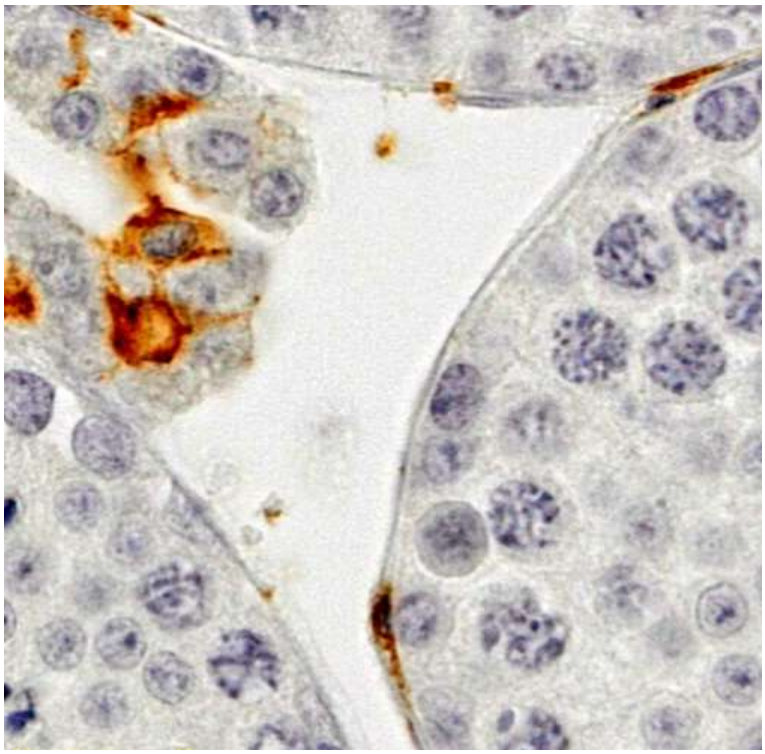

Journal of Reproductive Immunology 151 (2022) 103618

Contents lists available at ScienceDirect

Journal of Reproductive Immunology

journal homepage: www.elsevier.com/locate/jri

Regulation of macrophage number and gene transcript levels by activin A and its binding protein, follistatin, in the testes of adult mice

Sneha Biniwale [a,b,c,*], Rukmali Wijayarathna [a,b], Christiane Pleuger [c,d], Sudhanshu Bhushan [c,d], Kate L. Loveland [a,b], Andreas Meinhardt [a,c,d], Mark P. Hedger [a,b]

[a] Centre for Reproductive Health, Hudson Institute of Medical Research, Clayton, Victoria, Australia
[b] Department of Molecular and Translational Sciences, School of Clinical Sciences, Monash University, Clayton, Victoria, Australia
[c] Institute of Anatomy and Cell Biology, Justus-Liebig University Giessen, Giessen, Germany
[d] The Hessian Centre of Reproductive Medicine, Justus-Liebig-University, Giessen, Germany

ARTICLE INFO

Keywords:
Testicular macrophages
Activin A
Follistatin
Morphometry
Macrophage function

ABSTRACT

The cytokine activin A is expressed throughout testicular development and is a critical regulator of macrophage function, but its effects on the testicular macrophages are not well-defined. Macrophage distribution and gene transcript levels were examined in testes of adult mice with reduced levels of either activin A (*Inhba*$^{+/-}$), or its binding protein, follistatin (TghFST315). Macrophages were identified using F4/80 immunohistochemistry and enumerated by morphometry. Transcript levels were measured in testis extracts by qRT-PCR and Fluidigm ™ analyses. Interstitial macrophages were twice as numerous as peritubular macrophages in *Inhba*$^{+/-}$ and TghFST315 mice and their littermate controls. Macrophage numbers were significantly reduced in all regions of the *Inhba*$^{+/-}$ testis, and the volume density of peritubular and subcapsular macrophages was significantly reduced compared to littermate controls (by 52.9% and 36.3% respectively). Transcripts encoding macrophage chemokines, *Csf1* and *Ccl2*, and receptor *Csf1r*, were elevated (by 35%, 44% and 27% respectively) in *Inhba*$^{+/-}$ testes, but *Cx3cl1* and their receptors, *Cx3cr1* and *Ccr2*, were not altered. Transcripts encoding MHC class II antigens and the co-stimulatory molecule *Cd86,* also increased (by 32% and 60% respectively), but other co-stimulatory molecules *Cd80* and *Cd274*, and the scavenger receptor *Mrc1* (CD206), were unaffected. In the follistatin-deficient testes, macrophage numbers and most macrophage-specific transcripts were not significantly affected, but *Mrc1* expression was reduced by 35%. These data indicate that activin A maintains macrophage numbers, but selectively inhibits the levels of key transcripts associated with macrophage antigen-presentation, recruitment and differentiation in the adult mouse testis.

1. Introduction

Macrophages are the most abundant immune cells in the testicular interstitium. Testicular macrophages, like macrophages in other tissues, are potent regulators of immunity and inflammation (Hedger, 2015; Bhushan et al., 2020). They also perform testis-specific functions, regulating testicular development, steroidogenesis, the spermatogonial niche and retinoic acid biosynthesis (Defalco et al., 2015; Bhushan and Meinhardt, 2017; Tong et al., 2013), in addition to typical macrophage functions, such as homeostatic maintenance, tissue-remodelling, and the killing and phagocytosis of pathogens. Recent studies have shown that the tissue-resident macrophages in the murine testis are derived from several waves of hematopoiesis, initially arising from primitive yolk-sac macrophages, followed by fetal monocytes and later from nascent bone marrow-derived cells (Wang et al., 2021). In the absence of inflammation or endocrine disruption, they are largely self-maintaining with minimal replenishment from circulating monocytes (Lokka et al., 2020; Wang et al., 2021; Meinhardt et al., 2021).

Resident testicular macrophage populations have been identified by their localization as either interstitial or peritubular (Hume et al., 1984; Defalco et al., 2015), and are heterogenous in phenotype and function (Wang et al., 1994; Gerdprasert et al., 2002). In mice, although both of these populations express tissue-resident macrophage markers, including F4/80, CD11b and CX3CR1 (Defalco et al., 2015), they differ in expression of other myeloid cell markers, including colony-stimulating factor 1 receptor (CSF1R), major histocompatibility

* Correspondence to: Hudson Institute of Medical Research, 27-31 Wright Street, Clayton 3168, VIC, Australia.
E-mail address: Sneha.biniwale@monash.edu (S. Biniwale).

https://doi.org/10.1016/j.jri.2022.103618
Received 6 December 2021; Received in revised form 14 March 2022; Accepted 23 March 2022
Available online 26 March 2022

complex II antigens (MHCII) (Defalco et al., 2015) and CD64 (Gautier et al., 2012). Generally, CSF1/CSF1R signaling plays an important role in maintaining macrophage numbers and is responsible for their proliferation, maturation and differentiation (Chitu and Stanley, 2006). Macrophages can express MHCII, usually in conjunction with the co-stimulatory molecules, CD80 and CD86, to act as antigen-presenting cells (APCs) for T-cell activation (Gordon et al., 2014). While testicular interstitial macrophages are predominantly $CSF1R^{hi}CD64^{hi}MHCII^{-}$, peritubular macrophages are $CSF1R^{lo}CD64^{lo}MHCII^{+}$, indicating different functional roles (Defalco et al., 2015; Mossadegh-Keller et al., 2017). Interstitial macrophages also preferentially express CD206, a classical anti-inflammatory (M2) macrophage marker, which is absent on peritubular macrophages (Lokka et al., 2020).

Chemokine monocyte chemoattractant protein-1 (MCP-1/CCL2) is responsible for the recruitment of new macrophages to inflammation sites and to replenish the existing pool of macrophages, by increasing the expression of its receptor, CCR2 (Charo et al., 1994; Serbina and Pamer, 2006). In the testis, CCL2 is produced by Sertoli cells, Leydig cells, peritubular cells, endothelial cells, fibroblasts, and macrophages (Gerdprasert et al., 2002; Jiang et al., 2020).

Activins are members of the transforming growth factor-β (TGF-β) family of cytokines, which regulate development, tissue remodeling and immunoregulation (Wijayarathna and De Kretser, 2016). Activin A is produced by several cell types in the testis, particularly Sertoli cells, and is a regulator of Sertoli cell proliferation and germ cell development in fetal and post-natal life (Mithraprabhu et al., 2010; Mendis et al., 2011). Crucially, activin A is an important regulator of macrophage and dendritic cell development and function, and its endogenous binding protein, follistatin, has been found to be therapeutic in a number of inflammatory and immunological disease models (Hedger and De Kretser, 2013). Recently, our studies demonstrated that chronically-increased activin A levels further reduces MHCII expression by $CD206^{+}$ macrophages in the adult testis (Indumathy et al., 2020).

The aim of the current study was to investigate regulation by activin of the number and distribution of macrophages in different compartments of the adult testis using classical macrophage marker F4/80, using mice with reduced levels of either activin A or follistatin. Level of transcripts involved in macrophage regulation and function were also examined in comparison with that of other testicular somatic cells.

2. Materials and methods

2.1. Animals and tissue collection

Inhba$^{+/-}$ mice with 50% reduction in serum and testicular activin A transcript and protein levels, and their homozygous (*Inhba*$^{+/+}$) littermate controls, were produced as described previously (Matzuk et al., 1995a; Mendis et al., 2011; Wijayarathna et al., 2018b). Follistatin-deficient TghFST315 (*Fst*$^{h315/-}$) mice in which the endogenous *Fst* gene is replaced by a transgene encoding the circulating human follistatin isoform, FST315, and *Fst*$^{+/+}$ littermate controls were produced as described previously (Lin et al., 2008). Body weights of both *Inhba*$^{+/-}$ and TghFST315 adult mice are normal (Wijayarathna et al., 2017; Wijayarathna et al., 2018b). Serum total follistatin levels are reduced by more than 50% in the TghFST315 mice (Wijayarathna et al., 2017). Homozygous deletions of either *Inhba* or *Fst* are lethal at birth due to developmental defects, and were not available for analysis. Animal experiments at Monash University were conducted according to the National Health and Medical Research Council Code of Practice for the Care and Use of Animals for Experimental Purposes and approved by the Animal Ethics Committee of Monash Medical Centre. Transmission Electron Microscopy (TEM) studies were performed using adult C57BL/6 J mice at Justus-Liebig-University following Guidelines for the Care and Use of Laboratory Animals of the German law for animal welfare and the European legislation for the protection of animals for scientific purposes. All mice were between 8 and 10 weeks of age. Animals were euthanized using carbon dioxide overdose. Testes were collected and fixed in Bouin's solution for 5 h at room temperature for macrophage enumeration studies. Testes were punctured at both poles with a 23 G needle after 1 h for better penetration of the fixative and then incubated for 4 more hours. Tissues were washed with PBS three times to remove excess fixative, stored in 70% alcohol overnight at 4 °C and embedded in paraffin. Whole testes were snap-frozen and stored at − 80 °C until further processing for mRNA analysis.

2.2. Immunohistochemistry

Macrophages were localized in Bouin's-fixed, paraffin-embedded 5 μm thick whole transverse sections from the medial region of the testis using an antibody raised in rats against the macrophage-specific antigen, F4/80 (cat # MCA497G; Bio-rad Laboratories, Herculus, CA) (Hume et al., 1984; Defalco et al., 2015) in *Inhba*$^{+/+}$ (n = 6), *Inhba*$^{+/-}$ (n = 5), *Fst*$^{+/+}$ (n = 4) and *Fst*$^{h315/-}$ (n = 5) mouse testes. Heat-mediated antigen retrieval was performed in citrate buffer (pH 6.0) by boiling the sections at high power (800 watts) for one minute followed by the defrost cycle for 15 min. The slides were allowed to cool and then the sections were treated with 10% goat serum in Tris-buffered saline with 0.1% Tween-20 (TTBS) to block non-specific binding. Sections were incubated with the anti-F4/80 antibody at 1:100 dilution in 2.5% bovine serum albumin (BSA) in TBS in a humid chamber overnight at 4 °C. Negative controls were incubated with 2.5% BSA in 1X PBS alone. Staining was visualized using a biotinylated goat anti-rat secondary antibody (cat # BA-9401; Vector Laboratories, Burlingame, CA) at 1:300 for one hour in a humid chamber, followed by Vectastain Elite kit reagents (Vector Laboratories Inc., Burlingame, CA) at room temperature for 30 min. Diaminobenzidine (DAB) (Dako North America Inc., Carpinteria, CA) at 1:100 was added to the sections and colour development was monitored (10–20 min) under a wet-mount microscope. Sections were counter-stained with hematoxylin, cover slipped and mounted with DPX, and scanned using an Olympus VS120 brightfield slide scanner (Monash Histology Platform, MHTP) for imaging and macrophage quantification.

2.3. Macrophage enumeration strategy

Macrophages were counted using an established immunohistochemical morphometric technique to determine the volume density (Nv) of testicular macrophages in sections of constant thickness, as previously described (Wang et al., 1994). The scanned immunostained sections were analyzed using ImageJ with a cell counter plug-in (Schindelin et al., 2012). Briefly, between 100 and 200 visible nuclear profiles of F4/80 labelled cells (replicate numbers in Section 2.2, above) were counted in twenty-five equally-spaced grids of equal size (100,000 μm^2) across each transverse section. The mean nuclear diameter for each macrophage population was determined from the average of the longest and shortest axes of the nuclear profile of 10 randomly selected macrophage nuclei/section that were $F4/80^{+}$. In order to compensate for partial nuclear profiles at the periphery of the section, only the largest 30% of measurements was used to calculate the mean nuclear diameter. The testis parenchyma was divided into three compartments: intertubular interstitium (IT), seminiferous tubules (ST) and the subcapsular interstitial region (SC). Macrophages within the tunica albuginea were not counted, as this structure was not always completely retained. The total volume of the testis was estimated from testis weights, and the relative volumes of each compartment were determined by the point-counting method in each whole transverse section. Macrophage numbers were estimated from their volume density in sections of the whole testis (total) and compartments (Wang et al., 1994).

2.4. Transmission electron microscopy

Testes were collected and small pieces were fixed in 1.5% glutaraldehyde, 1.5% formaldehyde, 0.15 mol/L HEPES/KOH (pH 7.4) at 4 °C until embedding and sectioning. For epoxy resin embedding, samples were post-fixed in 1% osmium tetroxide in distilled water, stained in half-saturated watery uranyl acetate, dehydrated in an ascending ethanol series and finally embedded in Agar 100 (Agar scientific Ltd., Stansted, UK). Ultrathin sections were cut using an ultramicrotome and examined by TEM (Zeiss EM 902, Oberkochen, Germany). Digital images were captured with a slow-scan 2 K CCD camera (TRS, Tröndle, Moorenweis, Germany).

2.5. Quantitative RT-PCR and Fluidigm analysis

Snap-frozen tissues were homogenized using stainless steel beads and the Qiagen TissueLyser II (Qiagen GmBH, Hilden, Germany) in *Inhba*$^{+/+}$ (n = 6–9), *Inhba*$^{+/-}$ (n = 6–7), *Fst*$^{+/+}$ (n = 5–7) and *Fst*$^{h315/+}$ (n = 6–8) mouse testes. RNA extraction was carried out using the RNeasy mini kit (Qiagen GmBH) according to the manufacturer's instructions. On-column DNAse digestion was performed using DNase I (Qiagen GmBH). cDNA was synthesized using the Superscript III first-strand

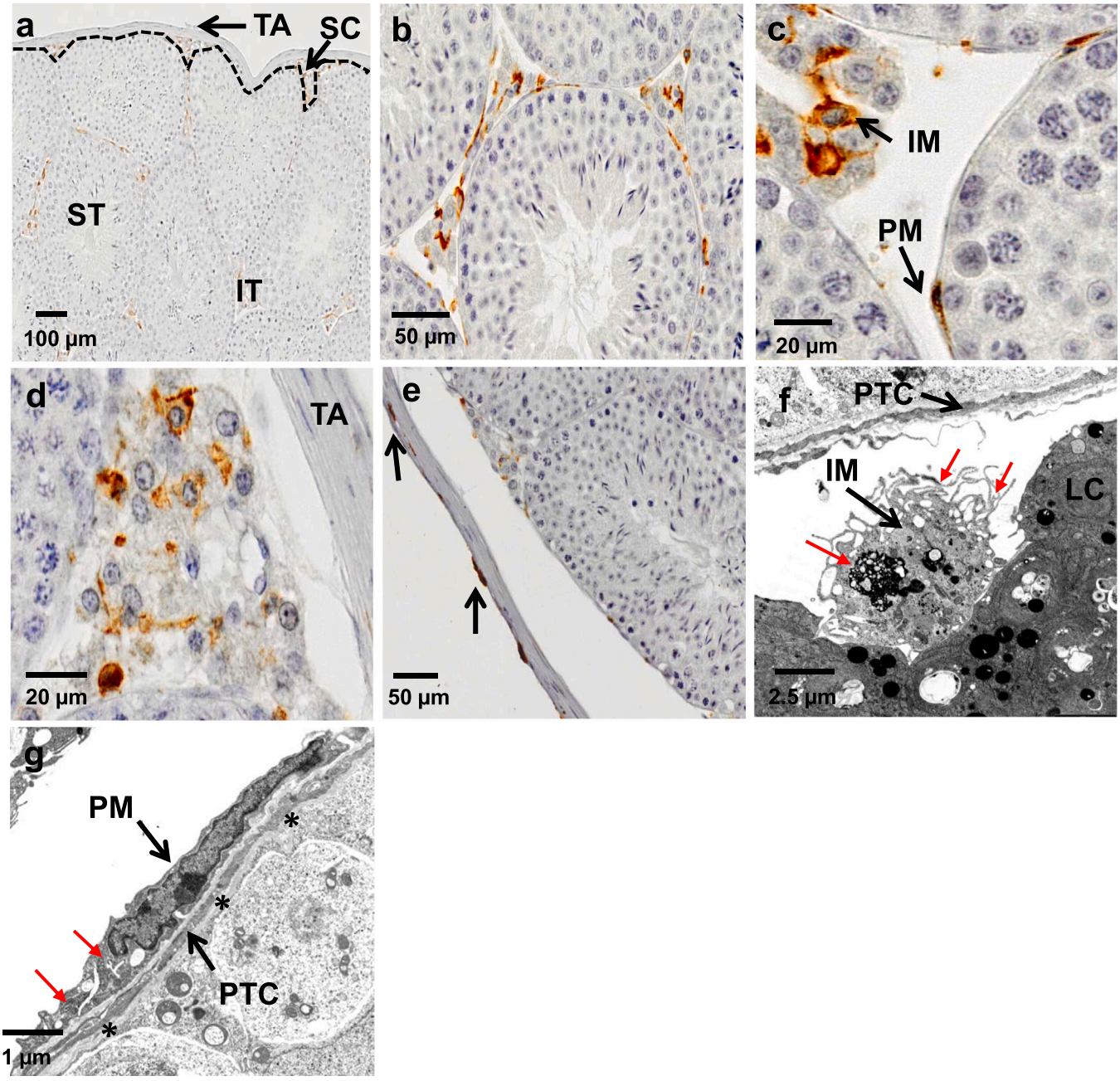

Fig. 1. Immunohistochemical staining of F4/80^{+} macrophages (brown signal) in the normal adult mouse testis: a) Based on the histology, the adult testis was compartmentalized into intertubular interstitial tissue (IT), seminiferous tubules (ST), subcapsular interstitial tissue (SC) and capsule/tunica albuginea (TA). b) Rounded interstitial macrophages (IM) and elongated peritubular macrophages (PM) were found throughout the parenchyma of the testis. c) Higher power micrograph of F4/80^{+} interstitial and peritubular macrophages in the intertubular interstitial and seminiferous tubule compartments. d) Macrophages in the subcapsular interstitial tissue compartment appear elongated and flattened. e) Macrophages embedded within and on the surface of the tunica albuginea (TA). f and g) Ultrastructure of interstitial and peritubular macrophages: PTC, peritubular myoid cell, LC, Leydig cell: ***, basement membrane. Cellular processes and intracytoplasmic vacuoles/phagosomes are indicated by small red arrows. Size markers indicated on each panel.

synthesis kit (Life Technologies, Carlsbad, CA) from 100 ng total RNA per reaction. Primers were designed to amplify short regions of the target genes spanning an intron/exon boundary. Transcript levels were measured using SYBR green (Applied Biosystems, MA, USA) in a final reaction volume of 10 μL. Each sample was measured in triplicate. For fluidigm analysis, TaqMan assays were obtained from Life Technologies. Assays and samples were combined in a 48.48 Dynamic array IFC according to Fluidigm® 48.48 Real-Time PCR Workflow Quick Reference PN 6800088. The primer sequences for qRT-PCR and details of the TaqMan probes are described in Supplementary Tables 1 and 2, respectively. The relative expression level of each target transcript was normalized to that of the reference transcript ribosomal protein, large, P0 (*Rplp0*) and *Hprt*, and was quantified using the ΔΔCt method.

2.6. Statistical analysis

Data are presented as individual values and mean ± standard error of the mean (SEM). Graphpad Prism 9 software (Graphpad software Inc., La Jolla, CA) was used for all analyses. An unpaired t-test was used for all comparisons. Significant differences were identified at $p < 0.05$.

3. Results

3.1. Macrophages in the parenchyma, subcapsular region and tunica albuginea of the adult mouse

Numerous F4/80$^+$ macrophages were observed throughout the testis parenchyma (Fig. 1a-c), subcapsular region (Fig. 1d), and the tunica albuginea (Fig. 1e). The demarcation between the intertubular interstitium (IT), seminiferous tubules (ST) and subcapsular interstitial tissue (SC) was defined histologically (Fig. 1a). Intertubular and subcapsular interstitial macrophages were closely associated with adjacent Leydig cells, and they were polygonal in shape, with round or ovoid nuclei (Fig. 1c and d). Peritubular macrophages were more sparsely distributed within the basal lamina of the seminiferous tubules, and were elongated in shape with narrow, elongated nuclei (Fig. 1c). The mean nuclear

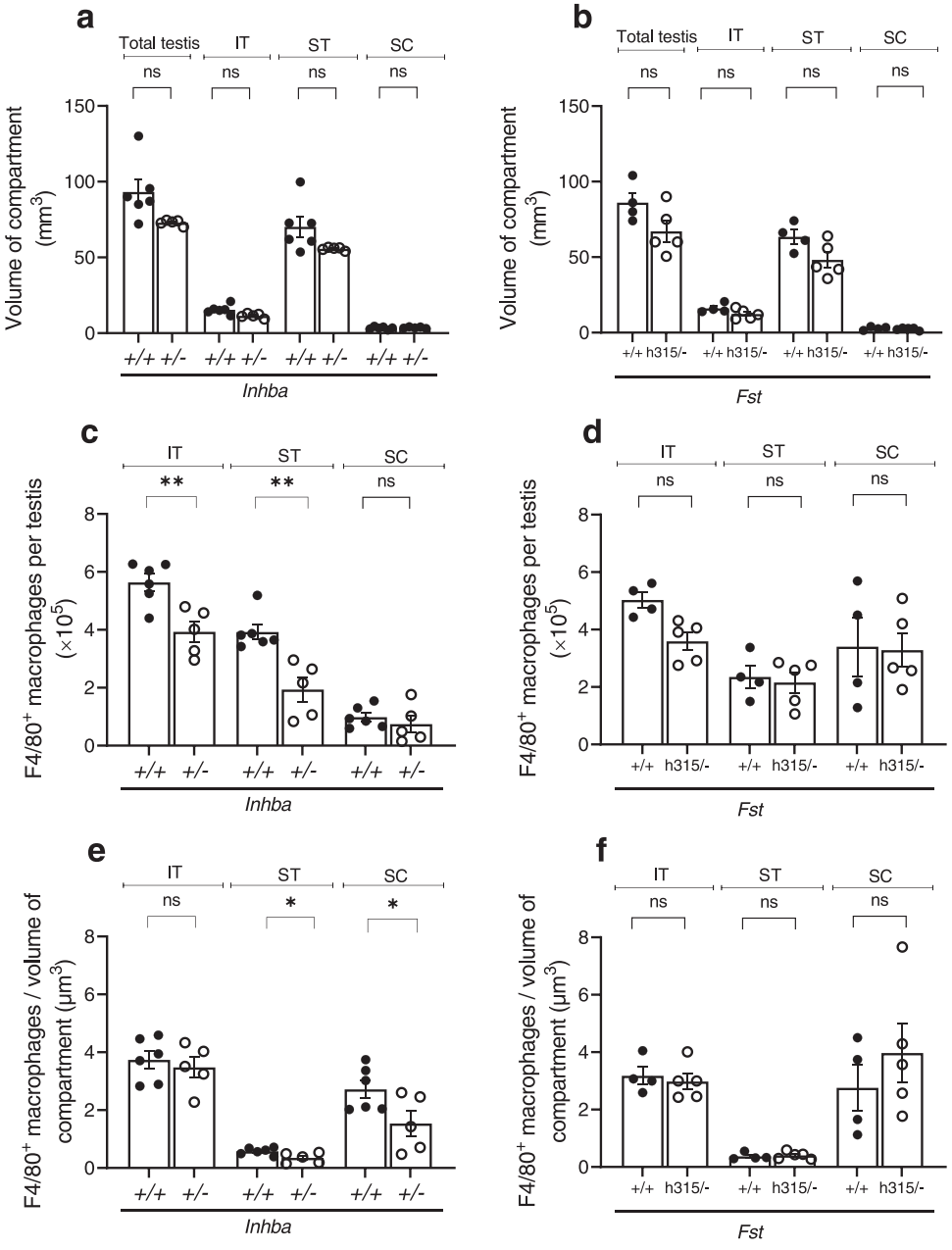

Fig. 2. Compartment volumes and quantification of macrophages in Inhba$^{+/-}$, TghFST315 and littermate control adult mouse testes. IT: Interstitial compartment (interstitial macrophages); ST: Seminiferous tubules (peritubular macrophages); SC: Subcapsular interstitial tissue (subcapsular macrophages). a and b) Volume of testes and tissue compartments. c and d) Total number of macrophages per testis in the interstitial, tubular and subcapsular testicular compartments. e and f) Volume density of macrophages in tissue compartments. Values are mean ± S.E.M (n = 6 *Inhba*$^{+/+}$; n = 5 *Inhba*$^{+/-}$; n = 4 *Fst*$^{+/+}$; n = 5 *Fst*$^{h315/-}$); *$p < 0.05$, **$p < 0.01$, ns not significantly different. Each data point represents a single animal.

diameter of intertubular and subcapsular interstitial macrophages was 3.78 μm, and 4.3 μm for peritubular macrophages. Elongated F4/80^{+} macrophages were also frequently observed within and along the surface of the tunica albuginea (Fig. 1e).

Electron micrographs containing interstitial macrophages (Fig. 1f) show their numerous intracellular inclusions and classical long cytoplasmic processes, and their close association with multiple Leydig cells, identified by their lipid droplets and dense smooth endoplasmic reticulum. Peritubular macrophages have a distinctly different morphology compared to interstitial macrophages (Fig. 1g). They have a spindle-shaped flat appearance and less cytoplasm than interstitial macrophages. Both macrophage populations contain similar vacuole/phagosome structures that are not found in peritubular cells. Peritubular macrophages were also differentiated from peritubular myoid cells by several additional criteria: (i) macrophages formed an additional layer to the single layer of peritubular cells (Fig. 1g), (ii) basement membrane is typically found between the peritubular cells and the seminiferous epithelium (Fig. 1f), but this was absent for macrophages (Fig. 1g), and (iii) macrophages had much fewer collagen fibers in their vicinity than peritubular cells (Fig. 1f, g).

3.2. Quantification of macrophages in the normal, activin-deficient and follistatin-deficient mouse testes

Although the average volumes of the *Inhba*$^{+/-}$ and TghFST315 testes and the individual tissue compartments were consistently smaller than their littermate controls by about 20%, as reported previously (Wijayarathna et al., 2017), these differences did not reach significance in the present study due to testis weight variability (Fig. 2a and b). Overall, interstitial macrophages were approximately twice as numerous as peritubular macrophages (Fig. 2c and d). Although subcapsular macrophages comprised a relatively small proportion of total testicular macrophages, their volume density was similar to macrophages in the intertubular region (Fig. 2e and f). There was a significant decrease in the number of intertubular interstitial macrophages (by 30.8%) and peritubular macrophages (by 48.5%) per testis in the *Inhba*$^{+/-}$ mice (Fig. 2c). The volume densities of the peritubular macrophages and subcapsular macrophages were also significantly reduced (by 52.9% and 36.3%, respectively), although the volume density in the intertubular regions was not significantly different from controls (Fig. 2e). Overall, these data indicate a significant reduction in the macrophage population in all compartments of the *Inhba*$^{+/-}$ testis. By contrast, there was no significant alteration in macrophage numbers in any compartment of the TghFST315 testis (Fig. 2b, d and f).

3.3. Expression of key macrophage functional genes in Inhba$^{+/-}$ and TghFST315 testes

As previously observed (Wijayarathna et al., 2018b), the *Inhba* transcript was reduced by 50% in the *Inhba*$^{+/-}$ testis (Fig. 3a), and the mouse *Fst* transcript was undetectable in the TghFST315 mouse testis (supplemental Fig. 1a). *Ccl2* was increased (by 44%) in the activin-deficient mouse testis (Fig. 3b), but its cognate receptor (*Ccr2*) was not altered (Fig. 3c). Additionally, *Csf1* and its receptor, *Csf1r*, were increased (by 35% and 27%, respectively) in the *Inhba*$^{+/-}$ testis (Fig. 3d and e). However, expression of the fractalkine (*Cx3cl1*) gene and its receptor, Cx3cr1, was not altered (Fig. 3f and g). Transcripts encoding MHC class II molecules (*H2-Ab1*) and the co-receptor *Cd86*, were increased in the activin-deficient testes (Fig. 3i and j), but transcripts for other antigen-presentation co-receptors (*Cd80* and *Cd274*) were not altered (Fig. 3h and k). In contrast, the only macrophage-specific transcript altered in the follistatin-deficient TghFST315 mouse testis was the scavenger receptor, *Mrc1* (Fig. 3l). Crucially, relative expression of the F4/80 transcript (*Adgre1*) was not altered in either genotype (supplemental Fig. 1b), indicating that the reductions in macrophage transcript levels were not attributable to the reduction in macrophage numbers. There was no difference in expression of the pan-leukocyte marker *Ptprc* (Cd45) (supplemental Fig. 1c) or the T-cell specific transcripts, *Cd3*, *Cd4* and *Cd8* (data not shown), in either activin- or follistatin-deficient mice.

3.4. Levels of somatic cell functional transcripts in Inhba$^{+/-}$ and TghFST315 testes

In order to establish the specificity of the macrophage-specific transcript level changes in the activin- and follistatin-deficient mice, the expression of transcripts associated with other somatic cells of the testis were also examined. Several transcripts encoding functionally important products of the Sertoli cells were significantly upregulated in the *Inhba*$^{+/-}$ testis: *Fshr* (increased by 17%), *Cp* (40%), *Pdgfb* (26%), *Sema4g* (24%) and *Vdr* (27%) (Table 1). Conversely, several Sertoli cell function-related transcripts were significantly lower in TghFST315 testes: *Amhr2* (decreased by 42%), *Trf* (33%) and *Serpina5* (50%), and the gap junction and tight junction related transcripts, *Cldn11* (25%), C*ldn3* (27%), O*cln* (27%) and Gja1 (40%). These data indicate that Sertoli cell function, in general, is inversely related to bioactive activin levels in the testis, with the exception of *Gdnf* expression, which was upregulated by 35% in TghFST315 testes.

A substantial reduction in transcripts related to steroidogenesis was observed in the TghFST315 testes: *Hsd17b3* (by 47%), *Cypa11a1* (59%) and *Cyp17a1* (66%), although *Hsd3b1* and *Insl3* remained unchanged (Table 1). Transcripts associated with peritubular myoid cell function also were reduced: *αSMA* (by 42%), *Fn1* (25%), *Dcn* (37%) and *Nid1* (28%). Altogether, these data indicate that, even though macrophage numbers and function were largely unaffected in the TghFST315 testis, the functions of other testicular somatic cells were significantly affected. Additional transcripts that were analyzed, but showed no changes in either mouse model, are listed in the Supplemental Table 2.

4. Discussion

Activins are known to play an important role in maintaining the immune environment of many tissues and are involved in the recruitment, maturation and activation of macrophages (Chen and Ten Dijke, 2016). Activin A has both pro-inflammatory and anti-inflammatory/tolerogenic activities and has differential effects on macrophage function based on their activation status and the dose and length of exposure (reviewed by Hedger et al., 2011). The results in the present study indicate that activin A exerts its action on the developing or mature testis to maintain macrophage numbers throughout all testicular compartments. Furthermore, the effects of changing activin A and follistatin levels on transcript levels indicate that activin A exerts cell-specific effects on macrophage function, distinct from its effects on Sertoli cells, Leydig cells and peritubular myoid cells.

In our previous study (Indumathy et al., 2020), using F4/80 as a macrophage marker in multi-color flow cytometry, a reduction in the proportion of F4/80^{+}CD206^{+} macrophages that expressed MHC class II antigen was observed in *Inha*$^{+/-}$ adult mice with elevated activin A, but the total macrophage number did not appear to be significantly altered in either the *Inha*$^{+/-}$ or *Inhba*$^{+/-}$ adult testis. Using a stereological approach, however, a reduction in the total number and volume density of macrophages was clearly evident in the testicular compartments, suggesting that changes in macrophage numbers in the earlier study may have been obscured by the normalisation of the data to total leukocytes (CD45^{+}), which was necessary to compensate for differential recovery of testicular cells for flow cytometry (Millard et al., 2021). Secondly, the observation that a reduction of follistatin activity did not have the inverse effect of increasing macrophage numbers in the adult testis suggests that the mode of action of activin A may be to maintain, rather than stimulate, macrophage numbers. Alternatively, activin protein levels may not be sufficiently increased in the TghFST315 mice to have a significant effect, as indicated in previous studies (Wijayarathna et al., 2017).

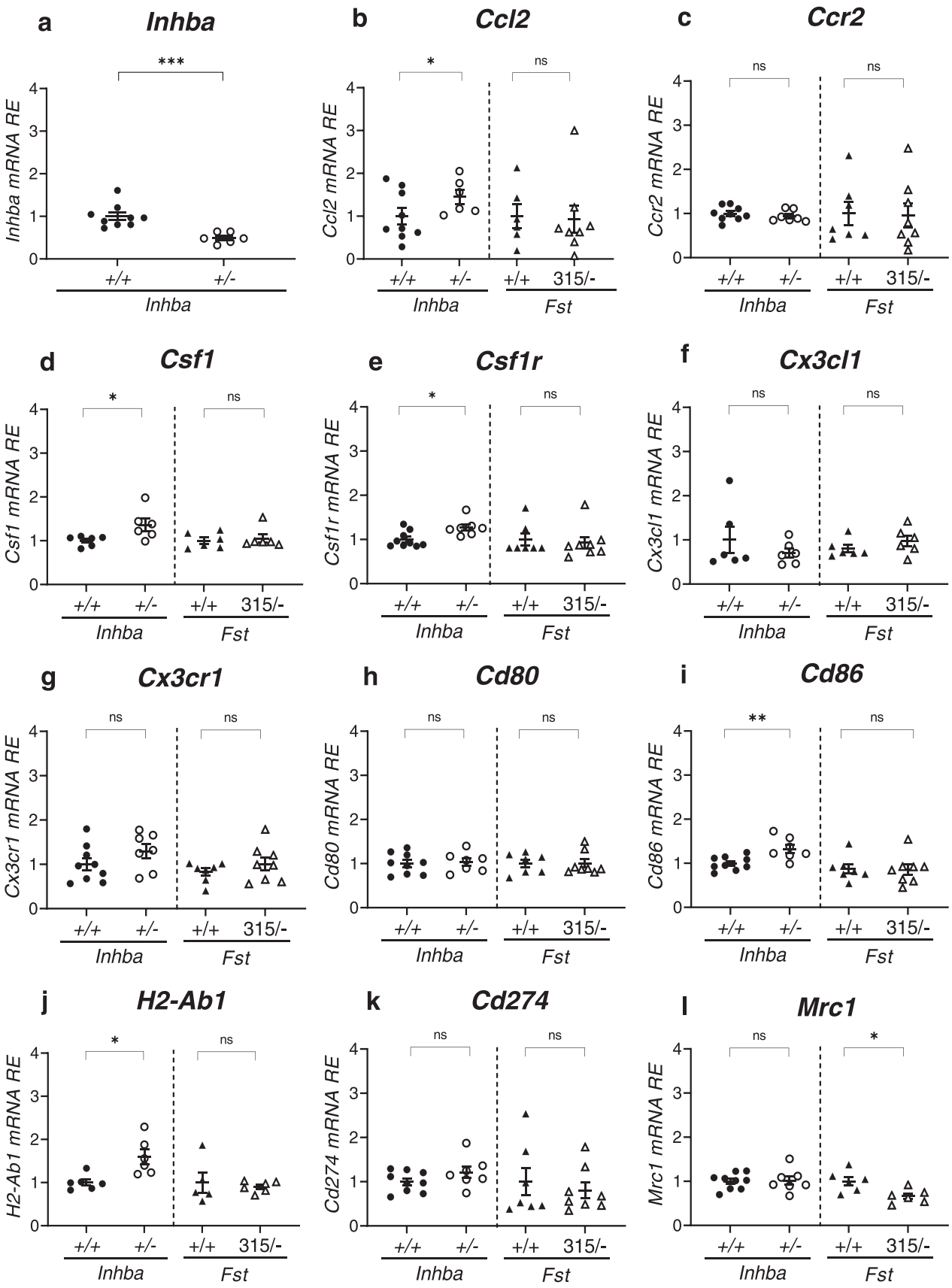

Fig. 3. Relative transcript levels of genes involved in macrophage regulation and function in the testes of *Inhba*$^{+/-}$, TghFST315 and littermate controls. Values are mean ± S.E.M (n = 6–9 *Inhba*$^{+/+}$; n = 6–7 *Inhba*$^{+/-}$; n = 5–7 *Fst*$^{+/+}$; n = 6–8 *Fst*$^{h315/+}$); *p < 0.05, **p < 0.01, ***p < 0.001; ns not significantly different. All *Inhba*$^{+/+}$ and *Fst*$^{+/+}$ control values are set to 1.

Table 1
Relative expression of mRNA transcripts involved in somatic cell function. All the values of associated with the transcript levels were normalized to the mean of the corresponding wild-type genotype. All values are mean ± SEM of 6 replicates; *p < 0.05; * *p < 0.01; [ns]not significantly different (p > 0.05). All other comparisons that were not significantly different are not included in the table (full list of analyzed transcripts in Supp. Table 2).

Gene Name	*Inhba*$^{+/+}$	*Inhba*$^{+/-}$	*Fst*$^{+/+}$	*Fst*$^{h315/+}$
Fshr	1.00 ± 0.07	1.18 ± 0.16*	1.00 ± 0.17	1.08 ± 0.16^{ns}
Cp	1.00 ± 0.26	1.40 ± 0.35*	1.00 ± 0.17	1.05 ± 0.23^{ns}
Pdgfb	1.00 ± 0.11	1.26 ± 0.22*	1.00 ± 0.19	0.97 ± 0.17^{ns}
Sema4g	1.00 ± 0.14	1.24 ± 0.18*	1.00 ± 0.18	1.00 ± 0.21^{ns}
Vdr	1.00 ± 0.11	1.28 ± 0.21*	1.00 ± 0.12	0.94 ± 0.17^{ns}
Amhr2	1.00 ± 0.62	1.30 ± 0.51^{ns}	1.00 ± 0.23	0.58 ± 0.13**
Trf	1.00 ± 0.38	1.47 ± 0.40^{ns}	1.00 ± 0.26	0.67 ± 0.15*
Serpina5	1.00 ± 0.61	1.32 ± 0.48^{ns}	1.00 ± 0.41	0.50 ± 0.36*
Gdnf	1.00 ± 0.22	1.05 ± 0.15^{ns}	1.00 ± 0.09	1.35 ± 0.14*
Cldn11	1.00 ± 0.46	1.27 ± 0.32^{ns}	1.00 ± 0.16	0.74 ± 0.23*
Cldn3	1.00 ± 0.36	1.23 ± 0.38^{ns}	1.00 ± 0.09	0.73 ± 0.12*
Ocln	1.00 ± 0.34	1.30 ± 0.35^{ns}	1.00 ± 0.18	0.73 ± 0.12*
Gja1	1.00 ± 0.50	0.56 ± 0.41^{ns}	1.00 ± 0.21	0.60 ± 0.12**
Hsd17b3	1.00 ± 0.46	1.67 ± 0.60^{ns}	1.00 ± 0.41	0.531 ± 0.10*
Cyp11a1	1.00 ± 0.74	1.67 ± 0.85^{ns}	1.00 ± 0.46	0.41 ± 0.19*
Cyp17a1	1.00 ± 0.75	1.65 ± 0.94^{ns}	1.00 ± 0.44	0.40 ± 0.15*
αSMA	1.00 ± 0.57	1.49 ± 0.58^{ns}	1.00 ± 0.32	0.58 ± 0.17*
Fn1	1.00 ± 0.32	1.33 ± 0.31^{ns}	1.00 ± 0.16	0.74 ± 0.21*
Dcn	1.00 ± 0.354	1.62 ± 0.73^{ns}	1.00 ± 0.33	0.63 ± 0.21*
Nid1	1.00 ± 0.37	1.43 ± 0.39^{ns}	1.00 ± 0.22	0.72 ± 0.16*

The increased level of transcripts encoding proteins involved in monocyte/macrophage chemotaxis (CCL2) and development (CSF1/CSFR1) in the activin-deficient mice suggests an effect of activin A on macrophage recruitment, differentiation and/or proliferation. CCL2 is responsible for recruitment of macrophages in the testis and other tissues in inflammatory conditions, but is less important for homeostatic and developmental regulation of macrophages (Charo et al., 1994; Serbina and Pamer, 2006). *Csf1* is required for macrophage survival in the testis by triggering CSF1/CSF1R signaling and the effects of CSF1 are CSF1R-dependent (Wang et al., 2021; Sauter et al., 2014; Stanley and Chitu, 2014). Though CSF1 and CCL2 have been reported to be expressed by other testicular cells, Leydig cells and peritubular cells in particular, CSF1R expression is macrophage-specific in the mouse testis (Lei et al., 2018, Defalco et al., 2015, Sauter et al., 2014). Notably, expression of the *Ccr2* transcript, presumably by macrophages, and that of another macrophage recruitment cytokine and its receptor, *Cx3Cl1/Cx3Cr1*, remained unchanged. Overall, the upregulation of *Ccl2, Csf1* and *Csf1r* in the activin-deficient testes, even though macrophage numbers were decreased, suggests that these changes could actually be a compensatory response by the macrophages and other cell types within the testis to the reduction in macrophage numbers, rather than a direct effect of activin itself.

Furthermore, activin inhibited level of some transcripts associated with antigen-presentation (MHC II, CD86), thereby potentially regulating the ability of testicular macrophages to activate CD4^{+} Th or Treg cells. The specificity of this response was indicated by the fact that expression of other co-stimulatory genes, *Cd80* and the inhibitory co-receptor, *Cd274*, were unaltered. MHC class II antigen, the scavenger receptor CD206 and the co-stimulatory B7 family of molecules (CD80, CD86 and CD274) are much more highly expressed on ''professional'' antigen-presenting cells (i.e., macrophages and dendritic cells), than on any other cell type, and that the significant changes seen almost certainly represent changes in expression by these cells (Defalco et al., 2014, Mossadegh-Keller et al., 2017). In the testis, it has been established that MHCII is most highly expressed on peritubular macrophages, and is weakly or sparsely expressed by interstitial macrophages (Defalco et al., 2015). The data suggest that activin A normally inhibits CD86 and MHCII expression by testicular antigen-presenting cells, which are predominantly macrophages in the mouse testis, consistent with a role in suppressing the antigen-presentation process in the mouse testis. These results are consistent with the results from our previous study (Indumathy et al., 2020), which showed that elevated activin further reduced MHCII expression on the CD206^{+} (i.e., predominantly interstitial) macrophages. In the current study, although activin deficiency did not affect CD206 transcript levels, the reduction of CD206 expression in the presence of reduced follistatin levels is indirect evidence that endogenous activin levels can regulate the inflammatory/anti-inflammatory macrophage (M1/M2) balance in the testis.

Finally, the divergent responses of somatic cell associated transcripts in the two mouse models investigated also confirm that the effects of activin A on the macrophages are cell type-specific. While the response to reduced activin was reduction in macrophage numbers and an increase in expression of genes associated with macrophage development and antigen-presentation, as well as several genes involved in Sertoli cell function, most testicular gene transcripts were not altered in the *Inhba*$^{+/-}$ mouse testis. In the follistatin-deficient model, there was a significant reduction in transcripts involved in formation of the blood-testis barrier and steroidogenesis, but no effect on macrophage-related genes. While it is not possible to establish from the present data whether the changes in transcript levels of somatic cell were in response to the changes in macrophage number and activity, or to the altered activin and follistatin levels, it is known that macrophages regulate Leydig cell development and steroidogenesis, in particular (Nes et al., 2000), and that activin has a regulatory effect on both Leydig cells and the integrity of the blood-testis barrier (Nicholls et al., 2012). The specific inter-relationship between activin A, the testicular macrophages and other somatic cells merit further study.

Acknowledgements

The authors thank Rosemary Genovese for maintaining and breeding the mouse colonies, as well as the Monash Histology Platform and Monash Health Translation Precinct Medical Genomics Facility for the provision of training, instrumentation and technical support.

Funding information

The research was supported by a grant from the Deutsche Forschungsgemeinschaft (DFG) and Monash University to the International Research Training Group (IRTG) on 'Molecular pathogenesis of male reproductive disorders' between Justus-Liebig-University, Giessen and Monash University (GRK 187/1), grants from the National Health and Medical Research Council, Australia to MPH and KAL (NHMRC APP1184867) and the Victorian Government's Operational Infrastructure Support Programme.

CRediT authorship contribution statement

SB (Sneha Biniwale)- Performing experiments, study design, data analysis, manuscript writing; RW- tissue collection, study design, technical and scientific guidance, critical review of the manuscript; CP-TEM experiments; SB (Sudhanshu Bhushan), KAL and AM- technical and scientific guidance, critical review of the manuscript; MH- study design, technical and scientific guidance and critical review of the manuscript.

Declaration of interest

None.

Appendix A. Supporting information

Supplementary data associated with this article can be found in the online version at doi:10.1016/j.jri.2022.103618.

References

Aubry, F., Habasque, C., Satie, A.P., Jégou, B., Samson, M., 2000. Expression and regulation of the CC-chemokine monocyte chemoattractant protein-1 in rat testicular cells in primary culture. Biol. Reprod. 62, 1427–1435.

Bhushan, S., Theas, M.S., Guazzone, V.A., Jacobo, P., Wang, M., Fijak, M., et al., 2020. Immune cell subtypes and their function in the testis. Front. Immunol. 11, 583304-583304.

Bhushan, S., Meinhardt, A., 2017. The macrophages in testis function. J. Reprod. Immunol. 119, 107–112.

Charo, I.F., Myers, S.J., Herman, A., Franci, C., Connolly, A.J., Coughlin, S.R., 1994. Molecular cloning and functional expression of two monocyte chemoattractant protein 1 receptors reveals alternative splicing of the carboxyl-terminal tails. Proc. Natl. Acad. Sci. U.S.A. 91, 2752–2756.

Chen, W., Ten Dijke, P., 2016. Immunoregulation by members of the TGFβ superfamily. Nat. Rev. Immunol. 16 (12), 723–740.

Chitu, V., Stanley, E.R., 2006. Colony-stimulating factor-1 in immunity and inflammation. Curr. Opin. Immunol. 18, 39–48.

Defalco, T., Potter, S.J., Williams, A.V., Waller, B., Kan, M.J., Capel, B., 2015. Macrophages contribute to the spermatogonial niche in the adult testis. Cell Rep. 12, 1107–1119.

Defalco, T., Bhattacharya, I., Williams, A.V., Sams, D.M., Capel, B., 2014. Yolk-sac–derived macrophages regulate fetal testis vascularization and morphogenesis. Proc. Natl. Acad. Sci. U.S.A. 111, E2384–E2393.

Gautier, E.L., Shay, T., Miller, J., 2012. Gene-expression profiles and transcriptional regulatory pathways that underlie the identity and diversity of mouse tissue macrophages. Nat. Immunol. 13, 1118–1128.

Gerdprasert, O., O'Bryan, M.K., Nikolic-Paterson, D.J.K., Sebire, K., De Kretser, D., Hedger, M.P., 2002. Expression of monocyte chemoattractant protein-1 and macrophage colony-stimulating factor in normal and inflamed rat testis. Mol. Hum. Reprod. 8, 518–524.

Gordon, S., Pluddemann, A., Estrada, F.M., 2014. Macrophage heterogeneity in tissues: phenotypic diversity and functions. Immunol. Rev. 262, 36–55.

Hedger, M.P., 2015. The immunophysiology of male reproduction. In: Plant, T.M., Zeleznik, A.J. (Eds.), Knobil and Neill's Physiology of Reproduction, fourth ed. Elsevier.

Hedger, M.P., De Kretser, D., 2013. The activins and their binding proteins, follistatis-Dianostic and therapeutic targets in inflammatory disease and fibrosis. Cytokine Growth Factor Rev. 24, 285–295.

Hedger, M.P., Winnall, W.R., Phillips, D.J., De Kretser, D., 2011. Regulation and function of activin and follistatin in inflammation and immunity. Vitam. Horm. 85, 255–297.

Hume, D.A., Halpin, D., Charlton, H., Gordon, S., 1984. The mononuclear phagocyte system of the mouse defined by immunohistochemical localization of antigen F4/80: Macrophages of endocrine organs. Proc. Natl. Acad. Sci. U.S.A. 81, 4174–4177.

Indumathy, S., Pueschl, D., Klein, B., Fietz, D., Bergmann, M., Schuppe, H.C., et al., 2020. Testicular immune cell populations and macrophage polarisation in adult male mice and the influence of altered activin A levels. J. Reprod. Immunol. 142, 103204.

Jiang, Q., Maresch, C.C., Petry, S.F., Paradowska-Dogan, A., Bhushan, S., Chang, Y., et al., 2020. Elevated CCL2 causes Leydig cell malfunction in metabolic syndrome. JCI Insight 5, e134882.

Lei, T., Moos, S., Klug, J., Aslani, F., Bhushan, S., Wahle, E., et al., 2018. Galectin-1 enhances TNFα-induced inflammatory responses in Sertoli cells through activation of MAPK signalling. Sci. Rep. 8, 1–15.

Lin, S.Y., Craythorn, R.G., O'Connor, A.E., Matzuk, M.M., Girling, J.E., Morrison, J.R., et al., 2008. Female infertility and disrupted angiogenesis are actions of specific follistatin isoforms. Mol. Endocrinol. 22, 415–429.

Lokka, E., Lintukorpi, L., Cisneros-Montalvo, S., Mäkelä, J.A., Tyystjärvi, S., Ojasalo, V., et al., 2020. Generation, localization and functions of macrophages during the development of testis. Nat. Commun. 11, 4375.

Matzuk, M.M., Kumar, T.R., Bicjenbach, J.R., Vassalli, A., Roop, D.R., Jaenisch, R., et al., 1995a. Functional analysis of activins during mammalian development. Nature 374, 354–356.

Meinhardt A., Dejucq-Rainsford N. Bhushan S. 2021. Testicular macrophages: Development and function in health and disease. Trends in immunology. Article in Press.

Mendis, S.H.S., Meachem, S.J., Sarraj, M.A., Loveland, K.L., 2011. Activin A balances sertoli and germ cell proliferation in the fetal mouse testis1. Biol. Reprod. 84, 379–391.

Millard SM, Heng O., Opperman KS, Sehgal A., Irvine KM, Kaur S. et al. 2021. Fragmentation of macrophages during isolation confounds analysis of single cell preparations from mouse hematopoietic tissues. *bioRxiv*.

Mithraprabhu, S., Mendis, S., Meachem, S.J., Tubino, L., Matzuk, M.M., Brown, C.W., et al., 2010. Activin bioactivity affects germ cell differentiation in the postnatal mouse testis in vivo. Biol. Reprod. 82, 980–990.

Mossadegh-Keller, N., Gentek, R., Gimenez, G., Bigot, S., Mailfert, S., Sieweke, M.H., 2017. Developmental origin and maintenance of distinct testicular macrophage populations. J. Exp. Med. 214, 2829–2841.

Nes, W.D., Lukyanenko, Y.O., Jia, Z.H., Quideau, S., Howald, W.N., Pratum, T.K., et al., 2000. Identification of the lipophilic factor produced bymacrophages that stimulates steroidogenesis. Endocrinology 141, 953–958.

Nicholls, P.K., Stanton, P.G., Chen, J.L., Olcorn, J.S., Haverfield, J.T., Qian, H., et al., 2012. Activin signaling regulates sertoli cell differentiation and function. Endocrinology 153, 6065–6077.

Sauter, K.A., Pridans, C., Sehgal, A., Tsai, Y.T., Bradford, B.M., Raza, S., et al., 2014. Pleiotropic effects of extended blockade of CSF1R signaling in adult mice. J. Leukoc. Biol. 96, 265–274.

Schindelin, J., Arganda-Carreras, I., Frise, E., Kaynig, V., Longair, M., Pietzsch, T., et al., 2012. Fiji: an open-source platform for biological-image analysis. Nat. Methods 9, 676–682.

Serbina, N.V., Pamer, E.G., 2006. Monocyte emigration from bone marrow during bacterial infection requires signals mediated by chemokine receptor CCR2. Nat. Immunol. 7, 311–317.

Stanley, E.R., Chitu, V., 2014. CSF-1 receptor signaling in myeloid cells. Cold Spring Harb. Perspect. Biol. 6, a021857.

Tong, M.H., Yang, Q.E., Davis, J.C., Griswold, M.D., 2013. Retinol dehydrogenase 10 is indispensible for spermatogenesis in juvenile males. Proc. Natl. Acad. Sci. U.S.A. 110, 543–548.

Wang, J., Wreford, N.G.M., Lan, H.Y., Atkins, R., Hedger, M.P., 1994. Leukocyte populations of the adult rat testis following removal of the leydig- cells by treatment with ethane dimethane sulfonate and subcutaneous testosterone implants. Biol. Reprod. 51, 551–561.

Wang, M., Yang, Y., Cansever, D., Wang, Y., Kantores, C., Messiaen, S., et al., 2021. Two populations of self-maintaining monocyte-independent macrophages exist in adult epididymis and testis. Proc. Natl. Acad. Sci. U.S.A. 118.

Wijayarathna, R., De Kretser, D., 2016. Activins in reproductive biology and beyond. Hum. Reprod. Update 22, 342–357.

Wijayarathna, R., De Kretser, D., Sreenivasan, R., Ludlow, H., Middendorff, R., Meinhardt, A., et al., 2018b. Comparative analysis of activins A and B in the adult mouse epididymis and vas deferens. Reproduction 155, 15–23.

Wijayarathna, R., Sarraj, M.A., Genovese, R., Girling, J.E., Michel, V., Ludlow, et al., 2017. Activin and follistatin interactions in the male reproductive tract: activin expression and morphological abnormalities in mice lacking follistatin 288. Andrology 5, 578–588.

Chapter 3: Analysis of the distribution and phenotypes of macrophages in the normal, activin-deficient, and infected adult mouse testis identifies multiple macrophage subpopulations

Complete manuscript in preparation for submission to Journal (to be decided)

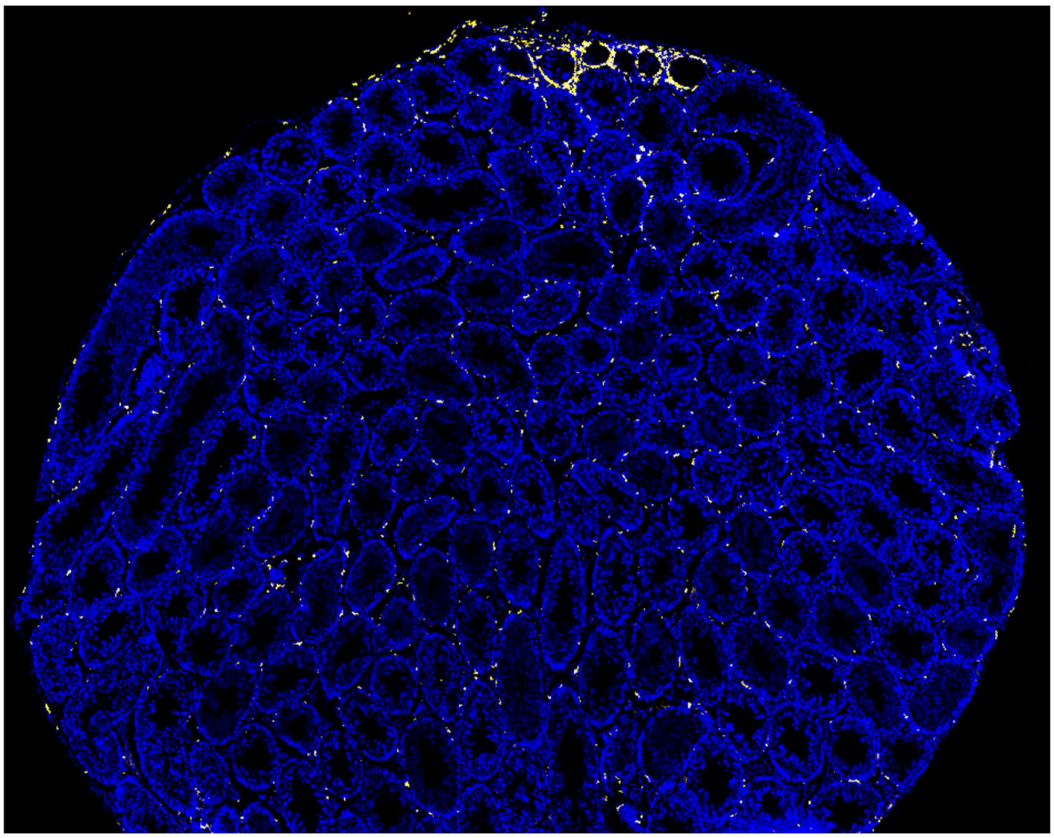

Analysis of the distribution and phenotypes of macrophages in the normal, activin-deficient, and infected adult mouse testis identifies multiple macrophage subpopulations

Sneha Biniwale[1,2,3], Rukmali Wijayarathna[1,2], Rosemary Genovese[1,2], Sudhanshu Bhushan[3,4], Christiane Pleuger[3,4], Kate L Loveland[1,2], Andreas Meinhardt[1,3,4], Mark P Hedger[1,2]

[1]Centre for Reproductive Health, Hudson Institute of Medical Research, Clayton, Victoria, Australia

[2]Department of Molecular and Translational Sciences, School of Clinical Sciences, Monash University, Clayton, Victoria, Australia

[3]Institute of Anatomy and Cell Biology, Justus-Liebig University Giessen, Giessen, Germany

[4]The Hessian Centre of Reproductive Medicine, Justus-Liebig-University, Giessen, Germany

Corresponding author: Sneha.biniwale@monash.edu

Postal address: Hudson Institute of Medical Research, 27-31 Wright Street, Clayton 3168, VIC Australia

Abstract

The rete testis and subcapsular regions are primary sites of disease onset in murine experimental auto-immune orchitis, but the macrophage population within these compartments have not been well-characterized. The aim of this study was to evaluate the macrophage populations in the rete testis, subcapsule and tunica albuginea in comparison with parenchymal phenotypes in normal and activin A-deficient adult mice and following bacterial infection. Human testis samples were also examined. We hypothesized that macrophage populations in these less-studied compartments have a different phenotype and functions than macrophages in rest of the testis. Macrophages were identified by immunofluorescence using an anti-F4/80 antibody in testis sections from adult wild-type C57BL/6J mice and in mice expressing a GFP-transgene at the locus of the macrophage chemokine receptor, CX_3CR_1 ($Cx_3cr_1^{gfp/+}$). $Cx_3cr_1^{gfp/+}$ mice deficient in activin A ($Cx_3cr_1^{gfp/+}Inhba^{+/-}$) were compared with their homozygous littermate controls ($Cx_3cr_1^{gfp/+}Inhba^{+/+}$). Sections were co-labelled by immunofluorescence for the anti-inflammatory macrophage marker, CD206, and the antigen-presenting MHC class II molecule (I-A/1-E), expressed by activated macrophages. Sections were scanned using an Olympus VS120 slide scanner and macrophages were quantified using established stereological techniques using QuPath software. Compared with the parenchyma surrounding the seminiferous tubules in the wild-type mouse testis, the volume density of macrophages ($F4/80^+$) was 8-9-fold higher in the interstitial and peri-epithelial regions of the rete testis. Macrophages ($CD68^+$) were also abundant in the interstitial and peri-epithelial regions of the human rete testis, although their volume density was not appreciably higher than that of the parenchyma, which may be attributed to the more extensive interstitial structure of the human rete testis. Macrophage density in the subcapsular region of the mouse testis was similar to that of the rest of the interstitium. The proportion of interstitial macrophages that expressed CX_3CR_1 was similar in the rete testis (80%) and inter-tubular parenchyma (88%), respectively, although expression of CD206 by interstitial macrophages in the rete testis was slightly lower (71%) than parenchymal interstitial macrophages. However, in contrast to the parenchyma, where the majority (95%) of interstitial macrophages lacked detectable MHCII expression, 75% of interstitial macrophages in the rete testis were positive for MHCII. This indicates the presence of a major subset of $F4/80^+CD206^+MHCII^+$ macrophages in the interstitial

tissue surrounding the rete testis, which is relatively rare throughout the rest of the interstitium. The number of macrophages expressing MHC class II in the subcapsular region was intermediate between that of the rete testis and the rest of the interstitial tissue. The proportion of CX_3CR_1 expression was lower (70-75%) in the rete testis peri-epithelial and peritubular macrophage populations, than in the interstitial population. The peri-epithelial macrophages in the rete testis were principally $F4/80^+MHCII^+$ (94%), similar to the peritubular macrophages (99%). However, 47% of peri-epithelial macrophages in the rete testis were also $CD206^+$, compared with only 16% in the seminiferous tubules. Additionally, there were significant increases in the volume density of both $MHCII^+$ (10%) and $MHCII^-$ (5%) macrophages respectively in the interstitium of the rete testis of activin A-deficient testis. When testes infected with uropathogenic *E. coli* were investigated, there was a clearly observable increase in $CX_3CR_1^+MHCII^+$ interstitial and peri-epithelial macrophages at day 10 post-infection in the rete testis and adjacent regions. Most of these macrophages were also $CD206^+$. This increase was found to be resolved by day 28 post-infection.

These data indicate that there is a large subset of macrophages within the interstitium and peri-epithelium of the mouse rete testis and subcapsular macrophages that expresses both CD206 and MHC class II, which is a minor subset in the rest of the testis. This is indicative of an activated, potentially anti-inflammatory, phenotype. Accordingly, these macrophages may play a role in recognizing sperm antigens and inducing tolerance to the emerging spermatozoa, in addition to providing protection from ascending infections. Alterations to the protective function of these macrophages during inflammatory disease, such as UPEC infection, may be a cause of sperm autoimmunity or more severe inflammatory damage.

1 Introduction

In the testis, sperm are produced in the seminiferous tubules surrounded by the interstitial tissue and are collected in the rete testis before transfer and storage in the epididymis. The cellular organization of the rete testis (RT) epithelium is notably different from that of the seminiferous epithelium. The mature rete testis consists of anastomosing channels lined by flattened or squamous to cuboidal-shaped epithelial cells, which are structurally different from the Sertoli cells in the seminiferous epithelium, surrounded by a basal lamina (Malolina and Kulibin, 2019). The rete testis and seminiferous tubules are linked by the transition region (TR), also known as the tubuli recti, consisting of cells resembling the Sertoli cells, referred to as 'modified' Sertoli cells or transition region Sertoli cells (TRSCs) (Kulibin and Malolina, 2020, Figueiredo *et al.,* 2021, Major *et al.,* 2021). These TRSCs are columnar cells with oval-shaped nuclei, peripheral heterochromatin, and small nucleoli (Aiyama *et al.,* 2015, Dym, 1974). The rete testis is connected to the efferent ducts (ED), which are small parallel tubules connecting the testis to the epididymis. The epithelium of the efferent ducts consists of cuboidal/columnar cells that may be either ciliated or nonciliated (Hess, 2002), and the epithelium is surrounded by a basement membrane and a smooth muscle layer with basal cells and intra-epithelial lymphocytes or macrophages evident in some species (Hess, 2002).

Resident macrophages have been most intensively studied in the parenchyma of the testis and comprise both interstitial (IT) and peritubular macrophages (PT). They differ in terms of location, morphology and function and have heterogenous phenotypic markers (Hume *et al.,* 1984, DeFalco *et al.,* 2015). In the mouse, these macrophages express common tissue-resident markers, such as F4/80, CD11b and CX_3CR_1, but differ in expression of functional markers, such as major histocompatibility complex II antigens (MHCII) and the anti-inflammatory scavenger receptor, CD206. While the interstitial macrophages are predominantly $F4/80^+CD206^+MHCII^-$, peritubular macrophages are $F4/80^+CD206^-MHCII^+$, indicating different functional roles (Lokka *et al.,* 2020, DeFalco *et al.,* 2015, Mossadegh-Keller *et al.,* 2017). The $CD206^+MHCII^-$ cells are present from birth and are associated with vascular cells, whereas $CD206^-MHCII^+$ cells appear at two weeks postnatally and are less frequently associated with the vasculature (Lokka *et al.,* 2020). In adult mice infected with Uropathogenic *E. coli* (UPEC), cellular infiltrates filled up the interstitial space by 10 days post-infection,

accompanied by impaired spermatogenesis, loss of germ cells and tubules with Sertoli cells only (Klein *et al.,* 2020). These cellular infiltrates included F4/80^{+} macrophages and showed simultaneous upregulation of transcripts for *Ccl2* and *Adgre1* (the gene encoding F4/80) (Wang *et al.,* 2021, Klein *et al.,* 2020). Interestingly, the testes showed complete recovery from the signs of testicular inflammation and the disruption of spermatogenesis by 31 days post-infection. A role for the testicular macrophages in inflammation resolution and bacterial clearance is indicated. Inflammation increases the resident as well as the infiltrating macrophage population (Wang *et al.,* 2021, Davies *et al.,* 2013, Jenkins *et al.,* 2011).

Tung and his colleagues reported that F4/80^{+} interstitial macrophages were more abundant in the rete testis and tunica albuginea (TA) adjacent to the rete testis of the mouse and many of these macrophages were MHCII^{+} in normal mice (Tung *et al.,* 1987). This was later confirmed by Takahashi and colleagues (Takahashi *et al.,* 2007). These observations were further studied in younger mice, and showed that an influx of F4/80^{+} macrophages in the rete testis occurs between day 21 and day 28 after birth (Itoh *et al.,* 1999). The efferent ducts were also found to be surrounded by numerous F4/80^{+}MHCII^{+} macrophages. Additionally, Takahashi and colleagues described penetration by macrophages in the epithelium within the terminal segment of the tubuli recti/ transition region by transmission electron microscopy in normal mice (Takahashi *et al.,* 2007). The rete testis and subcapsule (SC) are the primary sites of disease initiation in murine experimental auto-immune orchitis (EAO) (Tung *et al.,* 1987). Tung and his colleagues showed that the rete testis, the straight tubules, and ductus efferentes were the predominant sites of inflammation in passive EAO triggered by using donor T cells immunized with homologous testicular antigens (Tung *et al.,* 1987). Later, Itoh and colleagues showed that lymphocytic infiltration of autoimmune origin starts in the transition region and spreads to surrounding seminiferous tubules, when susceptible mouse strains were immunized using syngeneic testicular germ cells (TGC) alone (Itoh *et al.,* 1991). They also showed an accumulation of CD4^{+} and CD8^{+} T-cells around the transition region at the onset of EAO, before spreading around the seminiferous tubules after the onset of EAO, followed by the accumulation of B-cells (Naito *et al.,* 2009). These lymphocytes migrated to the wall of the TR and secreted cytokines, including IL-1, IL-6, IL-2, IL-10, IFN-γ and TNF, thereby disrupting the TR epithelium (Naito *et al.,* 2009). A similar effect was observed after LPS treatment in

mice for 36 hours starting with alterations in the TR at 6 hours post-LPS treatment (Figueiredo *et al.,* 2021).

Activins are members of the transforming growth factor-β (TGF-β) family of cytokines, which regulate development, tissue remodeling and immunoregulation (Wijayarathna and de Kretser, 2016). In the previous study (Chapter 2), it was demonstrated that activin A maintains F4/80^{+} macrophage numbers in the interstitial and peritubular regions surrounding the seminiferous tubules and in the subcapsule region (Biniwale *et al.,* 2022). Conversely, chronically increased activin A levels reduced MHCII expression by CD206^{+} macrophages, whereas reduced activin A increased MHCII gene expression in the adult testis [Indumathy *et al.,* 2020, chapter 2 (Biniwale *et al.,* 2022)]. The current understanding of the testicular macrophages revolves around the macrophages in the parenchyma around the seminiferous tubules, and investigation of other testicular compartments, such as the rete testis, the subcapsule, tunica albuginea, transition region and the efferent ducts has been less comprehensive. The aim of this study was to compare the distribution of macrophages and their phenotypes in these individual testicular compartments with the established parenchymal macrophage phenotypes, and their responses to activin-deficiency and infection.

2 Materials and Methods

2.1 Animals

2.1.1 CX_3CR_1-GFP transgenic (*Cx$_3$cr$_1^{GFP/+}$*) and activin A-deficient (*Inhba$^{+/-}$*) mice

The *Cx$_3$cr$_1^{GFP/+}$* mouse contains an inactivating insertion of the sequence encoding green fluorescent protein (GFP) within the first 390 base pairs of the CX3CR1 gene (Jung *et al.,* 2000). For this study, *Cx$_3$cr$_1^{GFP/+}$* mice were obtained by mating wild-type C57BL/6J mice (from the Monash Animal Research Platform) with *Cx$_3$cr$_1^{GFP/GFP}$* adults. Use of homozygous *Cx$_3$cr$_1^{GFP/GFP}$* adult mice, which therefore lack a functional CX_3CR_1 receptor, for these immune cell analyses was precluded because of the importance of CX_3CR_1 in leukocyte adhesion and migration (Jung *et al.,* 2000, Fong *et al.,* 1998, Imai *et al.,* 1997). *Inhba$^{+/-}$* mice, which display a 50% reduction in serum and intratesticular activin A protein levels, and their homozygous normal (*Inhba$^{+/+}$*) littermate controls, were produced as described previously (Matzuk *et al.,* 1995c, Mendis *et al.,* 2011, Wijayarathna *et al.,* 2018). Homozygous deletions of *Inhba* are lethal at birth due to developmental defects, and were not available for analysis.

Inhba$^{+/-}$ mice were crossed with mice that were homozygous for the CX_3CR_1-GFP transgene resulting in *Cx₃cr₁*$^{GFP/+}$*Inhba*$^{+/-}$ mice and their homozygous littermate controls (*Cx₃cr₁*$^{GFP/+}$*Inhba*$^{+/+}$). The maintenance of the *Cx₃cr₁*$^{GFP/+}$ mice was undertaken, as described previously (Indumathy *et al.,* 2020). Tissues from mice heterozygous for both the *Cx₃cr₁* and *Inhba* genes (*Cx₃cr₁*$^{GFP/+}$*Inhba*$^{+/-}$), and their *Inhba* homozygous (*Cx₃cr₁*$^{GFP/+}$*Inhba*$^{+/+}$) littermates were collected at 8 weeks of age (n=6 from each group).

2.1.2 Uropathogenic *E. coli* (UPEC) infected mice

Adult C57BL/6J male mice (Charles River Laboratories, Sulzfeld, Germany; 10–12 weeks of age) were anesthetised with an intraperitoneal injection of ketamine and xylazine, and bacterial epididymo-orchitis was established, as previously described (Michel et al. 2016). Briefly, a scrotal incision was made to expose the reproductive tract, and the vasa deferentia were ligated to prevent spreading of the infection anterograde towards the urethra. Ten µL of uropathogenic *E. coli* strain 536 (UPEC) in a saline (0.9% sodium chloride solution) suspension (about 5×10^5 bacteria) were injected bilaterally into the vas deferens proximal to the ligation site and distal to the cauda epididymis using 30 G needle. Sham-operated mice were injected with saline. Mice were killed at Day 10 and Day 28 post-inoculation (p.i.), and testes were collected. The time points were chosen based on the results of a previous study (Michel *et al.,* 2016). At Day 3 p.i., bacteria were present in the cauda epididymidis, but little histological damage was apparent. At Day 7 p.i., bacteria had ascended to the testis with severe damage evident in the cauda epididymidis. With bacteria ascending to the testis past the caput by Day 7 p.i., an assessment at Day 10 p.i. would allow sufficient time for any possible pathological alteration to become visible. Day 31 p.i. was chosen because the previous study showed that the infection had resolved at this time point in the testis, although not in the epididymis.

Inhba$^{+/-}$ and *Cx₃cr₁*$^{GFP/+}$*Inhba*$^{+/-}$ mice and their littermates were housed at the Monash Medical Centre animal facility. Experiments at Monash University were conducted according to the National Health and Medical Research Council Code of Practice for the Care and Use of Animals for Experimental Purposes and approved by the Animal Ethics Committee of Monash Medical Centre. UPEC-infected mice were housed at Justus-Liebig-University following Guidelines for the Care and Use of Laboratory

Animals of the German law for animal welfare and the European legislation for the protection of animals for scientific purposes.

2.2 Tissue collection

Animals were euthanized by carbon dioxide overdose. Testes were collected and fixed in Bouin's solution (for immunohistochemical studies) or 4% paraformaldehyde (PFA) (Alfa Aesar, Thermo Fisher Scientific, UK) (for immunofluorescence studies) at room temperature. Testes were punctured at both poles with a 23G needle after 1 hour for better penetration of the fixative and then incubated for 4 more hours. Tissues were washed with 0.01M PBS three times to remove excess fixative and stored in 70% alcohol overnight at 4°C. Bouin's-fixed testes were embedded in paraffin, while 4% PFA-fixed testes were embedded in Tissue-Tek OCT (Sakura Finetek, USA) and snap-frozen on dry ice.

Human testes were collected from body donors (>70 years of age). Cadavers were fixed in 3% formalin, 65% isopropanol, 3,8% phenoxetol (alcohol mix), 3,8% glycerin in water. Post-fixation of specimens was performed in 3% formalin in water. The collected testes were post-fixed in 3% formalin again for 72 hours, followed by 24 hours incubation in each of the increasing isopropanol solutions (30%, 50%, 70% and 90%) and 2 changes of 100% isopropanol for 24 hours each. Specimens were then embedded in paraffin.

2.3 Immunohistochemistry

Mouse testes

Immunohistochemistry using Bouin's-fixed, paraffin-embedded 5 µm thick whole transverse adult mouse testis sections containing the rete testis and/or testis capsule was performed, as previously described in chapter 2 (Biniwale *et al.,* 2022). Briefly, macrophages were detected by a well-characterized macrophage-specific antigen, F4/80, using a rat monoclonal antibody (see supplementary table 1 for all antibody details) (Bio-Rad Laboratories, Herculus, CA) (Hume *et al.,* 1984, DeFalco *et al.,* 2015). Heat-mediated antigen retrieval was performed in citrate buffer (pH 6.0) by boiling the sections at high power (800 watts) for one minute followed by the defrost cycle for 15 minutes. The slides were allowed to cool and then the sections were treated with 10% goat serum in Tris-buffered saline with 0.1% Tween-20 (TTBS) to block non-specific binding. Sections were incubated with the anti-F4/80 antibody at

1:100 dilution in 2.5% bovine serum albumin (BSA) in TBS in a humid chamber overnight at 4°C. Negative controls were incubated with 2.5% BSA in 0.01M PBS alone. Staining was visualized using a biotinylated goat anti-rat secondary antibody conjugated to horseradish peroxidase (Vector Laboratories, Burlingame, CA) at 1:300 for one hour in a humid chamber, followed by Vectastain Elite kit reagents (Vector Laboratories Inc., Burlingame, CA) at room temperature for 30 minutes. Diaminobenzidine (DAB) (Dako North America Inc., Carpinteria, CA) at the concentration recommended by the manufacturer was added to the sections and color development was monitored (10-20 minutes) under a wet-mount microscope. Sections were counter-stained with hematoxylin, cover-slipped and mounted with DPX, and scanned using an Olympus VS120 brightfield slide scanner (Monash Histology Platform, MHTP) for imaging and macrophage quantification.

Human testes

Immunohistochemistry using formalin-fixed, paraffin-embedded 5 µm thick whole transverse adult human testis sections containing the rete testis was performed. Macrophages were detected using a monoclonal mouse anti-human anti-CD68 marker at 1:500 (DAKO Agilent, CA, USA) (Klein *et al.,* 2016). Heat-mediated antigen retrieval was performed using citrate buffer (pH 6.0) at 800 watts (5 min) and 450 watts (9 mins). Sections were treated with 3% hydrogen peroxide for 20 mins after a brief wash in miliQ water. They were washed twice in Tris-buffered saline (TBS) and incubated with 5% BSA in TBS for 1 hour in a humid chamber to block non-specific binding before incubating it for anti-CD68 antibody overnight at 4°C. Staining was visualized using a biotinylated rabbit anti-mouse secondary antibody conjugated to horseradish peroxidase (Invitrogen, WA, USA) at 1:500 for one hour in a humid chamber followed by the DAB detection process used for mouse sections.

2.4 Immunofluorescence

Immunofluorescence studies were performed using the protocol described previously (Indumathy *et al.,* 2020). Briefly, cryosections of testis containing the rete testis from *Cx$_3$cr$_1^{GFP/+}$ Inhba$^{+/-}$* (n=6) and their littermate controls, *Cx$_3$cr$_1^{GFP/+}$ Inhba$^{+/+}$* (n=6 were air-dried for 20 mins and rehydrated in 0.01M PBS for 10 mins. Antigen retrieval was performed using 1% SDS for 5 mins, followed by PBS washes. The sections were incubated with 2% mouse on mouse (M.O.M) block (Vector laboratories, Burlingame,

CA) for 1h followed by 30 minutes blocking with 2% BSA in PBS. These tissue sections were then incubated overnight at 4°C with the same anti-F4/80 primary antibody (1:800) used for immunohistochemistry (supplementary table 1). Antibody combinations of anti-F4/80 with fluorescently labelled anti-MHCII, anti-CD206 or unconjugated anti-laminin (all at 1:500) were used on sections. The following day, sections were washed in 2.7% NaCl in PBS and incubated with the appropriate secondary antibodies conjugated to Alexa fluor 647 (Life technology, Carlsbad, USA), Alexa fluor 546 (Invitrogen, WA, USA) or Alexa fluor 555 (Invitrogen, WA, USA) for 1 hour in a humid chamber (supplementary table 1). Excess secondary antibodies were washed in 2.7% NaCl in PBS and sections were incubated with DAPI (Invitrogen, WA, USA) at 1:1000 for 15 minutes, washed, mounted with Mowiol 4-88 (Calbiochem, Damstadt, Germany) and dried overnight covered with foil at 4°C. Slides were scanned using an Olympus VS120 brightfield slide scanner (Monash Histology Platform, MHTP) for imaging and macrophage quantification.

2.5 Macrophage enumeration

Macrophages were counted using an established immunohistochemical morphometric technique to determine the volume density (Grubman *et al.,* 2021) of testicular macrophages in sections of constant thickness, as previously described in chapter 2 (Wang *et al.,* 1994, Biniwale *et al.,* 2022). The scanned immunostained sections were analyzed using QuPath with a cell counter plug-in (Bankhead *et al.,* 2017). The testes were segregated into six compartments: interstitium and seminiferous tubules of the parenchyma (defined as all tissue, excluding the rete testis and regions adjacent to the capsule), interstitial and tubular compartments of the rete testis, the subcapsular interstitium and the tunica albuginea, as previously described in chapter 2. Briefly, between 100-200 visible nuclear profiles of F4/80 labelled cells were counted in twenty-five equally spaced grids of equal size (100,000 μm^2) across each transverse section to quantitate macrophages in the interstitial and peritubular compartments of the parenchyma (n=6 mice / group and 3 sections / mouse were assessed). The mean nuclear diameter for each macrophage population was determined from the average of the longest and shortest axes of the nuclear profile of 10 randomly selected $F4/80^+$ macrophage nuclei/section. In order to compensate for partial nuclear profiles at the periphery of the section, only the largest 30% of measurements was used to calculate the mean nuclear diameter in the parenchyma. All macrophages in the rete testis,

subcapsule and the tunica albuginea sections were used for quantification, The total volume of the testis was estimated from the testis weights, and the relative volumes of each compartment were determined by the point-counting method in each whole transverse section. Macrophage numbers were estimated from their volume density in sections of the whole testis (total) and compartments, while cell proportions were calculated against the total F4/80^{+} macrophages in the same sections (Wang *et al.,* 1994). Volume density estimates for the peritubular and peri-epithelial macrophages were calculated using the total volume of the seminiferous tubule and rete duct compartments.

2.6 Statistical analysis

Data are presented as mean ± standard error of the mean (SEM). GraphPad Prism 9 software (GraphPad software Inc., La Jolla, CA) was used for all analyses. An unpaired t-test was used for all comparisons. Significant differences were identified at $p<0.05$.

3 Results

3.1 Distribution of macrophages in the rete testis, subcapsular region and tunica albuginea of the *Cx$_3$cr$_1^{GFP/+}$Inhba$^{+/+}$* adult mouse and human rete testis determined by immunohistochemistry and immunofluorescence

Histologically, macrophages were assigned by visual inspection to the interstitial tissue, and peritubular region in the testis parenchyma (here defined as the testis tissue, excluding the rete testis, subcapsular region and capsule), subcapsule and tunica albuginea. In the region of the rete testis, macrophages were assigned to the interstitial tissue (IT) or peri-epithelial (PE) regions. Numerous macrophages were identified in all compartments of the testis using the F4/80 and CX_3CR_1 markers (Fig. 1a, 1b, 1c and 1d). Notably, macrophages were considerably more numerous in the region of the rete testis than in the parenchyma. When total F4/80^{+} macrophages were quantified, the volume density of the rete testis interstitial and peri-epithelial macrophages was approximately 9-fold higher than that of the parenchymal interstitial and peritubular macrophages (Fig. 1e). Additionally, the density of macrophages in the SC was similar to IT macrophages in the parenchyma, but the tunica albuginea had a 2-fold higher density of macrophages than the SC (Fig. 1e). Macrophages within the human rete testis region (Fig. 1f, f') seemed to be similarly distributed to those of

the parenchyma, with a similar volume density in both rete testis and parenchyma. However, the human rete testis is much more extensive and contains a much larger proportion of interstitial tissue relative to the ducts than in the mouse.

3.2 Immunoregulatory macrophage phenotypes in the rete testis, subcapsule and tunica albuginea of the *Cx$_3$cr$_1^{GFP/+}$Inhba$^{+/+}$* adult mouse testis determined by immunofluorescence

The majority of interstitial macrophages in the rete testis were F4/80$^+$CX$_3$CR$_1^+$CD206$^+$ (Fig. 2a and a'') and F4/80$^+$CX$_3$CR$_1^+$MHCII$^+$ (Fig. 3a and a''), in contrast to the macrophage phenotypes (CD206$^+$ and MHCII$^{low/-}$) in the interstitium of the parenchyma testis (Fig. 2c, 2c'', 3c, 3c', 4c, and 4c'') (quantification is presented in Fig. 7d-i, Section 3.4). Consequently, most interstitial macrophages in the rete testis were both MHCII$^+$ and CD206$^+$, indicating a potentially immunoregulatory and tolerogenic phenotype (Fig. 4a and 4a''). Most F4/80$^+$CX$_3$CR$_1^+$ macrophages in the peri-epithelium of the rete testis were CD206$^+$ (Fig. 2a and 2a'). Moreover, a small number of F4/80$^+$ macrophages were both CD206$^+$ and MHCII$^+$ in the peri-epithelium of the rete testis (Fig. 4a and 4a'). Interestingly, peritubular macrophages surrounding the seminiferous tubules adjacent to the rete testis were predominantly CD206$^+$, compared with the peritubular macrophages more distal to the rete testis, which did not express CD206 (Fig. 2f and 2f'). Conversely, macrophages located in the interstitium around seminiferous tubules that were adjacent to the rete testis tubule expressed MHCII (Fig. 3f and 3f') more frequently than in the parenchyma (Fig. 3c). Several interstitial and peritubular macrophages co-expressed CD206 and MHCII in the seminiferous tubules adjacent to the rete testis (Fig. 4f, f' and f'').

Even though subcapsular macrophages were F4/80$^+$CX$_3$CR$_1^+$CD206$^+$ (Fig. 2b and b'), similar to interstitial macrophages in the parenchyma, they also expressed MHCII (Fig. 3b, 3b', 4b and 4b'). In the tunica albuginea, approximately half of the F4/80$^+$ macrophages were CX$_3$CR$_1^+$ and few co-expressed CD206 or MHCII (Fig. 2d, 3d and 4d). However, the capsule adjacent to the rete testis showed a higher density of F4/80$^+$ macrophages that were either MHCII$^+$, CD206$^+$ or co-expressed both these markers than the capsular region more distal to the rete testis (Fig. 2e, 3e and 4e).

3.3 Phenotypes of macrophages in the transition region and efferent ducts of the *Cx$_3$cr$_1^{GFP/+}$Inhba$^{+/+}$* adult mouse testis determined by immunofluorescence

Histological examination of an adult mouse testis longitudinal section highlights the transition region, a short structure between the seminiferous tubules and the rete testis (Fig. 5a, a' and a''). A valve-like structure is formed by the epithelial cells of the transition region as they project towards the rete testis and the basement membrane in this region is thicker than that of the adjacent ST (Fig. 5a''). The volume density of macrophages was higher in the interstitium within the transition region and decreased progressively away from this region (Fig. 5b, b'' and b'''). All interstitial macrophages were F4/80$^+$CX$_3$CR$_1^+$. Similar volume density results were obtained using F4/80, CX$_3$CR$_1$ and MHCII markers (Fig. 5c), where the density of interstitial macrophages was highest around the rete testis (Fig. 5c') and progressively declined with increasing distance from the TR (Fig. 5c'', 5c'''). Most notably, the interstitial macrophages around the rete testis were F4/80$^+$CX$_3$CR$_1^+$MHCII$^+$ (Fig 5c'), unlike the interstitial macrophages in the parenchyma, which were predominantly MHCII$^-$ or MHCII^{low}. Most interstitial macrophages around the rete testis and transition region were CD206$^+$ (Fig. 5d, d', d''). Most peri-epithelial macrophages in the rete testis and transition region were F4/80$^+$CX$_3$CR$_1^+$CD206$^+$, in contrast to very few F4/80$^+$CX$_3$CR$_1^+$ peritubular macrophages that were CD206$^+$ in the parenchyma (Fig 5d'''). Additionally, following co-labelling with CD45, the pan-leukocyte marker, most interstitial, and peritubular macrophages in the transition region were CX$_3$CR$_1^+$CD45$^{+/low}$F4/80$^+$ (supplementary Fig 1).

Macrophage phenotypes similar to those of the transition region were observed within the efferent ducts, where most intra-epithelial macrophages were either F4/80$^+$CX$_3$CR$_1^+$CD206$^+$ or F4/80$^+$CX$_3$CR$_1^+$MHCII$^+$ (Fig, 6a, a', b and b'); however, the interstitial macrophages were mostly CX$_3$CR$_1^-$ (i.e., F4/80$^+$CX$_3$CR$_1^-$MHCII$^+$ or F4/80$^+$CX$_3$CR$_1^-$CD206$^+$). In contrast to the testis and rete testis, macrophages in the efferent ducts were also located within the duct epithelium (Fig, 6a'' and 6b''), similar to the distribution of intra-epithelial macrophages in the caput epididymis (Da Silva and Barton, 2016, Da Silva and Smith, 2015). Additionally, most interstitial and peritubular macrophages in the efferent ducts were CX$_3$CR$_1^+$CD45$^{+/low}$F4/80$^+$ (supplementary Fig 1).

3.4 Quantification of macrophage phenotypes in the *Cx3cr1*$^{GFP/+}$*Inhba*$^{+/+}$ adult mouse testis

Having identified multiple macrophage subsets in the mouse testis by immunofluorescence using several antibody markers (F4/80, CX_3CR_1, CD206 and MHCII), detailed quantification of these subsets was undertaken. In the interstitial tissue, the volume density of F4/80$^+$ macrophages expressing CX_3CR_1 (32.4 ± 6.0 macrophages/μm^3) was significantly higher (10-fold; $p < 0.05$) in the rete testis than in the parenchyma (3.7 ± 0.2 macrophages/μm^3) (Fig. 7a and appendix Fig 1a). There was also a fraction of interstitial macrophages in the RT interstitium that were F4/80$^+$$CX_3CR_1^-$ (3.5 ± 0.3 macrophages/μm^3) than in the parenchyma (0.4 ± 0.04 macrophages/μm^3) (Fig. 7a and appendix fig 1a). Similarly, the F4/80$^+$ interstitial macrophages in the RT also expressed higher numbers of CD206 (14.5 ± 1.8 macrophages/μm^3) and MHCII (15.7 ± 2.5 macrophages/μm^3) than in the parenchyma (4.9 ± 0.5 macrophages/μm^3 and 0.2 ± 0.06 macrophages/μm^3 respectively) (Fig. 7d, 7g and appendix Fig. 1d, 1g). In the peri-epithelial region of the RT, most F4/80$^+$ macrophages were $CX_3CR_1^+$ (5.8 ± 0.9 macrophages/μm^3) or MHCII$^+$ (3.1 ± 0.5 macrophages/μm^3) (Fig. 7b, 7h and appendix figures 1b, 1h). Interestingly, the volume density of F4/80$^+$CD206$^+$ and F4/80$^+$CD206$^-$ macrophages in this region was almost equal, i.e., 3.1 ± 0.5 macrophages/μm^3 and 3.5 ± 0.7 macrophages/μm^3 respectively, confirming the visual observation (see section 3.2) indicating a changing immune environment in the RT (Fig. 7e and appendix figure 1e). When the SC and TA were compared, it was observed that the major subset of F4/80$^+$ macrophages in the SC were either $CX_3CR_1^+$ (2.9 ± 0.3 macrophages/μm^3) or CD206$^+$ (2.0 ± 0.3 macrophages/μm^3) (Fig. 7c, 7f and appendix figures 1c, 1f) but equal number of MHCII$^+$ and MHCII$^-$ phenotypes respectively (1.4 ± 0.3 macrophages/μm^3 and 1.1 ± 0.1 macrophages/μm^3) (Fig. 7c, 7f, 7i and appendix figures 1c, 1f, 1i). In contrast, the tunica albuginea had a higher volume density of $CX_3CR_1^-$ (3.8 ± 0.5 macrophages/μm^3), CD206$^-$ (2.9 ± 0.3 macrophages/μm^3) and MHCII$^+$ (2.7 ± 0.4 macrophages/μm^3) macrophages (Fig 7c, 7e, 7f and appendix figures 1c, 1e and 1f).

3.5 Effect of activin A-deficiency on macrophage number and phenotypes in the *Cx3cr1*$^{GFP/+}$ adult mouse

The mean testicular volume was 80.7 ± 5.7 mm^3 for *Cx3cr1*$^{GFP/+}$*Inhba*$^{+/+}$ (littermate control) mouse testes and was significantly reduced in *Cx3cr1*$^{GFP/+}$*Inhba*$^{+/-}$ mouse

testes to 63.5 ± 4.4 mm^3 (supplementary Fig. 1). The mean volumes of the individual compartments (interstitial and seminiferous tubule regions of the parenchyma, subcapsule and tunica albuginea) in *Cx3cr1*$^{GFP/+}$*Inhba*$^{+/+}$ (control) mice were 13.8 mm^3, 60.2 mm^3, 3.02 mm^3 and 2.36 mm^3, respectively, and although compartment volumes were slightly reduced, there was no statistically significant difference for any individual compartment. There was a significant increase ($p < 0.05$) in the volume density of both MHCII$^+$ (10%) and MHCII$^-$ macrophages (5%) in the interstitium of the rete testis from the activin-deficient (*Inhba*$^{+/-}$) mice (Fig. 8g). However, activin A deficiency had marginal or no significant effects on the expression of CX_3CR_1 or CD206 by macrophages in any compartment of the testis (Fig. 8a-f, appendix Fig. 2a-f). There was no corresponding increase in the volume density of peri-epithelial macrophages in the rete testis in the activin-deficient testis, but there was a significant ($p < 0.05$) reduction of 4% in the proportion of these macrophages that expressed MHCII (appendix Fig. 2h). Expression of MHCII was not affected by activin-deficiency in the subcapsule region or tunica albuginea.

3.6 Macrophage infiltration in testicular compartments following infection by Uropathogenic *E. coli* (UPEC)

At 10 days after UPEC infection, the rete testis compartment was filled with large numbers of $CX_3CR_1^+$F4/80$^+$MHCII$^+$ macrophages, the majority of which (~90%) were also CD206$^+$ (Fig. 9a, 9b and 9e). By 28 days after UPEC infection, the number of macrophages had largely returned to normal (Fig. 9c and d). A similar large increase in $CX_3CR_1^+$F4/80$^+$MHCII$^+$CD206$^+$ macrophage numbers was observed in the subcapsule region adjacent to the rete testis (Fig. 11a and 11b) and tunica albuginea (Fig. 12a and 12b) at 10 days after UPEC infection, but not at day 28 after infection (Fig 11c, 11d and 12c, 12d). In contrast, there was little change in the number of interstitial and peritubular macrophages in the parenchyma except that many F4/80$^+$ interstitial macrophages were MHCII$^+$ in the parenchyma at day 10 post-infection, compared to the usual MHCII^{low} or MHCII$^-$ phenotype of interstitial macrophages under normal conditions (Fig. 10b, 10d). The presence of small numbers of intraluminal macrophages that were F4/80$^+$MHCII$^+$CD206$^{low/-}$ (2-3 macrophages/rete testis) was also observed (Fig 9d’’’) in the day 10 UPEC-infected testis. These intraluminal cells were never observed in the rete testis of normal or sham control mice.

4 Discussion

The current study evaluated and quantified macrophage phenotypes in the testis parenchyma and less well-studied testicular compartments of the testis: the rete testis, subcapsular region, tunica albuginea, transition region, as well as the efferent ducts in adult mice. The most significant observation of the present study was that the volume density of F4/80$^+$ interstitial and peri-epithelial macrophages was considerably (up to 9-fold) higher in the rete testis than in the corresponding interstitial and peritubular regions of the parenchyma, and that these cells display a unique anti-inflammatory and activated phenotype indicated by co-expression of both CD206 and MHCII. Evidence suggests that this region lacks the effective blood-testis barrier normally maintained by the elaborate tight junctions between adjacent Sertoli cells (Major *et al.,* 2021). These macrophages might be present in higher numbers in this region as part of a mechanism to protect the sperm traveling from the seminiferous tubules to the epididymis or to protect the organ from ascending infections, or both.

CX_3CR_1 is a G-protein-coupled receptor expressed predominantly on mononuclear phagocytes, and in subsets of natural killer (NK) and T cells that may vary between species (Jung *et al.,* 2000). It recognizes the chemokine, CX3CL1 (fractalkine) and facilitates leukocyte adhesion and migration (Imai *et al.,* 1997). In adult $CX_3CR_1^{GFP/+}$ mice, $CX_3CR_1^+$ macrophages surround the seminiferous tubules and reside within the interstitium, implicating a role for fractalkine in their recruitment and regulation (DeFalco *et al.,* 2015). This observation was confirmed in the present study, the majority of macrophages expressing CX_3CR_1 in all testis compartments, with the exception of a significant population of macrophages lacking CX_3CR_1 expression in the peri-epithelial region of the rete testis and in the tunica albuginea, which are presumably not regulated by fractalkine. It will be interesting to study if these macrophages have the same origin as parenchymal macrophages.

CD206, a mannose-specific scavenger receptor, is a transmembrane glycoprotein that belongs to the C-type lectin family expressed predominantly by most tissue macrophages, dendritic cells (DCs) and selected lymphatic or liver endothelial cells (Taylor *et al.,* 2005). It is a characteristic marker of anti-inflammatory/M2 macrophage subsets, and CD206$^+$ macrophages also play an active role in the induction of T cell tolerance (Schuette *et al.,* 2016). In the testis, CD206$^+$MHCII$^-$ macrophages are associated with the vasculature and Leydig cells in the interstitium, while CD206$^-$

MHCII$^+$ macrophages are localized around the tubules and are suspected to respond to sperm auto-antigens through antigen presentation (Lokka *et al.,* 2020, DeFalco *et al.,* 2015). In the rete testis, however, the proportion of CD206$^+$ macrophages in the interstitium were 20% lower than in the parenchyma, while about half of the peri-epithelial macrophages were CD206$^+$. The proportion of interstitial macrophages expressing CD206 was also significantly lower in the subcapsule region, in comparison with the parenchyma. In contrast to the parenchyma, a majority of interstitial macrophages in the rete testis also expressed MHCII, while expression of MHCII by the peri-epithelial macrophages was similar to that of the peritubular compartment. More than half of the macrophages in the subcapsular region and tunica albuginea also expressed MHCII.

Altogether, these data indicate that there is a significant subset of macrophages that expresses both CD206 and MHCII in the interstitium and peri-epithelial regions of the rete testis, and in the subcapsule region These macrophages have yet to be functionally characterized, but would appear to be active antigen-presenting cells with an anti-inflammatory and/or tolerogenic function. The role of these macrophages in the onset of orchitis, which preferentially involves the subcapsular region and rete testis (Tung et al 1987), and in defense against ascending infections, also deserves further exploration.

The immune environment of the transition region associated with the transition region Sertoli cells (TRSCs) has not been studied before (Takahashi *et al.,* 2007, Figueiredo *et al.,* 2021). There was a notable increase in the expression of MHCII$^+$ of interstitial macrophages positioned near the transition region of a tubule in comparison to the macrophages adjacent to normal seminiferous tubules. This suggests that the immune environment in the transition region is intermediate between the rete testis and the parenchyma of the testis surrounding the seminiferous tubules. Similar intra-epithelial F4/80$^+$CX$_3$CR$_1^+$MHCII$^+$ and F4/80$^+$CX$_3$CR$_1^+$CD206$^+$ macrophages were observed in the efferent ducts leading to the epididymis. These macrophages were phenotypically similar to the rete testis macrophages, but in location and morphology were more similar to the intra-epithelial epididymal macrophages.

In chapter 2 (Biniwale et al 2022), it was shown that activin A regulates total macrophage numbers in the testis, although this could not be attributed to a significant

differential effect on any of the major macrophage subsets identified in the present study. However, activin A deficiency resulted in a significant increase in the volume density of both F4/80^{+}MHCII^{+} and F4/80^{+}MHCII^{-} interstitial macrophages, and a small, but significant, reduction in the proportion of MHCII^{+} peri-epithelial macrophages in the rete testis. Since transcript levels of MHCII and its co-stimulatory molecules CD80 and CD86 were increased in whole testis extracts of activin-deficient mice in the previous study, this suggests that activin A specifically regulates the number and antigen-presenting functions of macrophages in the rete testis. It would be worth studying whether production of activin A by cells in the rete testis is higher than that produced by cells in rest of the parenchyma to test this hypothesis.

During inflammation caused by infection, macrophage populations at the infected sites expand, both by rapid recruitment of blood monocytes and by proliferation of the resident macrophages (Wang *et al.,* 2021). The increase in F4/80^{+} interstitial macrophages in the parenchyma occurred at day 10 post UPEC infection in adult mice, a time-point when the infection was at its peak (Klein *et al.,* 2020). In the current study, there was an increase in F4/80^{+}CD206^{+}MHCII^{+} macrophages in the rete testis, the subcapsule and tunica albuginea at day 10 post-infection, which decreased by day 28. By contrast, there was little change in the macrophage population of the parenchyma. It may be proposed that the vasculature surrounding the rete testis serves as a port of entry for the infiltration of macrophages into the testis, which then spread to the subcapsule and tunica albuginea, but with minimal spread into the parenchyma or due to an increase in proliferation of the resident macrophages. However, it was observed that many F4/80^{+} interstitial macrophages were MHCII^{+} in the parenchyma at day 10 post-infection, compared to the usual MHCII^{low} or MHCII^{-} phenotype of interstitial macrophages under normal conditions (Lokka *et al.,* 2020).

As in the mouse, CD68^{+} Interstitial and peritubular macrophages were found throughout the human rete testis, as has been reported previously, but their volume density was similar to other regions of the human testis (Fietz and Bergmann, 2017). This may be due to the much larger structure of the rete testis, with more extensive interstitial tissue, in the human testis. Whether the functional phenotype of these macrophages in the human rete testis is similar to those of the mouse rete testis deserves further investigation.

In conclusion, this study has identified new macrophage populations in the testicular compartments that have received little attention in the past - the rete testis, subcapsule and the tunica albuginea - and indicated that the phenotype of the macrophages and therefore, most likely, the immune environment in these compartments is different from the rest of the testis. These macrophages may play an important role in maintaining tolerance and providing immunoprotection of the sperm, as opposed to the parenchymal macrophages that appear to be mainly involved in suppressing inflammation and regulating spermatogenesis and steroidogenesis.

Acknowledgements

The authors thank Angela Vais (immunofluorescent slide scanning using Olympus VS120 slide scanner) and Paula Gillis (cryotomy containing rete testis sections) from the Monash Histology Platform without whom this project would not have been possible.

Funding information

The research was supported by a grant from the National Health and Medical Research Council of Australia (Grant # APP1184867 to MPH) and the grants from Monash University and Deutsche Forschungsgemeinschaft (DFG) to the International Research Training Group (IRTG) on 'Molecular pathogenesis of male reproductive disorders' between JLU Giessen and Monash University (GRK 187/1), and the Victorian Government's Operational Infrastructure Support Programme.

Declaration of interest

None

Author contributions

SB (Sneha Biniwale) – tissue collection, performing experiments, study design, data analysis, manuscript writing; RW - technical and scientific guidance, critical review of the manuscript; CP and SB (Sudhanshu Bhushan) – UPEC infection experiments: KAL and AM – collection of human material, technical and scientific guidance, critical review of the manuscript; MH - study design, technical and scientific guidance, and critical review of the manuscript.

References

Aiyama, Y., Tsunekawa, N., Kishi, K., Kawasumi, M., Suzuki, H., Kanai-Azuma, M., Kurohmaru, M. & Kanai, Y. 2015. A Niche for GFRα1-Positive Spermatogonia in the Terminal Segments of the Seminiferous Tubules in Hamster Testes. *Stem Cells,* 33**,** 2811-2824.

Bankhead, P., Loughrey, M. B., Fernández, J. A., Dombrowski, Y., Mcart, D. G., Dunne, P. D., Mcquaid, S., Gray, R. T., Murray, L. J., Coleman, H. G., James, J. A., Salto-Tellez, M. & Hamilton, P. W. 2017. QuPath: Open source software for digital pathology image analysis. *Scientific Reports,* 7**,** 16878.

Biniwale, S., Wijayarathna, R., Pleuger, C., Bhushan, S., Loveland, K. L., Meinhardt, A. & Hedger, M. P. 2022. Regulation of macrophage number and gene transcript levels by activin A and its binding protein, follistatin, in the testes of adult mice. *Journal of Reproductive Immunology,* 151**,** 103618.

Da Silva, N. & Barton, C. R. 2016. Macrophages and dendritic cells in the post-testicular environment. *Cell and Tissue Research,* 363**,** 97-104.

Da Silva, N. & Smith, T. B. 2015. Exploring the role of mononuclear phagocytes in the epididymis. *Asian Journal Of Andrology,* 17**,** 591.

Davies, L. C., Rosas, M., Jenkins, S. J., Liao, C.-T., Scurr, M. J., Brombacher, F., Fraser, D. J., Allen, J. E., Jones, S. A. & Taylor, P. R. 2013. Distinct bone marrow-derived and tissue-resident macrophage lineages proliferate at key stages during inflammation. *Nature Communications,* 4**,** 1-10.

Defalco, T., Bhattacharya, I., Williams, A. V., Sams, D. M. & Capel, B. 2014. Yolk-sac–derived macrophages regulate fetal testis vascularization and morphogenesis. *Proceedings of the National Academy of Sciences of the United States of America,* 111**,** E2384-E2393.

Defalco, T., Potter, S. J., Williams, A. V., Waller, B., Kan, M. J. & Capel, B. 2015. Macrophages Contribute to the Spermatogonial Niche in the Adult Testis. *Cell Reports,* 12**,** 1107-1119.

Dym, M. 1974. The fine structure of monkey Sertoli cells in the transitional zone at the junction of the seminiferous tubules with the tubuli recti. *American Journal of Anatomy,* 140**,** 1-25.

Fietz D. and Bergmann M. 2017. Functional anatomy and histology of the testis. *In:* Simoni, M. & Huhtaniemi, I.T. (eds.) *Endocrinology of the testis and male reproduction.* Cham Switzerland: Springer International Publishing, 313-341.

Figueiredo, A. F. A., Hess, R. A., Batlouni, S. R., Wnuk, N. T., Tavares, A. O., Abarikwu, S. O., Costa, G. M. J. & França, L. R. 2021. Insights into differentiation and function of the transition region between the seminiferous tubule and rete testis. *Differentiation,* 120**,** 36-47.

Fong, A. M., Robinson, L. A., Steeber, D. A., Tedder, T. F., Yoshie, O., Imai, T. & Patel, D. D. 1998. Fractalkine and CX3CR1 mediate a novel mechanism of leukocyte capture, firm adhesion, and activation under physiologic flow. *Journal of Experimental Medicine,* 188**,** 1413-1419.

Grubman, A., Choo, X. Y., Chew, G., Ouyang, J. F., Sun, G., Croft, N. P., Rossello, F. J., Simmons, R., Buckberry, S., Landin, D. V., Pflueger, J., Vandekolk, T. H., Abay, Z., Zhou, Y., Liu, X., Chen, J., Larcombe, M., Haynes, J. M., Mclean, C., Williams, S., Chai, S. Y., Wilson, T., Lister, R., Pouton, C. W., Purcell, A. W., Rackham, O. J. L., Petretto, E. & Polo, J. M. 2021. Transcriptional signature in microglia associated with Aβ plaque phagocytosis. *Nature Communications,* 12**,** 3015.

Hess, R. A. 2002. The efferent ductules: structure and functions. In: Robaire, B & Hinton, B. T. (eds) *The epididymis: from molecules to clinical practice: A comprehensive Survey of the Effeent ducts, the Epididymis and the Vas Deferens.* Boston, MA: Springer US, 49-80.

Hume, D. A., Halpin, D., Charlton, H. & Gordon, S. 1984. The mononuclear phagocyte system of the mouse defined by immunohistochemical localization of antigen F4/80: Macrophages of endocrine organs. *Proceedings of the National Academy of Sciences of the United States of America,* 81**,** 4174-4177.

Imai, T., Hieshima, K., Haskell, C., Baba, M., Nagira, M., Nishimura, M., Kakizaki, M., Takagi, S., Nomiyama, H., Schall, T. J. & Yoshie, O. 1997. Identification and Molecular Characterization of Fractalkine Receptor CX3CR1, which Mediates Both Leukocyte Migration and Adhesion. *Cell,* 91**,** 521-530.

Indumathy, S., Pueschl, D., Klein, B., Fietz, D., Bergmann, M., Schuppe, H. C., Da Silva, N., Loveland, B. E., Hickey, M. J., Hedger, M. P. & Loveland, K. L. 2020. Testicular immune cell populations and macrophage polarisation in adult male mice and the influence of altered activin A levels. *Journal of Reproductive Immunology,* 142**,** 103204.

Itoh, M., Hiramine, C. & Hojo, K. 1991. A new murine model of autoimmune orchids induced by immunization with viable syngeneic testicular germ cells alone. I. Immunological and histological studies. *Clinical & Experimental Immunology,* 83**,** 137-142.

Itoh, M., Xie, Q., Miyamoto, K. & Takeuchi, Y. 1999. F4/80-positive cells rapidly accumulate around tubuli recti and rete testis between 3 and 4 weeks of age in the mouse: an immunohistochemical study. *American Journal of Reproductive Immunology,* 42**,** 321-326.

Jenkins, S. J., Ruckerl, D., Cook, P. C., Jones, L. H., Finkelman, F. D., Van Rooijen, N., Macdonald, A. S. & Allen, J. E. 2011. Local macrophage proliferation, rather than recruitment from the blood, is a signature of TH2 inflammation. *Science,* 332**,** 1284-1288.

Jung, S., Aliberti, J., Graemmel, P., Sunshine, M. J., Kreutzberg, G. W., Sher, A. & Littman, D. R. 2000. Analysis of Fractalkine Receptor CX3CR1 Function by Targeted Deletion and Green Fluorescent Protein Reporter Gene Insertion. *Molecular and Cellular Biology,* 20**,** 4106-4114.

Klein, B., Bhushan, S., Günther, S., Middendorff, R., Loveland, K. L., Hedger, M. P. & Meinhardt, A. 2020. Differential tissue-specific damage caused by bacterial epididymo-orchitis in the mouse. *Molecular Human Reproduction,* 26**,** 215-227.

Klein, B., Haggeney, T., Fietz, D., Indumathy, S., Loveland, K. L., Hedger, M., Kliesch, S., Weidner, W., Bergmann, M. & Schuppe, H.-C. 2016. Specific immune cell and cytokine characteristics of human testicular germ cell neoplasia. *Human Reproduction,* 31**,** 2192-2202.

Kulibin, A. Y. & Malolina, E. A. 2020. Formation of the rete testis during mouse embryonic development. *Developmental Dynamics,* 249**,** 1486-1499.

Lokka, E., Lintukorpi, L., Cisneros-Montalvo, S., Mäkelä, J.-A., Tyystjärvi, S., Ojasalo, V., Gerke, H., Toppari, J., Rantakari, P. & Salmi, M. 2020. Generation, localization and functions of macrophages during the development of testis. *Nature Communications,* 11**,** 4375.

Major, A. T., Estermann, M. A. & Smith, C. A. 2021. Anatomy, Endocrine Regulation and Embryonic Development of the Rete Testis. *Endocrinology*, 162.

Malolina, E. A. & Kulibin, A. Y. 2019. The rete testis harbors Sertoli-like cells capable of expressing DMRT1. *Reproduction,* 158**,** 399-413.

Matzuk, M. M., Kumar, T. R., Bicjenbach, J. R., Vassalli, A., Roop, D. R., Jaenisch, R. & Bradley, A. 1995c. Functional analysis of activins during mammalian development. *Nature,* 374**,** 354-356.

Mendis, S. H. S., Meachem, S. J., Sarraj, M. A. & Loveland, K. L. 2011. Activin A Balances Sertoli and Germ Cell Proliferation in the Fetal Mouse Testis1. *Biology of Reproduction,* 84**,** 379-391.

Michel, V., Duan, Y., Stoschek, E., Bhushan, S., Middendorff, R., Young, J. M., Loveland, K. L., de Kretser, D. M., Hedger, M. P. & Meinhardt, A. 2016. Uropathogenic Escherichia coli causes fibrotic remodelling of the epididymis. *The Journal of Pathology,* 240**,** 15-24.

Mossadegh-Keller, N., Gentek, R., Gimenez, G., Bigot, S., Mailfert, S. & Sieweke, M. H. 2017. Developmental origin and maintenance of distinct testicular macrophage populations. *The Journal of Experimental Medicine,* 214**,** 2829-2841.

Naito, M., Terayama, H., Hirai, S., Qu, N., Kawata, S. & Itoh, M. 2009. Histopathology of the tubuli recti at the start of experimental autoimmune orchitis in mice. *Medical Molecular Morphology,* 42**,** 230-235.

Schuette, V., Embgenbroich, M., Ulas, T., Welz, M., Schulte-Schrepping, J., Draffehn, A. M., Quast, T., Koch, K., Nehring, M., König, J., Zweynert, A., Harms, F. L., Steiner, N., Limmer, A., Förster, I., Berberich-Siebelt, F., Knolle, P. A., Wohlleber, D., Kolanus, W., Beyer, M., Schultze, J. L. & Burgdorf, S. 2016. Mannose receptor induces T-cell tolerance via inhibition of CD45 and up-regulation of CTLA-4. *Proc Proceedings of the National Academy of Sciences U S A,* 113**,** 10649-54.

Takahashi, K., Naito, M., Terayama, H., Qu, N., Cheng, L., Tainosho, S. & Itoh, M. 2007. Immunomorphological aspects of the tubuli recti and the surrounding interstitium in normal mice. *International Journal Of Andrology,* 30**,** 21-27.

Taylor, P. R., Martinez-Pomares, L., Stacey, M., Lin, H.-H., Brown, G. D. & Gordon, S. 2005. Macrophage receptors and immune recognition. *Annual review of immunology,* 23**,** 901-944.

Tung, K. S., Yule, T. D., Mahi-Brown, C. A. & Listrom, M. B. 1987. Distribution of histopathology and Ia positive cells in actively induced and passively transferred experimental autoimmune orchitis. *The Journal of Immunology,* 138**,** 752-759.

Wang, J., Wreford, N. G. M., Lan, H. Y., Atkins, R. & Hedger, M. P. 1994. Leukocyte Populations of the Adult Rat Testis Following Removal of the Leydig- Cells by Treatment with Ethane Dimethane Sulfonate and Subcutaneous Testosterone Implants. *Biology of Reproduction,* 51**,** 551-561.

Wang, M., Yang, Y., Cansever, D., Wang, Y., Kantores, C., Messiaen, S., Moison, D., Livera, G., Chakarov, S. & Weinberger, T., Stremmel, C., Fijak, M., Klein, B., Pleuger, C., Lian, Z., Ma, W., Liu, Q., Klee, K., Händler, K., Ulas, T., Schlitzer, A., Schultze, J. L., Becher, B., Greter, M., Liu, Z., Ginhoux, F., Epelman, S., Schulz, C., Meinhardt, A. & Bhushan, S. 2021. Two populations of self-maintaining monocyte-independent macrophages exist in adult epididymis and testis. *Proceedings of the National Academy of Sciences USA,* 118.

Wijayarathna, R. & de Kretser, D. M. 2016. Activins in reproductive biology and beyond. *Human Reproduction Update,* 22**,** 342-357.

Wijayarathna, R., de Kretser, D. M., Sreenivasan, R., Ludlow, H., Middendorff, R., Meinhardt, A., Loveland, K. L. & Hedger, M. P. 2018. Comparative analysis of activins A and B in the adult mouse epididymis and vas deferens. *Reproduction,* 155**,** 15-23.

Figure 1:

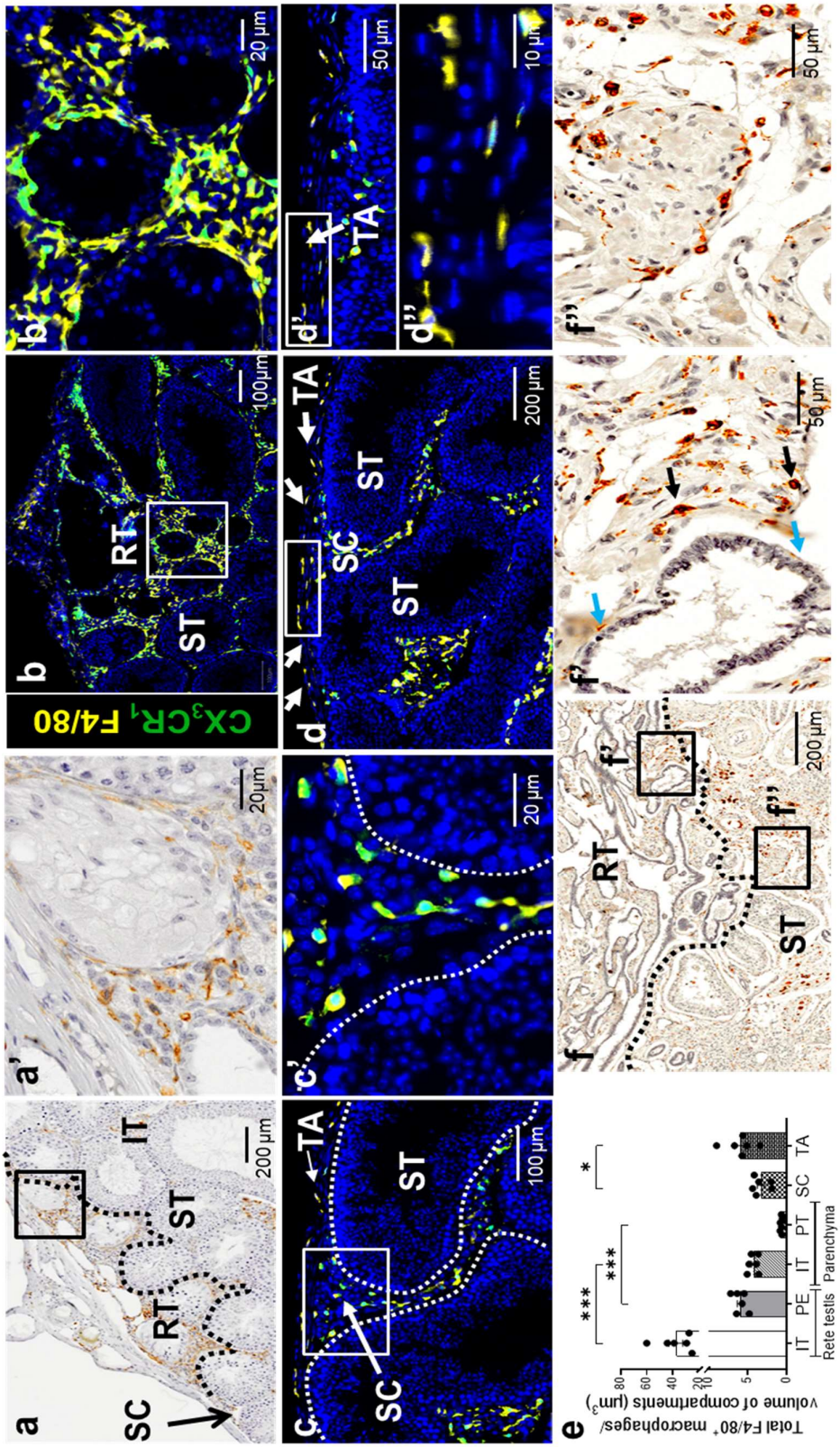
a
SC
RT
ST
IT
200 µm
a'
20µm
b
RT
ST
100µm
CX3CR1 F4/80
b'
20 µm
c
SC
TA
ST
100 µm
c'
20 µm
d
SC
TA
ST
200 µm
d'
TA
50 µm
d''
10 µm
e
Total F4/80+ macrophages/ volume of compartments (µm3)
***
***
*
IT
PE
IT
PT
SC
TA
Rete testis
Parenchyma
f
RT
ST
f'
f''
200 µm
f'
50 µm
f''
50 µm

Figure 1: *Localization of macrophages in different compartments of the adult mouse and human testis.* ***a and a')*** *Immunohistochemical localization of F4/80^{+} macrophages in the interstitial tissue (IT), seminiferous tubules (ST), subcapsular interstitial tissue (SC), capsule/tunica albuginea (TA) and rete testis (RT) of the adult $Cx_3cr_1^{GFP/+}Inhba^{+/+}$ mouse testis. Broken line indicates the border of the RT region. Panels a', b', c', d'', f' and f'' are higher power images of the enclosed box from the preceding corresponding panel.* ***b and b')*** *Immunofluorescence localization of CX_3CR_1 and F4/80^{+} in interstitial and peri-epithelial macrophages in the rete testis and parenchyma of the $Cx_3cr_1^{GFP/+}$ adult mouse testis.* ***c and c', d and d')*** *Immunofluorescence localization of F4/80 and CX_3CR_1 macrophages in the subcapsule region and tunica albuginea (TA) of the $Cx_3cr_1^{GFP/+}$ adult mouse testis. Broken line indicates the peritubular border of the ST. Arrow in panel c indicates the SC region. Arrows in panel d and d' indicate the TA region.* ***e)*** *Volume density of macrophages in all compartments of the mouse testis; PE: peri-epithelial.* ***f, f', f'')*** *Localization of CD68^{+} macrophages in the rete testis and parenchyma of the adult human testis. Broken line indicates the border of the RT region. *p<0.05; ***p<0.001, ****p<0.0001; all other comparisons were not significantly different (p>0.05).*

Figure 2:

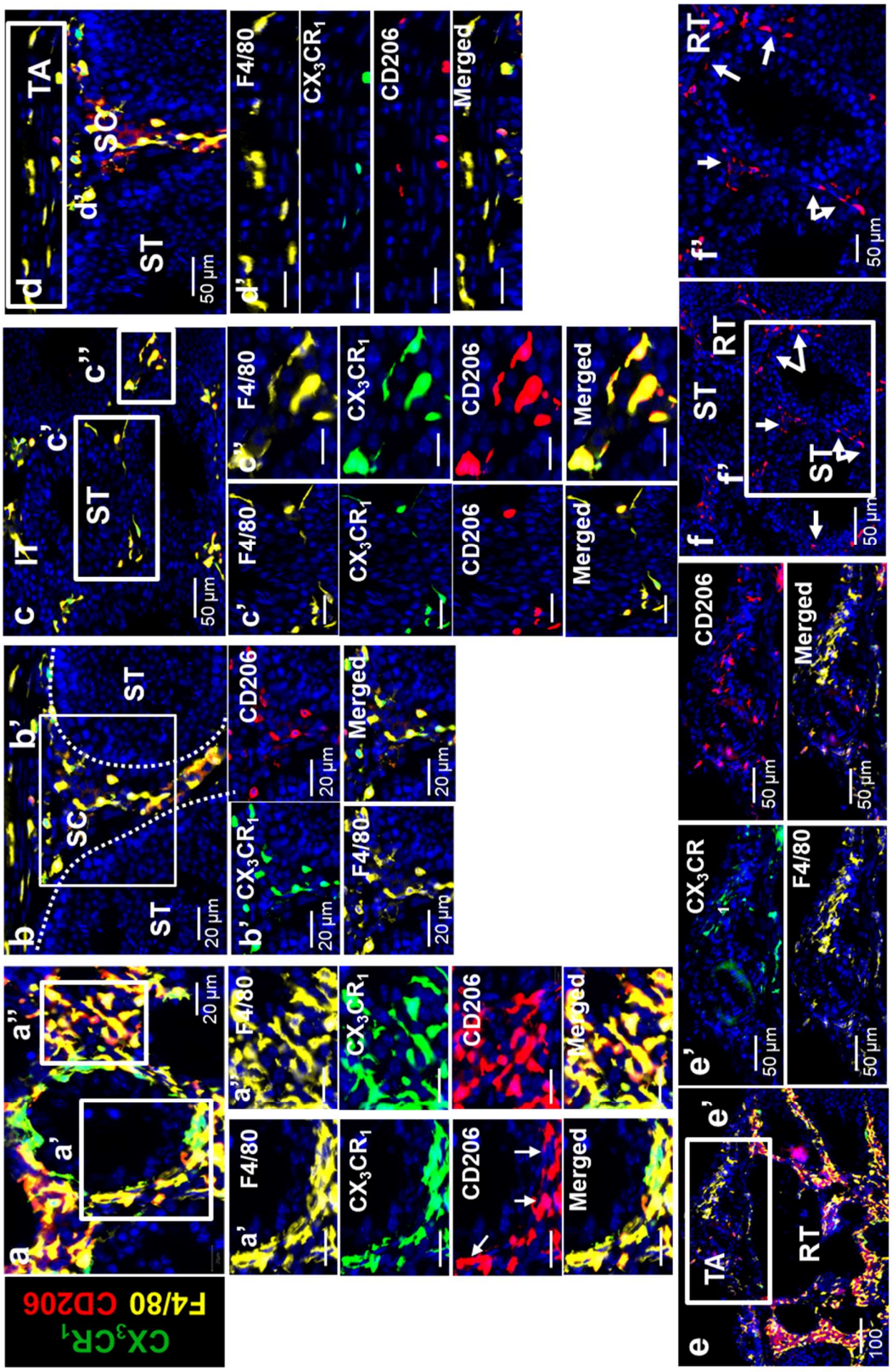
CX3CR1
F4/80 CD206
a
a'
a''
b
b'
c
c'
c''
d
d'
e
e'
f
f'
TA
ST
SC
RT
F4/80
CX3CR1
CD206
Merged
20 µm
50 µm
100

Figure 2: *Distribution and quantification of macrophages in testicular compartments of adult $Cx_3cr_1^{GFP/+}Inhba^{+/+}$ mouse using F4/80 (yellow), CX_3CR_1 (green) and CD206 (red) markers where the adult testis was compartmentalized into interstitial tissue (IT) and seminiferous tubules (ST) of parenchyma, subcapsular interstitial tissue (SC), tunica albuginea (TA) and the rete testis (RT). Panels a', a'', b', c', c'', d', e' and f' are higher power images of the enclosed box from the preceding corresponding panel.* ***a)*** *Peri-epithelial and interstitial tissue of the rete testis.* ***b)*** *Subcapsule.* ***c)*** *Parenchymal interstitium and peritubular regions.* ***d)*** *Tunica albuginea.* ***e)*** *Tunica albuginea adjacent to the rete testis.* ***f)*** *Parenchyma adjacent to the rete testis.*

Figure 3:

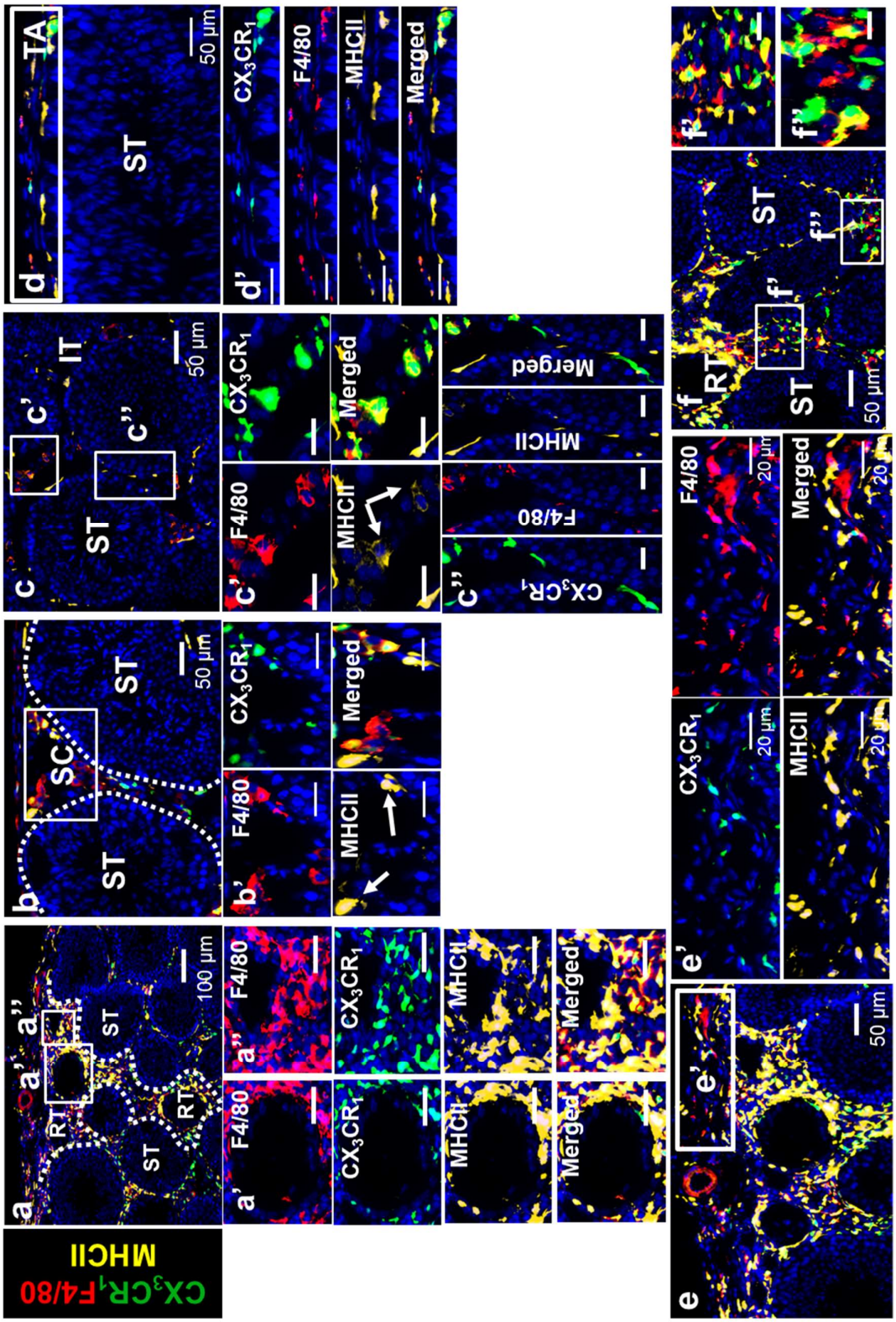
CX3CR1F4/80
MHCII
a
a'
a''
RT
ST
100 µm
b
SC
50 µm
c
c'
c''
IT
d
TA
e
e'
20 µm
f
f'
f''
F4/80
CX3CR1
MHCII
Merged

Figure 3: *Distribution and quantification of macrophages in testicular compartments of adult $Cx_3cr_1^{GFP/+}Inhba^{+/+}$ mouse using F4/80 (red), CX_3CR_1 (green) and MHCII (yellow) markers where the adult testis was compartmentalized into interstitial tissue (IT) and seminiferous tubules (ST) of parenchyma, subcapsular interstitial tissue (SC), tunica albuginea (TA) and the rete testis (RT). Panels a', a'', b', c', d', e' and f' are higher power images of the enclosed box from the preceding corresponding panel.* ***a)*** *Peri-epithelial and interstitial tissue of the rete testis.* ***b)*** *Subcapsule.* ***c)*** *Parenchymal interstitium and peritubular regions.* ***d)*** *Tunica albuginea.* ***e)*** *Tunica albuginea adjacent to the rete testis.* ***f)*** *Parenchyma adjacent to the rete testis.*

Figure 4:

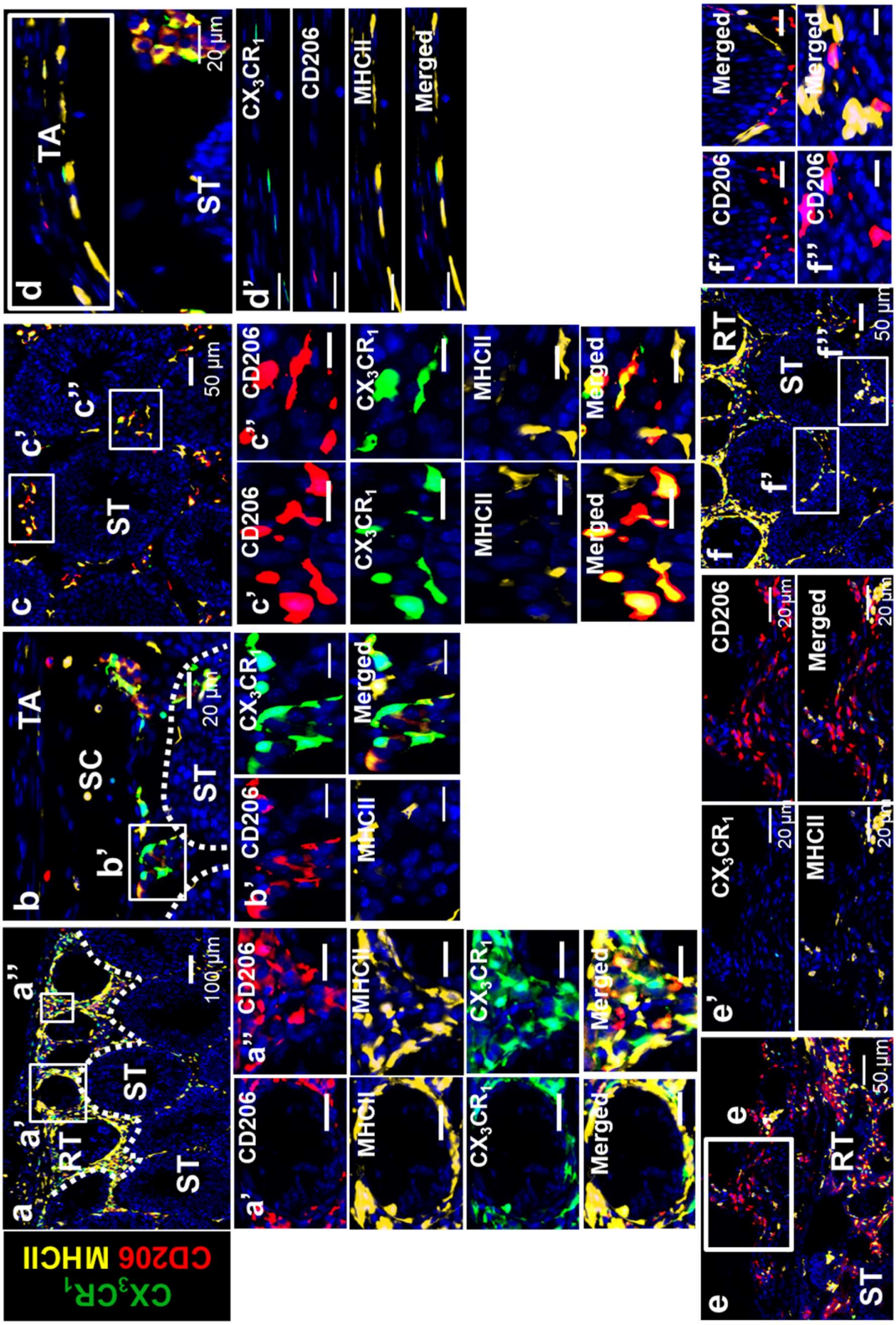
CX3CR1
CD206 MHCII
a
a'
a''
RT
ST
ST
100 µm
b
b'
TA
SC
ST
20 µm
c
c'
c''
ST
50 µm
d
d'
TA
ST
20 µm
CX3CR1
CD206
MHCII
Merged
e
e'
RT
ST
50 µm
20 µm
f
f'
f''
RT
ST
50 µm

Figure 4: *Distribution of macrophages in testicular compartments of adult* $Cx_3cr_1^{GFP/+}Inhba^{+/+}$ *mouse using CD206 (red),* CX_3CR_1 *(green) and MHCII (yellow) markers where the adult testis was compartmentalized into interstitial tissue (IT) and seminiferous tubules (ST) of parenchyma, subcapsular interstitial tissue (SC), tunica albuginea (TA) and the rete testis (RT). Panels a', a'', b', c', d', e', f' and f'' are higher power images of the enclosed box from the preceding corresponding panel.* ***a)*** *Peri-epithelial and interstitial tissue of the rete testis.* ***b)*** *Subcapsule.* ***c)*** *Parenchymal interstitium and peritubular regions.* ***d)*** *Tunica albuginea.* ***e)*** *Tunica albuginea adjacent to the rete testis.* ***f)*** *Parenchyma adjacent to the rete testis.*

Figure 5:

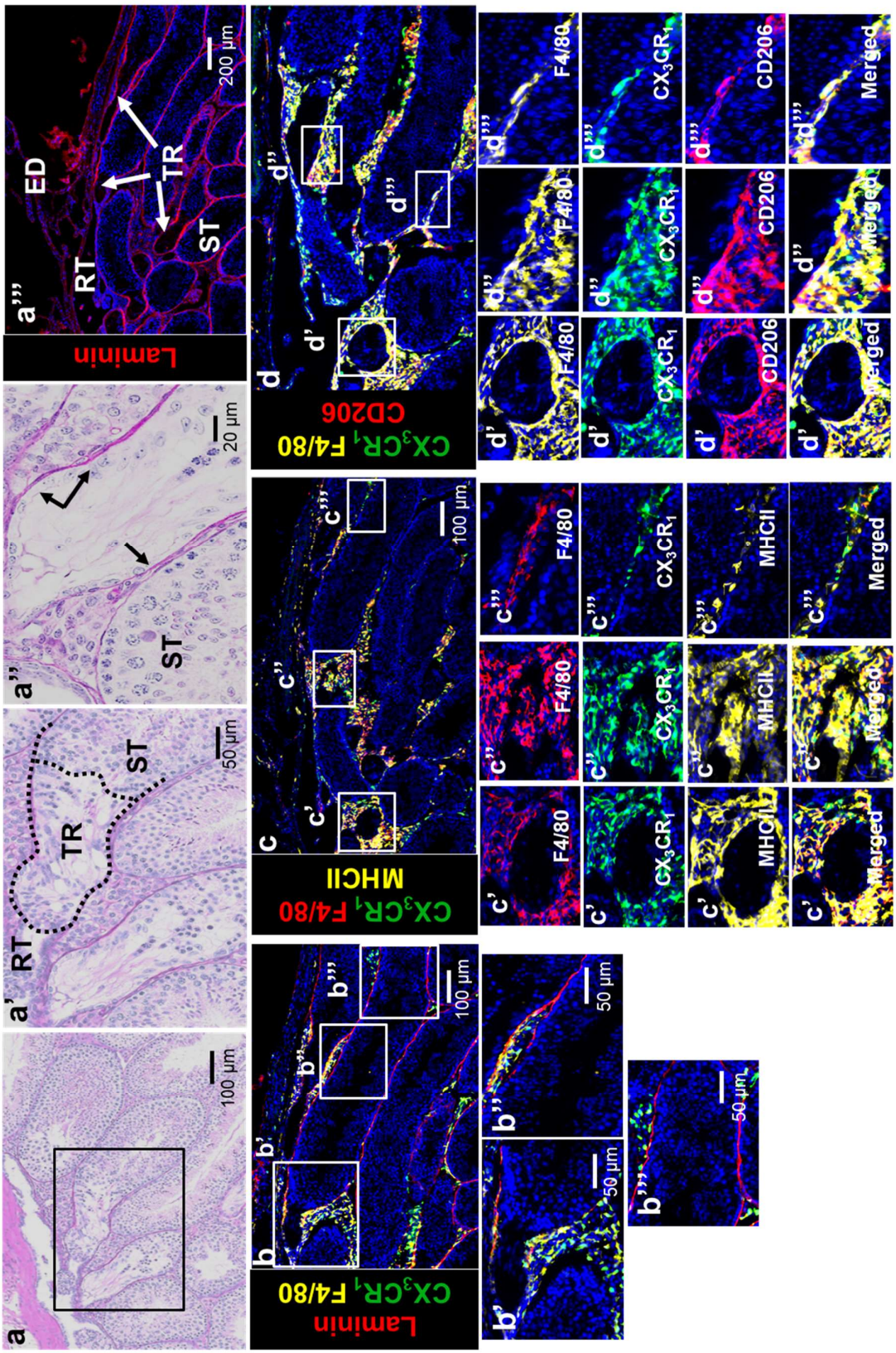
a
a'
RT
TR
ST
100 µm
50 µm
a''
ST
20 µm
a'''
Laminin
ED
RT
TR
ST
200 µm
b
b'
b''
b'''
Laminin CX3CR1 F4/80
100 µm
50 µm
50 µm
c
c'
c''
c'''
CX3CR1 F4/80 MHCII
100 µm
F4/80
CX3CR1
MHCII
Merged
d
d'
d''
d'''
CX3CR1 F4/80 CD206
F4/80
CX3CR1
CD206
Merged

Figure 5: *Macrophage distribution and phenotypes in the transition region (TR) of adult $CX_3CR_1^{GFP/+}Inhba^{+/+}$ mouse testis using CX_3CR_1, F4/80, MHCII and CD206 markers where compartments were distinguished as seminiferous tubules (ST), subcapsular interstitial tissue (SC), transition region (TR), rete testis (RT) and efferent ducts (ED) in $Cx_3cr_1^{GFP/+}$ adult mouse testis. Panels a', a'', a''', b', b'', b''', c', c'', c''', d', d'' and d''' are higher power images of the enclosed box from the preceding corresponding panel.* ***a, a', a'', a''')*** *PAS and laminin staining of adult mouse testis section shows the transition region (boxed and marked with dotted line) and by white arrows.* ***b)*** *Distribution of macrophages around TR (shown by box and magnified image b'), center of normal seminiferous tubule (shown by box and magnified image b'') and the region away from TR (shown by box and magnified image b''') using macrophage markers (CX_3CR_1 – green; F4/80 - yellow), basement membrane marker (laminin - red) and nuclei (DAPI-blue).* ***c)*** *Distribution of macrophages around the rete testis (RT) (shown by box and magnified image c'), normal seminiferous tubule near the TR (shown by box and magnified image c'') and the region surrounding TR (shown by box and magnified image c''') using macrophage markers (F4/80 – red; CX_3CR_1 – green, MHCII - yellow) and nuclei (DAPI-blue).* ***d)*** *Distribution of macrophages around the TR using macrophage markers (F4/80 – yellow; CX_3CR_1 – green, CD206 - red) and nuclei (DAPI-blue) shows rete testis (d') Transition region (d''), parenchymal interstitium (d''').*

Figure 6:

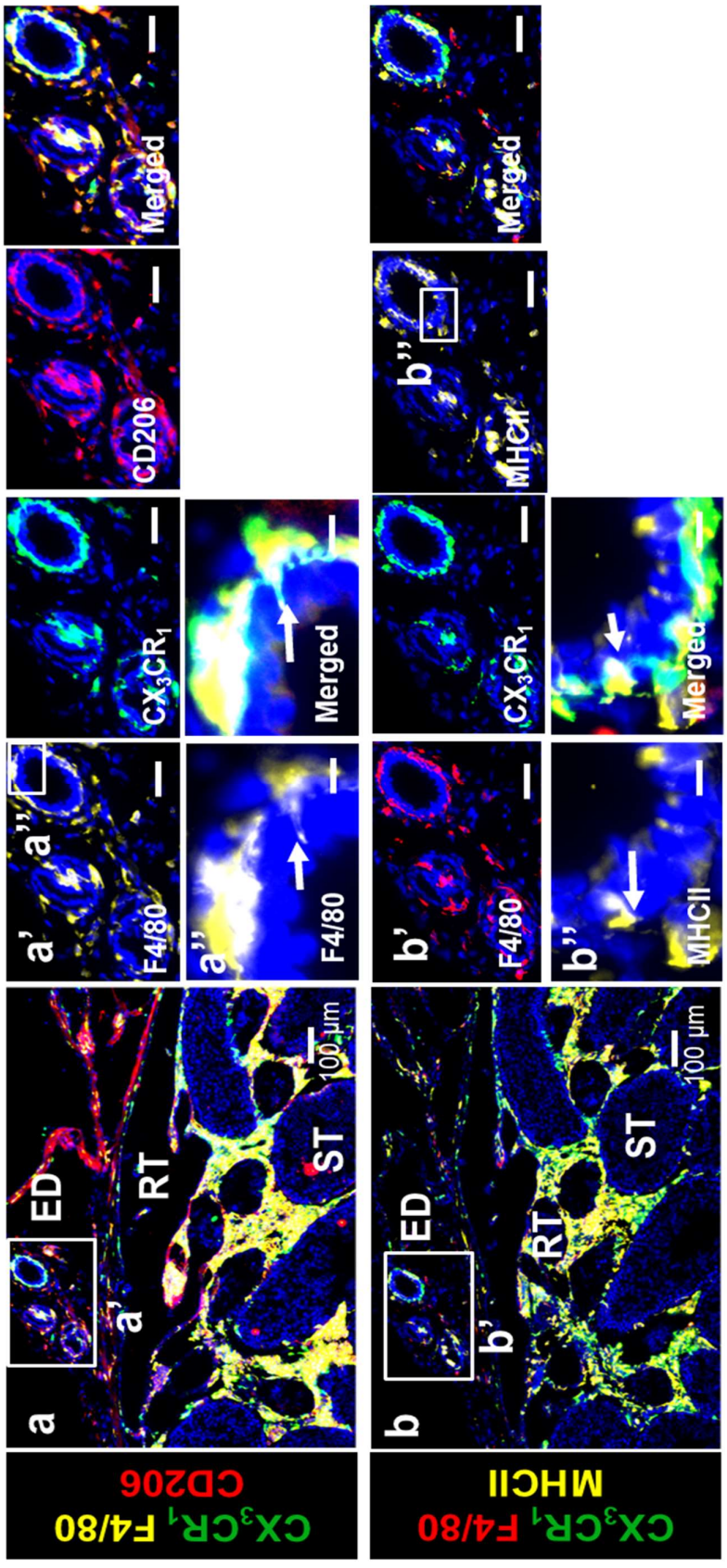
CX3CR1 F4/80
CD206
CX3CR1 F4/80
MHCII
a
a'
a''
b
b'
b''
ED
RT
ST
100 µm
F4/80
CX3CR1
CD206
MHCII
Merged

Figure 6: *Macrophage distribution and phenotypes in the efferent ducts (ED) where compartments were distinguished as seminiferous tubules (ST), subcapsular interstitial tissue (SC), rete testis (RT) and efferent ducts (ED) in* $Cx_3cr_1^{GFP/+}Inhba^{+/+}$ *adult mouse testis in a longitudinal cryosection (10µm).* ***a)*** *Macrophage phenotypes in the efferent ducts of adult mouse testis using markers for macrophages (*CX_3CR_1*, F4/80, CD206) and nuclei (DAPI) where a' and a'' shows interstitial and intraepithelial macrophage subsets.* ***b)*** *Macrophage phenotypes in the efferent ducts of adult mouse testis using markers for macrophages (*CX_3CR_1*, F4/80, MHCII) and nuclei (DAPI) where b' and b'' shows interstitial and intraepithelial macrophage subsets. Scale bar at 20µm (a' and b'), 5µm (a'' and b'').*

Figure 7:

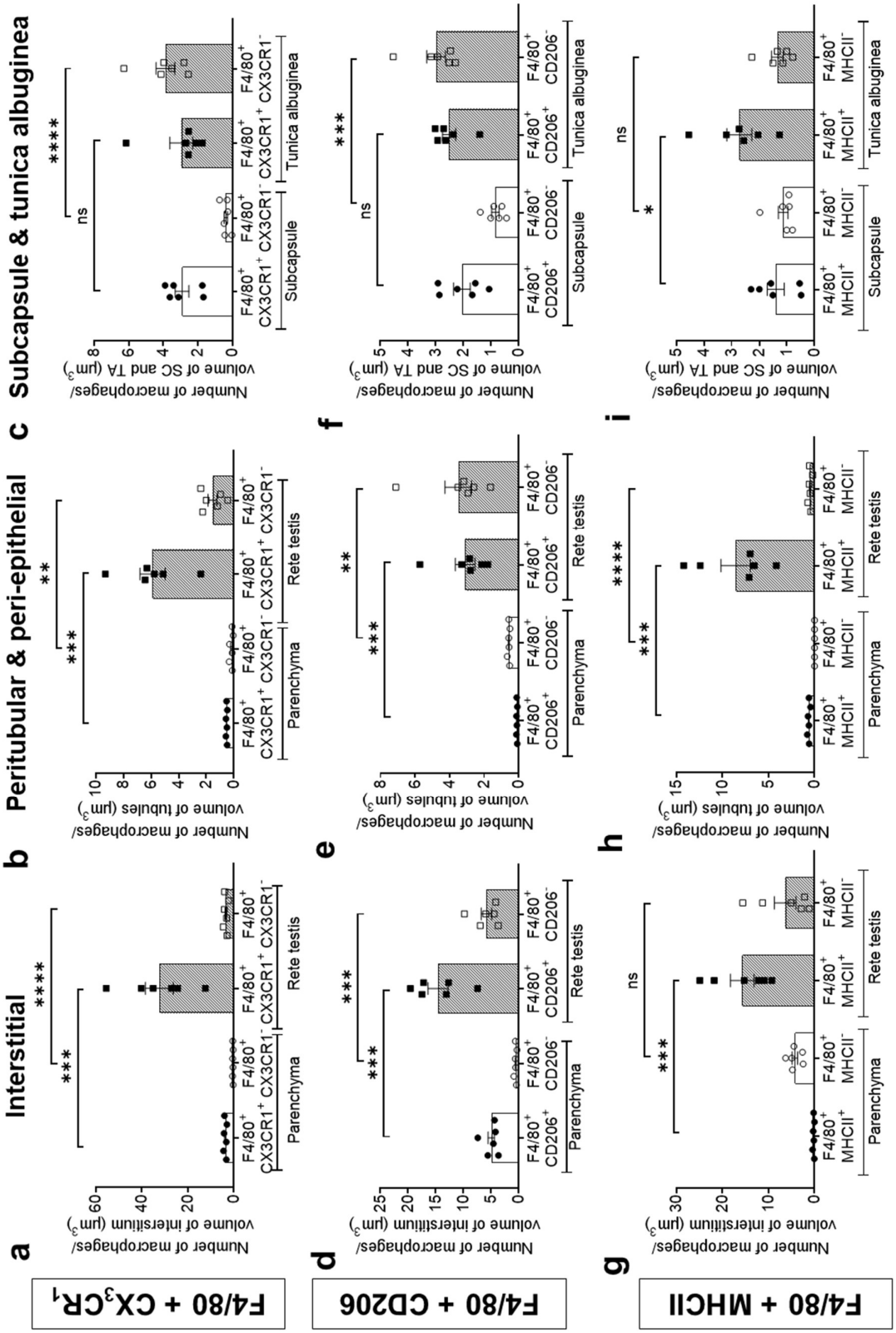
a
Interstitial
b
Peritubular & peri-epithelial
c
Subcapsule & tunica albuginea
F4/80 + CX3CR1
d
e
f
F4/80 + CD206
g
h
i
F4/80 + MHCII
Number of macrophages/ volume of interstitium (µm3)
Number of macrophages/ volume of tubules (µm3)
Number of macrophages/ volume of SC and TA (µm3)
F4/80+ CX3CR1+ CX3CR1- CX3CR1-
F4/80+ CX3CR1- CX3CR1+ CX3CR1-
F4/80+ CX3CR1- CX3CR1- CX3CR1-
F4/80+ CD206+ CD206-
F4/80+ MHCII+ MHCII-
Parenchyma
Rete testis
Subcapsule
Tunica albuginea
ns
*
**
***
****

Figure 7: *Quantification of macrophages in testicular compartments of adult $Cx_3cr_1^{GFP/+}Inhba^{+/+}$ mouse using CX_3CR_1 and F4/80 markers (**a, b, c**) F4/80 and CD206 markers (**d, e, f**) and F4/80 and MHCII markers (**g, h, i**), where the testis section was compartmentalized into interstitial tissue (IT) and seminiferous tubules (ST) of parenchyma, subcapsular interstitial tissue (SC), tunica albuginea (TA) and the rete testis (RT) was divided into interstitium (IT) and peri-epithelium (PE). Panels a, b, d, e, g and h compare parenchyma and rete testis subsets, whereas panels c, f and I compare subsets of subcapsule and tunica albuginea. Values are mean ± S.E.M (n=6 $Cx_3cr_1^{GFP/+}$ $Inhba^{+/+}$); *p<0.05, **p<0.01, ***p<0.001, ****p<0.0001, ns- not significantly different. Each data point represents a single animal expressed as a mean of 3 sections/ animal.*

Figure 8:

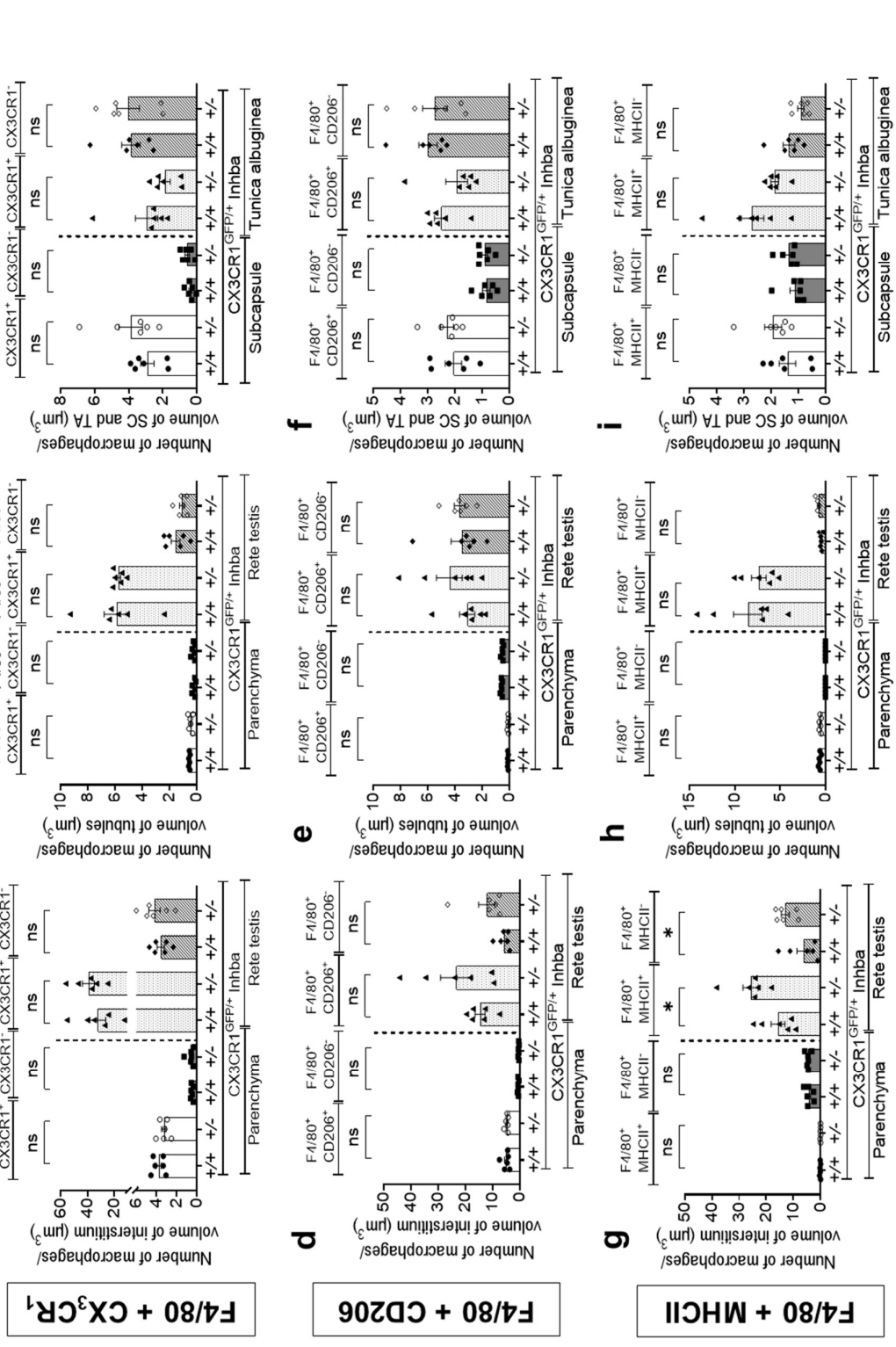
a
Interstitial
b
Peritubular & Peri-epithelial
c
Subcapsule & Tunica albuginea
d
e
f
g
h
i
F4/80 + CX3CR1
F4/80 + CD206
F4/80 + MHCII
Number of macrophages/ volume of interstitium (µm3)
Number of macrophages/ volume of tubules (µm3)
Number of macrophages/ volume of SC and TA (µm3)
F4/80+ CX3CR1+
F4/80+ CX3CR1-
F4/80+ CD206+
F4/80+ CD206-
F4/80+ MHCII+
F4/80+ MHCII-
ns
*
+/+ +/- +/+ +/- +/+ +/-
CX3CR1GFP/+ Inhba
Parenchyma
Rete testis
Subcapsule
Tunica albuginea

Figure 8: *Quantification of macrophages in testicular compartments of adult $Cx_3cr_1^{GFP/+}Inhba^{+/-}$ (activin A-deficient) mouse using CX_3CR_1 and F4/80 markers (**a, b, c**) F4/80 and CD206 markers (**d, e, f**) and F4/80 and MHCII markers (**g, h, i**) where the testis section was compartmentalized into interstitial tissue (IT) and seminiferous tubules (ST) of parenchyma, subcapsular interstitial tissue (SC), tunica albuginea (TA) and the rete testis (RT) was divided into interstitium (IT) and peri-epithelium (PE). Panels a, b, d, e, g and h compare parenchyma and rete testis subsets whereas panels c, f and I compare subsets of subcapsule and tunica albuginea. Values are mean ± S.E.M (n=6 $Cx_3cr_1^{GFP/+}$; n=6 $Cx_3cr_1^{GFP/-}$); *p<0.05, **p<0.01, ***p<0.001, ****p<0.0001, ns- not significantly different. Each data point represents a single animal expressed as a mean of 3 sections/ animal.*

Figure 9:

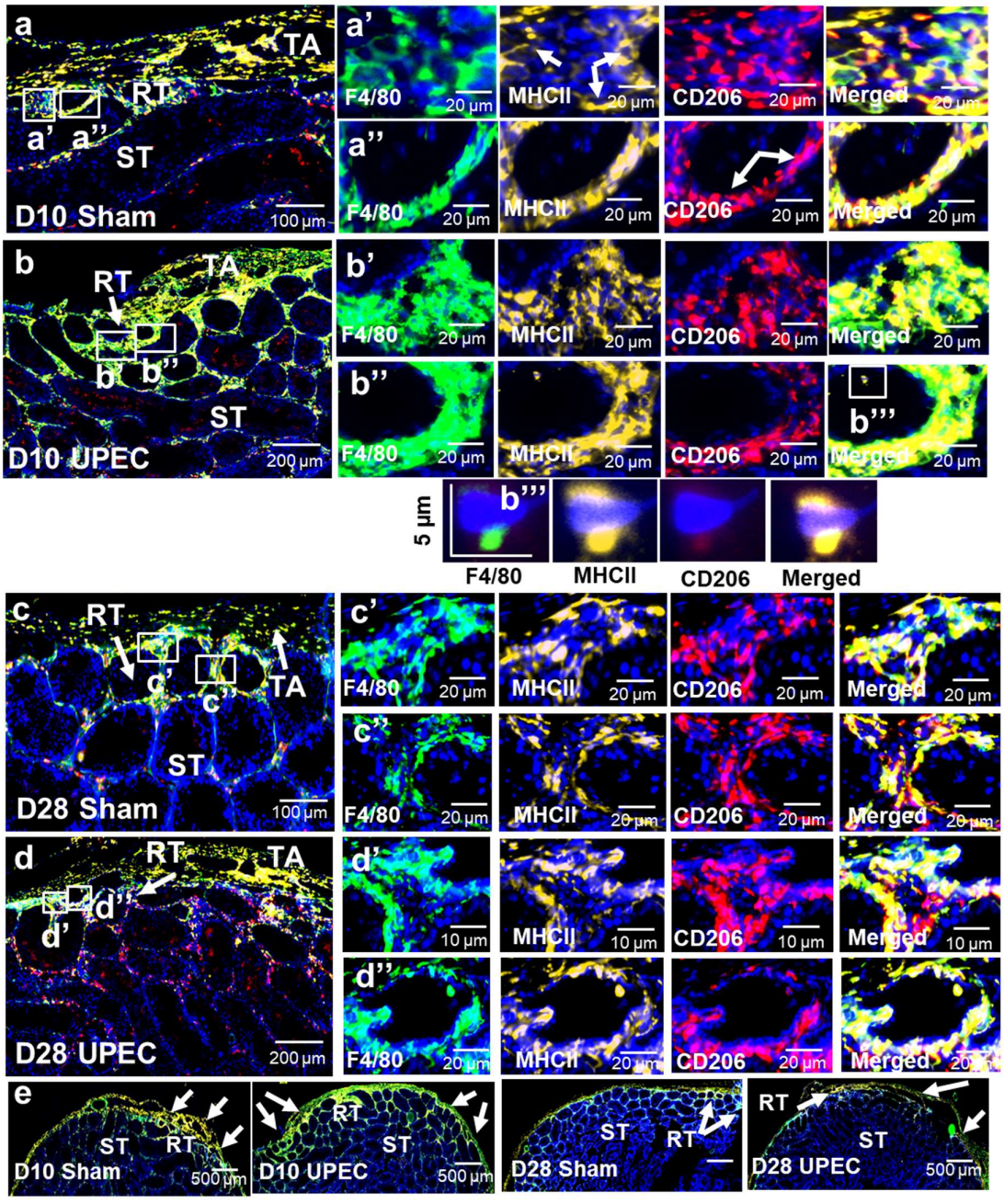
a
TA
RT
a'
a''
ST
D10 Sham
100 µm
a'
F4/80
20 µm
MHCII
20 µm
CD206
20 µm
Merged
20 µm
a''
F4/80
20 µm
MHCII
20 µm
CD206
20 µm
Merged
20 µm
b
RT
TA
b
b''
ST
D10 UPEC
200 µm
b'
F4/80
20 µm
MHCII
20 µm
CD206
20 µm
Merged
20 µm
b''
F4/80
20 µm
MHCII
20 µm
CD206
20 µm
b'''
Merged
20 µm
5 µm
b'''
F4/80
MHCII
CD206
Merged
c
RT
c'
c''
TA
ST
D28 Sham
100 µm
c'
F4/80
20 µm
MHCII
20 µm
CD206
20 µm
Merged
20 µm
c''
F4/80
20 µm
MHCII
20 µm
CD206
20 µm
Merged
20 µm
d
RT
TA
d''
d'
D28 UPEC
200 µm
d'
10 µm
MHCII
10 µm
CD206
10 µm
Merged
10 µm
d''
F4/80
20 µm
MHCII
20 µm
CD206
20 µm
Merged
20 µm
e
ST
RT
D10 Sham
500 µm
RT
ST
D10 UPEC
500 µm
ST
RT
D28 Sham
RT
ST
D28 UPEC
500 µm

Figure 9: *Distribution of macrophage subsets in the rete testis of UPEC- infected adult mouse testes evaluated 10-days and 28-days post-infection using F4/80 (green), CD206 (red) and MHCII (yellow) markers where the adult testis was compartmentalized into interstitial tissue (IT) and seminiferous tubules (ST) of parenchyma, subcapsular interstitial tissue (SC), tunica albuginea (TA) and the rete testis (RT). Panels a', a'', b', b'', c', c'', d' and d'' are higher power images of the enclosed box from the preceding corresponding panel.* ***a)*** *Day 10 sham control.* ***b)*** *Day 10 UPEC infected.* ***c)*** *Day 28 sham control.* ***d)*** *Day 28 UPEC-infected.* ***e)*** *Overview of macrophage infiltration in the rete testis at d10 sham, d10 UPEC, d28 sham and d28 UPEC samples.*

Figure 10:

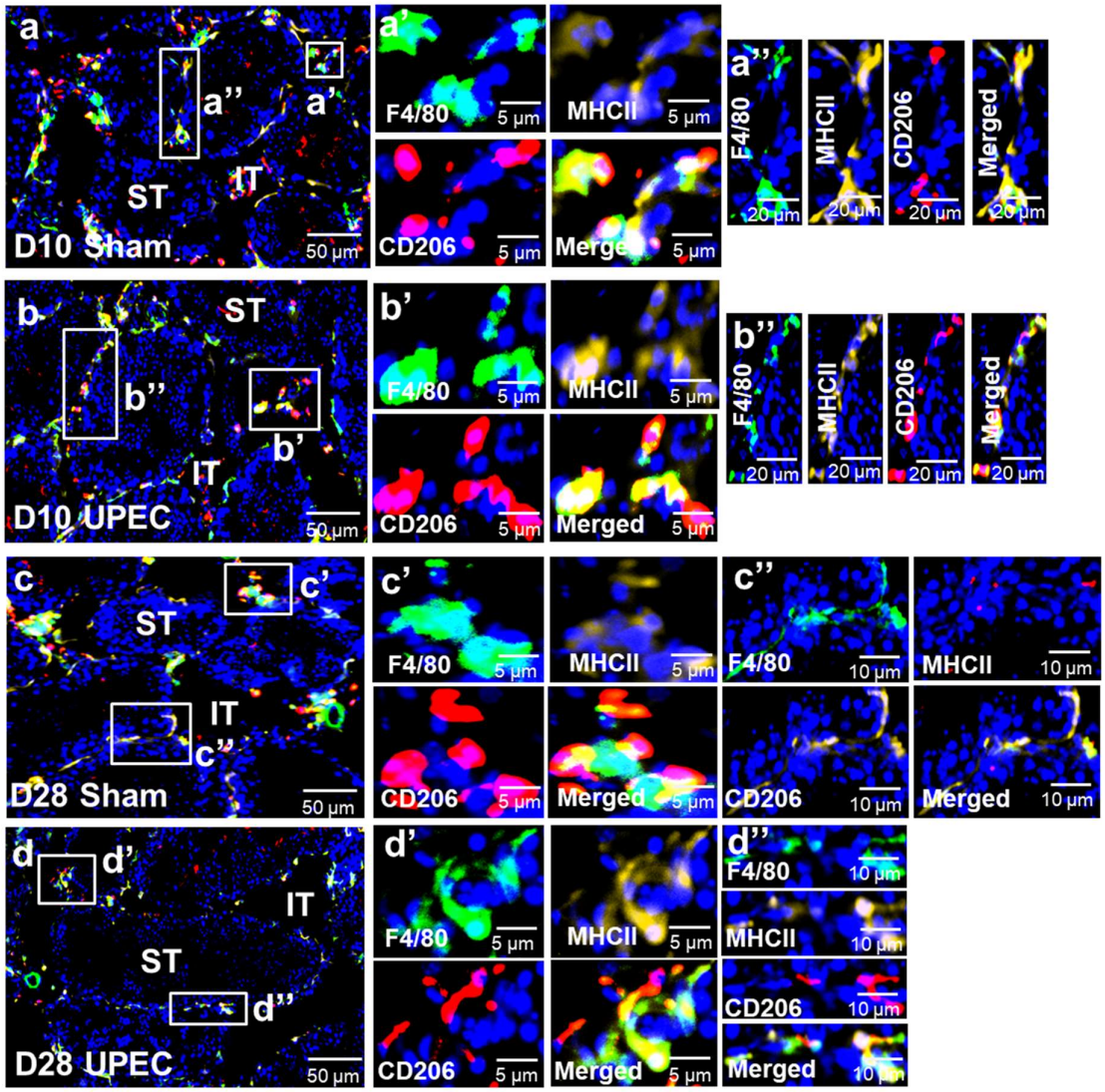
a
a''
a'
ST
IT
D10 Sham
50 µm
a'
F4/80
5 µm
MHCII
5 µm
CD206
5 µm
Merge
5 µm
a''
F4/80
MHCII
CD206
Merged
20 µm
b
ST
b''
b'
IT
D10 UPEC
50 µm
b'
F4/80
5 µm
MHCII
5 µm
CD206
5 µm
Merged
5 µm
b''
F4/80
MHCII
CD206
Merged
20 µm
c
c'
ST
IT
c''
D28 Sham
50 µm
c'
F4/80
5 µm
MHCII
5 µm
CD206
5 µm
Merged
5 µm
c''
F4/80
10 µm
MHCII
10 µm
CD206
10 µm
Merged
10 µm
d
d'
IT
ST
d''
D28 UPEC
50 µm
d'
F4/80
5 µm
MHCII
5 µm
CD206
5 µm
Merged
5 µm
d''
F4/80
10 µm
MHCII
10 µm
CD206
10 µm
Merged
10 µm

Figure 10: *Distribution of macrophage subsets in the parenchyma of UPEC-infected adult mouse testes evaluated 10-days and 28-days post-infection using F4/80 (green), CD206 (red) and MHCII (yellow) markers where the adult testis was compartmentalized into interstitial tissue (IT) and seminiferous tubules (ST) of parenchyma, subcapsular interstitial tissue (SC), tunica albuginea (TA) and the rete testis (RT). Panels a', a'', b', b'', c', c'', d' and d'' are higher power images of the enclosed box from the preceding corresponding panel.* ***a)*** *Day 10 sham control.* ***b)*** *Day 10 UPEC-infected.* ***c)*** *Day 28 sham control.* ***d)*** *Day 28 UPEC-infected.*

Figure 11:

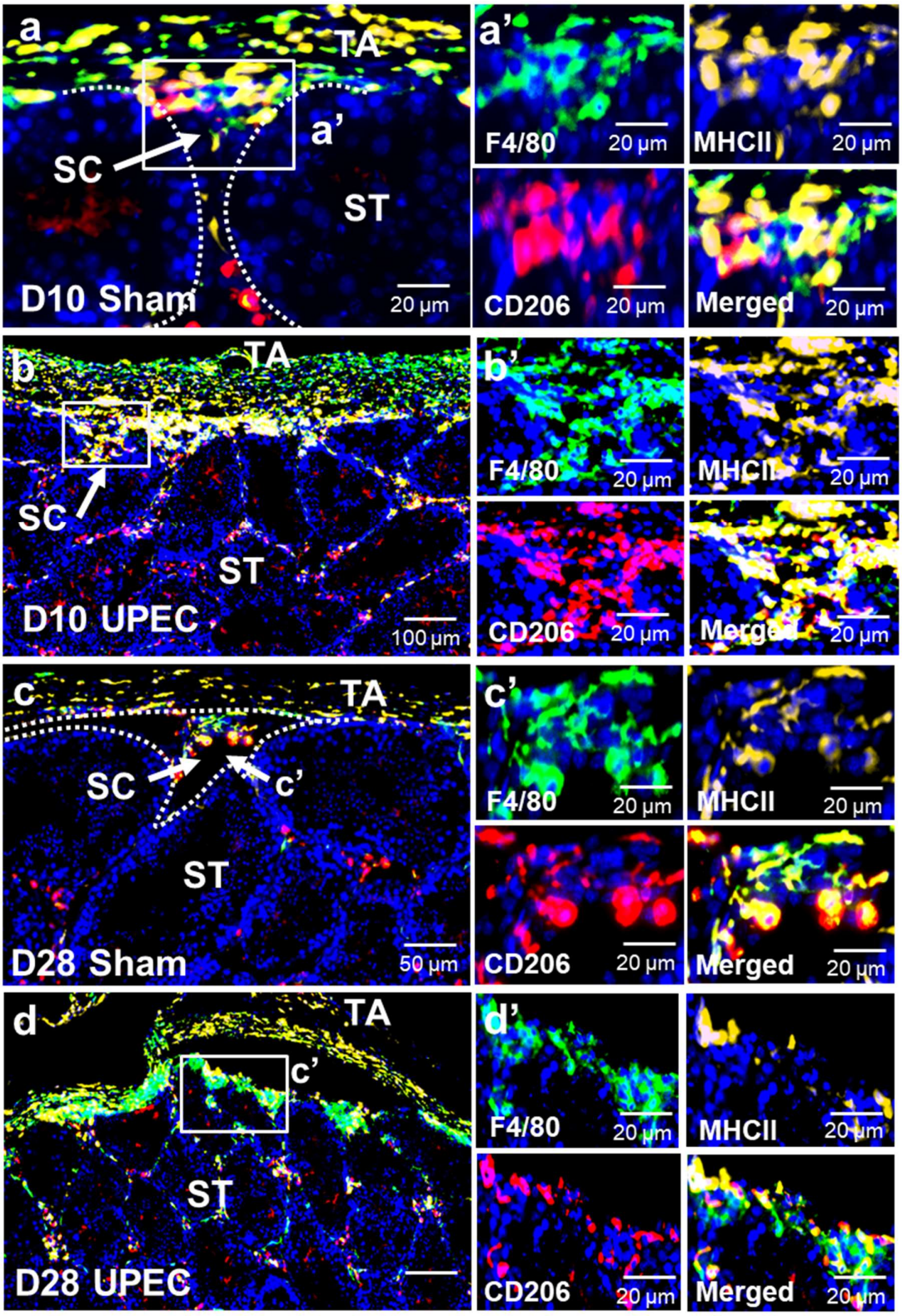
a
TA
a'
SC
ST
D10 Sham
20 µm
a'
F4/80
20 µm
MHCII
20 µm
CD206
20 µm
Merged
20 µm
b
TA
SC
ST
D10 UPEC
100 µm
b'
F4/80
20 µm
MHCII
20 µm
CD206
20 µm
Merged
20 µm
c
TA
SC
c'
ST
D28 Sham
50 µm
c'
F4/80
20 µm
MHCII
20 µm
CD206
20 µm
Merged
20 µm
d
TA
c'
ST
D28 UPEC
d'
F4/80
20 µm
MHCII
20 µm
CD206
20 µm
Merged
20 µm

Figure 11: *Distribution of macrophage subsets in the subcapsule of WT C57BL/6J adult mice infected with saline or UPEC evaluated 10-days and 28-days post-infection using F4/80 (green), CD206 (red) and MHCII (yellow) markers where the adult testis was compartmentalized into interstitial tissue (IT) and seminiferous tubules (ST) of parenchyma, subcapsular interstitial tissue (SC), tunica albuginea (TA) and the rete testis (RT). Panels a', b', c' and d' are higher power images of the enclosed box from the preceding corresponding panel.* ***a)*** *Day 10 sham control.* ***b)*** *Day 10 UPEC-infected.* ***c)*** *Day 28 sham control.* ***d)*** *Day 28 UPEC-infected.*

Figure 12:

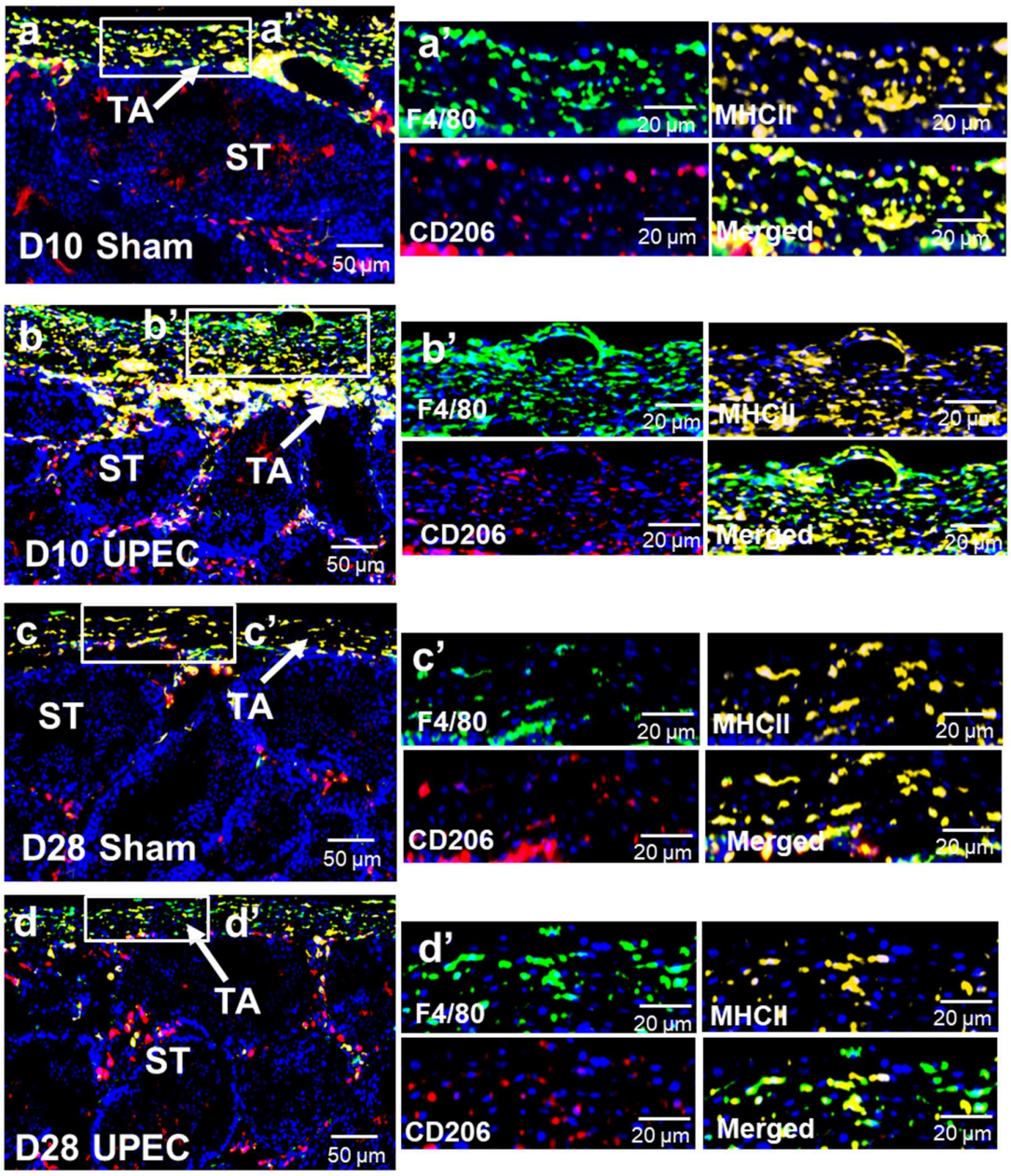
a
a'
TA
ST
D10 Sham
50 µm
a'
F4/80
20 µm
MHCII
20 µm
CD206
20 µm
Merged
20 µm
b
b'
ST
TA
D10 UPEC
50 µm
b'
F4/80
20 µm
MHCII
20 µm
CD206
20 µm
Merged
20 µm
c
c'
ST
TA
D28 Sham
50 µm
c'
F4/80
20 µm
MHCII
20 µm
CD206
20 µm
Merged
20 µm
d
d'
TA
ST
D28 UPEC
50 µm
d'
F4/80
20 µm
MHCII
20 µm
CD206
20 µm
Merged
20 µm

Figure 12: *Distribution of macrophage subsets in the tunica albuginea of WT C57BL/6J adult mice infected with saline or UPEC evaluated 10-days and 28-days post-infection using F4/80 (green), CD206 (red) and MHCII (yellow) markers where the adult testis was compartmentalized into interstitial tissue (IT) and seminiferous tubules (ST) of parenchyma, subcapsular interstitial tissue (SC), tunica albuginea (TA) and the rete testis (RT). Panels a', b', c' and d' are higher power images of the enclosed box from the preceding corresponding panel.* ***a)*** *Day 10 sham control.* ***b)*** *Day 10 UPEC-infected.* ***c)*** *Day 28 sham control.* ***d)*** *Day 28 UPEC-infected.*

Supplementary figure 1:

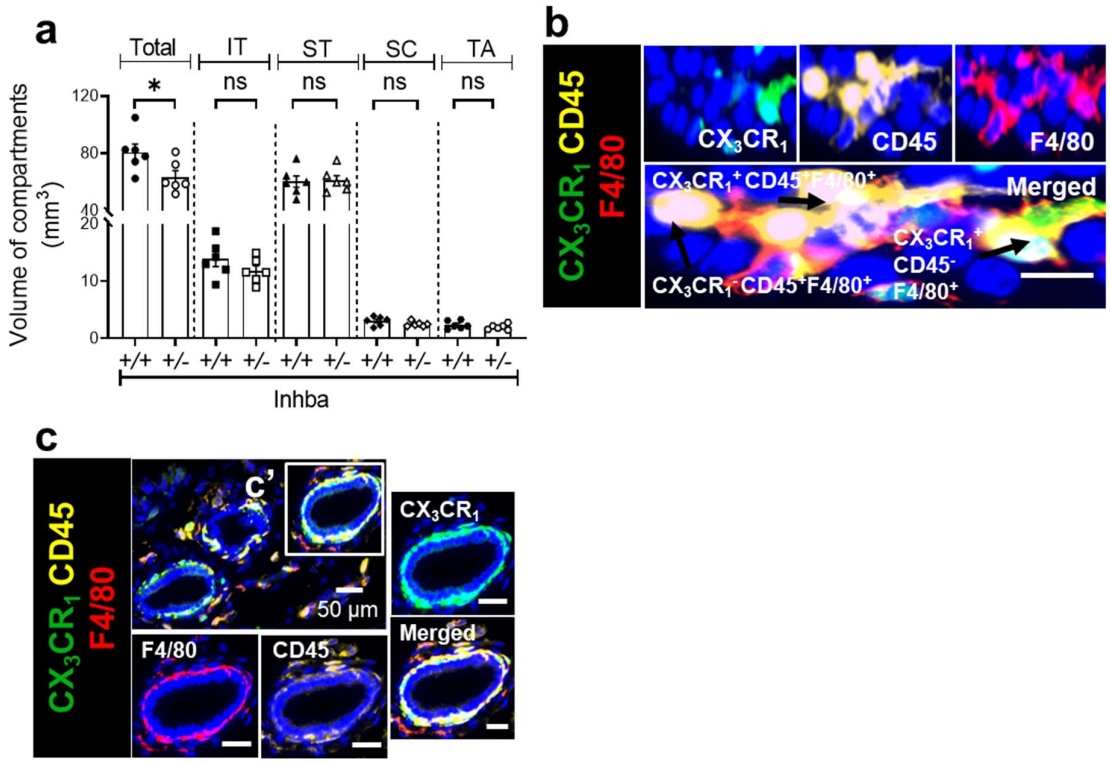

Supplementary figure 1: ***a)*** *Volume of testicular compartments,* ***b)*** *Co-staining of CX_3CR_1 (green), CD45 (yellow) and F4/80 (red) and DAPI (blue) in the transition region (TR) interstitium and* ***c)*** *intra-epithelial macrophages seen in the efferent ducts. Panel c' is a higher power image of the enclosed box from the preceding corresponding panel.*

Supplementary table 1: Details of antibodies used in immunohistochemical and immunofluorescence studies

Marker	Company	Cat #	Clone	Stock conc.	Dilution
Primary unconjugated and conjugated antibodies					
Rat anti-mouse F4/80	Bio-Rad	MCA497G	Cl: A3-1	0.5mg/ml	1:100 (Bouin's fixed paraffin sections) 1:800 (PFA fixed cryosections)
Rat anti-mouse 1-A/1-E (MHCII) Alexa Fluor 647	BioLegend	107618	M5/114.15.2	0.5mg/ml	1:500
Rat anti-mouse CD206 Alexa Fluor 594	BioLegend	141726	C068C2	0.5mg/ml	1:500
Rat anti-mouse CD45 conjugated to APC	BD Pharmingen	559864	30-F11	0.2 mg/ml	1:50
Rabbit anti-laminin	Sigma-Aldrich	L9393	Polyclonal	0.2 mg/ml	1:1000
Mouse anti-human CD68	DAKO	M0867	PG-M1	40mg/ml	1:500
Secondary antibodies					
Biotinylated goat anti-rat conjugated to HRP	Vector labs	BA-9401	-	0.5 mg/ml	1:300
Biotinylated rabbit anti-mouse conjugated to HRP	Invitrogen	A15170	-	2 mg/ml	1:500
Goat anti-rat Alexa Fluor 647	Life technologies	A21247	-	2 mg/ml	1:500
Goat anti-rat Alexa Fluor 546	Invitrogen	A11081	-	2 mg/ml	1:500
Donkey anti-rabbit Alexa Fluor 555	Invitrogen	A31572	-	2 mg/ml	1:500

Chapter 4: Isolation and gene expression analysis of highly purified testicular macrophages from adult mouse testes

Complete manuscript in preparation for submission to Journal (to be decided)

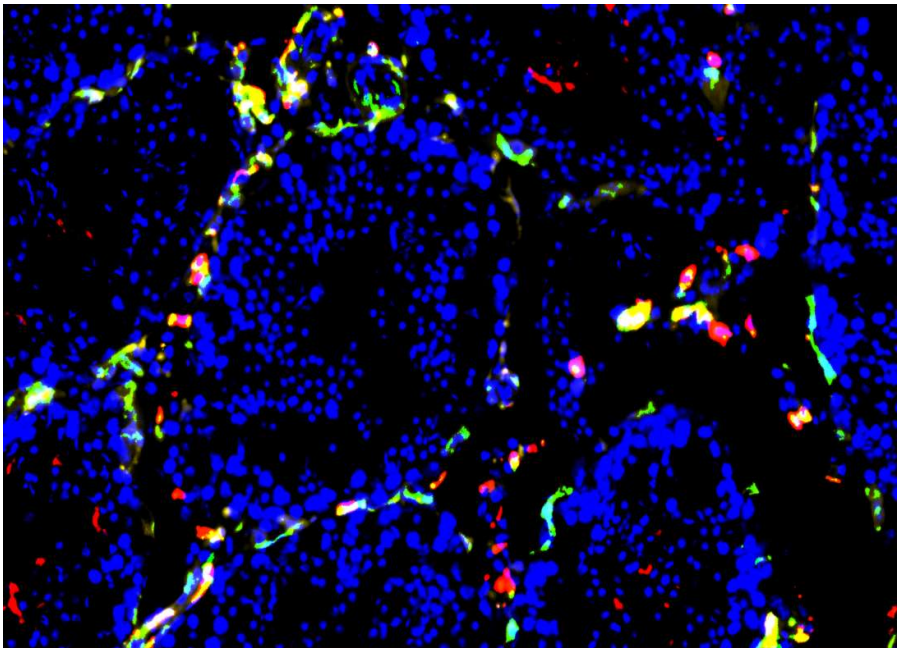

Isolation and gene expression analysis of highly purified testicular macrophages from adult mouse testes

Sneha Biniwale[1,4,5], Rukmali Wijayarathna[1,4], Linden J Gearing[3,4], Paul Hertzog[2,3,4], Sudhanshu Bhushan[5,6], Kate L Loveland[1,4], Andreas Meinhardt[1,4,5], Mark P Hedger[1,4]

[1]Centre for Reproductive Health, Hudson Institute of Medical Research, Clayton, Victoria, Australia

[2]Department of Microbiology and Immunology, The University of Melbourne at the Peter Doherty Institute for Infection and Immunity Melbourne Victoria Australia

[3]Centre for Innate Immunity and Infectious Diseases, Hudson Institute of Medical Research Clayton Victoria Australia

[4]Department of Molecular and Translational Sciences, School of Clinical Sciences, Monash University, Clayton, Victoria, Australia

[5]Institute of Anatomy and Cell Biology, Justus-Liebig University Giessen, Giessen, Germany

[6]The Hessian Centre of Reproductive Medicine, Justus-Liebig-University, Giessen, Germany

Corresponding author: Sneha.biniwale@monash.edu

Postal address: Hudson Institute of Medical Research, 27-31 Wright Street, Clayton 3168, VIC Australia

Abstract

Testicular macrophages have been functionally evaluated *in vivo* and *in vitro* in both rats and mice and have been shown to exhibit anti-inflammatory and tolerogenic properties. The two main subpopulations of testicular macrophages, *i.e.*, interstitial and peritubular, have been studied most extensively in mice: interstitial macrophages are characterized by expression of an anti-inflammatory marker, the mannose receptor (MRC1/CD206), and although peritubular macrophages have elevated expression of MHC class II antigens, they exhibit similar anti-inflammatory gene signatures. However, detailed examination of the functional properties of the testicular macrophages, particularly in the mouse, has been compromised by the difficulties of obtaining sufficient numbers of purified macrophages for analysis. The aim of the current study was to establish a method to isolate purified testicular macrophages (TMs) from adult mice, in order to establish their complete transcriptomic profile. Bone marrow-derived macrophages (BMMs) matured in the presence of colony-stimulating factor-1 (CSF1) were used for baseline comparison. Highly purified (>99%) macrophages were isolated from adult mouse testes by enriching the immune cell component by magnetic separation with CD45 microbeads (MACS), followed by FACS to isolate F4/80^{+} macrophages. A novel multiplex RNAseq method capable of analyzing samples with very low RNA yields was employed.

The analysis revealed that TMs express significantly higher levels of genes encoding proteins involved in antigen-presentation (MHC class II antigens, *Cd80*, *Cd86*, *Ciita*), anti-inflammatory genes (*Il10*, *Socs1*, *Nfkbiz*) and markers of alternatively activated, or M2, macrophages (*Mrc1*/CD206, *Stat3*, *Stat6*, *Gata3, Egfr*), relative to the BMMs. Most notably, TMs were unresponsive to stimulation by bacterial lipopolysaccharide (LPS), which correlated with low expression of genes involved in the LPS-regulated toll-like receptor (TLR4) signaling pathway (*Tlr4, Cd14, Ly96*, *Tirap, Tram1*), and higher expression of genes encoding proteins that inhibit TLR signaling via NF-κB (*Chuk, Ptpn6, Sigirr, Ikbkb*). Some transcripts involved in regulating anti-viral responses, including *Irf5 and* several interferon-stimulated gene transcripts (*Ifitm2*, *Ifitm3*, *Ifi35*, *Oas1a*, *Oas1g*, *Oas3*), also displayed lower expression in TMs, but other crucial anti-viral genes (*Tlr3, Tlr7, Irf1, Irf3, Mx, Ddx58*) were higher. Transcripts encoding proteins of the mTOR/PI3K/AKT signaling pathway also were expressed in TMs, notably *Mtor*, *Akt2* and several PI3K catalytic subunits, but key regulators of this

pathway that promote the anti-inflammatory/M2 phenotype (*Akt1, Pten*, *Inpp5d*, *Tsc1, Pik3r2*) were elevated in expression. Furthermore, the crucial gene responsible for reprogramming glucose metabolism towards oxidative phosphorylation, characteristic of anti-inflammatory/M2 macrophages, *Shpk* (CARKL), as well as several genes encoding enzymes that link glycolysis to the TCA cycle and oxidative phosphorylation (*Me1*, *Pdha2*, *Dlst*) were elevated in TMs. Most transforming growth factor (TGFβ)/activin signaling genes were more highly expressed in TMs, including *Tgfb1*, *Tgfb2*, the activin and TGFβ type 2 receptors (*Acvr2a*, *Acvr2b, Tgfbr2*), and *Smads* 2, 3 and 4, although the type 1 receptors (*Acvr1b, Tgfbr1*) were lower in expression. Overall, this analysis has unequivocally confirmed that the gene expression pattern of the testicular macrophages is that of the anti-inflammatory/M2/tolerogenic phenotype and has identified a number of crucial genes and pathways that may be responsible for regulating this phenotype. The data indicate that the testicular macrophage population has significantly diminished machinery for inflammatory and some antimicrobial responses, but that a significant proportion of these cells are capable of antigen-presentation and regulation of T cell responses, even in the absence of activation stimulii.

1 Introduction

The testis is known to be an immune-privileged organ along with other immune-privileged sites, such as the brain, anterior chamber of the eye, uterus during pregnancy and tumor-draining lymph nodes (Fijak and Meinhardt, 2006, Mellor and Munn, 2008). Macrophages, the most abundant immune cells in the testis, have an important role in maintaining this immune privilege in conjunction with the androgen producing Leydig cells in the interstitium and Sertoli cells in the seminiferous tubules (Meinhardt and Hedger, 2011). Additionally, several animal studies involving ablation of macrophages by a variety of methods showed their significance in overall testicular development and the postnatal development and steroidogenic function of the Leydig cells (Gaytan *et al.,* 1994, Cohen *et al.,* 1996).

It has long been known that macrophages isolated from rat or mouse testis have reduced pro-inflammatory responses, and an immunoregulatory, anti-inflammatory phenotype in comparison with other resident macrophages (Kern *et al.,* 1995, Hayes *et al.,* 1996, Bryniarski *et al.,* 2004). Our studies previously had shown that the immune response of isolated rat testicular macrophages is skewed towards an alternatively activated, or M2, phenotype following treatment with classical (LPS and interferon-IFNγ) or alternative (interleukin-4; IL-4) activation ligands, with expression of high levels of anti-inflammatory cytokines, including interleukin-10 (Il10), TGFβ1, CXCL2 (macrophage inflammatory protein-2α) and suppressor of cytokine signalling-1 (SOCS1) (Winnall *et al.,* 2011). Further studies established that rat testicular macrophages express low levels of the toll-like receptor-4 (TLR4) co-receptors, CD14, MD-2, and the adaptor protein, MyD88, which are required for response to LPS, and had reduced ability to activate NF-κB signaling pathway following stimulation by LPS or another TLR ligand, poly (I:C) (Bhushan *et al.,* 2015, Wang *et al.,* 2017). Typically, however, studies on testicular macrophage function *in vitro* have been complicated by the fact that macrophages represent a very small proportion of cells in the testis, and preparations contain significant cellular contamination, primarily by Leydig cells, which maintain tight junctional specializations with the macrophages in the rat and mouse (Hutson 2006). Consequently, it is very difficult to obtain sufficient numbers of purified testicular macrophages for functional studies, especially in the case of the mouse.

More recently, studies have sought to circumvent these problems by analyzing the phenotype of highly purified, FACS-sorted macrophages at the transcriptome level.

Two main subpopulations have been identified in the mouse, based primarily on their differential expression of MHC class II antigens, the Fc receptor, CD64, and the mannose receptor (MRC1/CD206), corresponding to the interstitial and peritubular macrophage populations *in vivo*. Mossadegh-Keller and colleagues separated interstitial ($CD64^{+}MHCII^{-}$) and peritubular ($CD64^{-}MHCII^{+}$) macrophages from adult mouse testes to study gene expression by nanofluidic fluidigm array real-time PCR (Mossadegh-Keller *et al.,* 2017). In addition to confirming the higher expression of MHCII-related transcripts in peritubular macrophages, they showed that both macrophage populations have similar gene expression profiles of immunosuppressive and M2-type activation genes, with the exception of IL10 and the scavenger receptor, MARCO (higher expression in interstitial macrophages) and IL1β (higher expression in peritubular macrophages). More recently, a comprehensive RNAseq analysis comparing total resident macrophages in the mouse testis to epididymal macrophages and microglia, has been performed (Wang *et al.,* 2021). However, a detailed comparative transcriptome of purified testicular macrophages, specifically related to their inflammatory (M1) and anti-inflammatory/tolerogenic (M2) functions, has not been investigated previously.

The current study was performed with the following aims:

1. Establish a technique to isolate testicular macrophages (TMs) from adult mice, with minimal contamination by other testicular cells, and
2. Investigate the differential gene expression and regulation of these TMs, in comparison with unstimulated and LPS-activated bone marrow-derived macrophages (BMM).

2 Materials and Methods

2.1 Animals

Adult (54 - 58 days old) wild-type (WT) C57BL/6J male mice were purchased from the Monash Animal Research Platform (MARP), Clayton, Australia. Animal experiments were conducted according to the National Health and Medical Research Council Code of Practice for the Care and Use of Animals for Experimental Purposes and approved by the Animal Ethics Committee of Monash Medical Centre. Animals were euthanized using carbon dioxide overdose. Testes and bone marrow were collected immediately

before each testicular macrophage isolation or bone marrow-derived macrophage isolation experiment.

2.2 Primary testicular macrophage isolation

Testicular macrophages were isolated from mechanically-dispersed mouse testes by enrichment with anti-CD45-conjugated microbeads using magnetic separation (Magnetic-Activated Cell Sorting – MACS) to positively select immune cells, and F4/80^{+} macrophages were subsequently collected for downstream processing using Fluorescence-Activated Cell Sorting (FACS) to obtain >99% pure testicular macrophages (based on F4/80 staining). After extensive optimization studies, a robust isolation method was established using 24 testes from 12 adult mice (Fig. 1a). The testes were collected into Dulbecco's modified Eagle's medium (DMEM) medium, on ice. DMEM containing 4.5 g/L D-glucose + L-glut (ThermoFisher Scientific, MA, USA) was supplemented with 100 U/ml penicillin/streptomycin (Gibco, Grand Island, NY, USA), 0.39% sodium bicarbonate (Sigma Aldrich, MO, USA), 0.094% D, L- lactic acid (MP Biomedicals LLC, Ohio, USA) and 0.2% sodium pyruvate (Sigma Aldrich, MO, USA). Multiple (5-6) testes were decapsulated in a petri dish containing DMEM medium and the capsule was discarded. As macrophages rapidly adhere to the petri dish surface, dissociation of the interstitial tissue from the seminiferous tubules was performed as fast as possible on ice with care to minimize breaking the tubules, reducing the leakage of spermatogenic cells from the seminiferous tubules into the medium. No enzymes were used for the dissociation, in order to avoid effects of proteolytic activity on the macrophages (Johnston *et al.,* 1981, Bryniarski *et al.,* 2005). Each testis was dissociated carefully to release the interstitial tissue into the medium within 3 minutes, and the tubules and interstitial cell suspension were collected in a fresh 50ml Falcon tube. This suspension was inverted 3X gently and kept at room temperature (RT) for 5 minutes until the tubules settled. The cell suspension, excluding the tubules, which consisted of interstitial cells and a proportion of peritubular cells (including the peritubular macrophages), was then transferred to a fresh falcon tube (10-15 million cells/ml). The cell suspension was pipetted up and down vigorously multiple times to break up the clumps of macrophages and Leydig cells, then centrifuged at 320 x g for 5 minutes, the supernatant was discarded and 5 ml RBC lysis solution (eBiosciences, MA, USA) was added. After 5 minutes, the reaction was stopped by adding an equal volume of FACS buffer (0.01M PBS, 5 mM EDTA, 1%

heat-inactivated FBS). The cell suspension was centrifuged for 5 mins at 320 x g, the pellet was resuspended in 1 ml FACS buffer and the cell suspension was then filtered through a 35µm mesh, incubated with anti-mouse CD45-conjugated microbeads (Clone 30F11.1; Miltenyi Biotec, Cologne, Germany) at 1:10 per 1 million cells/ml for 20 minutes at 4°C and magnetically separated by Magnetic-activated cell sorting (MACS) into $CD45^+$ and $CD45^-$ fractions, as per the manufacturer's instructions. The $CD45^+$ immune cells were then labelled with an anti-mouse F4/80 APC antibody at 1:800 dilution for 1 hour at 4°C covered with foil (Clone BM8; eBiosciences, MA, USA) and $F4/80^+$ live macrophages were collected by FACS (BD FACSAria™ Fusion, Franklin lakes, NJ, USA) at Monash University Flow Core (Clayton, Australia). The gating strategy was based on selecting singlets followed by gating-in non-debris (FSC vs SSC) and finally gating on $F4/80^+$ live cells [F4/80 vs propidium iodide (PI) as a viability marker] where PI was prepared in-house from commercially sourced powder and used at 0.3µl/ml. This concentration is a routinely known concentration that do not damage the cells used for culturing. After FACS sort, cells were washed once to remove the residual PI before culturing. In general, 24 testes produced a yield of 4-5 × 10^5 $F4/80^+$ macrophages (>99% pure) in total. The proportion of $F4/80^+$ testicular macrophages (TMs) was approximately 1% of total dissociated cells at the start of the experiment, so that this was a 100x enrichment of the macrophages. Final macrophage numbers obtained in this procedure (7 replicates studied and reported) were on average 4-5% of total testicular macrophages, calculated by morphometric studies performed on testis sections in chapter 2 (approximately 500,000 $F4/80^+$ macrophages/ testis). While this might seem low, it is comparable to the results of other isolation results for highly purified cells from complex tissues. The macrophages were divided equally into 2 wells (2-2.5 × 10^5 macrophages/ treatment group and 400µl per well) in a 48-well flat-bottomed culture plate and incubated at 37°C, 5% CO_2 for 1 hour to acclimatize the macrophages. They were incubated in the presence or absence of 100 ng/ml LPS from *E. Coli* K235 (Sigma Aldrich, MO, USA) for a further 3 hours. Cells were harvested, RNA was extracted for each untreated control (UTC) and LPS-treated cells (LPS) and samples were subjected to multiple RNAseq experiments. In total, five- individual isolation procedures and cultures were analyzed.

2.3 Flow cytometry

Flow cytometry was performed to monitor and validate the enrichment of immune cells by anti-CD45 microbeads. Propidium iodide (PI) (0.33 µg/ml) was used a live-dead cell marker. After magnetic cell separation, $CD45^+$ and $CD45^-$ fractions were assessed by flow cytometry using an anti-CD45 antibody AF488 at 1:200 dilution (clone 30-F11; BioLegend, San Diego, USA) to check the enrichment and rat IgG2b, κ FITC was used as an isotype control (BD pharma, Franklin lakes, NJ, USA) (Fig. 1b). It was observed that $CD45^+$ immune cells were enriched by at least 30-fold, reducing the starting number of cells for subsequent FACS. and that the $CD45^-$ testicular cell fraction did not contain any $CD45^+$ immune cells. Flow cytometric analysis was performed on BD LSR-Fortessa X20 (Franklin lakes, NJ, USA) and data was analyzed using FlowJo software version 10.8.0 (Tree Star, Ashland, OR, USA).

2.4 Primary bone marrow- derived macrophage isolation

Mouse BMMs were derived from mouse bone marrow cells in culture using 25 ng/ml recombinant mouse CSF1 (Miltenyi Biotec, Cologne, Germany), as previously described (Fleetwood *et al.,* 2009). Maturation of BMMs in the presence of CSF1 tends to skew cell development away from an inflammatory/M1 phenotype towards the alternatively activated/M2 program (Hamilton, 2011), so these BMMs can be considered to be baseline M0/M2 cells for comparison. Each replicate was generated from the femur and tibia from a single mouse. Briefly, the bone marrow was flushed into 0.01M PBS with a 1 ml syringe and centrifuged at 220 × g for 6 min at RT. The cell pellet was resuspended in 2 ml RBC lysis buffer for 3 min, then centrifuged at 300 x g for 5 min at RT, before being resuspended again in RPMI-1640 medium supplemented with 10% FBS and 1% penicillin/streptomycin. The cell seeding density was adjusted to 2×10^6 cells/ well in 12-well flat-bottom culture plates and incubated at 37°C in an atmosphere containing 5% CO_2 for 30 min. Finally, the isolated cells were cultured with RPMI 1640 medium containing 10% FBS, 50µg/ml penicillin/streptomycin, and 25 ng/ml CSF-1. Fresh medium containing CSF1 was replaced on day 3 and day 6. After changing the media on day 7, the cells were incubated in the presence or absence of 100 ng/ml LPS for 3 hours and cells were harvested. RNA was extracted from 4 separate cultures, one from each mouse.

2.5 RNA isolation

RNA extraction was carried out using the RNeasy micro kit (Qiagen GmBH, Germany) (for TMs) and RNeasy mini kit (Qiagen GmBH, Germany) (for BMMs) according to the manufacturer's instructions. On-column DNAse digestion was performed using DNase I (Qiagen GmBH). Extracted RNA was submitted to Medical Genomics Facility at MHTP, Clayton, Australia for multiplex RNAseq analysis.

2.6 Multiplex RNAseq analysis

As an alternative to conventional RNA-Seq where sequencing libraries are prepared from RNA individually, we used a new method of multiplex RNAseq developed by Dr. Trevor Wilson (Scientific Manager, Medical Genomics Facility at MHTP). One of the advantages of the multiplex approach is that samples with as little as 500 pg RNA are able to be processed (Grubman *et al.,* 2021). Briefly, multiplex RNAseq was performed on TM (UTC and LPS; n=5) and BMM (UTC and LPS: n=4) samples by the MHTP Medical Genomics Facility. Total RNA samples were subjected to quality control. RIN scores measured on bioanalyzer (Model # 2100, Agilent technologies, CA, USA) were 8.8-9.8 for BMMs, while F4/80 sorted TMs had low RIN scores (2.5-3). Samples were diluted into appropriate range and quantitated by Qubit (ThermoFisher Scientific). All samples were processed starting with 30 ng of total RNA. For the cDNA library construction, index was added during individual pA priming and first strand synthesis. Samples were then pooled and amplified using template switching oligo. P5 was added by PCR and P7 by Nextera transposase. Sequencing was performed on a NextSeq2000 P2 run using 19bp forward read (8nt index and UMI) and 101bp reverse reads (cDNA), to generate ~400 million read pairs.

2.7 Bioinformatics and statistical analysis

RNA-seq read alignment, gene quantification, differential expression analyses and gene set tests were performed in R (v4.1.0) (Team, R.C. 2021). The scPipe package (v1.8.0) was employed to process and de-multiplex the data (Tian *et al.,* 2018). A combined FASTQ file was created from the R1 and R2 FASTQ files, by trimming the sample barcode and UMI sequences and storing them in the read header using the sc_trim_barcode function (with bs2 = 0, bl2 = 8, us = 8, ul = 9). Due to problems with N bases appearing at the end of the R1 sequences, just the first 9 bases of the full 10-base UMI were used. Read alignment was performed using the Rsubread package

(v2.0.1) (Liao *et al.,* 2019). An index was built using the Ensembl *Mus musculus* GRCm38 primary assembly genome file and alignment performed with default settings.

Aligned reads were mapped to exons using the sc_exon_mapping function with the Ensembl *Mus musculus* GRCm38 version 100 GFF3 annotation file. The BAM file was de-multiplexed and reads mapping to exons were associated with each individual sample using the sc_demultiplex functiom. An overall count for each gene for each was sample was generated, taking the UMI into account, using the sc_gene_counting function (with UMI_cor = 1). Ensembl gene IDs were annotated using the biomaRt package (v2.48.2).

A DGEList object was created with the UMI counts and gene annotation using the edgeR package (v3.34.0) (Robinson *et al.,* 2010). One TM sample with almost no reads (TM.4_LPS) and an outlying BMM control sample (BMM.6_UTC) were excluded. A design matrix was constructed incorporating the sample groups. Lowly expressed genes were removed using the filterByExpr function and normalization factors were calculated using the TMM method (Robinson and Oshlack, 2010).

Counts were transformed using the voom function from the limma package (v3.48.1) and a linear model was fit using the lmFit function, using replicate as blocking factor, to account for matched UTC and LPS samples, with a consensus correlation of 0.417 (Law *et al.,* 2014, Ritchie *et al.,* 2015).

Comparisons were made between groups using the contrasts.fit function and empirical Bayes moderated t-tests were performed against a 1.2-fold-change threshold and p-values obtained using treat. Differentially expressed genes were determined using a false discovery rate (FDR)-adjusted p-value < 0.05 (McCarthy and Smyth, 2009).

Hallmark, Reactome and Gene Ontology Biological Processes (GO BP) gene set collections were obtained from the Broad Institute Molecular Signature Database, via the msigdbr package (v7.4.1) (Subramanian *et al.,* 2005, Dolgalev 2021). Gene set testing was performed using the camera function from the limma package (Wu and Smyth, 2012). Camera results are shown as bar plots or heat maps. For the camera bar plots, the length of the bar indicates the significance of the gene set ($-\log_{10}$ adjusted p-value), the width of the bar indicates the relative gene set size and the color indicates the average $\log_2$ fold changes of all genes in the gene set. The dashed line

indicates the adjusted p-value cut-off of 0.05. For other bar graphs, GraphPad Prism 9 software (GraphPad software Inc., La Jolla, CA) was used where X-axis represents average log_2 FC values for the pathways listed on the Y- axis. For camera heat maps, the color represents the average log_2 fold changes of all genes in the gene set and the adjusted *p*-value is indicated, if significant (* p < 0.05, ** p < 0.01, *** p < 0.001, **** p < 0.0001; more significant *p*-values are shown as an inequality, such as p < 1e−5).

For heat maps showing gene expression, log_2 counts per million (cpm) expression values were calculated using the edgeR cpm function for individual samples. Average cpm values for each of the 4 groups (TM UTC, TM LPS, BMM UTC, BMM LPS) were also calculated for each gene. Adjusted p-value where p < 0.05 when TM UTC and BMM UTC were compared are shown by *. LPS groups were not compared as there was no effect of LPS on TMs. Morpheus software (https://software.broadinstitute.org/morpheus) was used to prepare the heat maps where row minimum and maximum were considered for comparison giving distinct colors (for each gene).

3 Results

3.1 Comparison of total gene expression profiles of mouse testicular macrophages and CSF1-matured bone marrow-derived macrophages

The multidimensional scaling (MDS) plot for all TM and BMM genes expressed indicated that TMs and BMMs display very different gene expression profiles (Fig. 2a). Further segregation was observed for untreated and LPS-treated BMMs, but the untreated and LPS-treated TMs were similarly distributed. A volcano plot comparing untreated TM and BMM gene expression (Fig. 2b) shows that 5500 genes (in red) were more highly expressed in TMs, whereas 4392 genes (in blue) were more highly expressed in BMMs, and that 4144 genes were not significantly different in their expression. No genes were significantly altered by LPS-treatment in TMs (Fig. 2c), confirming the BMS plot data. However, LPS-treatment of the BMMs led to upregulation of 1444 genes, and downregulation of 1284 genes, while 11308 genes were unaffected (Fig. 2d). A Venn diagram of total gene expression in the TM UTC, BMM UTC and BMM LPS groups is shown in Fig. 2e.

Pathway analysis of gene expression in untreated TMs and BMMs was compared using the Hallmark (Fig. 3), Reactome (Fig. 4) and Gene Ontology (GO) (Fig. 5)

datasets. These analyses indicated that the TMs had significantly lower expression of a number of gene sets, compared with untreated BMMs, including oxidative phosphorylation, glycolysis and respiratory electron transport, mTORC1 signaling, cholesterol homeostasis, protein targeting to the membrane and reactive oxygen species pathways (Fig. 3a, 4a and 5a). In the TMs, the gene sets that were significantly more highly expressed were the TRAF-AP2, PD1 and K-RAS signaling pathways (Figs. 3b, 4b and 5b), steroid hormone responses, and spermatogenesis (Fig. 3b).

When pathway analysis of TMs was performed against BMMs, both before and after LPS treatment using Hallmark, Reactome and Gene Ontology (GO) datasets (Figs. 6a, 6b, 6c, respectively), the gene sets that were most upregulated by LPS in BMMs were related to inflammatory responses: type 1 interferon (IFN) and IFNγ signaling, tumor necrosis factor (TNF) and JAK-STAT signaling, interleukin signaling pathways as well as bacterial and viral defense system-related genes. As predicted by the MDS and Volcano plot data, none of these gene sets or pathways were significantly altered by LPS treatment in the TMs.

When individual genes were analyzed in all four experimental groups (i.e., TM UTC, TM LPS, BMM UTC and BMM LPS), expression of classical macrophage markers and chemokines was clearly different between the two macrophage types. A heat map for classical macrophage markers and regulatory chemokines and receptors (Fig. 7a) indicates that TMs express significantly higher levels of several macrophage marker genes, including *Csf1r* (0.7 $\log_2$ FC), *Ccr2* (1.9 $\log_2$ FC), *Mertk* (2.5 $\log_2$ FC), *Cx3cr1* (4.9 $\log_2$ FC) and *Ptprc* (CD45) (0.5 $\log_2$ FC), than unstimulated BMMs, but lower levels of other macrophage marker genes, including *Adgre1* (F4/80) (1.1 $\log_2$ FC), *Slamf8* (2.3 $\log_2$ FC), *Itgam* (CD11b) (0.6 $\log_2$ FC), and *Fcgr1* (CD64) (0.6 $\log_2$ FC). Furthermore, the TMs displayed elevated constitutive expression of genes encoding MHC class II antigens (*H2-Ab1*, *H2-Ob*, *H2-Oa*, *H2-DMa* with $\log_2$ FC of 3.8, 4.0, 3.4 and 2.0, respectively) that play important roles in the generation of the MHCII-peptide complex in antigen presenting cells and the alternatively-activated/M2 macrophage scavenger receptor, *Mrc1* (CD206) (2.5 $\log_2$ FC) (Fig. 7b and 7d), indicating that both peritubular and interstitial macrophages were represented in the isolated cell preparation.

Activin and TGFβ are key regulators of macrophage number and function (Wijayarathna and de Kretser, 2016), including macrophages in the testis (Biniwale *et al.,* 2022). Most activin/TGFβ signaling genes were more highly expressed in TMs as compared to BMMs, including *Tgfb1* (log_2 FC of 1.6), *Tgfb2* (log_2 FC of 6.0), the activin and TGFβ type 2 receptors (*Acvr2a*, *Acvr2b, Tgfbr2* with log_2 FC of 1.4 – 1.8), and *Smads* 2, 3 and 4 with log_2 FC of 0.4 – 1.2 (Fig. 7c). The type 1 receptors (*Acvr1b, Tgfbr1* with log_2 FC of 0.5 - 1.4) were lower in expression in TMs. Expression of the gene encoding the activin A subunits, *Inhba*, was similar in both macrophage types, but some antagonists of activin/TGFβ signaling, specifically the gene encoding the inhibitory inhibin α subunit (*Inha*) and the TGFβ inhibitory protein, follistatin-like 1 (*Fstl1*), were significantly higher in expression in TMs with log_2 FC of 6.9 and 1.9.

Several genes encoding enzymes and transporters involved in steroid and androgen biosynthesis were more highly expressed in TMs than in BMMs, including the key rate-limiting proteins, steroid acute regulatory protein (*Star*), the cholesterol side-chain cleavage enzyme (*Cyp11a1*) and 17α-hydroxylase/C17,20 lyase (*Cyp17a1*) (log_2 FC of 6.9 - 8) (Fig. 7e) (Hedger, 2015). However, cholesterol 25-hydroxylase (*Ch25h*) was no higher in expression than in untreated BMMs. The top 10 most-affected transcripts (each with high and low expression in untreated TMs than BMMs) that are highly specific for spermatogenic cell development and sperm motility, including *Tnp1, Tulp2, Tnp2, Akap4, Hspa1l, Clgn, Pgk2* and *Ybx2*, were also more highly expressed in the TMs (log_2 FC of 7.3 – 8.2) (Fig. 7f) (Waclawska and Kurpisz, 2012, Ikawa *et al.,* 2011, Stouffs *et al.,* 2009, Gatta *et al.,* 2010). However, testicular macrophages are frequently observed phagocytosing sperm and Leydig cell cytoplasm during isolation, which may be a source of transcripts from these cell typesin the macrophage preparations.

3.2 Expression of genes involved in immunoregulation

Expression of genes encoding proteins required for antigen-presentation to $CD4^+$ T cells were significantly higher in the TMs than in unstimulated BMMs: these included several MHC class II antigens, the stimulatory co-receptors CD80 and CD86, and the essential activator of MHC class II gene transcription, C2TA (*Ciita*) (log_2 FC of 1.8, 2.6 and 5.4 respectively) (Fig. 7b and d) (Ting and Trowsdale, 2002, Gordon *et al.,* 2014). *Marchf1* encodes the MARCH1 enzyme E3 ubiquitin ligase that is responsible for the turnover of peptide-MHCII and hence its stability on the surface of an antigen-

presenting cell and was more highly expressed in TMs by 1.6-fold (Ohmura-Hoshino *et al.,* 2006). On the other hand, *Tollip*, *Ctss, Ctsl*, *Cdc42* and *Cd36* had lower expression in TMs (log_2 FC of 1.6, 1.6, 4.5, 1.6 and 3.7 respectively). The Toll-interacting protein (encoded by *Tollip*) regulates MARCH1 and hence increases MHC class II expression (Roche and Furuta, 2015). Cathepsin S and cathepsin L (encoded by *Ctss* and *Ctsl*) are lysosomal proteases that regulate endosomal and lysosomal proteolysis in antigen-presenting cells (APCs) (Lautwein *et al.,* 2002, Shi *et al.,* 1999). RHO GTPase cell division cycle 42 (encoded by *Cdc42*) regulates the formation of plasma membrane ruffles in micropinocytosis, one of the mechanisms of antigen acquisition and processing in APCs, had lower expression in TMs (log_2 FC of 1.6) (Garrett *et al.,* 2000). CD36 (encoded by *Cd36*) is a phagocytic receptor that recognizes ligands on pathogens and apoptotic cells and had a lower expression in TMs by 3.7-fold (Roche and Furuta, 2015).

Additionally, the TMs displayed higher constitutive expression of genes encoding anti-inflammatory proteins (*Il10*, *Socs1*, *Nfkbiz* by 1.3, 1.1 and 2.2 fold, respectively), transcription factors that regulate the alternatively-activated/M2 phenotype (*Stat3*, *Stat6*, *Gata3* by 0.3, 0.4 and 3.5 fold, respectively) and other anti-inflammatory and immunoregulatory proteins, including the scavenger receptor, MRC1/CD206, the anti-inflammatory transcription factor *Nfe2l2* (log_2 FC of 0.2) and the EGF receptor (*Egfr*) (log_2 FC of 6.9) (Fig.7b and 10b) (Viola *et al.,* 2019, de Groot and Pienta, 2018, Corliss *et al.,* 2016). Notably, however, a small number of transcripts that are typically associated with the anti-inflammatory/tolerogenic or M2 phenotype showed lower expression in TMs than in BMMs, including *Arg1*, *Cd274* (PD-L1), *Chil3* and *Pkm* (log_2 FC of 0.1, 1.0, 3.8 and 2.6, respectively) (de Groot and Pienta, 2018, Palsson-McDermott *et al.,* 2015).

3.3 Expression of genes involved in inflammatory responses and antimicrobial defense

Consistent with the absence of a response to bacterial LPS, genes involved in recognition of LPS via the TLR4 signaling pathway displayed low expression in TMs as compared to unstimulated BMMs, including the genes encoding the TLR4-receptor complex, TLR4 (*Tlr4*), CD14, and MD-2 (*Ly96*) (log_2 FC of 0.3, 2.3 and 1.1, respectively), and adapter proteins in its downstream signaling pathway (*Myd88*, *Tirap/Mal*, *Tram1*) (log_2 FC of 0.6, 1.2 and 0.8 respectively) (Fig. 8a and b) (Bhushan

et al., 2015, Bhushan and Meinhardt, 2017). Conversely, several genes that encode proteins that inhibit TLR signaling by NF-κB, including *Chuk, Ptpn6, Sigirr and Ikbkb* (log_2 FC of 1.2, 0.2, 1.6 and 0.5, respectively), were more highly expressed by TMs (Brint *et al.,* 2004, Kobayashi *et al.,* 2002).

Genes that were constitutively elevated in TMs and also upregulated by LPS in BMMs included *Stat1* and *Ccl17* (a T_{reg} cell chemoattractant) (log_2 FC of 1.0 and 5.0 respectively) (Viola *et al.,* 2019). Pro-inflammatory genes that were not elevated in TMs, but were induced by LPS in BMMs, included *Il1b*, *Il6*, *Il12, Tnf and Ccl2* (log_2 FC of 6.9, 8.1, 6.1, 2.8 and 6.6 respectively) and a number of proteins that mediate the interferon response (Fig. 8d and 7b).

The MTOR/PI3K/AKT pathway is important for regulating proinflammatory signals and promotes anti-inflammatory responses in TLR-stimulated macrophages. Transcripts encoding this signaling pathway were expressed in TMs, particularly *Mtor*, *Akt2* and several PI3K catalytic subunits, but key regulators of this pathway that promote the anti-inflammatory/M2 phenotype (*Akt1, Pten*, *Inpp5d* with log_2 FC of 1.0, 1.6 and 1.1, respectively) were also elevated in expression, whereas others, such as *Tsc1* (log_2 FC of 1.9) had low expression compared to BMMs (Fig. 9a, b) (Birkenkamp and Coffer, 2003, Fan *et al.,* 2010, Cuschieri *et al.,* 2008, Kral *et al.,* 2016). The Src homology 2 domain-containing inositol-5-phosphatase-1 (SHIP-1), encoded by the *Inpp5d* gene, degrades PI-3,4,5-P2, which is the bioactive mediator produced by PI3K. Furthermore, the enzyme pyruvate dehydrogenase kinase 1 (*Pdk1*), which activates AKT in TLR-stimulated macrophages, had lower expression in TMs than in BMMs (log_2 FC of 0.7) (Chaurasia *et al.,* 2010).

Anti-viral responses are initiated when viruses are detected by viral pattern recognition receptors, including TLR3 and 7 and the retinoic-acid inducible gene I (RIG-I). Some transcripts involved in regulating anti-viral responses, including *Irf5 and* several interferon-stimulated gene transcripts (*Ifitm2*, *Ifitm3*, *Ifi35*, *Oas1a*) displayed lower expression in TMs than in unstimulated BMMs (log_2 FC of 2.6, 0.9, 1.8, 1.1 and 2.6 respectively), but other crucial anti-viral genes (*Tlr3, Tlr7, Irf1 and Irf3* with log_2 FC of 1.5, 0.8, 1.3, 1.0 and 2.0) were higher in expression in the TMs (Fig. 8c) (Marks *et al.,* 2019).

3.4 Expression of genes related to tissue repair, fibrosis and phagocytosis

Amongst the tissue repair, fibrosis and phagocytosis-related macrophage genes (Fig. 9c, 9d and 10e), TMs had higher expression of *Myo18a, Retnla, Plod2, Ear2* and *Fn1* (log_2 FC of 1.3, 6.8, 2.8, 1.1 and 2.8 respectively), but lower expression of *Mmp9, Adora2b, Chil3* and *Itgb1* (log_2 FC of 6.1, 3.1, 0.6 and 1.4 respectively). The transcripts listed in Fig. 10e were the only few transcripts affected in the phagocytosis signaling pathway. Activation of macrophage-mediated tissue repair by Th2 cytokines involves macrophage-derived arginase 1 (*Arg 1*) and RELMα (*Retnla*), the enzyme lysyl hydrolase 2 (*Plod2*), as well as expression of matrix metalloproteinase 9 (*Mmp9*) promoted by RELMα, integrin beta 1 (*Itgb1*) and junctional adhesion molecule A (*F1lr*). Additionally, receptor myosin 18A (*Myo18a*), YM1 (*Chil3*), eosinophil-associated, ribonuclease A family, member 2 (*Ear2*), fibronectin 1 (*Fn1*) and A2B receptor (*Adora2b*) enhance both M2 macrophage activation and wound healing. Mincle (*Clec4e*), a C-type lectin expressed on macrophages, is a mediator of fibrosis and was less expressed in TMs (Kim and Nair, 2019, Borthwick *et al.,* 2016, Schingnitz *et al.,* 2010, Bosurgi *et al.,* 2017, Gause *et al.,* 2013). Genes playing an important role in apoptotic cell engulfment, or efferocytosis, requires the receptor tyrosine kinases *Axl* and *Mertk* from the tumor-associated macrophage (TAM) receptor tyrosine kinase family, whose activation is facilitated by TIM4 (*Timd4*) and downstream transcription factors, including LXRα, LXRβ and PPARγ (*Nr1h3*, *Nr1h2* and *Pparg*) (Kim and Nair, 2019). TMs had higher expression of *Axl, Mertk* and *Timd4* (1.7-, 2.5- and 6.9-fold) but lower expression of *Pparg* (3.1–fold). In addition, Fig. 10f shows the top 20 most-affected transcripts ($p < 0.05$) related to complement activation especially the highly expressed gene *Clu* (encodes CLU - clusterin), which is an important complement lysis inhibitor with 7-fold higher expression in TMs than BMMs. Additionally, clusterin regulates macrophage expansion, polarization and phagocytic activity in response to inflammation in the kidneys (Weng *et al.,* 2021, Weng *et al.,* 2022). *Spanxn4* gene (encodes SPANX family member N4) with 7.6-fold higher expression in TMs than BMMs plays an important role in spermiogenesis (Westbrook *et al.,* 2006).

3.5 Expression of genes involved in metabolism

Pro-inflammatory macrophages are dependent upon glycolysis, and exhibit impairment of the TCA cycle and oxidative phosphorylation (OXPHOS), whereas anti-inflammatory macrophages are more dependent upon OXPHOS, with downregulation

of glycolysis and the pentose phosphate pathway (PPP) (Viola *et al.,* 2019). Figure 10a shows an overall effect on selected metabolic pathway transcripts whereas figures 10b, 10c and 10d show the top 20 most-significantly affected transcripts ($p < 0.05$) in glycolysis, oxidative phosphorylation and TCA cycle respectively.

Crucially, the regulatory gene responsible for reprogramming glucose metabolism towards oxidative phosphorylation and the anti-inflammatory/M2 phenotype, *Shpk* (CARKL), as well as several genes encoding enzymes that link glycolysis to the TCA cycle and oxidative phosphorylation (*Me1*, *Pdha2*, *Dlst, Pfkm, Odghi*) and glutamine synthetase (*Glul*) were significantly elevated in TMs compared with unstimulated BMMs (Fig.10a) (Palsson-McDermott *et al.,* 2015, Palmieri *et al.,* 2017, Baardman *et al.,* 2018, Haschemi *et al.,* 2012). However, some glycolytic enzyme transcripts were more highly expressed in TMs than in unstimulated BMMs, including phosphoglycerate mutase 2 (*Pgam2*) and GADPH glyceraldehyde-3-phosphate dehydrogenase (*Gapdhs*) (Fig. 10b) (Viola *et al.,* 2019).

Metabolic genes that were expressed significantly lower in the TMs included glucose transporter 1 (*Slc2a1*), pyruvate kinase (*Pkm*), a regulator of glucose metabolism, phosphogluconate dehydrogenase (*Pgd*), an enzyme involved in ribulose-5-P formation, the mitochondrial dicarboxylate and tricarboxylate transport proteins, *Slc25a10* and *Slc25a1*, and acomitate decarboxylase, *Acod1* (Fig. 10a) (Freemerman *et al.,* 2014, Palsson-McDermott *et al.,* 2015, Baardman *et al.,* 2018, Palmieri *et al.,* 2017, Michelucci *et al.,* 2013). Overall, these gene expression profiles are consistent with the fact that the TMs are deviated towards the anti-inflammatory/M2 metabolic program.

4 Discussion

There have been numerous studies on isolated macrophages from rat and mouse testes. Isolating pure preparation of testicular macrophages is a particular challenge due to their very low numbers, especially from the mouse testis. In general, most studies on testicular macrophage function *in vitro* have used preparations with low purity (70-90%) (Kern *et al.,* 1995, Hayes *et al.,* 1996, Bryniarski *et al.,* 2004, Winnall *et al.,* 2011, Bhushan *et al.,* 2015, Zhang *et al.,* 2020, Gayer *et al.,* 2022). These studies have established that the testicular macrophages are anti-inflammatory/tolerogenic, with poor pro-inflammatory capacity, but the presence of

testicular spermatogenic and somatic cell contamination complicates these findings. More recent studies have sought to circumvent this problem by analyzing the phenotype of highly-purified, FACS-sorted testicular macrophages at the transcriptome level by gene expression profiling using microfluidic RT-PCR or RNAseq analysis (Mossadegh-Keller *et al.,* 2017, Wang *et al.,* 2021). However, these studies did not examine the response of these cells to pro-inflammatory stimuli, and used proteolytic dissociation of the testes to isolate cells, which has the capacity to alter macrophage inflammatory functions (Johnston *et al.,* 1981, Bryniarski *et al.,* 2005). Although it is well-established that the process of isolation and culturing macrophages inherently modifies their function, we have previously used gentle mechanical-dissociation of the testis to isolate rat and mouse testicular macrophages to reduce these complications (Winnall *et al.,* 2011, Indumathy *et al.,* 2020). This does not appear to substantially reduce the recovery of macrophages, and the isolates contain both interstitial and peritubular macrophages at approximately the proportions found *in vivo* (Indumathy *et al.,* 2020, Biniwale *et al.,* 2022).

In the present study, a new purification method for mouse testicular macrophages from mechanically-isolated testes were developed and validated. This involved an enrichment step with anti-CD45 magnetic microbeads to positively select testicular immune cells and FACS-sorting using the macrophage-specific surface protein F4/80 to achieve >99% pure mouse testicular macrophages. The purified macrophages were cultured for 3h in the presence or absence of LPS to provide untreated (baseline) and activated macrophage samples. Analysis of the macrophages was undertaken using a novel multiplex RNAseq method that enabled the analysis of very small samples of extracted RNA (Grubman *et al.,* 2021).

In general, the results showed that TMs are transcriptionally different from BMMs matured in the presence of CSF1. In particular, CSF1 tends to direct bone marrow-derived macrophages towards the alternative, immunosuppressive M2 phenotype or tissue-resident phenotype and hence it was considered as a more appropriate control for M2 and tissue-resident gene expression than a macrophage population deviated towards a pro-inflammatory/M1 program. It is important to note that this study investigated transcript levels, which can only give an indirect estimate of function, and not the protein levels or their activity. Based on the expression of both CD206 and MHC class II antigens, and other genes, the cell suspension taken for downstream

processing after the FACS sort was a mixture of interstitial and peritubular macrophages, as CD45, F4/80 and CD11b are expressed on both these cell populations in the testis (Indumathy *et al.,* 2020, Mossadegh-Keller *et al.,* 2017). In addition to MHCII, our study confirms that TMs also express higher levels of the co-stimulatory molecules, CD80 and CD86, which are likely preferentially expressed on peritubular macrophages as they are primed for antigen-presentation even in the absence of activation stimuli as (Lokka *et al.,* 2020, Gordon, 2014). Chemokines and their receptors [*Csf1r*, *Cx$_3$cr$_1$*, *Ccl2*] and interstitial macrophage markers [*Fcgr1* (CD64) and *Mertk*] that have been reported to be expressed on either or both of these macrophage populations in the testis have been confirmed here (Mossadegh-Keller *et al.,* 2017, DeFalco *et al.,* 2015). In addition to this, our study also shows that TMs express transcripts related to PD-1 signaling pathway (e.g., the *Cd274* gene that encodes PD-L1) at higher levels than BMMs, which is consistent with induction of tolerance.

An unpublished microarray analysis comparing murine TMs with BMMs, peritoneal macrophages and embryonic stem cell-derived macrophages cultured with and without LPS at same concentration and time-point as used in the current study showed that TLR4-related and other inflammatory pathways were activated after LPS stimulation in TMs; however, the TMs were less responsive than the other macrophages (unpublished data from our group). Similar reduced responses to LPS by macrophages isolated from rat and mouse testes have been reported in several published studies (Kern *et al.,* 1995, Hayes *et al.,* 1996, Bryniarski *et al.,* 2004, Winnall *et al.,* 2011, Bhushan *et al.,* 2015; Zhang *et al.,* 2020). These observations contrast with the inability of the highly purified macrophages in the present study to respond to LPS. However, the testicular macrophages in the microarray analysis were only 90% pure, with significant Leydig cell contamination, most likely due to their close physical association with the interstitial macrophages. Overall, this suggests that the response of isolated TMs to LPS observed in previous studies may have been due to contaminating testicular somatic cells, which can also respond to LPS (Hales *et al.,* 1992, Winnall *et al.,* 2009, 2011). Furthermore, even in the highly-purified macrophage preparation used in the present study there were significant transcripts associated with steroid biosynthesis and spermatogenesis. While macrophages are capable of steroidogenesis (Chen et al 2002), it is very unlikely that genes associated

with meiosis and spermiogenesis would be significantly expressed by these cells. Phagocytosis of sperm and Leydig cell cytoplasm by testicular macrophages can often be observed during the isolation procedure, and this process may explain the presence of many of these transcripts in the macrophage preparation. It is unlikely that any isolation procedure could avoid this complication.

Mossadegh-Keller and colleagues have shown previously that both interstitial and peritubular macrophages express transcripts related to an anti-inflammatory phenotype, with some minor differences. For example, *Il10* and *Marco* are more highly expressed by the interstitial macrophages and *Il1b* is more highly expressed by the peritubular macrophages (Mossadegh-Keller *et al.,* 2017). Our study showed that key transcripts for activation of anti-inflammatory pathway, such as *Stat6*, *Gata3* and the anti-inflammatory cytokine *Il10*, had higher expression in TMs, whereas lower levels of pro-inflammatory cytokines, such as *Il6*, *Il12*, *Nos2* and transcription factor *Stat3,* were observed. In addition, the metabolic signatures of pro-inflammatory and anti-inflammatory macrophages are different (Liu *et al.,* 2021, Viola *et al.,* 2019). Generally speaking, pro-inflammatory/M1 macrophages are dependent upon glycolysis, and exhibit impairment of the TCA cycle and oxidative phosphorylation (OXPHOS), whereas anti-inflammatory macrophages are more dependent upon OXPHOS, with downregulation of glycolysis and the pentose phosphate pathway (PPP) (Viola *et al.,* 2019). The TCA cycle in M1 macrophages is interrupted at multiple key points allowing accumulated signal metabolites, citrate, itaconate and succinate, to escape mitochondria and exert regulatory roles (Liu *et al.,* 2021, Jha *et al.,* 2015, McGettrick and O'Neill, 2013). In TMs in the present study, key transcripts related to glycolysis (*Slc2a1* and *Pkm*) and the pentose phosphate pathway had lower expression relative to the BMMs (Palsson-McDermott *et al.,* 2015, Freemerman *et al.,* 2014). Furthermore, the SLC25a1 enzyme (encoded by *Slc25a1*), which transports citrate to the cytosol, is often highly expressed in M1 macrophages because of the break in the TCA cycle and was expressed at lower levels in TMs (Infantino *et al.,* 2014). On the other hand, our results conform with a previous finding that expression of SDHA (succinate dehydrogenase, a mitochondrial enzyme encoded by *Sdha*) remains unchanged in BMMs treated with LPS as compared to untreated controls. This is due to the fact that SDHA is inhibited by itaconate in LPS-stimulated macrophages resulting in accumulation of succinate that results in similar expression in untreated

and LPS-treated BMM groups (Viola *et al.,* 2019). Moreover, a key enzyme GLUL (glutamate synthetase), encoded by *Glul* is barely detectable in M1 macrophages, but is highly expressed in M2 macrophages, and showed relatively higher expression in TMs (Palmieri *et al.,* 2017). These results indicate that the metabolic signatures of TMs are consistent with the anti-inflammatory macrophage phenotype. A further question is whether these signatures differ between interstitial and peritubular macrophages especially when these macrophage types only differ slightly in transcript levels of several pro-inflammatory and anti-inflammatory genes (Mossadegh-Keller *et al.,* 2017). In contrast to the other signatures of the metabolic pathways already discussed, several OXPHOS pathway transcripts had lower expression in unstimulated TMs in our study when compared to the BMMs.

The mTOR/PI3K/AKT signaling pathway plays a complex role in inflammation, and can stimulates NF-κB activation and the inflammatory response, but can also play an anti-inflammatory role (Vergadi *et al.,* 2017, Troutman *et al.,* 2012). Transcripts encoding this signaling pathway were expressed in TMs, particularly *Mtor*, *Akt2* and several PI3K catalytic subunits, but key regulators of this pathway that promote the anti-inflammatory/M2 phenotype (*Akt1, Pten*, *Inpp5d*) were also elevated in expression. Additionally, the enzyme PDK1 encoded by *Pdk1*, which activates AKT in TLR-stimulated macrophages, had lower expression in TMs than in BMMs (Chaurasia *et al.,* 2010). The low expression of *Pdk1* might be a result of a negative feedback mechanism, especially when transcript levels of PTEN encoded by *Pten*, a key negative regulator of this pathway, which plays a major role in controlling cell metabolism, was also highly expressed (Kral *et al.,* 2016). SHIP-1 (Src homology 2 domain-containing inositol-5-phosphatase-1) regulates the activity of PI3K by hydrolyzing its product, PI-3,4,5-P3 to inactive PI-3,4-P2, thus inhibiting NF-κB-dependent activation in response to stimulation and was more highly expressed in TMs than in BMMs (Conde *et al.,* 2011). The TMs also expressed relatively high levels of activin and follistatin signaling pathway-related transcripts, and activin A suppresses inflammatory responses in activated macrophages, at least in part through stimulation of SHIP-1 (Cuschieri *et al.,* 2008). It is well-established that activin A exerts complex effects on macrophage function, inducing pro-inflammatory gene expression in unstimulated macrophages, but reducing gene expression in activated (e.g., LPS-

stimulated) macrophages, hence acting as an anti-inflammatory regulator (Hedger *et al.,* 2011).

In the TLR4 signaling pathway, *Tlr4* and many of the key transcripts encoding co-receptors and adaptor molecules (MyD88, CD14, MD-2), MAP kinases, NF-κB subunits and MAL had low expression in TMs. This confirms a previous observation in a study performed in Wistar rats where these signaling molecules were downregulated in LPS-treated TMs (Bhushan *et al.,* 2015). On the contrary, one of the few MyD88-dependent negative regulators, *Ptpn6* had elevated levels in TMs providing further explanation for the lack of an LPS effect. In addition to the absent TLR4 signaling pathway, several key anti-viral related transcripts were expressed at low levels indicating that the response to some bacterial infections may be suppressed in TMs, but some anti-viral responses may be deficient as well. This may indicate that the resident TM population does not play a major role in responses to infection in the testis, and that such responses depend upon newly-recruited macrophages from the circulation.

A majority of the transcripts encoding proteins responsible for activation of M2 macrophage-mediated tissue repair by Th2 cytokines and wound healing were highly expressed in unstimulated TMs (*Myo18a, Retnla, Plod2, Ear2, Fn1*) and others had low expression (*Mmp9*, *Adora2b*, *Chil3*, *Itgb1*). Additionally, Clec4a, encoding a C-type lectin expressed on macrophages, is a mediator of fibrosis and was less expressed in TMs (Kim and Nair, 2019, Borthwick *et al.,* 2016, Schingnitz *et al.,* 2010, Bosurgi *et al.,* 2017, Gause *et al.,* 2013). This indicates that TMs play an important part in wound healing and tissue repair in the testis. Furthermore, receptors tyrosine kinases *Axl* and *Mertk* play an important role in apoptotic cell engulfment, or efferocytosis and their activation is facilitated by TIM4 (*Timd4*) and downstream transcription factors, including LXRα, LXRβ and PPARγ (*Nr1h3*, *Nr1h2* and *Pparg*) (Kim and Nair, 2019). These transcripts had high expression in TMs indicating their active role in phagocytosis. Transcripts such as *Clu*, which is an important complement lysis inhibitor, had higher expression in TMs. Additionally, clusterin regulates macrophage expansion, polarization and phagocytic activity in response to inflammation in the kidneys (Weng *et al.,* 2021, Weng *et al.,* 2022).

In conclusion, the gene expression pattern of the resident macrophages of the mouse testis indicates that these cells have a predominantly anti-inflammatory/M2 phenotype, with reduced capacity for responding to bacterial and viral infections, but appear to be actively involved in antigen-presentation. These data are further confirmation that the principal role of the resident macrophages is to suppress inflammatory immune responses and regulate tolerance to antigens within the testis environment. This analysis has identified a number of crucial genes and pathways that may be responsible for regulating this phenotype, and directions for further investigation of its regulation.

Acknowledgements

The authors thank Trevor Wilson from Monash Medical Genomics Facility, MHTP for performing the multiplex RNAseq analysis. Secondly, we like to thank Sivanjah Indumathy for providing the flow cytometry training required for validation studies. Additionally, we are indebted to A/Prof Ashley Mansell for providing invaluable scientific inputs during the data analysis. Furthermore, we thank Rosemary Genovese and Julie Muir for taking care of ordering mice from Monash Animal Research Platform, Clayton, Australia and providing training, instrumentation and technical support for tissue culture experiments.

Funding information

The research was supported by a grant from the National Health and Medical Research Council of Australia (Grant # APP1184867 to MPH) and the grants from Monash University and Deutsche Forschungsgemeinschaft (DFG) to the International Research Training Group (IRTG) on ‘Molecular pathogenesis of male reproductive disorders’ between JLU Giessen and Monash University (GRK 187/1), and the Victorian Government’s Operational Infrastructure Support Programme.

Declaration of interest

None

Author contributions

SB (Sneha Biniwale)- Performing experiments, study design, data analysis, manuscript writing; RW- tissue collection, study design, technical and scientific

guidance, critical review of the manuscript; JG – Bioinformatics and statistical analysis; PH, SB (Sudhanshu Bhushan), KAL and AM- technical and scientific guidance, critical review of the manuscript; MH- study design, technical and scientific guidance and critical review of the manuscript.

References

Baardman, J., Verberk, S. G. S., Prange, K. H. M., Van Weeghel, M., Van Der Velden, S., Ryan, D. G., Wüst, R. C. I., Neele, A. E., Speijer, D., Denis, S. W., Witte, M. E., Houtkooper, R. H., O'neill L, A., Knatko, E. V., Dinkova-Kostova, A. T., Lutgens, E., De Winther, M. P. J. & Van Den Bossche, J. 2018. A Defective Pentose Phosphate Pathway Reduces Inflammatory Macrophage Responses during Hypercholesterolemia. *Cell Reports,* 25**,** 2044-2052.e5.

Bhushan, S. & Meinhardt, A. 2017. The macrophages in testis function. *Journal of Reproductive Immunology,* 119**,** 107-112.

Bhushan, S., Tchatalbachev, S., Lu, Y., Fröhlich, S., Fijak, M., Vijayan, V., Chakraborty, T. & Meinhardt, A. 2015. Differential Activation of Inflammatory Pathways in Testicular Macrophages Provides a Rationale for Their Subdued Inflammatory Capacity. *The Journal of Immunology,* 194**,** 5455-5464.

Biniwale, S., Wijayarathna, R., Pleuger, C., Bhushan, S., Loveland, K. L., Meinhardt, A. & Hedger, M. P. 2022. Regulation of macrophage number and gene transcript levels by activin A and its binding protein, follistatin, in the testes of adult mice. *Journal of Reproductive Immunology,* 151**,** 103618.

Birkenkamp, K. U. & Coffer, P. J. 2003. FOXO transcription factors as regulators of immune homeostasis: molecules to die for? *Journal of Immunology,* 171**,** 1623-9.

Borthwick, L. A., Barron, L., Hart, K. M., Vannella, K. M., Thompson, R. W., Oland, S., Cheever, A., Sciurba, J., Ramalingam, T. R., Fisher, A. J. & Wynn, T. A. 2016. Macrophages are critical to the maintenance of IL-13-dependent lung inflammation and fibrosis. *Mucosal Immunology,* 9**,** 38-55.

Bosurgi, L., Cao, Y. G., Cabeza-Cabrerizo, M., Tucci, A., Hughes, L. D., Kong, Y., Weinstein, J. S., Licona-Limon, P., Schmid, E. T., Pelorosso, F., Gagliani, N., Craft, J. E., Flavell, R. A., Ghosh, S. & Rothlin, C. V. 2017. Macrophage function in tissue repair and remodeling requires IL-4 or IL-13 with apoptotic cells. *Science,* 356**,** 1072-1076.

Brint, E. K., Xu, D., Liu, H., Dunne, A., Mckenzie, A. N., O'neill, L. A. & Liew, F. Y. 2004. ST2 is an inhibitor of interleukin 1 receptor and Toll-like receptor 4 signaling and maintains endotoxin tolerance. *Nature Immunology,* 5**,** 373-9.

Bryniarski, K., Szczepanik, M., Maresz, K., Ptak, M. & Ptak, W. 2004. Subpopulations of Mouse Testicular Macrophages and their Immunoregulatory Function. *American Journal of Reproductive Immunology,* 52**,** 27-35.

Bryniarski, K., Szczepanik, M., Ptak, M. & Ptak, W. 2005. Modulation of testicular macrophage activity by collagenase. *Folia Histochemica et Cytobiologica,* 43**,** 37-41.

Chaurasia, B., Mauer, J., Koch, L., Goldau, J., Kock, A. S. & Brüning, J. C. 2010. Phosphoinositide-dependent kinase 1 provides negative feedback inhibition to Toll-like receptor-mediated NF-kappaB activation in macrophages. *Molecular and Cellular Biology,* 30**,** 4354-66.

Chen, J. J., Lukyanenko, Y. & Hutson, J. C. 2002. 25-hydroxycholesterol is produced by testicular macrophages during the early postnatal period and influences differentiation of Leydig cells in vitro. *Biology of Reproduction,* 66**,** 1336-41.

Cohen, P. E., Chisholm, O., Arceci, R. J., Stanley, E. R. & Pollard, J. W. 1996. Absence of Colony-Stimulating Factor-1 in Osteopetrotic ($csfm^{op}/csfm^{op}$) Mice Results in Male Fertility Defects. *Biology of Reproduction,* 55**,** 310-317.

Conde, C., Gloire, G. & Piette, J. 2011. Enzymatic and non-enzymatic activities of SHIP-1 in signal transduction and cancer. *Biochemical Pharmacology,* 82**,** 1320-1334.
Corliss, B. A., Azimi, M. S., Munson, J. M., Peirce, S. M. & Murfee, W. L. 2016. Macrophages: An Inflammatory Link Between Angiogenesis and Lymphangiogenesis. *Microcirculation,* 23**,** 95-121.
Cuschieri, J., Bulger, E., Grinsell, R., Garcia, I. & Maier, R. V. 2008. Insulin regulates macrophage activation through activin A. *Shock,* 29**,** 285-290.
De Groot, A. E. & Pienta, K. J. 2018. Epigenetic control of macrophage polarization: implications for targeting tumor-associated macrophages. *Oncotarget,* 9**,** 20908-20927.
Defalco, T., Potter, S. J., Williams, A. V., Waller, B., Kan, M. J. & Capel, B. 2015. Macrophages Contribute to the Spermatogonial Niche in the Adult Testis. *Cell Reports,* 12**,** 1107-1119.
Fan, W., Morinaga, H., Kim, J. J., Bae, E., Spann, N. J., Heinz, S., Glass, C. K. & Olefsky, J. M. 2010. FoxO1 regulates Tlr4 inflammatory pathway signalling in macrophages. *The European Molecular Biology Organization (EMBO) Journal,* 29**,** 4223-36.
Fijak, M. & Meinhardt, A. 2006. The testis in immune privilege. *Immunological reviews,* 213**,** 66-81.
Fleetwood, A. J., Dinh, H., Cook, A. D., Hertzog, P. J. & Hamilton, J. A. 2009. GM-CSF-and M-CSF-dependent macrophage phenotypes display differential dependence on type I interferon signaling. *Journal of leukocyte biology,* 86**,** 411-421.
Freemerman, A. J., Johnson, A. R., Sacks, G. N., Milner, J. J., Kirk, E. L., Troester, M. A., Macintyre, A. N., Goraksha-Hicks, P., Rathmell, J. C. & Makowski, L. 2014. Metabolic reprogramming of macrophages: glucose transporter 1 (GLUT1)-mediated glucose metabolism drives a proinflammatory phenotype. *Journal of Biological Chemistry,* 289**,** 7884-96.
Garrett, W. S., Chen, L. M., Kroschewski, R., Ebersold, M., Turley, S., Trombetta, S., Galán, J. E. & Mellman, I. 2000. Developmental control of endocytosis in dendritic cells by Cdc42. *Cell,* 102**,** 325-34.
Gatta, V., Raicu, F., Ferlin, A., Antonucci, I., Scioletti, A. P., Garolla, A., Palka, G., Foresta, C. & Stuppia, L. 2010. Testis transcriptome analysis in male infertility: new insight on the pathogenesis of oligo-azoospermia in cases with and without AZFc microdeletion. *BMC Genomics,* 11**,** 401.
Gause, W. C., Wynn, T. A. & Allen, J. E. 2013. Type 2 immunity and wound healing: evolutionary refinement of adaptive immunity by helminths. *Nature Reviews Immunology,* 13**,** 607-14.
Gayer, F. A., Reichardt, S. D., Bohnenberger, H., Engelke, M. & Reichardt, H. M. 2022. Characterization of testicular macrophage subpopulations in mice. *Immunology Letters,* 243**,** 44-52.
Gaytan, F., Bellido, C., Aguilar, E. & Van Rooijen, N. 1994. Requirement for testicular macrophages in Leydig cell proliferation and differentiation during prepubertal development in rats. *Journal of Reproduction and Fertility,* 102**,** 393-9.
Gordon, S. 2014. The M1 and M2 paradigm of macrophage activation: time for reassessment. *F1000Prime Reports,* 6**,** 787-95.
Gordon, S., Pluddemann, A. & Estrada, F. M. 2014. Macrophage heterogeneity in tissues: phenotypic diversity and functions. *Immunological Reviews,* 262**,** 36-55.

Grant, C. R., Liberal, R., Mieli-Vergani, G., Vergani, D. & Longhi, M. S. 2015. Regulatory T-cells in autoimmune diseases: challenges, controversies and—yet—unanswered questions. *Autoimmunity reviews,* 14**,** 105-116.

Grubman, A., Choo, X. Y., Chew, G., Ouyang, J. F., Sun, G., Croft, N. P., Rossello, F. J., Simmons, R., Buckberry, S., Landin, D. V., Pflueger, J., Vandekolk, T. H., Abay, Z., Zhou, Y., Liu, X., Chen, J., Larcombe, M., Haynes, J. M., Mclean, C., Williams, S., Chai, S. Y., Wilson, T., Lister, R., Pouton, C. W., Purcell, A. W., Rackham, O. J. L., Petretto, E. & Polo, J. M. 2021. Transcriptional signature in microglia associated with Aβ plaque phagocytosis. *Nature Communications,* 12**,** 3015.

Hales, D. B., Xiong, Y. & Tur-Kaspa, I. 1992. The role of cytokines in the regulation of Leydig cell P450c17 gene expression. *The Journal of Steroid Biochemistry and Molecular Biology,* 43**,** 907-914.

Hamilton, J. 2011. Colony stimulating factors and macrophage heterogeneity. *Inflammation and Regeneration,* 31**,** 228-236.

Haschemi, A., Kosma, P., Gille, L., Evans, C. R., Burant, C. F., Starkl, P., Knapp, B., Haas, R., Schmid, J. A., Jandl, C., Amir, S., Lubec, G., Park, J., Esterbauer, H., Bilban, M., Brizuela, L., Pospisilik, J. A., Otterbein, L. E. & Wagner, O. 2012. The sedoheptulose kinase CARKL directs macrophage polarization through control of glucose metabolism. *Cell Metabolism,* 15**,** 813-26.

Hayes, R., Chalmers, S. A., Nikolic-Paterson, D. J., Atkins, R. C. & Hedger, M. P. 1996. Secretion of Bioactive Interleukin 1 by Rat Testicular Macrophages In Vitro. *Journal of Andrology,* 17**,** 41-49.

Hedger, M. P. 2015. *The Immunophysiology of Male Reproduction In:* Plant, T. M. & Zeleznik, A. J. (eds) *Knobil and Neill's Physiology of Reproduction (Third edition).* St. Louis: Academic Press, 805-892.

Hedger, M. P., Winnall, W. R., Phillips, D. J. & de Kretser, D. M. 2011. Regulation and function of activin and follistatin in inflammation and immunity. *Vitamins Hormones,* 85**,** 255-297.

Hutson, J. C. 2006. Physiologic Interactions Between Macrophages and Leydig Cells. *Experimental Biology and Medicine,* 231**,** 1-7.

Igor Dolgalev (2021). msigdbr: MSigDB Gene Sets for Multiple Organisms in a Tidy Data Format. R package version 7.4.1. https://CRAN.R-project.org/package=msigdbr

Ikawa, M., Tokuhiro, K., Yamaguchi, R., Benham, A. M., Tamura, T., Wada, I., Satouh, Y., Inoue, N. & Okabe, M. 2011. Calsperin is a testis-specific chaperone required for sperm fertility. *Journal of Biological Chemistry,* 286**,** 5639-46.

Indumathy, S., Pueschl, D., Klein, B., Fietz, D., Bergmann, M., Schuppe, H. C., Da Silva, N., Loveland, B. E., Hickey, M. J., Hedger, M. P. & Loveland, K. L. 2020. Testicular immune cell populations and macrophage polarisation in adult male mice and the influence of altered activin A levels. *Journal of Reproductive Immunology,* 142**,** 103204.

Infantino, V., Iacobazzi, V., Menga, A., Avantaggiati, M. L. & Palmieri, F. 2014. A key role of the mitochondrial citrate carrier (SLC25A1) in TNFα-and IFNγ-triggered inflammation. *Biochimica et Biophysica Acta (BBA)-Gene Regulatory Mechanisms,* 1839**,** 1217-1225.

Jha, A. K., Huang, S. C.-C., Sergushichev, A., Lampropoulou, V., Ivanova, Y., Loginicheva, E., Chmielewski, K., Stewart, K. M., Ashall, J. & Everts, B. 2015. Network integration of parallel metabolic and transcriptional data reveals metabolic modules that regulate macrophage polarization. *Immunity,* 42**,** 419-430.

Johnston, R. B., Jr., Chadwick, D. A. & Cohn, Z. A. 1981. Priming of macrophages for enhanced oxidative metabolism by exposure to proteolytic enzymes. *Journal of Experimental Medicine,* 153**,** 1678-83.
Kern, S., Robertson, S. A., Mau, V. J. & Maddocks, S. 1995. Cytokine secretion by macrophages in the rat testis. *Biology of Reproduction,* 53**,** 1407-16.
Kim, S. Y. & Nair, M. G. 2019. Macrophages in wound healing: activation and plasticity. *Immunology & Cell Biology,* 97**,** 258-267.
Kobayashi, K., Hernandez, L. D., Galán, J. E., Janeway, C. A., Jr., Medzhitov, R. & Flavell, R. A. 2002. IRAK-M is a negative regulator of Toll-like receptor signaling. *Cell,* 110**,** 191-202.
Kral, J. B., Kuttke, M., Schrottmaier, W. C., Birnecker, B., Warszawska, J., Wernig, C., Paar, H., Salzmann, M., Sahin, E., Brunner, J. S., Österreicher, C., Knapp, S., Assinger, A. & Schabbauer, G. 2016. Sustained PI3K Activation exacerbates BLM-induced Lung Fibrosis via activation of pro-inflammatory and pro-fibrotic pathways. *Scientific Reports,* 6**,** 23034.
Lautwein, A., Burster, T., Lennon-Duménil, A. M., Overkleeft, H. S., Weber, E., Kalbacher, H. & Driessen, C. 2002. Inflammatory stimuli recruit cathepsin activity to late endosomal compartments in human dendritic cells. *European Journal of Immunology,* 32**,** 3348-57.
Law, C. W., Chen, Y., Shi, W. & Smyth, G. K. 2014. voom: Precision weights unlock linear model analysis tools for RNA-seq read counts. *Genome biology,* 15**,** 1-17.
Liao, Y., Smyth, G. K. & Shi, W. 2019. The R package Rsubread is easier, faster, cheaper and better for alignment and quantification of RNA sequencing reads. *Nucleic acids research,* 47**,** e47-e47.
Liu, Y., Xu, R., Gu, H., Zhang, E., Qu, J., Cao, W., Huang, X., Yan, H., He, J. & Cai, Z. 2021. Metabolic reprogramming in macrophage responses. *Biomarker Research,* 9**,** 1.
Lokka, E., Lintukorpi, L., Cisneros-Montalvo, S., Mäkelä, J.-A., Tyystjärvi, S., Ojasalo, V., Gerke, H., Toppari, J., Rantakari, P. & Salmi, M. 2020. Generation, localization and functions of macrophages during the development of testis. *Nature Communications,* 11**,** 4375.
Marks, Z. R. C., Campbell, N., Deweerd, N. A., Lim, S. S., Gearing, L. J., Bourke, N. M. & Hertzog, P. J. 2019. Properties and functions of the novel type I interferon epsilon. *Seminars in Immunology,* 43**,** 101328.
Mccarthy, D. J. & Smyth, G. K. 2009. Testing significance relative to a fold-change threshold is a TREAT. *Bioinformatics,* 25**,** 765-771.
Mcgettrick, A. F. & O'neill, L. A. 2013. How metabolism generates signals during innate immunity and inflammation. *Journal of Biological Chemistry,* 288**,** 22893-8.
Meinhardt, A. & Hedger, M. P. 2011. Immunological, paracrine and endocrine aspects of testicular immune privilege. *Molecular and Cellular Endocrinology,* 335**,** 60-8.
Mellor, A. L. & Munn, D. H. 2008. Creating immune privilege: active local suppression that benefits friends, but protects foes. *Nature Reviews Immunology,* 8**,** 74-80.
Michelucci, A., Cordes, T., Ghelfi, J., Pailot, A., Reiling, N., Goldmann, O., Binz, T., Wegner, A., Tallam, A., Rausell, A., Buttini, M., Linster, C. L., Medina, E., Balling, R. & Hiller, K. 2013. Immune-responsive gene 1 protein links metabolism to immunity by catalyzing itaconic acid production. *Proceedings of the National Acadamy of Sciences U S A,* 110**,** 7820-5.
Mossadegh-Keller, N., Gentek, R., Gimenez, G., Bigot, S., Mailfert, S. & Sieweke, M. H. 2017. Developmental origin and maintenance of distinct testicular macrophage populations. *The Journal of Experimental Medicine,* 214**,** 2829-2841.

Ohmura-Hoshino, M., Matsuki, Y., Aoki, M., Goto, E., Mito, M., Uematsu, M., Kakiuchi, T., Hotta, H. & Ishido, S. 2006. Inhibition of MHC class II expression and immune responses by c-MIR. *The Journal of Immunology,* 177**,** 341-54.

Palmieri, E. M., Menga, A., Martín-Pérez, R., Quinto, A., Riera-Domingo, C., De Tullio, G., Hooper, D. C., Lamers, W. H., Ghesquière, B. & Mcvicar, D. W. 2017. Pharmacologic or genetic targeting of glutamine synthetase skews macrophages toward an M1-like phenotype and inhibits tumor metastasis. *Cell Reports,* 20**,** 1654-1666.

Palsson-Mcdermott, E. M., Curtis, A. M., Goel, G., Lauterbach, M. A., Sheedy, F. J., Gleeson, L. E., Van Den Bosch, M. W., Quinn, S. R., Domingo-Fernandez, R. & Johnston, D. G. 2015. Pyruvate kinase M2 regulates Hif-1α activity and IL-1β induction and is a critical determinant of the warburg effect in LPS-activated macrophages. *Cell metabolism,* 21**,** 65-80.

Ritchie, M. E., Phipson, B., Wu, D., Hu, Y., Law, C. W., Shi, W. & Smyth, G. K. 2015. limma powers differential expression analyses for RNA-sequencing and microarray studies. *Nucleic acids research,* 43**,** e47-e47.

Robinson, M. D. & Oshlack, A. 2010. A scaling normalization method for differential expression analysis of RNA-seq data. *Genome biology,* 11**,** 1-9.

Robinson, M. D., Mccarthy, D. J. & Smyth, G. K. 2010. edgeR: a Bioconductor package for differential expression analysis of digital gene expression data. *Bioinformatics,* 26**,** 139-140.

Roche, P. A. & Furuta, K. 2015. The ins and outs of MHC class II-mediated antigen processing and presentation. *Nature Reviews Immunology,* 15**,** 203-216.

Schingnitz, U., Hartmann, K., Macmanus, C. F., Eckle, T., Zug, S., Colgan, S. P. & Eltzschig, H. K. 2010. Signaling through the A2B adenosine receptor dampens endotoxin-induced acute lung injury. *The Journal of Immunology,* 184**,** 5271-9.

Shi, G. P., Villadangos, J. A., Dranoff, G., Small, C., Gu, L., Haley, K. J., Riese, R., Ploegh, H. L. & Chapman, H. A. 1999. Cathepsin S required for normal MHC class II peptide loading and germinal center development. *Immunity,* 10**,** 197-206.

Stouffs, K., Tournaye, H., Liebaers, I. & Lissens, W. 2009. Male infertility and the involvement of the X chromosome. *Human Reproduction Update,* 15**,** 623-37.

Subramanian, A., Tamayo, P., Mootha, V. K., Mukherjee, S., Ebert, B. L., Gillette, M. A., Paulovich, A., Pomeroy, S. L., Golub, T. R. & Lander, E. S. 2005. Gene set enrichment analysis: a knowledge-based approach for interpreting genome-wide expression profiles. *Proceedings of the National Academy of Sciences,* 102**,** 15545-15550.

Team, R. C. (2021). R: A language and environment for statistical computing. R Foundation for Statistical Computing, Vienna, Austria. 2012.

Tian, L., Su, S., Dong, X., Amann-Zalcenstein, D., Biben, C., Seidi, A., Hilton, D. J., Naik, S. H. & Ritchie, M. E. 2018. scPipe: A flexible R/Bioconductor preprocessing pipeline for single-cell RNA-sequencing data. *PLoS computational biology,* 14**,** e1006361.

Ting, J. P. & Trowsdale, J. 2002. Genetic control of MHC class II expression. *Cell,* 109 Suppl**,** S21-33.

Troutman, T. D., Bazan, J. F. & Pasare, C. 2012. Toll-like receptors, signaling adapters and regulation of the pro-inflammatory response by PI3K. *Cell cycle,* 11**,** 3559-3567.

Vergadi, E., Ieronymaki, E., Lyroni, K., Vaporidi, K. & Tsatsanis, C. 2017. Akt Signaling Pathway in Macrophage Activation and M1/M2 Polarization. *The Journal of Immunology,* 198**,** 1006-1014.

Viola, A., Munari, F., Sánchez-Rodríguez, R., Scolaro, T. & Castegna, A. 2019. The Metabolic Signature of Macrophage Responses. *Frontiers in Immunology,* 10.

Waclawska, A. & Kurpisz, M. 2012. Key functional genes of spermatogenesis identified by microarray analysis. *Systems Biology in Reproductive Medicine,* 58**,** 229-235.

Wang, M., Fijak, M., Hossain, H., Markmann, M., Nusing, R. M., Lochnit, G., Hartmann, M. F., Wudy, S. A., Zhang, L., Gu, H., Konrad, L., Chakraborty, T., Meinhardt, A. & Bhushan, S. 2017. Characterization of the Micro-Environment of the Testis that Shapes the Phenotype and Function of Testicular Macrophages. *The Journal of Immunology,* 198**,** 1-14.

Wang, M., Yang, Y., Cansever, D., Wang, Y., Kantores, C., Messiaen, S., Moison, D., Livera, G., Chakarov, S. & Weinberger, T. 2021. Two populations of self-maintaining monocyte-independent macrophages exist in adult epididymis and testis. *Proceedings of the National Academy of Sciences,* 118.

Weng, X., Li, J., Guan, Q., Zhao, H., Wang, Z., Gleave, M. E., Nguan, C. Y., & Du, C. (2022). The functions of clusterin in renal mesenchymal stromal cells: Promotion of cell growth and regulation of macrophage activation. *Experimental cell research*, 413(2), 113081.

Weng, X., Zhao, H., Guan, Q., Shi, G., Feng, S., Gleave, M. E., Nguan, C. C., & Du, C. (2021). Clusterin regulates macrophage expansion, polarization and phagocytic activity in response to inflammation in the kidneys. *Immunology and cell biology*, 99(3), 274–287.

Westbrook, V. A., Schoppee, P. D., Vanage, G. R., Klotz, K. L., Diekman, A. B., Flickinger, C. J., Coppola, M. A., & Herr, J. C. (2006). Hominoid-specific SPANXA/D genes demonstrate differential expression in individuals and protein localization to a distinct nuclear envelope domain during spermatid morphogenesis. *Molecular human reproduction*, 12(11), 703–716.

Wijayarathna, R. & de Kretser, D. M. 2016. Activins in reproductive biology and beyond. *Human Reproduction Update,* 22**,** 342-357.

Winnall, W. R., Muir, J. A. & Hedger, M. 2011. Rat resident testicular macrophages have an alternatively activated phenotype and constitutively produce interleukin-10 in vitro. *Journal of Leukocyte Biology,* 90**,** 133-143.

Winnall, W. R., Okuma, Y., Saito, K., Muir, J. A., & Hedger, M. P. (2009). Regulation of interleukin 1alpha, activin and inhibin by lipopolysaccharide in Sertoli cells from prepubertal rats. *Molecular And Cellular Endocrinology*, *307*(1-2), 169–175.

Wu, D. & Smyth, G. K. 2012. Camera: a competitive gene set test accounting for inter-gene correlation. *Nucleic Acids Research,* 40**,** e133-e133.

Zhang, Z., Jiang, Z., Zhang, Y., Zhang, Y., Yan, Y., Bhushan, S., Meinhardt, A., Qin, Z. & Wang, M. 2020. Corticosterone Enhances the AMPK-Mediated Immunosuppressive Phenotype of Testicular Macrophages During Uropathogenic Escherichia coli Induced Orchitis. *Frontiers in immunology,* 11**,** 583276-583276.

Left blank on purpose

Figure 1:

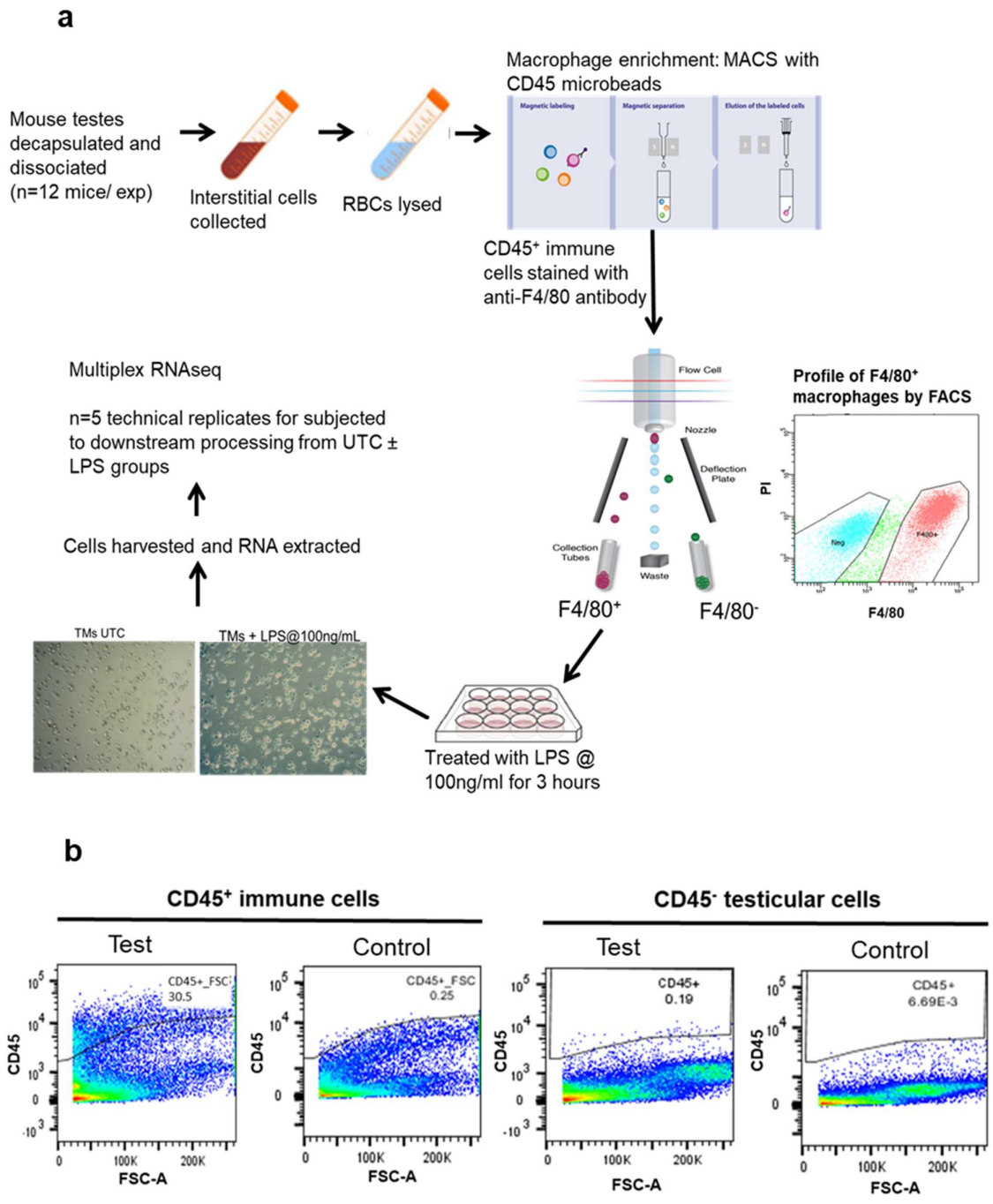
a
Mouse testes decapsulated and dissociated (n=12 mice/ exp)
Interstitial cells collected
RBCs lysed
Macrophage enrichment: MACS with CD45 microbeads
Magnetic labeling
Magnetic separation
Elution of the labeled cells
CD45+ immune cells stained with anti-F4/80 antibody
Flow Cell
Nozzle
Deflection Plate
Collection Tubes
Waste
F4/80+
F4/80-
Profile of F4/80+ macrophages by FACS
PI
Neg
F480+
F4/80
Multiplex RNAseq
n=5 technical replicates for subjected to downstream processing from UTC ± LPS groups
Cells harvested and RNA extracted
TMs UTC
TMs + LPS@100ng/mL
Treated with LPS @ 100ng/ml for 3 hours
b
CD45+ immune cells
CD45- testicular cells
Test
Control
Test
Control
CD45+_FSC 30.5
CD45+_FSC 0.25
CD45+ 0.19
CD45+ 6.69E-3
CD45
FSC-A
100K
200K

Figure 1: *Isolation and functional analysis of testicular macrophages from adult mouse testes.* ***(a)*** *Protocol for isolation of macrophages by mechanical dissociation, CD45-magnetic bead-enrichment and cell-sorting, and analysis of cultured cells incubated in the presence of LPS or in the absence of LPS (UTC).* (***b)*** *Flow cytometric analysis of* $CD45^{+}$ *and* $CD45^{-}$ *cells after magnetic cell separation (MACS) using CD45 microbeads, where control shows isotype control and test shows* $CD45^{+}$ *labelled cells. Cells were gated on CD45 expression and forward scatter (FSC), and 30.5% of cells in the CD45 microbead-bound fraction displayed CD45 fluorescence higher than the isotype control, while only 0.19% of cells in the unbound fraction were* $CD45^{+}$*. This analysis was repeated 3 times and representative data is shown.*

Figure 2:

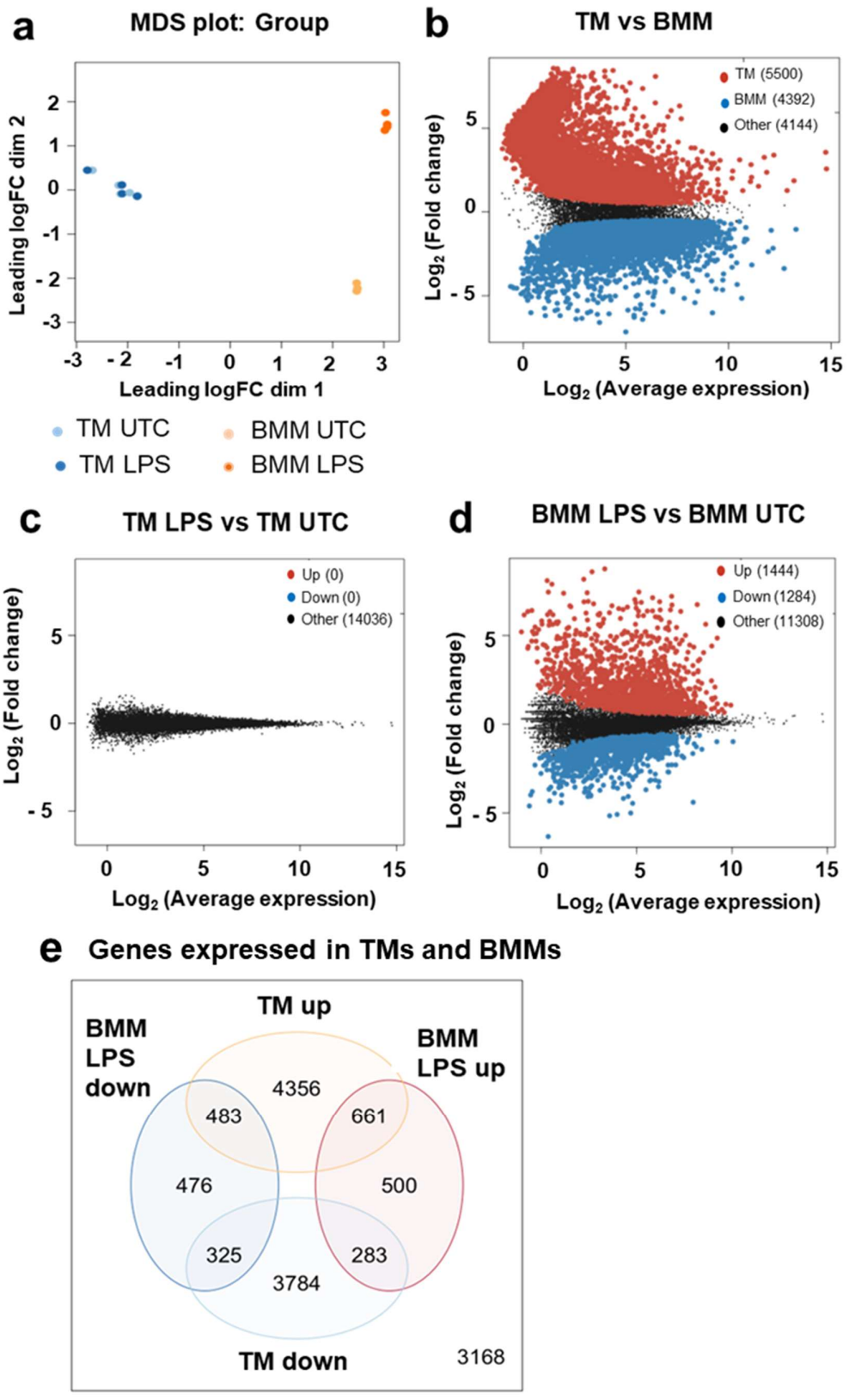
a
MDS plot: Group
Leading logFC dim 2
Leading logFC dim 1
TM UTC
TM LPS
BMM UTC
BMM LPS
b
TM vs BMM
TM (5500)
BMM (4392)
Other (4144)
Log2 (Fold change)
Log2 (Average expression)
c
TM LPS vs TM UTC
Up (0)
Down (0)
Other (14036)
Log2 (Fold change)
Log2 (Average expression)
d
BMM LPS vs BMM UTC
Up (1444)
Down (1284)
Other (11308)
Log2 (Fold change)
Log2 (Average expression)
e
Genes expressed in TMs and BMMs
TM up
BMM LPS down
BMM LPS up
4356
483
661
476
500
325
283
3784
TM down
3168

Figure 2: *Comparison of testicular macrophages (TM) with bone marrow-derived macrophages (BMM) by multiplex RNAseq analysis.* ***(a)*** *Group MDS plot of untreated (UTC) and LPS-treated (LPS) TMs and BMMs.* ***(b)*** *Volcano plot of gene expression by untreated TMs and BMMs. Genes expressed more highly by TMs are in red, and genes expressed more highly in BMMs are in blue.* ***(c****) Volcano plot of gene expression by untreated and LPS-treated TMs.* ***(d)*** *Volcano plot of gene expression by untreated and LPS-treated BMMs.* ***(e)*** *Venn diagram with comparison of genes expressed in BMM and TM groups where TM up means higher expression in TM UTC than BMM UTC, TM down means lower expression in TM UTC than BMM UTC, BMM LPS up means higher expression in BMM treated with LPS than TM LPS group and BMM LPS down means lower expression in BMM treated with LPS than TM LPS group.*

Figure 3:

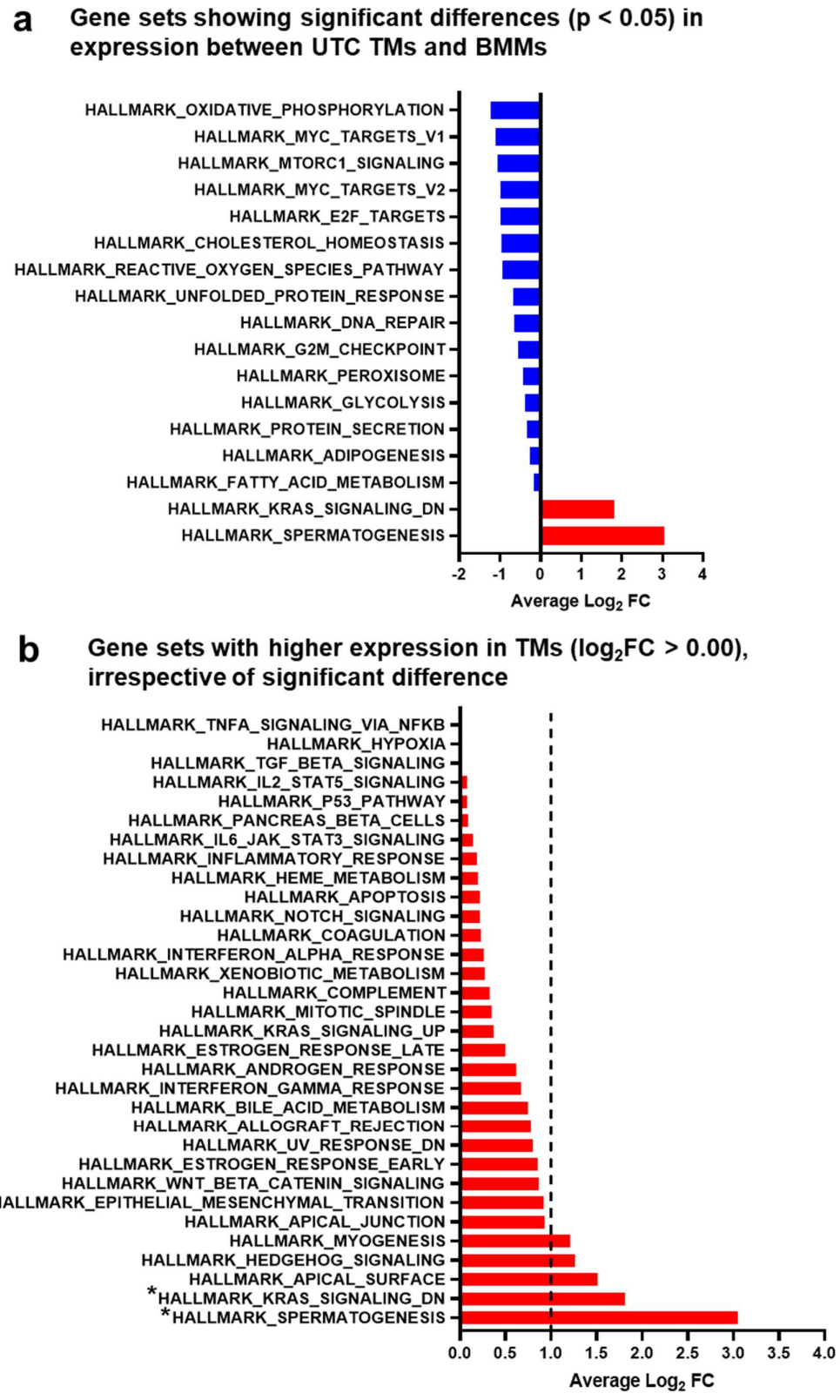
a
Gene sets showing significant differences (p < 0.05) in expression between UTC TMs and BMMs
HALLMARK_OXIDATIVE_PHOSPHORYLATION
HALLMARK_MYC_TARGETS_V1
HALLMARK_MTORC1_SIGNALING
HALLMARK_MYC_TARGETS_V2
HALLMARK_E2F_TARGETS
HALLMARK_CHOLESTEROL_HOMEOSTASIS
HALLMARK_REACTIVE_OXYGEN_SPECIES_PATHWAY
HALLMARK_UNFOLDED_PROTEIN_RESPONSE
HALLMARK_DNA_REPAIR
HALLMARK_G2M_CHECKPOINT
HALLMARK_PEROXISOME
HALLMARK_GLYCOLYSIS
HALLMARK_PROTEIN_SECRETION
HALLMARK_ADIPOGENESIS
HALLMARK_FATTY_ACID_METABOLISM
HALLMARK_KRAS_SIGNALING_DN
HALLMARK_SPERMATOGENESIS
-2 -1 0 1 2 3 4
Average Log2 FC
b
Gene sets with higher expression in TMs (log2FC > 0.00), irrespective of significant difference
HALLMARK_TNFA_SIGNALING_VIA_NFKB
HALLMARK_HYPOXIA
HALLMARK_TGF_BETA_SIGNALING
HALLMARK_IL2_STAT5_SIGNALING
HALLMARK_P53_PATHWAY
HALLMARK_PANCREAS_BETA_CELLS
HALLMARK_IL6_JAK_STAT3_SIGNALING
HALLMARK_INFLAMMATORY_RESPONSE
HALLMARK_HEME_METABOLISM
HALLMARK_APOPTOSIS
HALLMARK_NOTCH_SIGNALING
HALLMARK_COAGULATION
HALLMARK_INTERFERON_ALPHA_RESPONSE
HALLMARK_XENOBIOTIC_METABOLISM
HALLMARK_COMPLEMENT
HALLMARK_MITOTIC_SPINDLE
HALLMARK_KRAS_SIGNALING_UP
HALLMARK_ESTROGEN_RESPONSE_LATE
HALLMARK_ANDROGEN_RESPONSE
HALLMARK_INTERFERON_GAMMA_RESPONSE
HALLMARK_BILE_ACID_METABOLISM
HALLMARK_ALLOGRAFT_REJECTION
HALLMARK_UV_RESPONSE_DN
HALLMARK_ESTROGEN_RESPONSE_EARLY
HALLMARK_WNT_BETA_CATENIN_SIGNALING
HALLMARK_EPITHELIAL_MESENCHYMAL_TRANSITION
HALLMARK_APICAL_JUNCTION
HALLMARK_MYOGENESIS
HALLMARK_HEDGEHOG_SIGNALING
HALLMARK_APICAL_SURFACE
*HALLMARK_KRAS_SIGNALING_DN
*HALLMARK_SPERMATOGENESIS
0.0 0.5 1.0 1.5 2.0 2.5 3.0 3.5 4.0
Average Log2 FC

Figure 3: *Pathway analysis comparing gene sets in TMs and BMMs using the Hallmark dataset.* ***(a)*** *Gene sets showing significant differences ($p < 0.05$) in expression between UTC TMs and BMMs, presented as average log_2 FC.* ***(b)*** *All gene sets with higher expression in TMs ($log_2FC > 0.00$), irrespective of significant difference. TM gene sets showing a significant difference against BMMs at $p < 0.05$ are marked with *. The dotted line denotes average log_2 FC of 1 log.*

Figure 4:

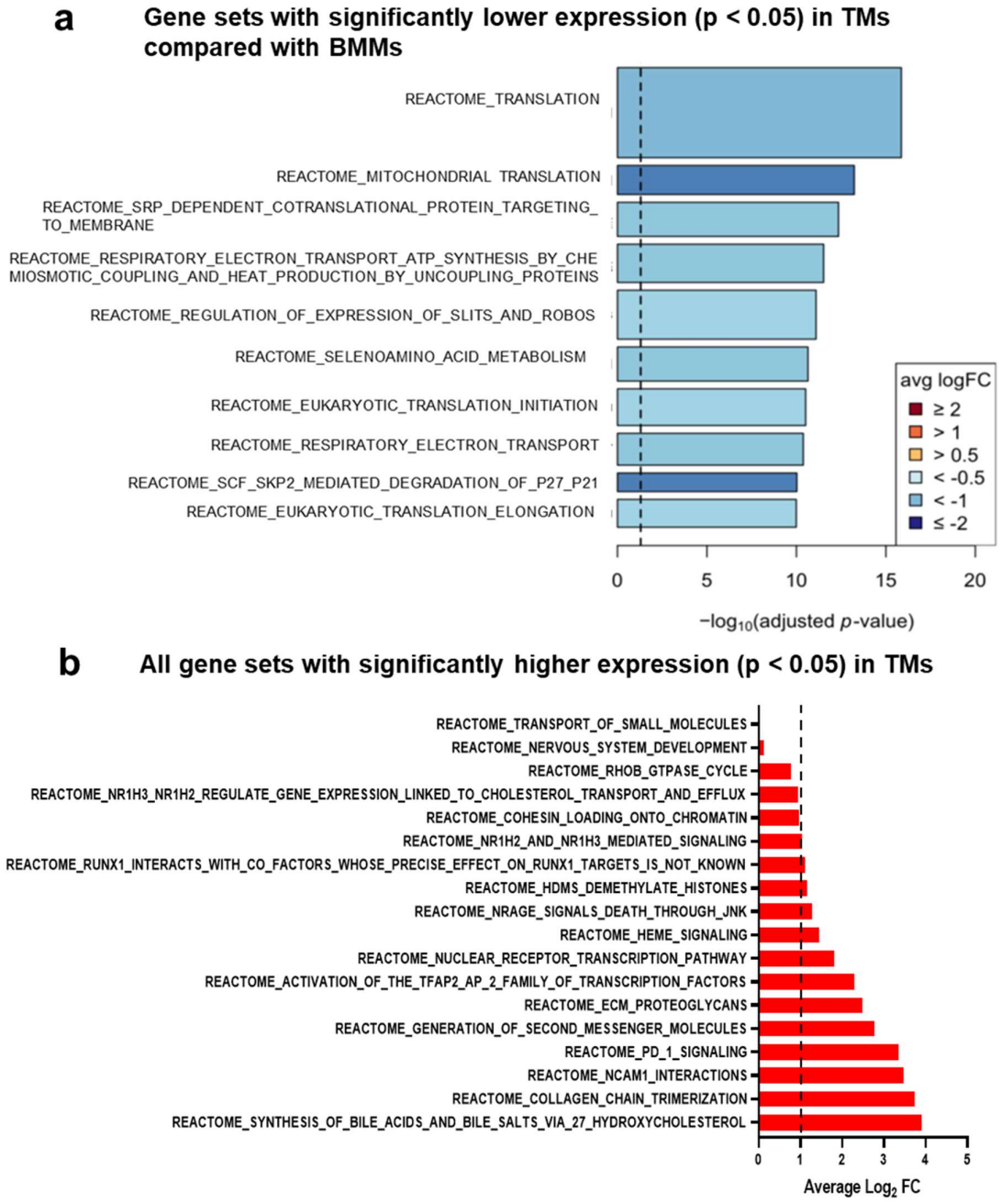

Figure 4: *Pathway analysis comparing gene sets in TMs and BMMs using the C2_CP: Reactome dataset,* ***(a)*** *Gene sets with significantly lower expression (p < 0.05) in TMs compared with BMMs.* ***(b)*** *All gene sets with significantly higher expression (p < 0.05) in TMs. The dotted lines denote average log_2 FC of 1 log.*

Figure 5:

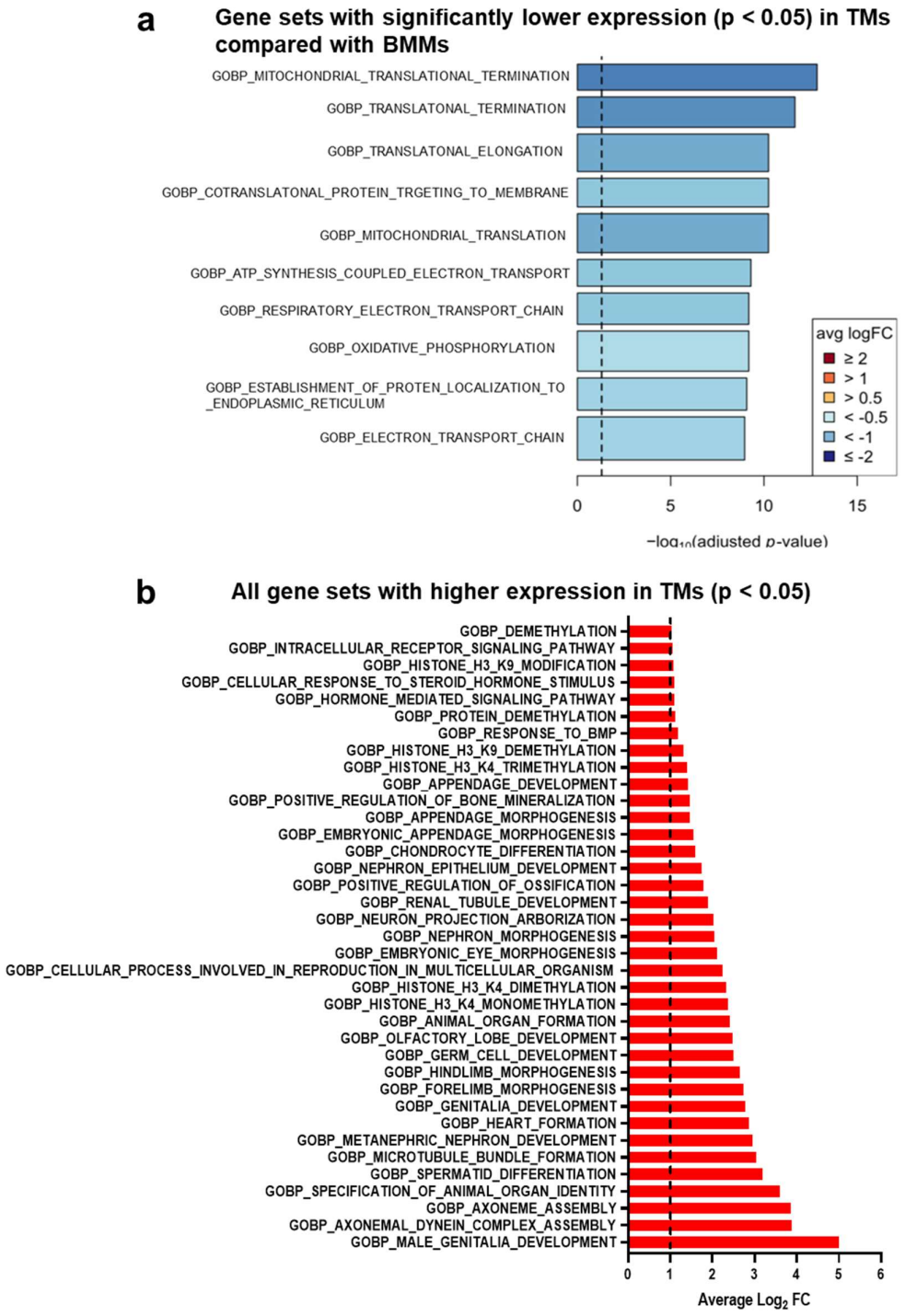

Figure 5: *Pathway analysis comparing gene sets in TMs and BMMs using the C5_Gene Ontology (GO): BP dataset.* ***(a)*** *Gene sets with significantly lower expression (p < 0.05) in TMs compared with BMMs.* ***(b)*** *All gene sets with higher expression in TMs (p < 0.05). The dotted lines denote average log_2 FC of 1 log.*

Figure 6:

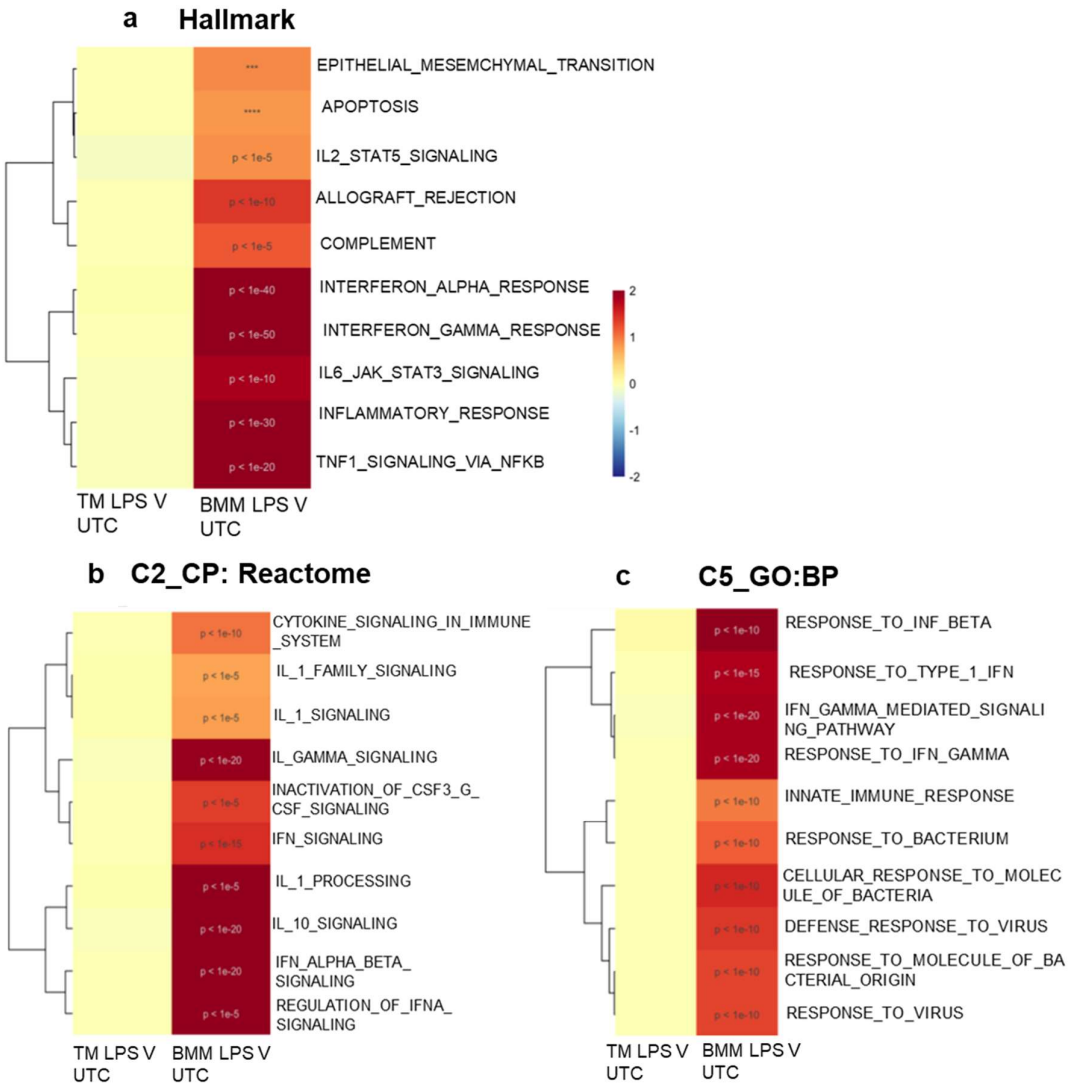

Figure 6: *Pathway analysis comparing gene sets in untreated and LPS-treated TMs and BMMs using* ***(a)*** *Hallmark* ***(b)*** *Reactome and* ***(c)*** *Gene Ontology (GO) datasets.*

Left blank on purpose

Figure 7:

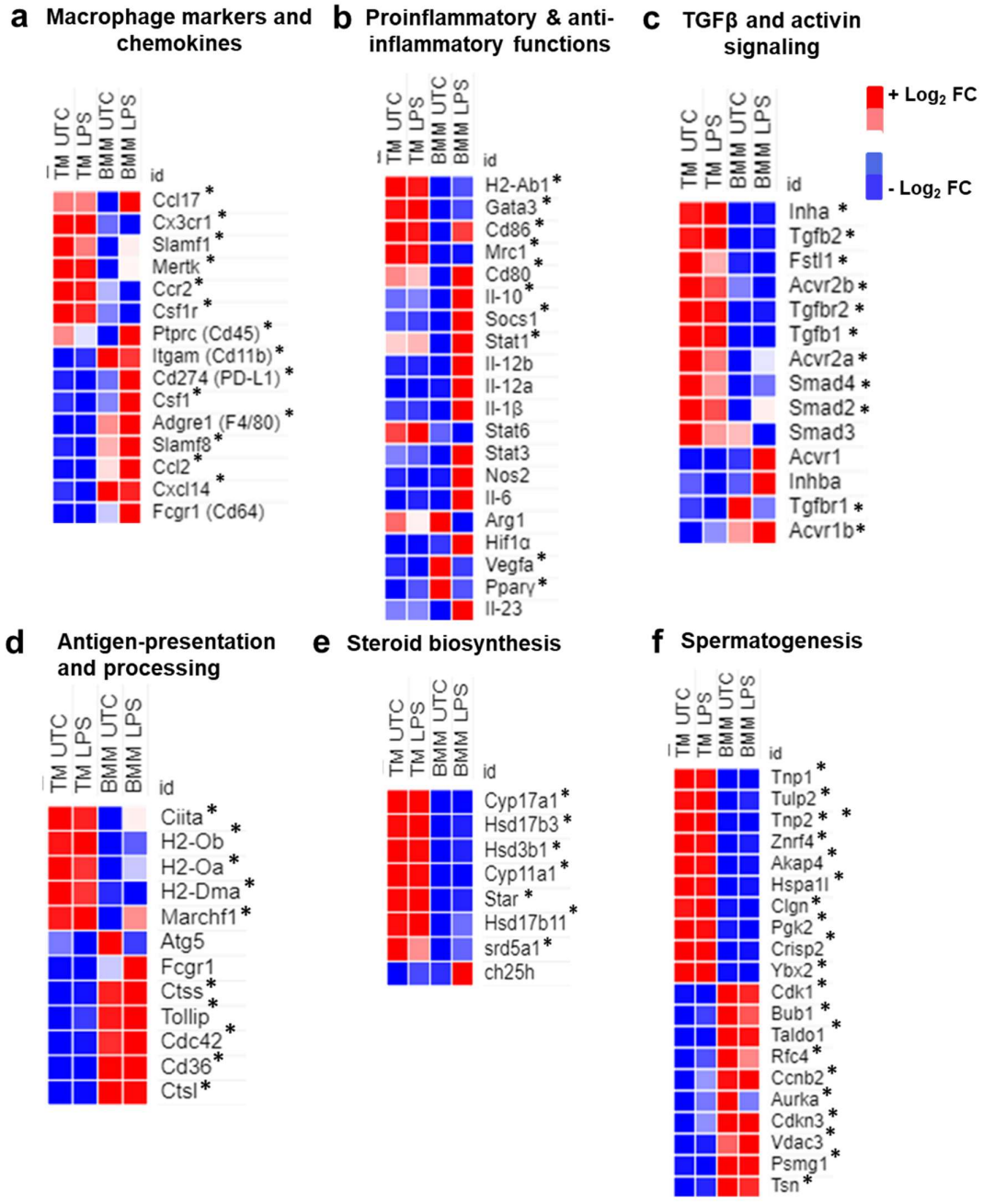
a Macrophage markers and chemokines
TM UTC
TM LPS
BMM UTC
BMM LPS
id
Ccl17 *
Cx3cr1 *
Slamf1 *
Mertk *
Ccr2 *
Csf1r *
Ptprc (Cd45) *
Itgam (Cd11b) *
Cd274 (PD-L1) *
Csf1 *
Adgre1 (F4/80) *
Slamf8 *
Ccl2 *
Cxcl14 *
Fcgr1 (Cd64)
b Proinflammatory & anti-inflammatory functions
TM UTC
TM LPS
BMM UTC
BMM LPS
id
H2-Ab1 *
Gata3 *
Cd86 *
Mrc1 *
Cd80 *
Il-10 *
Socs1 *
Stat1 *
Il-12b
Il-12a
Il-1β
Stat6
Stat3
Nos2
Il-6
Arg1
Hif1α
Vegfa *
Pparγ *
Il-23
c TGFβ and activin signaling
+ Log2 FC
- Log2 FC
TM UTC
TM LPS
BMM UTC
BMM LPS
id
Inha *
Tgfb2 *
Fstl1 *
Acvr2b *
Tgfbr2 *
Tgfb1 *
Acvr2a *
Smad4 *
Smad2 *
Smad3
Acvr1
Inhba
Tgfbr1 *
Acvr1b *
d Antigen-presentation and processing
TM UTC
TM LPS
BMM UTC
BMM LPS
id
Ciita *
H2-Ob *
H2-Oa *
H2-Dma *
Marchf1 *
Atg5
Fcgr1
Ctss *
Tollip *
Cdc42 *
Cd36 *
Ctsl *
e Steroid biosynthesis
TM UTC
TM LPS
BMM UTC
BMM LPS
id
Cyp17a1 *
Hsd17b3 *
Hsd3b1 *
Cyp11a1 *
Star *
Hsd17b11 *
srd5a1 *
ch25h
f Spermatogenesis
TM UTC
TM LPS
BMM UTC
BMM LPS
id
Tnp1 *
Tulp2 *
Tnp2 * *
Znrf4 *
Akap4 *
Hspa1l *
Clgn *
Pgk2 *
Crisp2 *
Ybx2 *
Cdk1 *
Bub1 *
Taldo1 *
Rfc4 *
Ccnb2 *
Aurka *
Cdkn3 *
Vdac3 *
Psmg1 *
Tsn *

Figure 7: *Heat maps of expression of genes related to macrophage marker genes and chemokines (**a**), proinflammatory and anti-inflammatory functions (**b**), TGFβ and activin signaling (**c**), antigen-presenting and processing (**d**), steroid biosynthesis (**e**) and spermatogenesis (**f**) in untreated (UTC) and LPS-stimulated (LPS) testicular macrophages (TM) and bone-marrow-derived macrophages (BMM) expressed as group average of counts per million (cpm). Color coding is based on row minimum and maximum values of each gene. Genes marked with * are significantly different in expression (adjusted p value < 0.05) in TM UTC as compared to BMM UTC. The LPS-treated expression groups were not compared as there was no effect in of LPS on TMs.*

Figure 8:

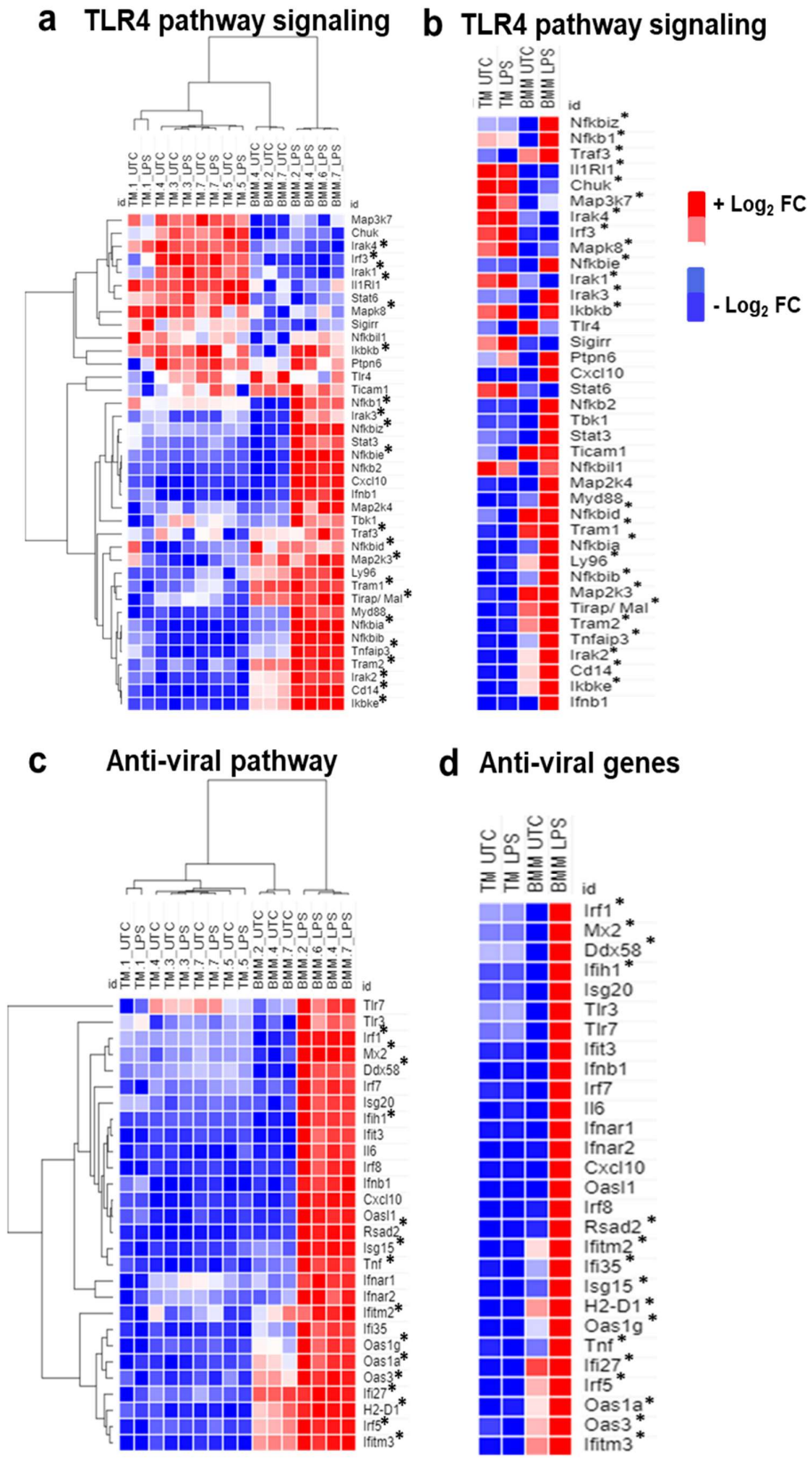
a TLR4 pathway signaling
b TLR4 pathway signaling
TM UTC
TM LPS
BMM UTC
BMM LPS
id
+ Log2 FC
- Log2 FC
c Anti-viral pathway
d Anti-viral genes

Figure 8: *Heat maps of expression of genes involved in TLR4 pathway signaling (**a,b**) and anti-viral genes (**c,d**) in untreated (UTC) and LPS-stimulated (LPS) testicular macrophages (TM) and bone-marrow-derived macrophages (BMM shown as individual replicates **(a,c)** and group average **(b,d)** expressed as counts per million (cpm). Color coding is based on row minimum and maximum values of each gene. Genes marked with * are significantly different in expression (adjusted p value < 0.05) in TM UTC as compared to BMM UTC. The LPS-treated expression groups were not compared as there was no effect in of LPS on TMs.*

Figure 9:

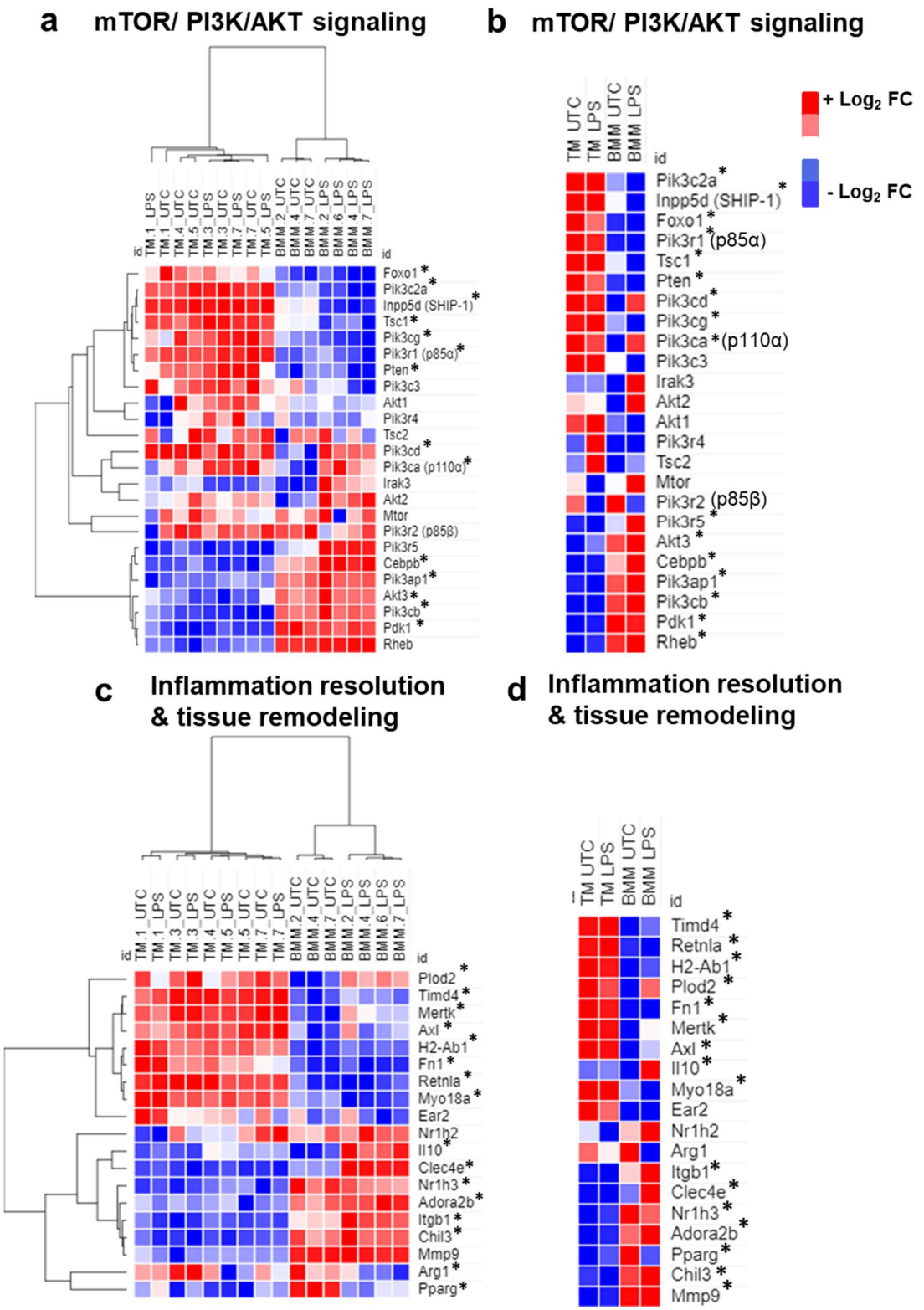
a
mTOR/ PI3K/AKT signaling
TM.1_LPS
TM.1_UTC
TM.4_UTC
TM.5_UTC
TM.3_LPS
TM.3_UTC
TM.7_LPS
TM.7_UTC
TM.5_LPS
BMM.2_UTC
BMM.4_UTC
BMM.7_UTC
BMM.2_LPS
BMM.6_LPS
BMM.4_LPS
BMM.7_LPS
id
Foxo1*
Pik3c2a*
Inpp5d (SHIP-1)*
Tsc1*
Pik3cg*
Pik3r1 (p85α)*
Pten*
Pik3c3
Akt1
Pik3r4
Tsc2
Pik3cd*
Pik3ca (p110α)*
Irak3
Akt2
Mtor
Pik3r2 (p85β)
Pik3r5
Cebpb*
Pik3ap1*
Akt3*
Pik3cb*
Pdk1*
Rheb
b
mTOR/ PI3K/AKT signaling
TM UTC
TM LPS
BMM UTC
BMM LPS
+ Log2 FC
- Log2 FC
id
Pik3c2a*
Inpp5d (SHIP-1)*
Foxo1*
Pik3r1 (p85α)*
Tsc1*
Pten*
Pik3cd*
Pik3cg*
Pik3ca*(p110α)
Pik3c3
Irak3
Akt2
Akt1
Pik3r4
Tsc2
Mtor
Pik3r2 (p85β)
Pik3r5*
Akt3*
Cebpb*
Pik3ap1*
Pik3cb*
Pdk1*
Rheb*
c
Inflammation resolution & tissue remodeling
TM.1_UTC
TM.1_LPS
TM.3_UTC
TM.3_LPS
TM.4_UTC
TM.5_LPS
TM.5_UTC
TM.7_UTC
TM.7_LPS
BMM.2_UTC
BMM.4_UTC
BMM.7_UTC
BMM.2_LPS
BMM.4_LPS
BMM.6_LPS
BMM.7_LPS
id
Plod2*
Timd4*
Mertk*
Axl*
H2-Ab1*
Fn1*
Retnla*
Myo18a*
Ear2
Nr1h2
Il10*
Clec4e*
Nr1h3*
Adora2b*
Itgb1*
Chil3*
Mmp9
Arg1*
Pparg*
d
Inflammation resolution & tissue remodeling
TM UTC
TM LPS
BMM UTC
BMM LPS
id
Timd4*
Retnla*
H2-Ab1*
Plod2*
Fn1*
Mertk*
Axl*
Il10*
Myo18a*
Ear2
Nr1h2
Arg1
Itgb1*
Clec4e*
Nr1h3*
Adora2b*
Pparg*
Chil3*
Mmp9*

Figure 9: *Heat maps of expression of genes involved in mTOR/PI3K/AKT signaling (**a,b**) and inflammation resolution and repair (**c,d**) in untreated (UTC) and LPS-stimulated (LPS) testicular macrophages (TM) and bone-marrow-derived macrophages (BMM) shown as individual replicates **(a,c)** and group average**(b,d)** expressed as counts per million (cpm). Color coding is based on row minimum and maximum values of each gene. Genes marked with * are significantly different in expression (adjusted p value < 0.05) in TM UTC as compared to BMM UTC. The LPS-treated expression groups were not compared as there was no effect in of LPS on TMs.*

Figure 10:

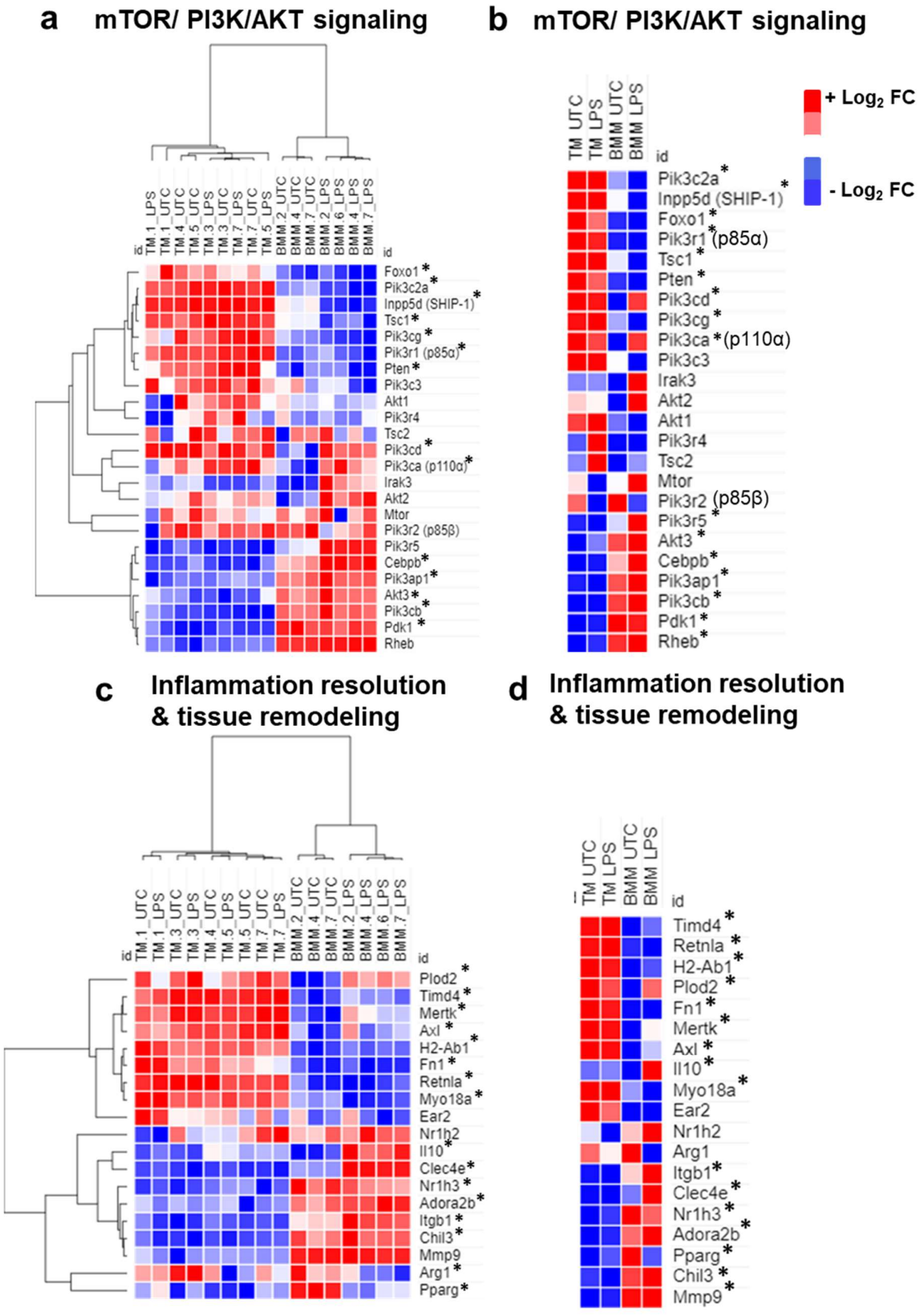
a
mTOR/ PI3K/AKT signaling
TM.1_LPS
TM.1_UTC
TM.4_UTC
TM.5_UTC
TM.3_LPS
TM.3_UTC
TM.7_LPS
TM.7_UTC
TM.5_LPS
BMM.2_UTC
BMM.4_UTC
BMM.7_UTC
BMM.2_LPS
BMM.6_LPS
BMM.4_LPS
BMM.7_LPS
id
Foxo1*
Pik3c2a*
Inpp5d (SHIP-1)*
Tsc1*
Pik3cg*
Pik3r1 (p85α)*
Pten*
Pik3c3
Akt1
Pik3r4
Tsc2
Pik3cd*
Pik3ca (p110α)*
Irak3
Akt2
Mtor
Pik3r2 (p85β)
Pik3r5
Cebpb*
Pik3ap1*
Akt3*
Pik3cb*
Pdk1*
Rheb
b
mTOR/ PI3K/AKT signaling
TM UTC
TM LPS
BMM UTC
BMM LPS
id
+ Log2 FC
- Log2 FC
Pik3c2a*
Inpp5d (SHIP-1)*
Foxo1*
Pik3r1 (p85α)*
Tsc1*
Pten*
Pik3cd*
Pik3cg*
Pik3ca (p110α)*
Pik3c3
Irak3
Akt2
Akt1
Pik3r4
Tsc2
Mtor
Pik3r2 (p85β)
Pik3r5*
Akt3*
Cebpb*
Pik3ap1*
Pik3cb*
Pdk1*
Rheb*
c
Inflammation resolution & tissue remodeling
TM.1_UTC
TM.1_LPS
TM.3_UTC
TM.3_LPS
TM.4_UTC
TM.5_LPS
TM.5_UTC
TM.7_UTC
TM.7_LPS
BMM.2_UTC
BMM.4_UTC
BMM.7_UTC
BMM.2_LPS
BMM.4_LPS
BMM.6_LPS
BMM.7_LPS
id
Plod2*
Timd4*
Mertk*
Axl*
H2-Ab1*
Fn1*
Retnla*
Myo18a*
Ear2
Nr1h2
Il10*
Clec4e*
Nr1h3*
Adora2b*
Itgb1*
Chil3*
Mmp9
Arg1*
Pparg*
d
Inflammation resolution & tissue remodeling
TM UTC
TM LPS
BMM UTC
BMM LPS
id
Timd4*
Retnla*
H2-Ab1*
Plod2*
Fn1*
Mertk*
Axl*
Il10*
Myo18a*
Ear2
Nr1h2
Arg1
Itgb1*
Clec4e*
Nr1h3*
Adora2b*
Pparg*
Chil3*
Mmp9*

Figure 10: *Heat maps of genes involved in metabolic pathways/PPP glycolysis/TCA cycle (**a**), glycolysis (**b**), oxidative phosphorylation (**c**) and the TCA cycle (**d**) in untreated (UTC) and LPS-stimulated (LPS) testicular macrophages (TM) and bone-marrow-derived macrophages (BMM) expressed as group average of counts per million (cpm). **(a)** Metabolic pathways overall: Selected genes of interest are presented in **(b)** Top 10 genes with highest and lowest expression in TMs, **(c, d)** Top 20 genes with highest and lowest expression in TMs with $p < 0.05$ (there were only 2 genes each for OXPHOS and TCA cycles that were highly expressed in TMs), **(e)** Phagocytosis-related and **(f)** Top 20 affected transcripts related to complement activation with 10-transcripts each with highest and lowest expression in TMs. Color coding is based on row minimum and maximum values of each gene. Genes marked with * are significantly different in expression (adjusted p value < 0.05) in TM UTC as compared to BMM UTC. The LPS-treated expression groups were not compared as there was no effect in of LPS on TMs.*

Chapter 5: General Discussion

Macrophages, which regulate inflammation and dictate the course of infection, are the most important immune cell type in the testis. It has been well-established that the majority of macrophages in the rodent testis are 'alternatively activated' (M2, or anti-inflammatory), consistent with the immune privilege of the tissue (Winnall *et al.,* 2011, Bhushan *et al.,* 2011). Significantly, activins have been implicated in regulating inflammatory responses by macrophages. The effects of activins on macrophages are complex and can lead to pro-inflammatory or anti-inflammatory phenotypes depending upon the environment and activation status of the macrophage itself. However, there had been no previous publications on the immunophysiology of the testis and the effects of altered activin and follistatin levels on testicular macrophages, prior to the present study. Additionally, the distribution and phenotypes of macrophages in several key testicular compartments, specifically the rete testis, the subcapsular interstitium, tunica albuginea, transition region and the efferent ducts had not been closely examined previously. Furthermore, previous analyses of the gene expression profiles and phenotype of the testicular macrophages, and their response to inflammation, had employed macrophage preparation that were significantly contaminated with other testicular cells or had been limited in their focus. The present study has addressed these issues.

The results of chapter two indicate that activin A exerts its action on the developing or mature testis to support and maintain total macrophage numbers throughout the testis. Furthermore, the effects of altered activin A and follistatin levels on gene expression in the testis indicate that activin A exerts cell-specific effects on macrophage function, distinct from its effects on Sertoli cells, Leydig cells and peritubular myoid cells. Regulation of macrophage numbers is probably most important during testicular development, when the TM populations are being established, but may also involve an ongoing regulatory/maintenance function when testis function is affected by disease or hormonal disturbance (Indumathy *et al.,* 2020). In this study, activin inhibited the expression of some transcripts associated with antigen-presentation (MHC II, CD86), thereby potentially regulating the ability of testicular macrophages to activate $CD4^+$ Th or Treg cells. The specificity of this response was indicated by the fact that expression of other co-stimulatory genes, *Cd80* and the inhibitory co-receptor, *Cd274*, were unaltered. MHC class II antigens, the scavenger receptor CD206 and the co-stimulatory B7 family of molecules (CD80, CD86 and CD274) are much more highly

expressed on ‘’professional’’ antigen-presenting cells (i.e., macrophages and dendritic cells), than on any other cell type, and the significant changes seen almost certainly represent changes in expression by the testicular macrophages (Mossadegh-Keller *et al.,* 2017, DeFalco *et al.,* 2014). The data indicated that activin A inhibits CD86 and MHCII expression by testicular antigen-presenting cells, which are predominantly macrophages, consistent with a role in controlling the antigen-presentation process in the mouse testis.

When macrophage distribution in the lesser-studied testicular compartments were studied in chapter three, it was found that macrophages have a much higher volume density and unique functional properties in the rete testis and subcapsular regions of the mouse testis, which are regions that are more susceptible to autoimmune responses (Tung *et al.,* 1987, Itoh *et al.,* 1995, Takahashi *et al.,* 2007). The sperm are probably most vulnerable to auto-immune damage while passing through the rete testis (Major *et al.,* 2021). It was shown that F4/80^{+} macrophages in the rete testis are not only considerably greater in number than those present in the parenchyma of the testis, but they are almost certainly functionally different, based on their expression of markers of antigen-presentation and inflammation-suppression. The F4/80^{+} interstitial and peri-epithelial macrophage subsets of the rete testis have an antigen-presenting phenotype (like peritubular macrophages, expressing MHCII^{+}), but are clearly anti-inflammatory/M2 (like interstitial macrophages, expressing CD206^{+}). These macrophages might be present in higher numbers in this region as part of a mechanism to protect the sperm traveling from the seminiferous tubules to the epididymis or to protect the testis from ascending infections, or both. It was recently reported that F4/80^{+} peritubular macrophages are present in the mouse testis parenchyma at 1-2 weeks after birth and probably earlier, but do not express MHCII at this age (Lokka *et al.,* 2020, Mossadegh-Keller *et al.,* 2017). Consequently, it will be interesting to investigate when the peri-epithelial and interstitial macrophage populations of the rete testis first appear and when they begin to express MHCII, given that mature sperm are not produced by the testis until about 4-5 weeks of age. In addition to this, a significant proportion of macrophages in the subcapsule and the tunica albuginea also expressed both MHCII and CD206, unlike the parenchymal interstitial cells, indicating these macrophages have a similar regulatory function to the macrophages of the rete testis. In this regard, it is significant that the subcapsular

region and rete testis are the regions of the testis most susceptible to auto-immune inflammation, and further detailed investigation of these cells is essential.

As demonstrated in chapter three, the number and, possibly, the function of the rete testis macrophages were regulated by activin and their numbers increased dramatically during bacterial infection. It is important to note that the transcript levels of MHCII and co-stimulatory molecules involved in antigen-presentation were upregulated in whole testis extracts of mice deficient in activin A (Chapter two). This suggests that endogenous production of activin A maintains macrophage numbers in the mouse testis, but reduces their antigen-presentation functions. It would be worth studying the production of activin A by cells in the rete testis region compared with the rest of the parenchyma, in order to assess the role of activin A in controlling the immune environment in the different testis compartments. Moreover, there was an increase in F4/80^{+}MHCII^{+} macrophages in the rete testis, the subcapsule and tunica albuginea following UPEC infection, which resolved several weeks later. There also was an observable increase in CD206 expression by interstitial macrophages at this time. We propose that the vasculature surrounding the rete testis serves as a port of entry for infiltration of circulating monocyte/macrophages into the testis, which then spread to the subcapsule and tunica albuginea, but with minimal spread into the parenchyma. Alternatively, the resident macrophages of the rete testis may be induced to proliferate in response to bacterial infection, but this seems less likely given the predominantly non-inflammatory nature of the testicular macrophage population. The respective roles of the resident macrophages versus new macrophages in responding to ascending bacterial infections needs further study.

Previous studies conducted in rat and mice (Kern *et al.,* 1995, Hayes *et al.,* 1996, Bryniarski *et al.,* 2004, Winnall *et al.,* 2011, Bhushan *et al.,* 2015, Zhang *et al.,* 2020, Gayer *et al.,* 2022) have established that the testicular macrophages are anti-inflammatory/tolerogenic, with poor pro-inflammatory capacity, but the presence of testicular spermatogenic and somatic cell contamination complicates these findings. In the present study (Chapter 4), a new purification method for mouse testicular macrophages from mechanically-isolated testes were developed and validated. In general, the results confirmed that TMs are transcriptionally different from a baseline of BMMs matured in the presence of CSF1. The gene expression profile confirms that the overall TM phenotype is predominantly homeostatic/anti-inflammatory/M2: TMs

displayed higher constitutive expression of genes encoding anti-inflammatory genes (*Il10*, *Socs1*, *Nfkbiz*), transcription factors that regulate the alternatively-activated/M2 phenotype (*Stat3*, *Stat6*, *Gata3*) and other anti-inflammatory and immunoregulatory proteins, including the scavenger receptor, CD206 (*Mrc1*), the anti-inflammatory transcription factor *Nfe2l2* and the EGF receptor (*Egfr*). However, the TMs showed higher expression of genes encoding proteins required for antigen-presentation to $CD4^+$ T cells, including several MHC class II antigens, the stimulatory co-receptors CD80 and CD86, the essential activator of MHC class II gene transcription, C2TA (*Ciita*) and MARCH1 (*Marchf1*) responsible for the turnover and stability of peptide-MHCII on the surface of an APC (Ting and Trowsdale, 2002, Gordon *et al.,* 2014). Overall, these gene expression data completely support the phenotypic data (Chapters two and three) indicating that the majority of macrophages in the adult mouse testis have an immunoregulatory and tolerogenic function.

This study also evaluated the expression of several key regulatory factors that we have been reported in the past to maintain the anti-inflammatory phenotype of macrophages in testis and other tissues, such as activin/TGFβ, SHIP-1 and mTOR/PI3K/AKT (Winnall *et al.,* 2011, Conde *et al.,* 2011, Vergadi *et al.,* 2017). Most activin/TGFβ signaling genes were more highly expressed in TMs as compared to BMMs, supporting the role of activins in maintaining the anti-inflammatory phenotype of macrophages in the testis at homeostasis (Indumathy *et al.,* 2020, Biniwale *et al.,* 2022). In addition, the highly purified testicular macrophages were not only unresponsive to LPS, but they had low expression of many key transcripts for the molecules in the TLR4-signalling pathway. This confirms the previous observation, in a study performed using less-purified LPS-treated TMs from Wistar rats, where this signaling pathway was similarly downregulated (Bhushan *et al.,* 2015). On the contrary, one of the few MyD88-dependent negative regulators, *Ptpn6* had elevated expression in TMs. Moreover, transcripts such as *Mtor*, *Akt2* and several PI3K catalytic subunits encoding the mTOR/PI3K/AKT signaling pathway were expressed in TMs, but key regulators of this pathway that promote the anti-inflammatory/M2 phenotype (*Akt1, Pten*, *Inpp5d*) were also elevated in expression. This signaling pathway plays a complex role in inflammation, and stimulates NF-κB activation, but can also play an anti-inflammatory role (Vergadi *et al.,* 2017, Troutman *et al.,* 2012). Additionally, SHIP-1 regulates the activity of PI3K by hydrolyzing its product, PI-3,4,5-P3 to inactive PI-

3,4-P2, thus inhibiting NF-κB-dependent activation in response to stimulation, and was more highly expressed in TMs than in BMMs (Conde *et al.,* 2011). Crucially, activin A has been shown to suppress inflammatory responses in activated macrophages through stimulation of SHIP1 (Cuschieri *et al.,* 2008).

It is important to note that the whole testis gene expression study in chapter 2 and multiplex RNAseq study in chapter 4 investigated gene transcript levels, which can only give an indirect estimate of function, and not the protein levels or their activity. More comprehensive functional studies will be required to explore the biological significance of these results, and the molecules and pathways that have been implicated.

Finally, in order to investigate the immune environment in the testicular compartments and role of activin A in regulating macrophage populations in these compartments in more detail, it will be interesting to study appearance of the immunoregulatory and tolerogenic phenotypes of peri-epithelial and interstitial macrophage populations of the rete testis and when they begin to express MHCII, given that mature sperm are not produced by the testis until about 4-5 weeks of age. In addition to this, it will be interesting to study the origin of subcapsule and capsular macrophages as they express MHCII and CD206, unlike parenchymal macrophages, to determine whether they originate from the same waves of hematopoiesis as interstitial and peritubular macrophages in the parenchyma and their time frame of development. As the effect of activin A on macrophage numbers and their phenotypes is compartment-specific, a further study is warranted to understand the production of activin A by cells in the rete testis region compared with the rest of the parenchyma, in order to assess the role of activin A in controlling the immune environment in the different testis compartments.

Figure 1:

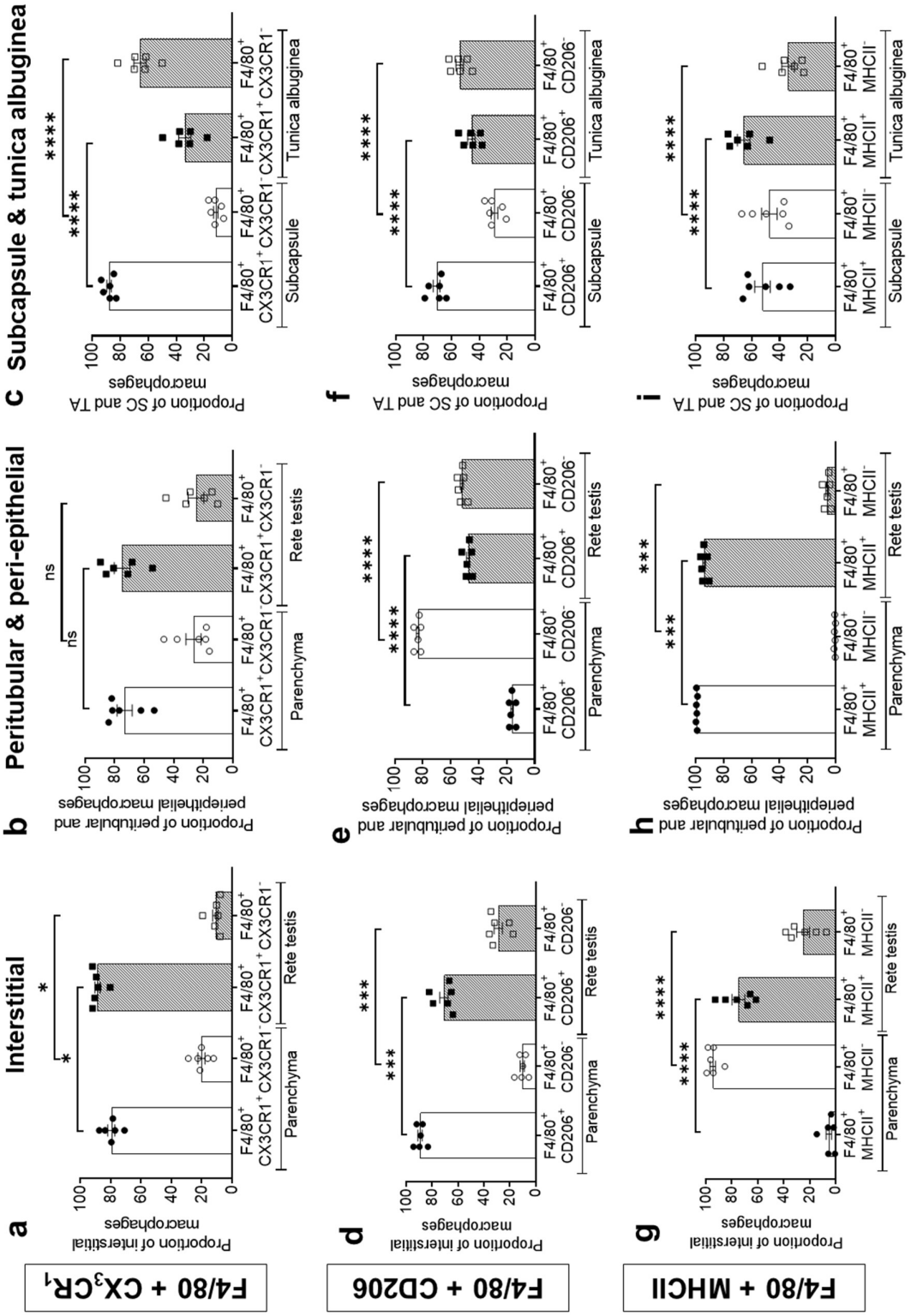
F4/80 + CX3CR1
F4/80 + CD206
F4/80 + MHCII
a
Interstitial
b
Peritubular & peri-epithelial
c
Subcapsule & tunica albuginea
d
e
f
g
h
i
Proportion of interstitial macrophages
Proportion of peritubular and periepithelial macrophages
Proportion of SC and TA macrophages
F4/80+ CX3CR1+ CX3CR1- CX3CR1+ CX3CR1-
F4/80+ CX3CR1+ CX3CR1- CX3CR1+ CX3CR1-
F4/80+ CD206+ F4/80+ CD206- F4/80+ CD206+ F4/80+ CD206-
F4/80+ MHCII+ F4/80+ MHCII- F4/80+ MHCII+ F4/80+ MHCII-
Parenchyma
Rete testis
Subcapsule
Tunica albuginea
ns
*
***
****

Figure 1: *Proportions of macrophages (%) in the testicular compartments of adult $Cx_3cr_1^{GFP/+}Inhba^{+/+}$ mouse using CX_3CR_1 and F4/80 markers (**a, b, c**) F4/80 and CD206 markers (**d, e, f**) and F4/80 and MHCII markers (**g, h, i**) where the testis section was compartmentalized into interstitial tissue (IT) and seminiferous tubules (ST) of parenchyma, subcapsular interstitial tissue (SC), tunica albuginea (TA) and the rete testis (RT) was divided into interstitium (IT) and periepithelium (PE). Panels a, b, d, e, g and h compare parenchyma and rete testis subsets whereas panels c, f and I compare subsets of subcapsule and tunica albuginea. Values are mean ± S.E.M (n=6 $Cx_3cr_1^{GFP/+}$ $Inhba^{+/+}$); *p<0.05, **p<0.01, ***p<0.001, ****p<0.0001, ns- not significantly different. Each data point represents a single animal expressed as a mean of 3 sections/ animal.*

Figure 2:

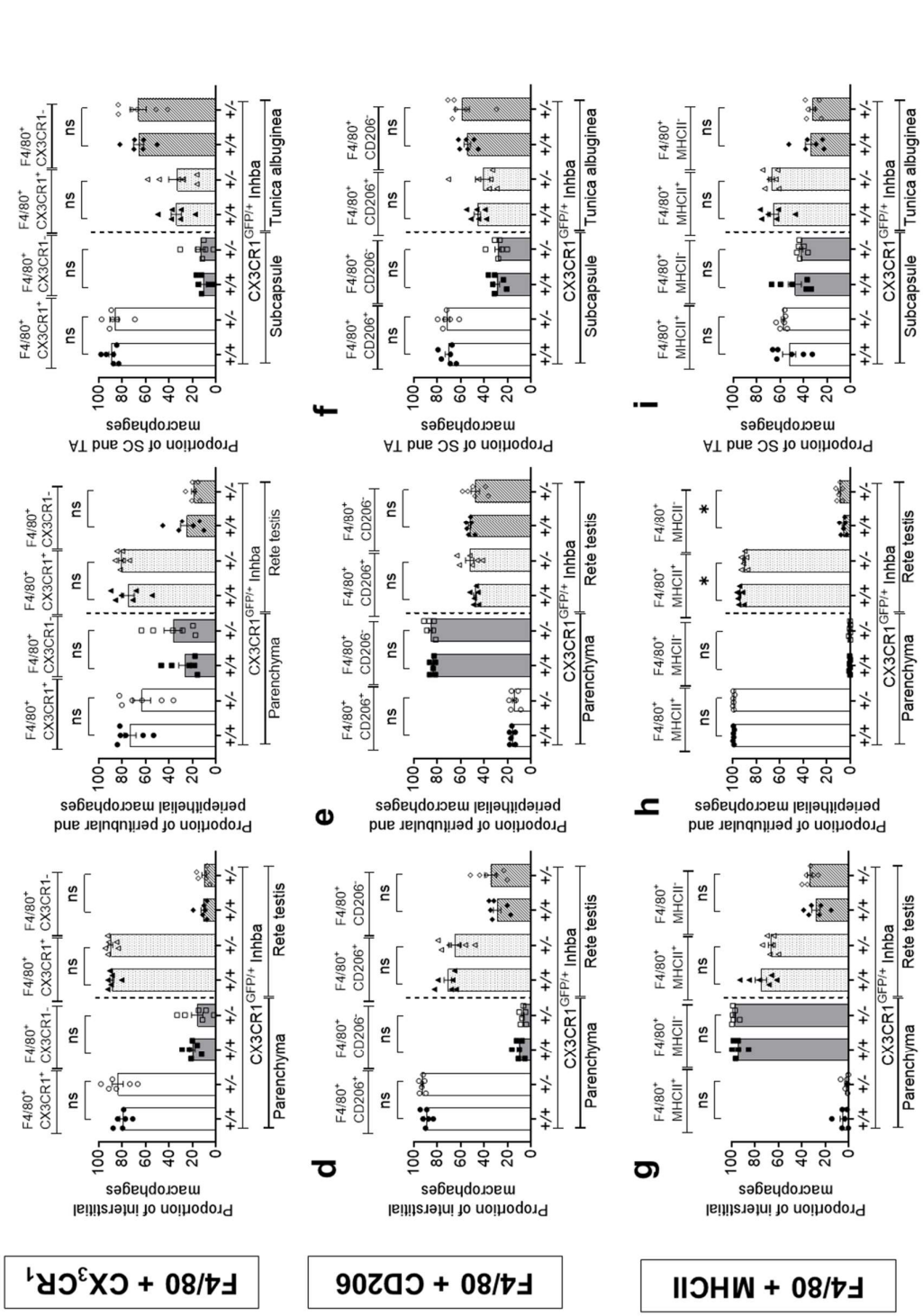
a Interstitial
b Peritubular & peri-epithelial
c Subcapsule & tunica albuginea
d
e
f
g
h
i
F4/80 + CX3CR1
F4/80 + CD206
F4/80 + MHCII
Proportion of interstitial macrophages
Proportion of peritubular and peripithelial macrophages
Proportion of SC and TA macrophages
F4/80+ CX3CR1+
F4/80+ CX3CR1-
F4/80+ CD206+
F4/80+ CD206-
F4/80+ MHCII+
F4/80+ MHCII-
ns
*
+/+ +/- +/+ +/- +/+ +/-
CX3CR1GFP/+ Inhba
Parenchyma
Rete testis
Subcapsule
Tunica albuginea

Figure 2: *Proportions of macrophages (%) in the testicular compartments of adult $Cx_3cr_1^{GFP/+}Inhba^{+/-}$ (activin A-deficient) mouse using CX_3CR_1 and F4/80 markers (**a, b, c**) F4/80 and CD206 markers (**d, e, f**) and F4/80 and MHCII markers (**g, h, i**) where the testis section was compartmentalized into interstitial tissue (IT) and seminiferous tubules (ST) of parenchyma, subcapsular interstitial tissue (SC), tunica albuginea (TA) and the rete testis (RT) was divided into interstitium (IT) and periepithelium (PE). Panels a, b, d, e, g and h compare parenchyma and rete testis subsets whereas panels c, f and I compare subsets of subcapsule and tunica albuginea. Values are mean ± S.E.M (n=6 $Cx_3cr_1^{GFP/+}$ $Inhba^{+/+}$; n=6 $Cx_3cr_1^{GFP/+}$ $Inhba^{+/-}$); *p<0.05, **p<0.01, ***p<0.001, ****p<0.0001, ns- not significantly different. Each data point represents a single animal expressed as a mean of 3 sections/ animal.*

Bibliography (Literature Review and General Discussion)

Ahmed, A., Schmidt, C. & Brunner, T. 2019. Extra-adrenal glucocorticoid synthesis in the intestinal mucosa: between immune homeostasis and immune escape. *Frontiers in Immunology,* 10**,** 1438.

Aiyama, Y., Tsunekawa, N., Kishi, K., Kawasumi, M., Suzuki, H., Kanai-Azuma, M., Kurohmaru, M. & Kanai, Y. 2015. A Niche for GFRα1-Positive Spermatogonia in the Terminal Segments of the Seminiferous Tubules in Hamster Testes. *Stem Cells,* 33**,** 2811-2824.

Anderson, R. A., Evans, L. W., Irvine, D. S., Mcintyre, M. A., Groome, N. P. & Riley, S. C. 1998. Follistatin and activin A production by the male reproductive tract. *Human Reproduction,* 13**,** 3319-3325.

Aratchige, P. E., Mcintyre, P. B., Quinn, H. E. & Gilbert, G. L. 2008. Recent increases in mumps incidence in Australia: the “forgotten” age group in the 1998 Australian Measles Control Campaign. *Medical Journal of Australia,* 189**,** 434-437.

Archambeault, D. R. & Yao, H. H.-C. 2010. Activin A, a product of fetal Leydig cells, is a unique paracrine regulator of Sertoli cell proliferation and fetal testis cord expansion. *Proceedings of the National Academy of Sciences,* 107**,** 10526-10531.

Avallet, O., Vigier, M., Leduque, P., Dubois, P. M. & Saez, J. M. 1994. Expression and regulation of transforming growth factor-β1 messenger ribonucleic acid and protein in cultured porcine Leydig and Sertoli cells. *Endocrinology,* 134**,** 2079-2087.

Banchereau, J. & Steinman, R. M. 1998. Dendritic cells and the control of immunity. *Nature,* 392**,** 245-252.

Barbara, N. P., Wrana, J. L. & Letarte, M. 1999. Endoglin is an accessory protein that interacts with the signaling receptor complex of multiple members of the transforming growth factor-β superfamily. *Journal of Biological Chemistry,* 274**,** 584-594.

Bhushan, S. & Meinhardt, A. 2017. The macrophages in testis function. *Journal of Reproductive Immunology,* 119**,** 107-112.

Bhushan, S., Hossain, H., Lu, Y., Geisler, A., Tchatalbachev, S., Mikulski, Z., Schuler, G., Klug, J., Pilatz, A., Wagenlehner, F., Chakraborty, T. & Meinhardt, A. 2011. Uropathogenic E. coli Induce Different Immune Response in Testicular and Peritoneal Macrophages: Implications for Testicular Immune Privilege. *PLoS ONE,* 6**,** e28452.

Bhushan, S., Tchatalbachev, S., Lu, Y., Fröhlich, S., Fijak, M., Vijayan, V., Chakraborty, T. & Meinhardt, A. 2015. Differential Activation of Inflammatory Pathways in Testicular Macrophages Provides a Rationale for Their Subdued Inflammatory Capacity. *The Journal of Immunology,* 194**,** 5455-5464.

Bhushan, S., Theas, M. S., Guazzone, V. A., Jacobo, P., Wang, M., Fijak, M., Meinhardt, A. & Lustig, L. 2020. Immune Cell Subtypes and Their Function in the Testis. *Frontiers in Immunology,* 11**,** 583304-583304.

Biniwale, S., Wijayarathna, R., Pleuger, C., Bhushan, S., Loveland, K. L., Meinhardt, A. & Hedger, M. P. 2022. Regulation of macrophage number and gene transcript levels by activin A and its binding protein, follistatin, in the testes of adult mice. *Journal of Reproductive Immunology,* 151**,** 103618.

Britannica, T. Editors of Encyclopaedia (2020, May 27). spermatogenesis. Encyclopedia Britannica. https://www.britannica.com/science/spermatogenesis.

Brosh, N., Sternberg, D., Honigwachs-Sha’anani, J., Lee, B. C., Shav-Tal, Y. & Tzehoval, E. 1995. The plasmacytoma growth inhibitor restrictin-P is an antagonist of interleukin 6 and interleukin 11. Identification as a stroma-derived activin A. *Journal of Biological Chemistry,* 270**,** 29594-29600.

Bryniarski, K., Szczepanik, M., Maresz, K., Ptak, M. & Ptak, W. 2004. Subpopulations of Mouse Testicular Macrophages and their Immunoregulatory Function. *American Journal of Reproductive Immunology,* 52**,** 27-35.

Carpenter, M. P. 1974. Prostaglandins of rat testis. *Lipids,* 9**,** 397-406.

Cesaris, P. D., Philippini, A., Cervelli, C., Riccioli, A., Muci, S. & Starace, G. 1992. Immunosuppressive molecules produced by Sertoli cells cultured in vitro: Biological effects on lymphocytes. *Biochemical and Biophysical Research Communications,* 186**,** 1639-1646.

Chen, W. & Ten Dijke, P. 2016. Immunoregulation by members of the TGFβ superfamily. *Nature Reviews Immunology,* 16**,** 723-740.

Chen, Z., Hagler, J., Palombella, V. J., Melandri, F., Scherer, D., BALLARD, D. & Maniatis, T. 1995. Signal-induced site-specific phosphorylation targets I kappa B alpha to the ubiquitin-proteasome pathway. *Genes & Development,* 9**,** 1586-1597.

Clulow, J., Jones, R., Hansen, L. & Man, S. 1998. Fluid and electrolyte reabsorption in the ductuli. *Journal of Reproduction and Fertility Supplement,* 53**,** 1-14.

Cohen, P. E., Chisholm, O., Arceci, R. J., Stanley, E. R. & Pollard, J. W. 1996. Absence of Colony-Stimulating Factor-1 in Osteopetrotic ($csfm^{op}/csfm^{op}$) Mice Results in Male Fertility Defects. *Biology of Reproduction,* 55**,** 310-317.

Conde, C., Gloire, G. & Piette, J. 2011. Enzymatic and non-enzymatic activities of SHIP-1 in signal transduction and cancer. *Biochemical Pharmacology,* 82**,** 1320-1334.

Cuschieri, J., Bulger, E., Grinsell, R., Garcia, I. & Maier, R. V. 2008. Insulin regulates macrophage activation through activin A. *Shock,* 29**,** 285-290.

de Kretser, D.M & Robertson, D. 1989. The isolation and physiology of inhibin and related proteins. *Biology of Reproduction,* 40**,** 33-47.

de Kretser, Temple-Smith, P. D., Kerr, J. B. 1982. Anatomical and functional aspects of the male reproductive organs. *In:* Bandhauer, J & Frick, K. (eds). *Disturbances in Male Fertility.* Berlin, Heidelberg: Springer Berlin Heidelberg, 1-131

Defalco, T., Bhattacharya, I., Williams, A. V., Sams, D. M. & Capel, B. 2014. Yolk-sac–derived macrophages regulate fetal testis vascularization and morphogenesis. *Proceedings of the National Academy of Sciences of the United States of America,* 111**,** E2384-E2393.

Defalco, T., Potter, S. J., Williams, A. V., Waller, B., Kan, M. J. & Capel, B. 2015. Macrophages Contribute to the Spermatogonial Niche in the Adult Testis. *Cell Reports,* 12**,** 1107-1119.

Dickson, C., Webster, D. R., Johnson, H., Millena, A. C. & Khan, S. A. 2002. Transforming growth factor-β effects on morphology of immature rat Leydig cells. *Molecular and Cellular Endocrinology,* 195**,** 65-77.

Dym, M. 1974. The fine structure of monkey Sertoli cells in the transitional zone at the junction of the seminiferous tubules with the tubuli recti. *American Journal of Anatomy,* 140**,** 1-25.

El-Demiry, M. I. M., Hargreave, T. B., Busuttil, A., James, K., Ritchie, A. W. S. & Chisholm, G. D. 1985. Lymphocyte Sub-populations in the Male Genital Tract. *British Journal of Urology,* 57**,** 769-774.

Eramaa, M., Hurme, M., Stenman, U. H. & Ritvos, O. 1992. Activin A/erythroid differentiation factor is induced during human monocyte activation. *Journal of Experimental Medicine,* 176**,** 1449-1452.

Fang, J., Yin, W., Smiley, E., Wang, S. Q. & Bonadio, J. 1996. Molecular cloning of the mouse activin βE subunit gene. *Biochemical and Biophysical Research Communications,* 228**,** 669-674.

Figueiredo, A. F. A., Hess, R. A., Batlouni, S. R., Wnuk, N. T., Tavares, A. O., Abarikwu, S. O., Costa, G. M. J. & França, L. R. 2021. Insights into differentiation and function of the transition region between the seminiferous tubule and rete testis. *Differentiation,* 120**,** 36-47.

Figueiredo, A., França, L., Hess, R. & Costa, G. 2016. Sertoli cells are capable of proliferation into adulthood in the transition region between the seminiferous tubules and the rete testis in Wistar rats. *Cell Cycle,* 15**,** 2486-2496.

Fijak, M., Bhushan, S. & Meinhardt, A. 2017. The Immune Privilage Of The Testis. *In:* Krause, W. K. H. & Naz, R. K. (eds.) *Immune Infertility: Impact of Immune Reactions on Human Fertility.* Springer International Publishing, 97-107.

Fijak, M., Pilatz, A., Hedger, M. P., Nicolas, N., Bhushan, S., Michel, V., Tung, K. S. K., Schuppe, H.-C. & Meinhardt, A. 2018. Infectious, inflammatory and 'autoimmune' male factor infertility: how do rodent models inform clinical practice? *Human Reproduction Update,* 24**,** 416-441.

Fijak, M., Schneider, E., Klug, J., Bhushan, S., Hackstein, H., Schuler, G., Wygrecka, M., Gromoll, J. & Meinhardt, A. 2011. Testosterone Replacement Effectively Inhibits the Development of Experimental Autoimmune Orchitis in Rats: Evidence for a Direct Role of Testosterone on Regulatory T Cell Expansion. *The Journal of Immunology,* 186**,** 5162-5172.

Frungieri, M. B., Calandra, R. S., Mayerhofer, A. & Matzkin, M. E. 2015. Cyclooxygenase and prostaglandins in somatic cell populations of the testis. *Reproduction*, 149, R169-80.

Funaba, M., Ikeda, T., Ogawa, K., Murakami, M. & Abe, M. 2003. Role of activin A in murine mast cells: modulation of cell growth, differentiation, and migration. *Journal of Leukocyte Biology,* 73**,** 793-801.

Gayer, F. A., Reichardt, S. D., Bohnenberger, H., Engelke, M. & Reichardt, H. M. 2022. Characterization of testicular macrophage subpopulations in mice. *Immunology Letters,* 243**,** 44-52.

Gaytan, F., Bellido, C., Aguilar, E. & Van Rooijen, N. 1994. Requirement for testicular macrophages in Leydig cell proliferation and differentiation during prepubertal development in rats. *Journal of Reproduction and Fertility,* 102**,** 393-9.

Gerdprasert, O., O'bryan, M. K., Muir, J. A., Caldwell, A. M., Schlatt, S., de Kretser, D. M. & Hedger, M. P. 2002a. The response of testicular leukocytes to lipopolysaccharide-induced inflammation: further evidence for heterogeneity of the testicular macrophage population. *Cell and Tissue Research,* 308**,** 277-285.

Gerdprasert, O., O'bryan, M. K., Nikolic-Paterson, D. J., K.Sebire, de Kretser, D. M. & Hedger, M. P. 2002. Expression of monocyte chemoattractant protein-1 and macrophage colony-stimulating factor in normal and inflamed rat testis. *Molecular and Human Reproduction,* 8**,** 518-524.

Gold, E., Jetly, N., O'bryan, M. K., Meachem, S., Srinivasan, D., Behuria, S., Sanchez-Partida, L. G., Woodruff, T., Hedwards, S., Wang, H., Mcdougall, H., Casey, V., Niranjan, B., Patella, S. & Risbridger, G. 2009. Activin C antagonizes activin A in vitro and overexpression leads to pathologies in vivo. *American Journal of Pathology,* 174**,** 184-195.

Gordon, S., Pluddemann, A. & Estrada, F. M. 2014. Macrophage heterogeneity in tissues: phenotypic diversity and functions. *Immunological Reviews,* 262**,** 36-55.

Gray, A. M. & Mason, A. J. 1990. Requirement for activin A and transforming growth factor-β1 pro-regions in homodimer assembly. *Science,* 247**,** 1328-1330.

Guo, Q., Kumar, T. R., Woodruff, T., Hadsell, L. A., Demayo, F. J. & Matzuk, M. M. 1998. Overexpression of mouse follistatin causes reproductive defects in transgenic mice. *Molecular Endocrinology,* 12**,** 96-106.

Harris, S. G., Padilla, J., Koumas, L., Ray, D. & Phipps, R. P. 2002. Prostaglandins as modulators of immunity. *Trends in Immunology,* 23**,** 144-150.

Hashimoto, O., Nakamura, T., Shoji, H., Shimasaki, S., Hayashi, Y. & Sugino, H. 1997. A novel role of follistatin, an activin-binding protein, in the inhibition of activin action in rat pituitary cells. Endocytotic degradation of activin and its acceleration by follistatin associated with cell-surface heparan sulfate. *Journal of Biological Chemistry,* 272**,** 13835-13842.

Hayes, R., Chalmers, S. A., Nikolic-Paterson, D. J., Atkins, R. C. & Hedger, M. P. 1996. Secretion of Bioactive Interleukin 1 by Rat Testicular Macrophages In Vitro. *Journal of Andrology,* 17**,** 41-49.

Head, J. R. & Billingham, R. E. 1985. Immune privilege of testis. II Evalution of potential local factors. *Transplantation,* 40**,** 269-275.

Head, J. R., Neaves, W. B. & Billingham, R. E. 1983. Immune privilege in the testis. I. Basic parameters of allograft survival. *Transplantation,* 36**,** 423-431.

Hedger, M. P. & Hales, D. B. 2006. Chapter 25 - Immunophysiology Of The Male Reproductive Tract. *In:* Neill, J. D., Plant, T. M., Pfaff, D. W., Challis, J. R., de Kretser, D. M., Richards, J. & Wassarman, P. M. (eds.) *Knobil and Neill's Physiology of Reproduction* (Third edition). St Louis: *Academic press,* 1195-1286.

Hedger, M. P. & de Kretser, D. M. 2013. The activins and their binding proteins, follistatis-Dianostic and therapeutic targets in inflammatory disease and fibrosis. *Cytokine and Growth Factor Reviews,* 24**,** 285-295.

Hedger, M. P. & Winnall, W. R. 2012. Regulation of activin and inhibin in the adult testis and the evidence for functional roles in spermatogenesis and immunoregulation. *Molecular and Cellular Endocrinology,* 59**,** 30-42.

Hedger, M. P. 2002. Marophages and the immune responsiveness of the testis. *Journal of Reproductive Immunology,* 57**,** 19-34.

Hedger, M. P. 2011. Immunophysiology and pathology of inflammation in the testis and epididymis. *Journal of Andrology,* 32**,** 625-640.

Hedger, M. P. 2015. The Immunophysiology of Male Reproduction *In:* Plant, T. M. & Zeleznik, A. J. (eds) *Knobil and Neill's Physiology of Reproduction* (Third edition). St. Louis: *Academic Press*, 805-892.

Hedger, M. P., Winnall, W. R., Phillips, D. J. & de Kretser, D. M. 2011. Regulation and function of activin and follistatin in inflammation and immunity. *Vitamins Hormones,* 85**,** 255-297.

Hermo, L. & Dworkin, J. 1988. Transitional cells at the junction of seminiferous tubules with the rete testis of the rat: their fine structure, endocytic activity, and basement membrane. *American Journal Of Anatomy,* 181**,** 111-131.

Hess, R. A. & Vogl, A. W. 2015. 1 - Sertoli cell anatomy and cytoskeleton. *In*: Griswold, M. D. (ed.) *Sertoli cell biology* (Second edition). Oxford: *Academic Press*, 1-55.

Hess, R. A. 2002. The efferent ductules: structure and functions. In: Robaire, B & Hinton, B. T. (eds) *The epididymis: from molecules to clinical practice: A comprehensive Survey of the Effeent ducts, the Epididymis and the Vas Deferens.* Boston, MA: Springer US, 49-80.

Hintz, M. & Goldberg, E. 1977. Immunohistochemical localization of LDH-x during spermatogenesis inmouse testes. *Developmental Biology,* 57**,** 375-384.

Hogarth, C. A. & Griswold, M. D. 2010. The key role of vitamin A in spermatogenesis. *The Journal Of Clinical Investigation,* 120**,** 956-962.

Hotten, G., Neidhardt, H., Schneider, C. & Pohl, J. 1995. Cloning of a new member of the TGF-β family: a putative new activin βC chain. *Biochemical and Biophysical Research Communications,* 206**,** 608-613.
Huber, S., Stahl, F. R., Schrader, J., Lüth, S., Presser, K., Carambia, A., Flavell, R. A., Werner, S., Blessing, M., Herkel, J. & Schramm, C. 2009. Activin A Promotes the TGF-β-Induced Conversion of CD4+CD25− T Cells into Foxp3+ Induced Regulatory T Cells. *Journal of Immunology,* 182**,** 4633-4640.
Hutson, J. C. 1992. Development of cytoplasmic digitations between Leydig cells and testicular macrophages of the rat. *Cell and Tissue Research,* 267**,** 385-389.
Hutson, J. C. 2006. Physiologic Interactions Between Macrophages and Leydig Cells. *Experimental Biology and Medicine,* 231**,** 1-7.
Ilio, K. Y. & Hess, R. A. 1992. Localization and activity of Na+, K+-ATPase in the ductuli efferentes of the rat. *The Anatomical Record,* 234**,** 190-200.
Indumathy, S., Pueschl, D., Klein, B., Fietz, D., Bergmann, M., Schuppe, H. C., Da Silva, N., Loveland, B. E., Hickey, M. J., Hedger, M. P. & Loveland, K. L. 2020. Testicular immune cell populations and macrophage polarisation in adult male mice and the influence of altered activin A levels. *Journal of Reproductive Immunology,* 142**,** 103204.
Inouye, S., Guo, Y., Depaolo, L., Shimonaka, M., Ling, N. & Shimasaki, S. 1991. Recombinant expression of human follistatin with 315 and 288 amino acids: chemical and biological comparison with native porcine follistatin. *Endocrinology,* 129**,** 815-822.
Itoh, M., De Rooij, D. G., Jansen, A. & Drexhage, H. A. 1995. Phenotypical heterogeneity of testicular macrophages/dendritic cells in normal adult mice: an immunohistochemical study. *Journal of Reproductive Immunology,* 28**,** 217-232.
Itoh, M., De-Rooij, D. & Takeuchi, Y. 1995. Mode of inflammatory cell infiltration in testes of mice injected with syngeneic testicular germ cells without adjuvant. *Journal of anatomy,* 187**,** 671.
Itoh, M., Hiramine, C. & Hojo, K. 1991. A new murine model of autoimmune orchitis induced by immunization with viable syngeneic testicular germ cells alone. I. Immunological and histological studies. *Clinical & Experimental Immunology,* 83**,** 137-142.
Jha, A. K., Huang, S. C.-C., Sergushichev, A., Lampropoulou, V., Ivanova, Y., Loginicheva, E., Chmielewski, K., Stewart, K. M., Ashall, J. & Everts, B. 2015. Network integration of parallel metabolic and transcriptional data reveals metabolic modules that regulate macrophage polarization. *Immunity,* 42**,** 419-430.
Kaur, G., Thompson, L. A. & Dufour, J. 2014. Sertoli cell-Immunological sentinels of spermatogenesis. *Seminars in Cell and Developmental Biology***,** 36-44.
Kaur, G., Vadala, S. & Dufour, J. M. 2017. An overview of a Sertoli cell transplantation model to study testis morphogenesis and the role of the Sertoli cells in immune privilege. *Environmental epigenetics,* 3**,** dvx012.
Kern, S., Robertson, S. A., Mau, V. J. & Maddocks, S. 1995. Cytokine secretion by macrophages in the rat testis. *Biology of Reproduction,* 53**,** 1407-16.
Klein, B., Bhushan, S., Günther, S., Middendorff, R., Loveland, K. L., Hedger, M. P. & Meinhardt, A. 2020. Differential tissue-specific damage caused by bacterial epididymo-orchitis in the mouse. *Molecular Human Reproduction,* 26**,** 215-227.
Knoblaugh, S. & True, L. 2012. 18 - Male Reproductive System. *In:* Treuting, P. M. & Dintzis, S. M. (eds.) *Comparative Anatomy and Histology.* San Diego: Academic Press, 285-308.

Kotsias, F., Cebrian, I. & Alloatti, A. 2019. Chapter Two - Antigen Processing And Presentation. *In:* Lhuillier, C. & Galluzzi, L. (eds.) *International Review of Cell and Molecular Biology.* Academic Press, 348:69-121.

de Kretser, D. M. , O'hehir, R. E., Hardy, C. L. & Hedger, M. P. 2012. The roles of activin A and its binding protein, follistatin, in inflammation and tissue repair. *Molecular and Cellular Endocrinology,* 359**,** 101-106.

Kulibin, A. Y. & Malolina, E. A. 2020. Formation of the rete testis during mouse embryonic development. *Developmental Dynamics,* 249**,** 1486-1499.

Kumar, A., Raut, S. & Balasinor, N. H. 2018. Endocrine regulation of sperm release. *Reproduction, Fertility and Development*, 30, 1595-1603.

Le Tortorec, A., Matusali, G., Mahé, D., Aubry, F., Mazaud-Guittot, S., Houzet, L. & Dejucq-Rainsford, N. 2020. From ancient to emerging infections: the odyssey of viruses in the male genital tract. Physiological reviews, 100, 1349-1414.

Li, X. 2009. Aromatase over expression transgenic murine models for aromatase inhibitor studies. *Molecular Human Reproduction,* 16**,** 80-86.

Lin, S. J., Lerch, T. F., Cook, R. W., Jardetzky, T. S. & Woodruff, T. K. 2006. The structural basis of TGF-beta, bone morphogenetic protein, and activin ligand binding. *Reproduction,* 132**,** 179-190.

Ling, N., Ying, S.-Y., Ueno, N., Shimasaki, S., Esch, F., Hotta, M. & Guillemin, R. 1986. Pituitary FSH is released by a heterodimer of the β-subunits from the two forms of inhibin. *Nature,* 321**,** 779-782.

Lokka, E., Lintukorpi, L., Cisneros-Montalvo, S., Mäkelä, J.-A., Tyystjärvi, S., Ojasalo, V., Gerke, H., Toppari, J., Rantakari, P. & Salmi, M. 2020. Generation, localization and functions of macrophages during the development of testis. *Nature Communications,* 11**,** 4375.

Lui, W. Y., Lee, W. M. & Cheng, C. Y. 2003. TGF-βs: their role in testicular function and Sertoli cell tight junction dynamics. *International Journal of Andrology,* 26**,** 147-160.

Mackenzie, K. F., Clark, K., Naqvi, S., Mcguire, V. A., Nöehren, G., Kristariyanto, Y., Van Den Bosch, M., Mudaliar, M., Mccarthy, P. C. & Pattison, M. J. 2013. PGE2 induces macrophage IL-10 production and a regulatory-like phenotype via a protein kinase A–SIK–CRTC3 pathway. *The Journal of Immunology,* 190**,** 565-577.

Major, A. T., Estermann, M. A. & Smith, C. A. 2021. Anatomy, Endocrine Regulation and Embryonic Development of the Rete Testis. *Endocrinology*, 162.

Malolina, E. A. & Kulibin, A. Y. 2019. The rete testis harbors Sertoli-like cells capable of expressing DMRT1. *Reproduction,* 158**,** 399-413.

Mantovani, A., Biswas, S. K., Galdiero, M. R., Sica, A. & Locati, M. 2013. Macrophage plasticity and polarization in tissue repair and remodelling. *The Journal of Pathology,* 229**,** 176-185.

Mather, J. P., Kenneth M. Attie, Woodruff, T. K., Rice, G. C. & Phillips, D. M. 1990. Activin Stimulates Spermatogonial Proliferation in Germ-Sertoli Cell Cocultures from Immature Rat Testis. *Endocrinology,* 127**,** 3206-3214.

Mathews, L. S. & Vale, W. W. 1991. Expression cloning of an activin receptor, a predicted transmembrane serine kinase. *Cell,* 65**,** 973-982.

Matzuk, M. M., Kumar, T. R. & Bradley, A. 1995a. Different phenotypes of mice deficient in either activins or activin receptor type II. *Nature,* 374**,** 356-360.

Matzuk, M. M., Lu, N., H.Vogel, Sellheyer, K., Roop, D. R. & Bradley, A. 1995b. Multiple defects and perinatal death in mice deficient in follistatin. *Nature,* 374**,** 360-363.

Matzuk, M. M., Kumar, T. R., Bicjenbach, J. R., Vassalli, A., Roop, D. R., Jaenisch, R. & Bradley, A. 1995c. Functional analysis of activins during mammalian development. *Nature,* 374**,** 354-356.
Mccabe, M. J., Foo, C. F., Dinger, M. E., Smooker, P. M. & Stanton, P. G. 2016. Claudin-11 and occludin are major contributors to Sertoli cell tight junction function, in vitro. *Asian Journal Of Andrology,* 18**,** 620.
Meinhardt, A. & Hedger, M. P. 2011. Immunological, paracrine and endocrine aspects of testicular immune privilege. *Molecular and Cellular Endocrinology,* 335**,** 60-8.
Meinhardt, A., Dejucq-Rainsford, N. & Bhushan, S. 2021. Testicular macrophages: development and function in health and disease. *Trends in Immunology*, 43, 51-62.
Meinhardt, A., Wang, M., Schulz, C. & Bhushan, S. 2018. Microenviornmental signals govern the cellular identity of testicular macrophages. *Journal of Leukocyte Biology,* 104**,** 757-766.
Meiser, J., Krämer, L., Sapcariu, S. C., Battello, N., Ghelfi, J., D'herouel, A. F., Skupin, A. & Hiller, K. 2016. Pro-inflammatory macrophages sustain pyruvate oxidation through pyruvate dehydrogenase for the synthesis of itaconate and to enable cytokine expression. *Journal of Biological Chemistry,* 291**,** 3932-3946.
Mendis, S. H. S., Meachem, S. J., Sarraj, M. A. & Loveland, K. L. 2010. Activin A Balances Sertoli and Germ Cell Proliferation in the Fetal Mouse Testis1. *Biology of Reproduction,* 84**,** 379-391.
Miller, S. C., Bowman, B. M. & Roberts, L. K. 1984. Identification and characterization of mononuclear phagocytes isolated from rat testicular interstitial tissues. *Journal of Leukocyte Biology,* 36**,** 679-687.
Morales, C., Hermo, L. & Clermont, Y. 1984. Endocytosis in epithelial cells lining the rete testis of the rat. *The Anatomical Record,* 209**,** 185-195.
Mossadegh-Keller, N., Gentek, R., Gimenez, G., Bigot, S., Mailfert, S. & Sieweke, M. H. 2017. Developmental origin and maintenance of distinct testicular macrophage populations. *The Journal of Experimental Medicine,* 214**,** 2829-2841.
Mosser, D. M. & Edwards, J. P. 2008. Exploring the full spectrum of macrophage activation. *Nature Reviews Immunology,* 8**,** 958-969.
Mruk, D. D. & Cheng, C. Y. 2015. The Mammalian Blood-Testis Barrier: Its Biology and Regulation. *Endocrine Reviews,* 36**,** 564-591.
Nes, W. D., Lukyanenko, Y. O., Jia, Z. H., Quideau, S., Howald, W. N., Pratum, T. K., West, R. R. & Hutson, J. C. 2000. Identification of the lipophilic factor produced bymacrophages that stimulates steroidogenesis. *Endocrinology,* 141**,** 953-958.
Nicolas, N., Michel, V., Bhushan, S., Wahle, E., Hayward, S., Ludlow, H., de Kretser, D. M. , Loveland, K. L., Schuppe, H.-C., Meinhardt, A., Hedger, M. P. & Fijak, M. 2017. Testicular activin and follistatin levels are elevated during the course of experimental autoimmune epididymo–orchitis in mice. *Scientific Reports,* 7**,** 1-15.
Nikolova, D. B., Kansheva, L. S., Surneva, M. D. & Martinova, Y. S. 1992. Species-specific effects of proteins secreted by cultured prepubertal rat Sertoli cells on natural killer cell activity. *Immunopharmacology,* 23**,** 15-20.
O'Bryan, M. K., Gerdprasert, O., Nikolic-Paterson, D. J., Meinhardt, A., Muir, J. A., Foulds, L. M., Phillips, D. J., de Kretser, D. M. & Hedger, M. P. 2005. Cytokine profiles in the testes of rats treated with lipopolysaccharide reveal localized suppression of inflammatory responses. *American Journal of Physiology Regulatoty, Integrative and Comparative Physiology,* 288**,** R1744-R1755.
O'Bryan, M. K., Schlatt, S., Phillips, D. J., de Kretser, D. M. & Hedger, M. P. 2000. Bacterial lipopolysaccharide-induced inflammation compromises testicularfunction at multiple levels in vivo. *Endocrinology,* 141**,** 238-246.

O'Donnell, L., Smith, L. B. & Rebourcet, D. 2022. Sertoli cells as key drivers of testis function. *Seminars in Cell & Developmental Biology,* 121**,** 2-9.
O'Donnell, L., Nicholls, P. K., O'Bryan, M. K., Mclachlan, R. I. & Stanton, P. G. 2011. Spermiation. *Spermatogenesis*, 1, 14-35.
Oda, S., Nishimatsu, S., Murakami, K. & Ueno, N. 1995. Molecular cloning and functional analysis of a new activin β subunit: a dorsal mesoderm-inducing activity in Xenopus. *Biochemical and Biophysical Research Communications,* 210**,** 581-588.
Ogawa, K., Funaba, M., Chen, Y. & Tsujimoto, M. 2006. Activin A Functions as a Th2 Cytokine in the Promotion of the Alternative Activation of Macrophages. *Journal of Immunology,* 177**,** 6787-6794.
Okuma, Y., O'connor, A. E., Hayashi, T., Loveland, K. L., de Kretser, D. M. & Hedger, M. P. 2006. Regulated production of activin A and inhibin B throughout the cycle of the seminiferous epithelium in the rat. *Endocrinology,* 190**,** 331-340.
Olaso, R., Pairault, C., Boulogne, B., Durand, P. J.-P. & Habert, R. 1998. Transforming growth factor β1 and β2 reduce the number of gonocytes by increasing apoptosis. *Endocrinology,* 139**,** 733-740.
Pace, J. L., Russell, S. W., Schreiber, R. D., Altman, A. & Katz, D. H. 1983. Macrophage activation: priming activity from a T-cell hybridoma is attributable to interferon-gamma. *Proceedings of the National Academy of Sciences,* 80**,** 3782-3786.
Pleuger, C., Silva, E. J. R., Pilatz, A., Bhushan, S. & Meinhardt, A. 2020. Differential Immune Response to Infection and Acute Inflammation Along the Epididymis. Frontiers in Immunology, 11.
Ritchie, A. W., Hargreave, T. B., James, K. & Chisholm, G. D. 1984. Intra-epithelial lymphocytes in the normal epididymis. A mechanism for tolerance to sperm auto-antigens? *British Journal of Urology,* 56**,** 79-83.
Robertson, D., Klein, R., De Vos, F., Mclachlan, R., Wettenhall, R., Hearn, M., Burger, H. & de Kretser, D.M 1987. The isolation of polypeptides with FSH suppressing activity from bovine follicular fluid which are structurally different to inhibin. *Biochemical And Biophysical Research Communications,* 149**,** 744-749.
Robson, N. C., Phillips, D. J., Mcalpine, T., Shin, A., Svobodova, S., Toy, T., Pillay, V., Kirkpatrick, N., Zanker, D., Wilson, K., Helling, I., Wei, H., Chen, W., Cebon, J. & Maraskovsky, E. 2008. Activin-A: a novel dendritic cell–derived cytokine that potently attenuates CD40 ligand–specific cytokine and chemokine production. *Blood,* 111**,** 2733-2743.
Roche, P. A. & Furuta, K. 2015. The ins and outs of MHC class II-mediated antigen processing and presentation. *Nature Reviews Immunology,* 15**,** 203-216.
Russell, L. D., Ren, H. P., Hikim, I. S., Schulze, W. & Hikim, A. P. S. 1990. A comparative study in twelve mammalian species of volume densities, volumes, and numerical densities of selected testis components, emphasizing those related to the sertoli cell. *American Journal of Anatomy,* 188**,** 21-30.
Rutherford, M. S., Witsell, A. & Schook, L. B. 1993. Mechanisms generating functionally heterogeneous macrophages: chaos revisited. *Journal of Leukocyte Biology,* 53**,** 602-618.
Saito, K., O'Donnell, L., Mclachlan, R. I. & Robertson, D. M. 2000. Spermiation failure is a major contributor to early spermatogenic suppression caused by hormone withdrawal in adult rats. *Endocrinology*, 141, 2779-85.
Schulz, C., Perdiguero, E. G., Chorro, L., Szabo-Rogers, H., Cagnard, N., Kierdorf, K., Prinz, M., Wu, B., Jacobsen, S. E. W., Pollard, J. W., Frampton, J., Liu, K. J. &

Geissmann, F. 2012. A lineage of myeloid cells independent of myb and hematopoietic stem cells. *Science,* 336**,** 86-90.
Schuppe, H. C. & Meinhardt, A. 2005. Immune privilege and inflammation of the testis. *Chemical Immunology and Allergy,* 88**,** 1-14.
Selawry, H. P., Kotb, M., Herrod, H. G. & Lu, Z. N. 1991. Production of a factor, or factors, suppressing IL-2 production and T cell proliferation by Sertoli cell-enriched preparations. A potential role for islet transplantation in an immunologically privileged site *Transplantation,* 52**,** 846-850.
Shimasaki, S., Koga, M., Esch, F., Cooksey, K., Mercado, M., Koba, A., Ueno, N., Ying, S.-Y., Ling, N. & Guillemin, R. 1988. Primary structure of the human follistatin precursor and its genomic organization. *Proceedings of the National Academy of Sciences,* 85**,** 4218-4222.
Sierra-Filardi, E., Nieto, C., Dominguez-Soto, A., Barroso, R., Sanchez-Mateos, P., Puig-Kroger, A., Lopez-Bravo, M., Joven, J., Mellado, M. & Corbi, A. L. 2014. CCL2 shapes macrophage polarization by GM-CSF and M-CSF: Identification of CCL2/CCR2-Dependent Gene Expression Profile. *The Journal of Immunology,* 192**,** 1-10.
Slominski, R. M., Tuckey, R. C., Manna, P. R., Jetten, A. M., Postlethwaite, A., Raman, C. & Slominski, A. T. 2020. Extra-adrenal glucocorticoid biosynthesis: Implications for autoimmune and inflammatory disorders. *Genes & Immunity,* 21**,** 150-168.
Sonoda, K.-H., Faunce, D. E., Taniguchi, M., Exley, M., Balk, S. & Stein-Streilein, J. 2001. NK T cell-derived IL-10 is essential for the differentiation of antigen-specific T regulatory cells in systemic tolerance. *Journal of Immunology,* 166**,** 42-50.
Stanton, P. G. 2016. Regulation of the blood-testis barrier. Seminars in cell & developmental biology. Elsevier, 59, 166-173.
Stein, M. 1992. Keshav S. Harris N, Gordon S. Interleukin 4 potently enhances murine macrophage mannose receptor activity: a marker of alternative immunologic macrophage activation. *Journal of Experimental Medicine,* 176**,** 287-92.
Sugino, K., Kurosawas, N., Nakamura, T., Takios, K., Shimasakill, S., Lingll, N., Titanill, K. & Sugino, H. 1993. Molecular heterogeneity of follistatin, an activin-binding protein. Higher affinity of the carboxyl-terminal truncated forms for heparan sulfate proteoglycans on the ovarian granulosa cell. *Journal of Biological Chemistry,* 268**,** 15579-15587.
Takahashi, K., Naito, M., Terayama, H., Qu, N., Cheng, L., Tainosho, S. & Itoh, M. 2007. Immunomorphological aspects of the tubuli recti and the surrounding interstitium in normal mice. *International Journal of Andrology,* 30**,** 21-27.
Ting, J. P. & Trowsdale, J. 2002. Genetic control of MHC class II expression. *Cell,* 109 Suppl**,** S21-33.
Troutman, T. D., Bazan, J. F. & Pasare, C. 2012. Toll-Like receptors, signaling adapters and regulation of the pro-inflammatory response by PI3K. *Cell cycle,* 11**,** 3559-3567.
Tsuchida, K., Nakatani, M., Yamakawa, N., Hashimoto, O., Hasegawa, Y. & Sugino, H. 2004. Activin isoforms signal through type I receptor serine/threonine kinase ALK7. *Molecular and Cellular Endocrinology,* 220**,** 59-65.
Tung, K. S. & Teusher, C. 1995. Mechanisms of autoimmune disease in the testis and ovary. *Human Reproduction Update,* 1**,** 35-50.
Tung, K. S. K., Harakal, J., Qiao, H., Rival, C., Li, J. C. H., Paul, A. G. A., Wheeler, K., Pramoonjago, P., Grafer, C. M., Sun, W., Sampson, R. D., Wong, E. W. P., Reddi, P. P., Deshmukh, U. S., Hardy, D. M., Tang, H., Cheng, C. Y. & Goldberg, E. 2017.

Egress of sperm autoantigen from seminiferous tubules maintains systemic tolerance. *Journal of Clinical Investigation,* 127**,** 1046-1060.
Tung, K. S., Yule, T. D., Mahi-Brown, C. A. & Listrom, M. B. 1987. Distribution of histopathology and Ia positive cells in actively induced and passively transferred experimental autoimmune orchitis. *The Journal of Immunology,* 138**,** 752-759.
Turner, T., Jones, C., Howards, S., Ewing, L., Zegeye, B. & Gunsalus, G. 1984. On the androgen microenvironment of maturing spermatozoa. *Endocrinology,* 115**,** 1925-1932.
Vale, W., Rivier, J., Vaughan, J., Mcclintock, R., Corrigan, A., Woo, W., Karr, D. & Spiess, J. 1986. Purification and characterization of an FSH releasing protein from porcine ovarian follicular fluid. *Nature,* 321**,** 776-779.
Vassalli, A., Matzuk, M. M., Gardner, H. A. R., Lee, K.-F. & Jaenisch, R. 1994. Activitn/inhibin βB subunit gene disruption leads to defects in eyelid development and female reproduction. *Genes and Development,* 8**,** 414-427.
Vergadi, E., Ieronymaki, E., Lyroni, K., Vaporidi, K. & Tsatsanis, C. 2017. Akt Signaling Pathway in Macrophage Activation and M1/M2 Polarization. *The Journal of Immunology,* 198**,** 1006-1014.
Walton, K.L., Makanji, Y & Harrison, C. A. 2012. New insights into the mechanisma of activin action and inhibition. *Molecular and Cellular Endocrinology*, 359, 2-12.
Wang, J., Wreford, N. G. M., Lan, H. Y., Atkins, R. & Hedger, M. P. 1994. Leukocyte Populations of the Adult Rat Testis Following Removal of the Leydig- Cells by Treatment with Ethane Dimethane Sulfonate and Subcutaneous Testosterone Implants. *Biology of Reproduction,* 51**,** 551-561.
Wang, M., Fijak, M., Hossain, H., Markmann, M., Nusing, R. M., Lochnit, G., Hartmann, M. F., Wudy, S. A., Zhang, L., Gu, H., Konrad, L., Chakraborty, T., Meinhardt, A. & Bhushan, S. 2017. Characterization of the Micro-Environment of the Testis that Shapes the Phenotype and Function of Testicular Macrophages. *The Journal of Immunology,* 198**,** 1-14.
Wang, M., Yang, Y., Cansever, D., Wang, Y., Kantores, C., Messiaen, S., Moison, D., Livera, G., Chakarov, S. & Weinberger, T. 2021. Two populations of self-maintaining monocyte-independent macrophages exist in adult epididymis and testis. *Proceedings of the National Academy of Sciences,* 118.
Welsh, M., Saunders, P. T. K., Atanassova, N., Sharpe, R. M. & Smith, L. B. 2009. Androgen action via testicular peritubular myoid cells is essential for male fertility. *Federation of American Societies for Experimental Biology (FASEB) Journal,* 23**,** 4218-4230.
Winnall, W. R. & Hedger, M. P. 2013. Phenotypic and functional heterogeneity of the testicular macrophage population: a new regulatory model. *Journal of Reproductive Immunology,* 97**,** 147-158.
Winnall, W. R., Ali, U., O'bryan, M. K., Hirst, J. J., Whiley, P. A., Muir, J. A. & Hedger, M. P. 2007. Constitutive expression of prostaglandin-endoperoxide synthase 2 by somatic and spermatogenic cells is responsible for prostaglandin E2 production in the adult rat testis. *Biology of Reproduction,* 76**,** 759-768.
Winnall, W. R., Muir, J. A. & Hedger, M. 2011a. Rat resident testicular macrophages have an alternatively activated phenotype and constitutively produce interleukin-10 in vitro. *Journal of Leukocyte Biology,* 90**,** 133-143.
Winnall, W. R., Muir, J. A. & Hedger, M. P. 2011b. Differential responses of epithelial Sertoli cells of the rat testis to Toll-like receptor 2 and 4 ligands: Implications for studies of testicular inflammation using bacterial lipopolysaccharides. *Innate Immunity,* 17**,** 123-136.

Wyatt, C. R., Law, L., Magnuson, J. A., Griswold, M. G. & Magnuson, N. S. 1988. Suppression of lymphocyte proliferation by proteins secreted by cultured Sertoli cells. *Journal of Reproductive Immunology,* 14**,** 27-40.

Yamashita, N., Nakajima, T., Takahashi, H., Kaneoka, H., Mizushima, Y. & Sakane, T. 1993. Effects of activin A on IgE synthesis and cytokine production by human peripheral mononuclear cells. *Clinical and Experimental Immunology,* 94**,** 214-219.

Zhang, Z., Jiang, Z., Zhang, Y., Zhang, Y., Yan, Y., Bhushan, S., Meinhardt, A., Qin, Z. & Wang, M. 2020. Corticosterone Enhances the AMPK-Mediated Immunosuppressive Phenotype of Testicular Macrophages During Uropathogenic Escherichia coli Induced Orchitis. *Frontiers in Immunology,* 11**,** 583276-583276.

Declaration

I declare that I have completed this dissertation single-handedly without the unauthorized help of a second party and only with the assistance acknowledged therein. I have appropriately acknowledged and referenced all text passages that are derived literally from or are based on the content of published or unpublished work of others, and all information that relates to verbal communications. I have abided by the principles of good scientific conduct laid down in the charter of the Justus-Liebig-University of Giessen in carrying out the investigations described in the dissertation.

Ich erkläre: Ich habe die vorgelegte Dissertation selbständig, ohne unerlaubte fremde Hilfe und nur mit den Hilfen angefertigt, die ich in der Dissertation angegeben habe. Alle Textstellen, die wörtlich oder sinngemäß aus veröffentlichten oder nicht veröffentlichten Schriften entnommen sind, und alle Angaben, die auf mündlichen Auskünften beruhen, sind als solche kenntlich gemacht. Bei den von mir durchgeführten und in der Dissertation erwähnten Untersuchungen habe ich die Grundsätze guter wissenschaftlicher Praxis, wie sie in der „Satzung der Justus-Liebig-Universität Gießen zur Sicherung guter wissenschaftlicher Praxis“ niedergelegt sind, eingehalten.

Signature:

Print name: Sneha Biniwale

Date: 30-08-22